The role of the Transient Receptor Potential Ankyrin-1 in the peripheral vasculature

Aubdool, Aisah Aniisah

Awarding institution:
King's College London

The role of the Transient Receptor Potential Ankyrin-1 in the peripheral vasculature

A thesis submitted for the degree of
Doctor of Philosophy
King's College London

Aisah Aniisah Aubdool

Cardiovascular Division
BHF Center of Research Excellence
King's College London
Franklin Wiklins Building
Waterloo Campus
London, SE1 9NH

Abstract

The phenomenon of cold-induced vasodilatation (CIVD) was discovered by Sir Thomas Lewis (1930) and has been extensively investigated as it is involved in protecting against local cold-induced injury. The mechanisms underlying this well-established protective response remain unclear. The non-selective cation channel, transient receptor potential ankyrin-1 (TRPA1) is expressed in a subset of sensory neurons and acts as a polymodal membrane channel for cold sensitivity, but this remains a controversial issue in the literature. Additionally, the role of TRPA1 as a vascular cold sensor is currently unknown. Previous studies in our group have shown that TRPA1 plays an important role in regulating peripheral blood vessel tone, with little information available on the downstream signalling mechanism. The aims of this PhD project were to investigate the effects of TRPA1 activation by an exogenous agonist cinnamaldehyde and local cold exposure on peripheral vascular responses in murine skin *in vivo.*

Using a combination of pharmacological antagonists and genetically modified mice, topical application of cinnamaldehyde (10%) was shown to increase blood flow in a TRPA1-dependent manner in the mouse ear model. This response was further shown to be dependent on the release of the potent microvascular vasodilator calcitonin gene-related peptide (CGRP), highlighting the involvement of a neurogenic component. This study provides novel evidence demonstrating the relative contribution of neuronal nitric-oxide synthase (nNOS)-derived nitric oxide and reactive oxygen species, downstream of TRPA1 activation by cinnamaldehyde. These findings highlight the prominent role of TRPA1 in mediating peripheral vasodilatation.

The project further progressed to the development and characterisation of a local cold model in the mouse hindpaw *in vivo*. Local cold exposure was shown to cause a rapid and transient vasoconstriction, followed by a prolonged vasodilatation phase to return blood flow to baseline, an essential physiological function for protecting against local cold-induced injury. The activation of TRPA1 in the peripheral vasculature was shown to drive this cold-induced vascular response at 10°C. This model enabled the determination of the relative role of sympathetic nerves, post-junctional α_2-adrenergic receptors and reactive oxygen species in the local cold-induced vasoconstriction. This study provides novel evidence showing that local cold exposure causes an increase in intracellular superoxide production in a TRPA1-dependent manner, which activates the Rho-kinase-mediated pathways and induces cold-induced α_{2C}-adrenergic vasoconstriction. The neuropeptide CGRP was subsequently shown to have a prominent role in the vasodilator phase.

This study provide novel evidence of a major involvement of TRPA1 in mediating cold-induced vasoconstriction *in vivo*, with a new perspective of the underlying mechanisms mediating the protection against local-cold induced injury.

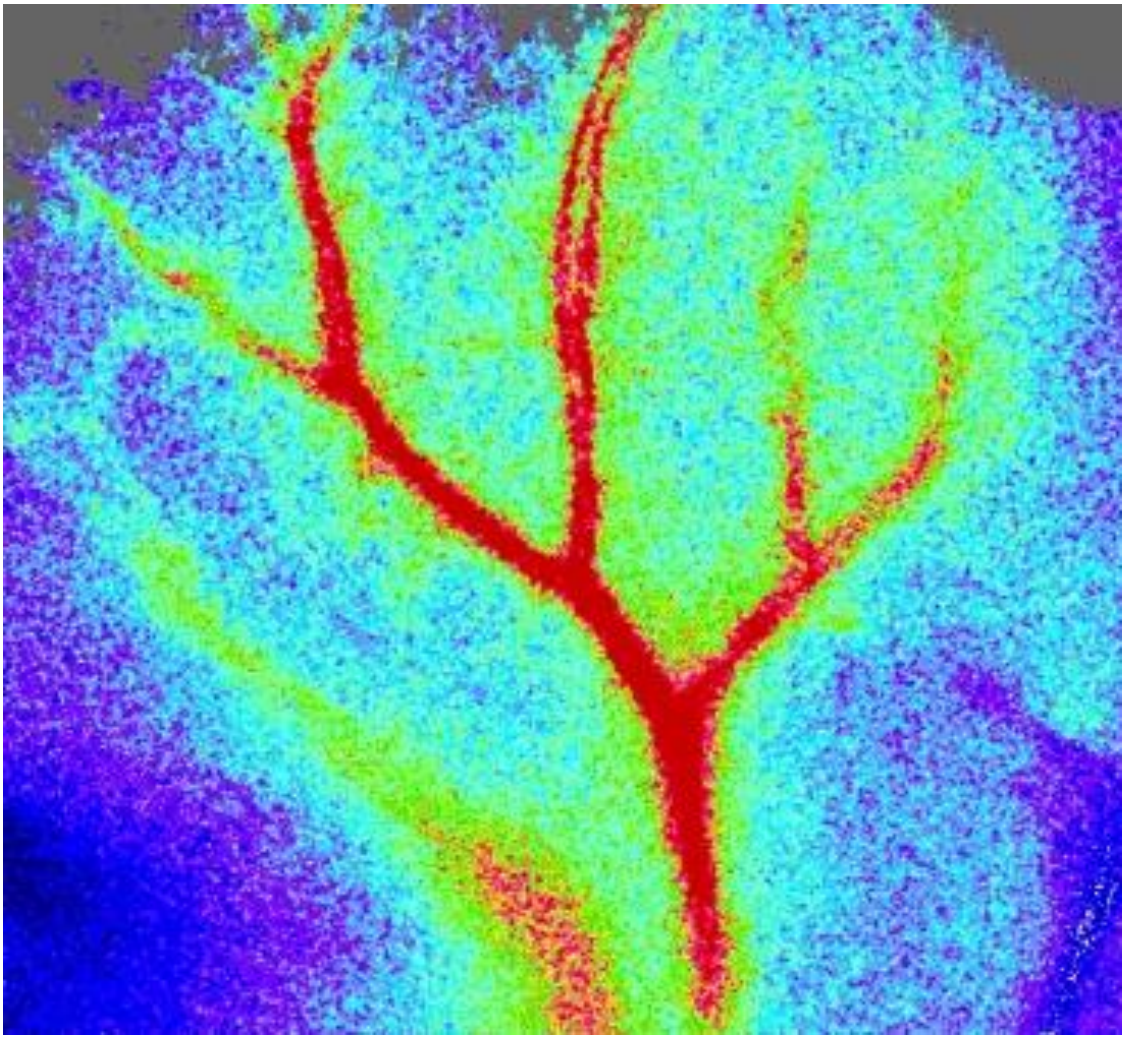

Cinnamaldehyde-induced increase in blood flow in the mouse ear following topical application

To Maa and Papa

Acknowledgements

My passion for understanding the function of TRPA1 initiated during my undergraduate degree in 2009. When I started my PhD project in the Brain Lab in 2010, I entered the world of vascular biology and started investigating the role of TRPA1 in regulating peripheral blood flow. I was ecstatic and it felt like one of my academic dreams came true. I have thoroughly enjoyed every single moment of the journey thus far and this would not have been possible without the constant support, guidance and inspiration from my supervisor Prof. Sue Brain. Sue, you made science fun and exciting, and you were my primary resource for getting my questions answered (from a knock on your door to emails sent out of office hours), and this enabled me to keep the experiments going day by day to be able to construct 'our story/pathway'. You have always been there answering my emails over the weekend when I am troubleshooting or having a 'cool moment' with my data ☺. Sometimes, I would even dream about my experiments. Over the last three years, you have taught me to be an ambitious but realistic scientist. Thank you! I hope to follow in your footstep and become a lively, enthusiastic and energetic Professor as you are in the near future.

The use of genetically modified mice and pharmacological antagonists was a major component of this project. This would not have been possible without the collaborations from Prof S. Bevan for the TRPA1 and TRPM8 KOs, and has always taken time to read my abstracts and paper, with insightful feedback and suggestions for future experiments, Mr C.Gentry for characterising AMTB, Dr A.Grant for TRPV4 KOs and Prof. A.Shah for NOX4 KOs. I would also like to thank Dr R.Graepel (my TRPA1 mentor) for teaching and training me to use the laser Doppler techniques and, developing and characterising the local cold-induced vascular model; the post-doctoral fellows Dr E.Fernandes, Dr J.Bodkin (my TRPA1 friend) and Dr S.Smillie for their time, encouragement and expertise throughout this project.

K.Alawi (TRPV1 Princess), a special thank you goes to you for always being there to listen to my stories on TRPA1 and where we are on the timeline of discoveries, teaching me about TRPV1 and the sympathetic nerve. Learning new techniques alongside with you for the last past 3 years has been amazing. S.Srivastava (Nrf2 Prince), a massive thank you for your willing help to develop and characterise the western blotting technique in order to quantify phosphorylated and total MLC in my tissues. I enjoyed our frequent critical discussion in exploring the role of reactive oxygen species and nitric oxide in my experiments, which usually always turns into little arguments or further experiments. Without my undergraduate student Ms X.Kodji (TRPA1Junior), the pursuit of the reactive oxygen species (superoxide) component of this project would not have started. Xenia has been an amazing star with her unflagging willingness to help and make this project scientifically wonderful.

Dr F.Russell, thank you for all your help, moral support and insightful suggestions for the last past few months. I am greatly indebted to you for your precious critique and proofreading of my thesis. Mr P.Thakore, I am grateful for your willingness to read my chapters as they were generated and your expertise in designing and drawing my schematic diagrams. I hope to return the favour when you produce your thesis. Lastly, I would like to thank Lihuan, Ross and Elena (Brain Lab) for an enjoyable atmosphere with great teamwork in the lab, and the rest of the members of the vascular biology department (especially Claire, Maria, Tabsy, Bijal, Shane, Chapplinicious, Jessal, Keith, Alessio) who I have worked with throughout this project.

Mr. P.Fox, a special thank you for all your advice and help on maintaining my TRPA1 colony. I gratefully acknowledge the support from the Centre of Integrative Biomedicine at KCL and BBSRC, which made my PhD project possible. On a personal note, I would like to thank my Maa, Papa, my two little siblings; Aadil and Aaqil who cannot wait to see the 'Book', my grandma (dadima) and the rest of my little family for their special love, support, advice and encouragement throughout this project. I hope you are all proud of me, you all read my thesis and love TRPA1 as much as I do.

List of Published Papers

Alexander R, Kerby A, **Aubdool AA**, Power AR, Grover S, Gentry C, Grant AD (2013). 4α-phorbol 12,13-didecanoate activates cultured mouse dorsal root ganglia neurons independently of TRPV4. *Br J Pharmacol.* 168: 761-762.

Fernandes ES, Vong CT, Quek S, Cheong J, Awal S, Gentry C, **Aubdool AA**, Liang L, Bodkin JV, Bevan S, Heads R, Brain SD (2013). Superoxide generation and leukocyte accumulation: key elements in the mediation of leukotriene B4-induced itch by transient receptor potential ankyrin 1 and transient receptor potential vanilloid 1. *FASEB J.* 27: 1664-73.

Ryckmans T, **Aubdool AA**, Bodkin JV, Cox P, Brain SD, Dupont T, Fairman E, Hashizume Y, Ishii N, Kato T, Kitchching L, Newman J, Omoto K, Rawson D, Strover J (2011). Design and pharmacolofical evaluation of PF-4840154, a non-electrophilic reference agonist of the TRPA1 channel. *Bioorg Med Chem Lett.* 21: 4857-9.

Aubdool AA, Brain SD (2011). Neurovascular aspects of skin neurogenic inflammation.*J Investig Dermatol Symp Proc.* 15:33-9.

Graepel R, Fernandes ES, **Aubdool AA**, Andersson DA, Bevan S, Brain SD (2011). 4-oxo-2-nonenal (4-ONE): evidence of transient receptor potential ankyrin 1-dependent and -independent nociceptive and vasoactive responses in vivo. *J Pharmacol Exp Ther.* 337:117-24.

List of Published Abstracts

Aubdool AA, Graepel R, Kodji X, Fernandes ES, Bevan S, Brain SD (2013). TRPA1 channels and cutaneous blood flow. *Proceedings of The Physiological Society.*Proc 37th IUPS, PCC413 (oral presentation).

Fernandes ES, Sand C, Salamon R, Bodkin JV, **Aubdool AA**, Brain SD (2013). TRPA1 mediates the cold-induced hemodynamic changes observed in the arthritic knee following exposure to low temperature. *Proceedings of The Physiological Society.* Proc 37th IUPS, PCD345 (poster presentation).

Thakore P, **Aubdool AA**, Brain SD, McFadzean I (2013). Investigating the role of perivascular adipose tissue on vasoconstriction in mouse mesenteric arteries. *Proceedings of The Physiological Society.* Proc 37th IUPS, PCD389 (poster presentation).

Aubdool AA, Kodji X, Fernandes ES, Bevan S, Brain SD (2013).Involvement of TRPA1 and reactive oxygen species in cinnamaldehyde-induced vasodilatation in the peripheral vasculature.*Proceedings of The Physiological Society.*Proc 37th IUPS, SA230 (poster presentation).

Graepel R, **Aubdool AA**, Kodji X, Fernandes ES, Bevan S, Brain SD (2013). TRPA1 channels play a critical role in cold-induced vasodilatation. *FASEB.* Joint Annual Meeting of the ASPET/BPS at Experimental Biology (EB), Boston (poster presentation).

Aubdool AA., Kodji X, Fernandes E, Bevan S, Brain SD (2013). The Participation of Reactive Oxygen Species and TRPA1 in Cinnamaldehyde-Induced Vasodilatation in the Peripheral Vasculature.*Heart* **99***:*A106-107. BSCR/BAS Joint Spring meeting (poster presentation).

Aubdool AA, Brain SD (2013). TRPA1-mediated vasodilatation in the peripheral vasculature. Neuropeptide Club Meeting, Poland (oral presentation).

Aubdool AA, Kodji X, Fernandes ES, Bevan S, Brain SD (2013). Cinnamaldehyde: evidence of TRPA1-dependent vasodilatation in the peripheral vasculature *in vivo* via a ROS-sensitive mechanism. *Microcirculation online*. BMS early career symposium (oral presentation).

Aubdool AA, Bodkin JV, Kodji X, King R, Gentry C, Liang L, Fernandes ES, Bevan S, Brain SD. (2012). Neurovascular effects of cinnamaldehyde through activation of TRPA1: mechanism underlying TRPA1-induced vasodilatation in the peripheral vasculature. *Proceedings of the British Pharmacological Society.pA2 online* BPS Winter Meeting (oral presentation).

Liang L, Chen C, **Aubdool A**, Brain SD (2012). A protective role of TRPV1 in hypertension induced by Angiotensin II. *Proceedings of the British Pharmacological Society.pA2 online* BPS Winter Meeting (poster presentation).

Aubdool AA, Kodji X, Fernandes ES, Bevan S, Brain SD. Cinnamaldehyde: evidence of TRPA1-dependent vasodilator responses in the peripheral vasculature in vivo via a CGRP and nitric oxide-sensitive mechanism (2011). *Proceedings of the British Pharmacological Society.pA2 online* BPS Winter Meeting (poster presentation).

Fernandes ES, Bodkin JV, **Aubdool AA**, Heads RJ, Brain SD (2011). LTB4-induced itch depends on TRPA1 activation: A role for superoxide production. *Proceedings of the British Pharmacological Society.pA2 online* BPS Winter Meeting (poster presentation).

Bodkin JV, **Aubdool AA**, Brain SD (2011). Investigating the role of TRPA1 in cardiovascular regulation. *Proceedings of the British Pharmacological Society.pA2 online* BPS Winter Meeting (poster presentation).

Aubdool AA, Kodji X, Fernandes ES, Bevan S, Brain SD (2011). Evidence that TRPA1 activation mediates CGRP-induced vasodilatation in the peripheral vasculature. *Proceedings of the British Pharmacological Society.pA2 online* BPS Winter Meeting (poster presentation).

Aubdool AA, Graepel R, Brain S (2011). A potential link between TRPA1 and TRPV1 receptors *in vivo*. *Inflammation Research*. *Inflammation Research.* S203. World Inflammation Congress (poster presentation).

Aubdool AA, Graepel R, Brain S. Interactions between TRPA1 and TRPV1 in the peripheral vasculature (2010). *Proceedings of the British Pharmacological Society.pA2 online* BPS Winter Meeting (poster presentation).

Abbreviations

1400W	N-(3-(Aminomethyl)benzyl)acetamidine
4HNE	4-Hydroxynonenal
4-ONE	4-Oxo-2-nonenal
A967079	(1E,3E)-1-(4-Fluorophenyl)-2-methyl-1-pentene-3-one oxime
α-adrenergic receptor	alpha-adrenergic receptor
α-CGRP	alpha-CGRP
AITC	allyl isothiocyanate
AMG7160	4-bromo-N-[2,2,2-trichloro-1-(4-chlorophenyl)sulfanylethyl]benzamide
AMG9810	(2E)-N-(2,3-Dihydro-1,4-benzodioxin-6-yl)-3-[4-(1,1-dimethylethyl)phenyl]-2-propenamide
AMTB	N-(3-Aminopropyl)-2-[(3-methylphenyl)methoxy]-N-(2-thienylmethyl)benzamide hydrochloride
ANS	autonomic nervous system
AP18	4-(4-Chlorophenyl)-3-methyl-3-buten-2-one oxime
APS	amonium persulfate
ATP	adenosine triphosphate
AVAs	arterio-venous anastomoses
B2R	bradykinin 2 receptor
β-actin	beta-actin
β-adrenergic receptor	beta-adrenergic receptor
BAEC	bovine aortic endothelial cells
β-CGRP	beta-CGRP
BH_4	tetrahydrobiopterin
BIBN4096BS	1-[3,5-Dibromo-N-[[4-(1,4-dihydro-2-oxo-3(2H)-quinazolinyl)-1-piperidinyl]carbonyl]-D-tyrosyl-L-lysyl]-4-(4-pyridinyl)-piperazine
BPB	3',3",5',5"-tetrabromophenolsulfonphthalein
BSA	bovine serum albumin
CA	cinnamaldehyde
$CaCl_2$	calcium chloride
CAMKII	Ca^{2+} /calmodulin-dependent protein kinase II
cAMP	cyclic adenosine monophosphate
CAT	catalase
CD1	congressional district 1
cDNA	complementary DNA
CFA	complete Freund's Adjuvant
cGMP	cyclic guanosine monophosphate
CGRP	calcitonin gene related peptide
CHO	chinese hamster ovary

CIVD	cold induced vasodilatation
CNS	central nervous system
COX2	cyclo-oxygenase
CRLR	calcitonin receptor-like receptor
CSL	complete sciatic lesion
Cys	cysteine
DAG	diacylglycerol
DMSO	dimethyl sulfoxide
DNA	deoxyribonucleic acid
DOCA	deoxycorticosterone acetate
DRG	dorsal root ganglion
EDTA	ethylenediaminetetraacetic acid
EMLA	eutectic mixture of local anesthetics
eNOS	endothelial nitric oxide synthase
ER	endoplasmic reticulum
ERK1/2	extracellular signal-regulated protein kinases 1 and 2
FLPI	full-field laser perfusion imager
GAPDH	glyceraldehyde 3-phosphate dehydrogenase
GPCR	G-protein coupled receptor
H_2O_2	hydrogen peroxide
H_2S	hydrogen sulphide
HC030031	2-(1,3-Dimethyl-2,6-dioxo-1,2,3,6-tetrahydro-7H-purin-7-yl)-N-(4-isopropylphenyl)acetamide
HCl	hydrochloride acid
HEK293	human embryonic kidney 293 cells
HRP	horseradish peroxidase
hTRPA1	human transient receptor potential ankyrin-1
i.p.	intraperitoneal
i.pl.	intraplantar
i.v.	intravenous
IB4	isolectin B4
iNOS	inducible nitric oxide synthase
IP_3	inosotal triphosphate
IRES	internal ribosome entre site
JP1302	N-[4-(4-Methyl-1-piperazinyl)phenyl]-9-acridinamine
K_{ATP}	ATP sensitive potassium channels
KO	knockout
L-NAME	NG-Nitro-L-arginine methyl ester
LTB_4	leukotriene B4
MLC	myosin light chain
MLCP	myosin light chain phosphatase

MnTMPyP	manganese(III) tetrakis(1-methyl-4-pyridyl)porphyrin
mRNA	messenger ribonucleic acid
mTRPA1	mouse TRPA1
MW	molecular weight
NaCl	sodium chloride
NADPH	nicotinamide adenine dinucleotide phosphate-oxidas
$NaH_2PO_4H_2O$	monosodium phosphate
$NaHCO_3$	sodium bicarbonate
NaHS	sodium hydrosulphide
NANC	non-adrenergic non-cholinergic
$NaPO_4$	sodium phosphate
NAV1.2	voltage gated sodium channel type II
NET	noradrenaline transporter
NFkb	nuclear factor kappa-light-chain-enhancer of activated B cells
NGF	nerve growth factor
NK_1	neurokinin-1
NMDA	N-methyl-D-aspartate
nNOS	neuronal nitric oxide synthase
NOMPC	no mechanoreceptor potential C
NOS	nitric oxide synthase
NOX2	NADPH oxidase 2
NOX4	NADPH oxidase 4
PBS	phosphate buffered saline
PCR	polymerase chain reaction
PET	positron emission tomography
PGE_2	prostaglandin E2
PGJ_2	prostaglandin J2
PIP_2	phosphatidylinositol 4,5-bisphosphate
PKA	protein kinase A
PKC	protein kinase C
PLC	phospholipase C
p-MLC	phosphorylated myosin light chain
Pvdf	polyvinylidene fluoride
qRT-PCR	quantitative real-time polymerase chain reaction
RAMP1	receptor activity modifying protein 1
RCP	receptor component protein
Rho-kinase/ROCK	rho-associated kinase
rhTRPA1	rhesus mokey transient receptor potential ankyrin-1
RNA	ribonucleic acid
ROI	region of interest

ROS	reactive oxygen species
rpm	revolutions per minute
rTRPA1	rat tranient receptor potential ankyrin-1
s.c.	subcutaneous
S.E.M.	standard error of mean
SB366791	4'-chloro-3-methoxycinnamanilide
SDS	sodium dodecyl sulfate
SMTC	s-methyl-L-thiocitrulline
SNI	spared nerve injury
SNS	sympathetic nervous system
SOD	superoxide dismutase
SR140333	1-[2-[(3S)-3-(3,4-Dichlorophenyl)-1-[2-[3-(1-methylethoxy)phenyl]acetyl]-3-piperidinyl]ethyl]-4-phenyl-1-azoniabicyclo[2.2.2]octane chloride
TAC-1	protachykinin-1
TBE	tris/borate/ethylenediaminetetraacetic acid
TBS	tris-buffered saline
TCS5861528	2-(1,3-Dimethyl-2,6-dioxo-1,2,3,6-tetrahydro-7H-purin-7-yl)-N-[4-(1-methylpropyl)phenyl]acetamide
TEMED	tetramethylethylenediamine
Tempol	1-Oxyl-2,2,6,6-tetramethyl-4-hydroxypiperidine
Thr	threonine
TRP	transient receptor potential
TRPA1	transient receptor potential anyrin-1
TRPC	transient receptor potential canonical
TRPM8	transient receptor potential melatonin 8
TRPML	transient receptor potential mucolipin
TRPP	transient Receptor Potential Polycystic
TRPV	transient Receptor Potential Vanilloid
UV	ultraviolet
WT	wild-type
Y27632	trans-4-[(1R)-1-Aminoethyl]-N-4-pyridinylcyclohexanecarboxamide

Table of Contents

List of Figures

List of Tables

Chapter 1 – Introduction

Chapter 1 – Introduction

1 Introduction

The stimulation of primary sensory neurons releases neuropeptides such as substance P and calcitonin gene-related peptide (CGRP), which are the main initiators of neurogenic-dependent vasodilatation in the peripheral vasculature (Holzer, 1992, Lembeck and Holzer, 1979, Brain et al., 1985). Although sensory neurons are known to have a physiological role in maintaining vascular haemostasis, the exact mechanism is unknown. The discovery of transient receptor potential ankyrin-1 (TRPA1), which is located on 60-75% of transient receptor potentials vanilloid-1 (TRPV1) expressing sensory neurons, has dramatically increased our understanding of the role of the sensory neurons in mediating vascular responses. Previous studies in our group have demonstrated a role of TRPA1 in regulating peripheral blood vessel tone using exogenous TRPA1 agonists such as mustard oil and cinnamaldehyde and, the endogenous agonist 4-oxononenal (4-ONE) via sensory neuropeptide-dependent mechanisms (Grant et al., 2005, Pozsgai et al., 2010, Graepel et al., 2011, Fernandes et al., 2011).

TRPA1 also acts as a polymodal membrane receptor for cold sensitivity (Story et al., 2003). Local cold exposure in mammals is known to lead to an initial cutaneous vasoconstrictor response, which acts to protect against excessive heat loss, and this is followed by a vasodilation phase, which protects against cold-induced injury in the periphery. Although the exact underlying mechanisms of this cold phenomenon remains unclear, sensory and sympathetic nerves have been proposed to play a prominent role. TRPA1 is activated at low temperatures but this remains a controversial issue as there are other cold sensitive TRP channels, such as the transient receptor potentials melastatin-8 (TRPM8). It is currently unknown whether TRPA1 acts a primary vascular cold sensor. Hence, in this study I investigated the vascular effects of TRPA1 activation *in vivo* using an exogenous agonist cinnamaldehyde in the mouse ear model and delineated the downstream mechanisms underlying the vasodilator response. Following on from this evidence, I further studied the role of TRPA1 as a primary vascular cold sensor by developing a local cold model in the mouse hindpaw *in vivo* and progressed on validating the potential protective role of TRPA1 in preventing against cold-induced injury in the peripheral vasculature.

To introduce this subject, this chapter will discuss the role of sensory neurons in mediating neurogenic-dependent vasodilatation, the current known vascular effects of TRPA1 and cold-induced vascular responses.

1.1 Innervation of skin vasculature

Several humoral meditators and the nervous system influence the vasomotor tone of cutaneous blood vessels. The sympathetic nervous system (SNS) innervation in the periphery is facilitated by pre- and post-ganglionic neurons. The pre-ganglionic neurons are known to originate from the thoracolumbar regions of the spinal cord (T1-L2), project to a ganglion such as the superior cervical ganglion and synapse with a post-ganglionic neuron which innervate the entire periphery (Arunodaya and Taly, 1995). It is well established that cutaneous nerves such as efferent autonomic sympathetic nerves and afferent non-adrenergic non-cholinergic (NANC) nerves innervating blood vessels can influence the control of skin temperature and blood flow. The autonomic nervous system (ANS) is a complex system, which consists of parasympathetic and sympathetic nerves that transmit their impulses to the effector via the neurotransmitters acetylcholine and noradrenaline/norepinephrine, respectively to respond to the stimuli. This response is known to be controlled by feedback and feedforward loops between various regions of the brain. The sympathetic division of the ANS is known to form distinct pathways, where the neural branch comprising the sympathetic nerve terminals innervate primarily the cardiovascular system and the sympathetic adrenal medullary branch releases catecholamines to target tissues and organs expressing adrenergic receptors (Kuntz and Hamilton, 1938, Brain, 1996).

The NANC nerves include peripheral sensory neurons that are polymodal and are found mainly close to the capillaries (Nelms, 1963). They can detect various external stimuli such as chemicals, temperature and pressure, and transmit the signal to the dorsal root ganglion (DRG) or to the trigeminal ganglia into the spinal cord, where the electrical impulse is then transmitted into the brain (ascending pathways). The cell bodies of the DRG produce neurotransmitters, neuropeptides and neurotrophic factors which are transported to both peripheral and central terminals (Bayliss, 1901).

1.1.1 Noradrenergic neurons

Small arteries and arterioles, and arteriovenous anastomoses (AVAs) are supplied with a dense innervation of noradrenergic neurons, which also innervate dermal smooth muscle and sebaceous glands in the cutaneous beds of fingers and toes (Norberg, 1964, Weihe and Hartschuh, 1988). Noradrenaline released from sympathetic nerves is known to be a potent vasoconstrictor in the microvasculature and continuous intravenous (*i.v.*) infusion of noradrenaline can lead to intermittent constriction of arterioles, further arresting flow in the nail bed capillaries (Greishman, 1954). Noradrenaline is known to stimulate α_1-adrenergic receptors on vascular smooth muscle cells in the skin, whilst both α_1- and α_2-adrenergic receptors have

been shown to be expressed in the hand vasculature (Coffman and Cohen, 1988). α-adrenergic receptors are known to be less sensitive to adrenaline (Ahlquist, 1948). Stimulation of α-adrenergic receptors of the vessel wall predominantly results in vasoconstriction or vasodilation depending on the site of action, whilst stimulation of β-adrenergic receptors leads to vasodilatation. Sympathetic neurons can form direct pathways through pre- and post-ganglionic nerves in the thoracic and lumbar spine area, which project and secrete acetylcholine locally, or to postganglionic motor nerves, and further stimulate noradrenaline activity on receptor sites. Apart from a role in vasoactive responses, noradrenaline is involved in cardiovascular effects such as increasing heart rate and cardiac contractility. Noradrenaline is known to be synthesised from the precursor tyrosine, which is actively transported into the varicosity of the postganglionic sympathetic nerve endings and packed into synaptic vesicles to be released following an action potential down the nerve endings (Eisenhofer et al., 2004).

1.1.2 Cholinergic neurons

Acetylcholine is known to be found in the skin in neuronal sites and endothelial cells (Parnavelas et al., 1985). Interestingly, electrical stimulation of the cat foot pad was shown to evoke sweat secretion and acetylcholine release in the venous effluent (Dale and Feldberg, 1934). Although the cholinergic nerve supply to the skin has been reported to be sparse, acetylcholinesterase has been shown to be localised with some nerves and acetylcholine receptors are found on cutaneous blood vessels. Hence, this suggests some involvement of cholinergic nerves in the cutaneous vasculature (Hurley and Mescon, 1956). Activation of parasympathetic nerves is known to result in vasodilatation. Acetylcholine is rapidly degraded and recycled and hence, investigating the biochemical activity of the parasympathetic nervous system branch can be challenging (Hurley and Mescon, 1956).

1.1.3 Non-adrenergic, non-cholinergic neurons

Earlier studies in 1880s showed that the nerves originating from the DRG release a vasodilator in the peripheral vasculature, in addition to transmitting information to the central nervous system (CNS) (Bayliss, 1901). Electrophysiological studies have demonstrated that there are different types of cutaneous afferent nerve endings which are encapsulated by a non-neural structure or a bare nerve ending, arising from the cell bodies of primary afferent nerve fibres in the DRG, and in the nodose and jugular ganglia, and can innervate peripheral tissues including cutaneous blood vessels (Perry and Lawson, 1998, Bennett et al., 1996). DRG neurons with encapsulated terminals sense the stimulus and mediate touch and pro-nociception, via rapidly conducting large-diameter, myelinated (Aα or Aβ) axons to the spinal cord, whilst DRG

neurons with bare nerve endings mediate painful or thermal sensations via slowly conducting small-diameter, unmyelinated (C-fibres afferents) or thinly myelinated (Aδ-fibres afferents) axons to the spinal cord. The proportions of C-, Aδ- and Aβ-fibres innervating the skin vary (70, 10 and 20%, respectively) and all three types of fibres can transmit non-nociceptive information under normal conditions. On the other hand, C- and Aδ-fibres can transmit nociceptive information (Millan, 1999).

There are different classes of Aδ- and C-fibres, and their characterisation has been reported to be complicated by several factors such as (1) terminological inconsistencies, (2) species differences and (3) glabrous or non-glabrous skin (Millan, 1999). There are two types of Aδ-fibres; type I Aδ-fibres consist of high threshold, rapidly-conducting mechanoreceptors that respond weakly to high intensity heat and cold stimuli (Treede and Magerl, 1995), whilst type II Aδ-fibres display a lower threshold to noxious heat stimuli (Treede et al., 1990, Treede et al., 1991). Type II Aδ-fibres are also more responsive to cooling than mechanical stimuli, as shown in studies using positron emission tomography (PET) in human brain (Craig et al., 1996). Upon exposure of the skin to a noxious stimulus, Aδ-fibres elicit a rapid first phase of pain which is commonly 'sharp' in nature and this is followed by a second wave of dull pain, mediated by C-fibres (Treede et al., 1992).

C-fibres are classified functionally or anatomically, where functionally they are polymodal and can respond to all or a subset of noxious stimuli such as thermal, mechanical and chemical (Caterina and Julius, 2001). Anatomically, one population of C-fibres is known to be regulated by nerve growth factor (NGF) and constitutively synthesises the neuropeptides CGRP and substance P, whilst the other population is non-peptidergic, with binding sites for the isolectin B4 (IB4). However, there is now evidence showing that IB4-positive neurons can also express CGRP and substance P, but the functional relevance of this finding is unknown (Hwang et al., 2005). The role of C-fibres in mediating the 'axon-flare response' is a component of neurogenic inflammation following nerve injury and has been widely documented (Schmidt et al., 1995, Lewis, 1927). Neurogenic inflammation is characterised by neuropeptide-induced oedema formation, increase in blood flow and recruitment of inflammatory cells (Jancso et al., 1967).

Earlier studies by Lewis showed that skin injury leads to (1) antidromic stimulation of sensory neurons with cutaneous vasodilatation, also known as an 'axon reflex flare', and (2) orthodromic stimulation of sensory neurons where there is orthodromic transmission of impulses to the spinal cord via connecting nerves to adjacent skin (Lewis, 1927). The role of sensory neurons in mediating antidromic stimulation was also shown by Jancso (1940) using the pungent extract of hot chilli peppers, capsaicin (Jancso et al., 1967). Capsaicin has been widely

used as a pharmacological tool to study sensory nerves and their contribution to neurogenic inflammation. Antidromic stimulation of sensory neurons consists of local depolarisation of the neuronal terminal and axon reflexes to evoke neuropeptide release which causes cutaneous vasodilatation (Jancso et al., 1967), leading to neurogenic inflammation. This vasodilator response was shown to be abolished by removal of afferent nerves from the dorsal root, causing degeneration of the peripheral nerve fibres rather than the disruption of the dorsal root between the ganglia and the spinal cord (Bayliss, 1901).

Langley (1923) and Lewis (1927) studied the physiological role of the antidromic vasodilation, which is described by three cardinal signs of inflammation termed as the 'triple response' which includes (1) redness due to local dilation of the minute cutaneous vessels, (2) flare due to widespread dilation of neighbouring arterioles and (3) wheal as a result of a local increase in blood vessels permeability (Figure 1.2) (Langley, 1923, Lewis, 1927). Following this theory, a number of studies focused on identifying the mediators responsible for this response; substance P (also called preparation P) and CGRP were later recognised as vasodilators (US and Gaddum, 1931, Lembeck, 1953, Brain et al., 1985). It is established that both these neuropeptides are localised in the peripheral endings of sensory neurons and stimulation of these neurons can lead to their release. This suggests that these mediators are involved in controlling local vascular tone and are the main initiators of neurogenic inflammation (Lundberg et al., 1985, Levine et al., 1984, Maggi and Meli, 1988, Holzer, 1992).

1.1.3.1 Calcitonin gene-related peptide

CGRP is a neuropeptide with 37-amino acid residues and was identified through molecular biological studies of the ageing rat (Amara et al., 1982, Amara et al., 1984). Although the calcitonin gene encodes for CGRP, alternate messenger ribosomal nucleic acid (mRNA) processing of the gene leads to producing CGRP in nervous tissue and calcitonin in the thyroid of the healthy subjects (Edbrooke et al., 1985). There are two isoforms of CGRP; α-CGRP and β-CGRP which are synthesised from two distinct genes at different sites on chromosome 11 in human (Wimalawansa et al., 1990) and share >90% homology with similar biological activities (Morris et al., 1984). α-CGRP is thought to be found mainly in the central and peripheral nervous system, whilst β-CGRP is more localised in the enteric nervous system (Brain, 1997). α-CGRP mRNA expression has been shown to be predominantly expressed in peptidergic nerves innervating skin, with little β-CGRP mRNA expression (Mulderry et al., 1988, Noguchi et al., 1990). However, there is now evidence using quantitative reverse transcription polymerase chain reaction (qRT-PCR) showing that epidermal keratinocytes also express β-

CGRP, with increased α-CGRP expression in sensory neurons (Hou et al., 2011). The role of β-CGRP in mediating vascular responses is yet to be investigated.

CGRP is known to act on $CGRP_1$ and $CGRP_2$ receptors to exert its biological effects, and it is important to note that the existence of both receptors have been debated for a number of years. It is generally now believed that CGRP-mediated effects are achieved through activation of $CGRP_1$ receptors (Dennis et al., 1989, Smillie and Brain, 2011). The CGRP receptor complex consists of ligand-binding protein calcitonin receptor-like receptor (CRLR), an accessory protein with a single transmembrane-spanning domain named receptor activity-modulating protein (RAMP1). RAMP1 is involved in trafficking CRLR to the cell surface membrane and produces pharmacological activity. Lastly, a peripheral membrane accessory protein termed CGRP-receptor component (RCP) couples to CRLR /RAMP1 to mediate the cellular signalling pathway (Figure 1.1) (Evans et al., 2000, Luebke et al., 1996, McLatchie et al., 1998, Prado et al., 2001).

The mechanisms underlying CGRP-induced responses have been reported to be tissue-specific (Brain, 1997). CGRP activates its receptors on arteriolar smooth muscles and endothelial cells to cause vasodilatation through endothelium-dependent and endothelium-independent mechanisms (Brain and Cox, 2006). The endothelium-independent vasodilator responses to CGRP are induced by an increase in intracellular cyclic adenosine monophosphate (cAMP) via adenylyl cyclase in vascular smooth muscle cells and cardiomyocytes (Tang et al., 1989). cAMP can further phosphorylate protein kinase A (PKA) and open ATP-sensitive potassium (K_{ATP}) channels, to mediate relaxation, as demonstrated using the K_{ATP} channel blocker glibenclamide in isolated rabbit mesenteric arteries (Figure 1.2) (Nelson et al., 1990).

Furthermore, CGRP is known to exert endothelium-dependent vasodilator responses where it was demonstrated to have nitric oxide-dependent vasodilator properties in foetal and peripheral vascular beds (Thakor and Giussani, 2005). In the presence of the endothelium, there is a significant increase in both cAMP and cyclic guanosine monophosphate (cGMP) which may lead to the release of nitric oxide from the endothelium (Gray and Marshall, 1992c, Gray and Marshall, 1992b), causing a relaxation in smooth muscle cells through soluble guanylyl cyclase (sGC) activation and cGMP accumulation (Gray and Marshall, 1992a). CGRP is also known to mediate its effects by activating endothelial nitric oxide synthase (eNOS) via the cAMP-PKA pathway.

CGRP has potent dilator properties in cerebral, coronary and kidney vascular beds with approximately 10-fold higher potency than prostaglandins and 10-100 fold higher potency than

acetylcholine and substance P. Intradermal (*i.d.*) administration of CGRP into the skin has been shown to cause erythema which lasts for 5-6 hours in human skin (Brain et al., 1986). CGRP is known to have a prominent role in decreasing blood pressure in both normotensive and hypertensive rats, in a nitric oxide-dependent and independent pathway, as shown in peripheral arterial vessels (Itabashi et al., 1988). CGRP acts as a vasodilator when given systemically to either healthy subjects or cardiovascular disease patients (Gennari and Fischer, 1985, Preibisz, 1993).

In terms of the cardiovascular properties of CGRP, basal blood pressure was shown to be similar in α-CGRP knockout (KO) and wild-type (WT) mice, which suggests that CGRP may not be involved in normal regulation of blood pressure (Lu et al., 1999). However, there are conflicting views in the literature depending on the type of α-CGRP KO mice used in these studies (Smillie and Brain, 2011). Injection (*i.v.*) of CGRP has also been shown to cause a vasodilator response with positive inotropic and chronotropic responses (Gardiner et al., 1991, Ando et al., 1990). Animal and human studies have shown that injection (*i.v.*) of CGRP causes peripheral vasodilation and hypotension (Ganten et al., 1991). This is supported by *in vitro* studies where CGRP causes dilatation of major resistance arterioles (Uddman et al., 1986).

CGRP receptor peptide antagonists were generated by removing the ring structure at the CGRP N-terminus, and have been widely used to understand the role of CGRP and its receptor. The peptide fragment $CGRP_{8-37}$ (Chiba et al., 1989) and the non-peptide compound BIBN4096BS (Doods et al., 2000) are two commonly used CGRP receptor antagonists that have been characterised in our group to understand the role of CGRP in mediating neurogenic inflammation (Grant et al., 2005, Grant et al., 2002, Starr et al., 2008). $CGRP_{8-37}$ was demonstrated to inhibit CGRP-induced vasodilatation in human forearm without affecting resting forearm blood flow (Vanmolkot et al., 2006). BIBN4096BS is known to have a greater affinity than $CGRP_{8-37}$ and it was shown to inhibit CGRP-induced cAMP levels, without any agonist activity at a concentration up to 10μM (Doods et al., 2000). Both CGRP receptor antagonists will be used later on in this project and further discussed to elucidate their role in neurogenic-dependent vasodilation in the peripheral vasculature.

The vasodilator properties of CGRP are well established in the literature. Furthermore, the plasma levels of CGRP were shown to be elevated in migraine patients and CGRP receptor antagonists may have the potential to be a major advancement in migraine therapy (Salvatore and Kane, 2011). It is generally believed that CGRP is released upon sensory nerve stimulation but there is now new evidence showing that non-neuronal cells such as endothelial cells also express or release CGRP (Fang et al., 2011). Studies over the last decade has focussed on

examining how CGRP is released from the nerve terminals and which receptors are expressed on the nerve terminals, to further elucidate the function of CGRP in the vasculature.

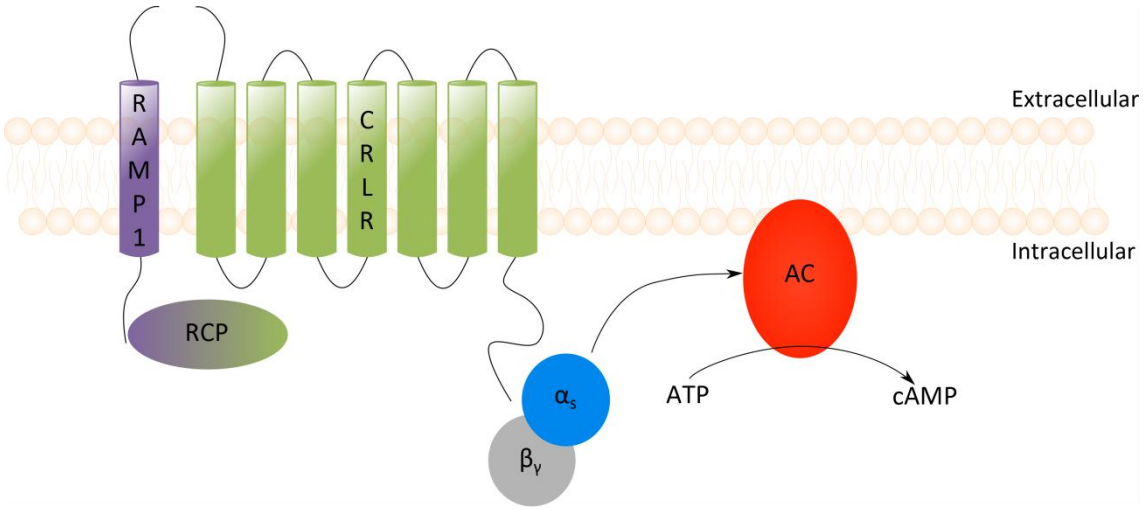

Figure 1.1 Model for functional CGRP receptor. The CGRP receptor complex consists of the seven transmembrane ligand binding protein CRLR, a small single transmembrane protein RAMP1 for trafficking and pharmacology and, an accessory protein RCP for coupling to cellular transduction pathways. This is mainly through Gαs and AC, resulting in elevating cAMP levels. Abbreviations: AC-adenylyl cyclase, cAMP-cyclic adenosine monophosphate, CRLR-calcitonin receptor-like receptor, Gαs-Gs protein, Gβγ-Gβ protein RAMP1- receptor activity modifying protein 1, RCP-receptor component protein.

1.1.3.2 Substance P

The stimulation of sensory neurons is also known to release substance P, which belongs to the tachykinin family of peptides (Euler and Nilsson, 1931, Chang et al., 1971). Substance P is synthesised within the neuronal cell bodies in the DRG (Harmar et al., 1981), and further transported via retrograde axonal transport to the release sites at the nerve endings or within the dorsal horn of the spinal cord (Reilly et al., 1997). There is evidence showing that CGRP is co-localised with substance P within the sensory nerves (Ribeiro-da-Silva and Hokfelt, 2000). Interestingly, substance P is also found in some sympathetic neurons (Kessler et al., 1983, Roach et al., 1987) and parasympathetic neurons innervating the salivary glands (al-Hadithi et al., 1988). Furthermore, substance P protein is localised in non-neuronal cells such as endothelial cells, as shown by electron and light microscope in coronary artery, brain microvessels and rat femoral and mesenteric arteries, (Milner et al., 1989, Milner et al., 1995,

Loesch and Burnstock, 1988) and, mRNA expression by qRT-PCR in human dermal skin (Milner et al., 2004).

Substance P is known to regulate its own release from primary sensory neurons via activation of neurokinin-1 (NK_1) receptors (Tang et al., 2007), and exerts its effects downstream via activation of phospholipase C (PLC) which hydrolyses the phospholipid PIP_2 to release DAG and IP_3(Nakajima et al., 1992, Burgess et al., 1984). IP_3 is known to stimulate calcium release from intracellular stores (Burgess et al., 1984) and DAG activates protein kinase C (PKC) (Figure 1.2) (Berridge and Irvine, 1984). Substance P has also been shown to trigger calcium mobilisation and cAMP accumulation downstream of NK_1 receptor activation (Sagan et al., 1996). Additionally, substance P is known to induce activation of ERK1/2 and p38 mitogen-activated protein (MAP) kinases, nuclear factor-kappa B (NFKβ) and PKC, increasing prostaglandin E_2 (PGE_2) production and COX2 expression (Fiebich et al., 2000, Ebner and Singewald, 2006, Koon et al., 2006).

Substance P has a prominent role in mediating neurogenic inflammation and in transmitting pain information to the CNS. Substance P-induced vasodilation via activation of NK_1 receptors on the endothelium is dependent on nitric oxide release in human coronary arteries (Bossaller et al., 1992). Indeed, substance P-induced local axon reflex erythema was shown to be significantly reduced by L-NAME. However, substance P-induced vasodilatation has been reported to decline during continuous infusion as a result of internalisation of NK_1 receptors (Wong et al., 2005). In the microvasculature, activation of NK_1 receptors on endothelial cells can lead to an increase in vascular permeability (Lembeck et al., 1992, Emonds-Alt et al., 1993) and initiation of plasma extravasation indirectly, through activation of mast cells (Foreman and Jordan, 1983, Coleman et al., 1986). Interestingly, substance P also has contractile effects on smooth muscle located in the intestines, airways, urinary system, uterus and other organs (Maggi et al., 1987, Maggi and Meli, 1988).

Substance P was first shown *in vivo* to decrease blood pressure in rabbit(Euler and Nilsson, 1931) and this response is dependent on vasodilatation mediated through the activation of NK_1 receptors (Maggi et al., 1987, Couture et al., 1989). However, activation of sensory C-fibres can cause mesenteric resistance arteries myogenic constriction via the release of substance P, which acts on post-junctional NK_1 receptors on vascular smooth muscle cells (Bayliss, 1901, Scotland et al., 2004). The pharmacological blockade of NK_1 receptors may hence be a novel therapeutic pathway to target in cardiovascular diseases where there is an altered myogenic responsiveness such as hypertension (Dunn et al., 1998, Izzard et al., 1996) and diabetes (Schofield et al., 2002, Scotland et al., 2004).

The availability of transgenic NK_1 receptor mice or selective NK_1 receptors antagonists has facilitated the research on the tachykinin system. Substance P-induced sensitivity to chemical pain (Cao et al., 1998) and oedema (Cao et al., 1999) were shown to be significantly decreased in NK_1 KO mice. CP-96345 was the first NK_1 receptor antagonist developed and was shown to be highly selective, orally active and stable *in vivo* (Snider et al., 1991). It was shown to inhibit plasma extravasation in rat hind paw caused by mustard oil or by stimulation of the saphenous nerve (Lembeck et al., 1992). The NK_1 receptor antagonist SR140333 has been widely used and was first demonstrated to inhibit substance P-induced hypotension in dogs, bronchoconstriction in guinea-pigs and plasma extravasation in rats (Emonds-Alt et al., 1993). Additionally, the compound SR140333 has also been used in our group to study neurogenic inflammation in the cutaneous vasculature following the topical application of capsaicin and mustard oil (Grant et al., 2002, Grant et al., 2005). It is important to note that although NK_1 receptor antagonists were proven to be effective in many animal models of inflammation, they failed to show efficacy in several clinical trials for pain (Pettitt et al., 2000), but prevented both acute and delayed chemotherapy-induced nausea and vomiting (Hargreaves et al., 2011). The effects of SR140333 on blood flow responses are studied later in the project to elucidate the mechanisms underlying neurogenic-dependent vasodilatation.

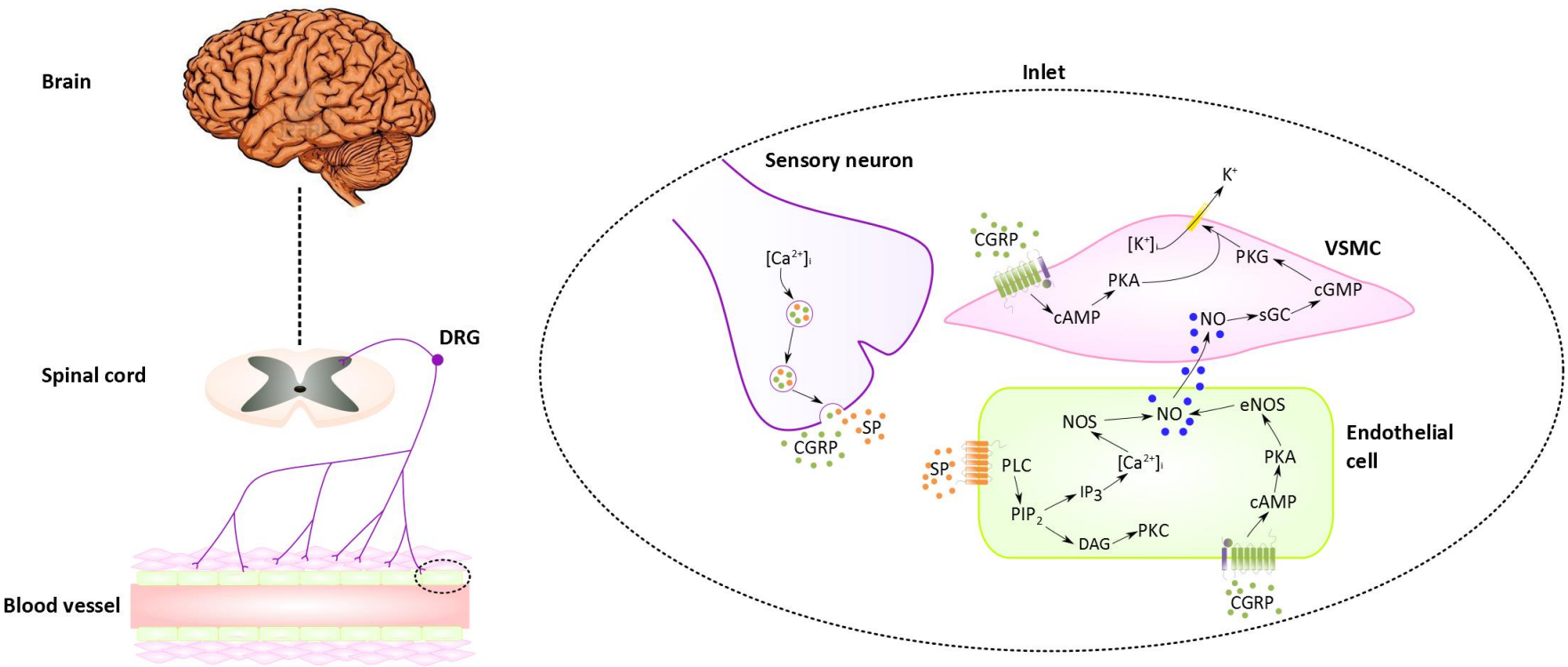

Figure 1.2 Schematic diagram representing neurogenic inflammation in the cutaneous vasculature Stimulation of the sensory nerve results in an electrical impulse being transmitted towards the spinal cord to the brain for pain transduction and an axon reflex to the peripheral vasculature where CGRP and SP are released from the nerve terminals acting on the arterioles, mediating vascular changes. CGRP can mediate its effects by binding to its receptor complex on the VSMC and mediate relaxation via the opening of K^+ channels on VSMC and in a NO-dependent manner in the endothelial cell. SP binds to neurokinin-1 (NK_1) receptor on the endothelial cell to mediate relaxation via the release of NO. Abbreviations: cAMP, cyclic adenosine monophosphate; cGMP, cyclic guanosine monophosphate; CGRP, Calcitonin gene-related peptide; DAG, diacylglycerol; DRG, dorsal root ganglion; IP_3, inositol triphosphate; NO, nitric oxide; NOS, nitric oxide synthase; PIP_2, phosphatidylinositol 4,5-bisphosphate; eNOS, endothelial NOS; PLC, phospholipase C; PKA, protein kinase A; PKC, protein kinase C; PKG, protein kinase G; SP, substance P; VSMC, vascular smooth muscle cell.

1.2 Transient receptor potential channels

TRP channels were first discovered in mutant Drosophila by Cosens and Manning (1969) and the identity of the mutated protein was cloned twenty years later (Cosens and Manning, 1969, Montell and Rubin, 1989). Using whole-cell recordings from Drosophila photoreceptors, Hardie and Minke further presented evidence that TRP consisted of an ion channel which opened in response to light stimulation (Hardie and Minke, 1992). TRP channels, a family of non-selective cation-permeable channels, are widely expressed in mammalian tissues and have six transmembrane regions, with a pore loop domain between the fifth and sixth transmembrane(Ramsey et al., 2006). The family is currently composed of 29 channels with seven subfamilies; including canonical (TRPC), vanilloid (TRPV), ankyrin (TRPA), melastatin (TRPM), polycystin (TRPP), no mechanoreceptor potential C (NOMPC) and mucolipin (TRPML) (Nassenstein et al., 2008). TRP channels have multiple functions as chemosensors in cells and are also involved in pain sensation and inflammatory diseases (Nilius, 2007). They respond to a great number of stimuli; such as natural chemical compounds, cold or hot temperatures, changes in lipid bilayer and are stimulated by mechanical stimuli as well as endogenous inflammatory mediators (Minke, 2006).

Capsaicin, a pungent chemical of chilli peppers at low doses has been shown to activate unmyelinated sensory C-fibres rather than myelinated Aδ-fibres on guinea-pig airways (Emery et al., 1983). Hence, capsaicin has been used to study the properties and functions of unmyelinated C-fibre afferents (Holzer, 1991, Kirchmair et al., 1994). Consequent studies have focussed on investigating the receptors expressed on the capsaicin-sensitive primary sensory neurons and these findings led to the discovery of neuronal TRP channels. TRPV1 is activated by capsaicin and capsaicin-induced nociception was significantly impaired in TRPV1 KO mice (Caterina et al., 1997, Caterina et al., 1999, Caterina et al., 2000).

1.3 Transient receptor potential ankyrin-1 (TRPA1)

1.3.1 Structure of TRPA1

TRPA1 is a non-selective cation channel, also known as the ankyrin like protein with six transmembrane domains, or the 'wasabi' receptor (Cordero-Morales et al., 2011). It is the only member of the TRPA subfamily and was first discovered by Jaquemar *et al*. (1999) as a 'transformation-sensitive' mRNA in cultured human lung fibroblasts (Jaquemar et al., 1999).

The long cytoplasmic N-terminal of TRPA1 consists of 18 ankyrin repeats and specific cysteine residues, which can undergo covalent modifications upon binding of electrophilic agonists, ultimately activating the channel (Figure 1.3) (Macpherson et al., 2007, Chung and Caterina, 2007). The N-terminal cysteine residues are involved in electrophilic activation by thiol-reactive compounds, which leads to altered interactions between subunits and promote conformational changes, thereby modifying the gating mechanism (Cvetkov et al., 2011, Wang et al., 2012). Deletion of these ankyrin repeats has been shown to negatively affect insertion of the channel into the plasma membrane (Nilius et al., 2011). The ankyrin motifs consist of 33 amino acid residues made up of anti-parallel α-helix-loop-α-helix-loop-β loop structures (Mosavi et al., 2004), which have presently been proposed to play a role in the mechanosensation of cutaneous Aβ-sensory fibres (Kwan et al., 2009) and vestibular functions of inner hair ear cells (Corey et al., 2004, Nagata et al., 2005).

There is also a canonical calcium-binding EF-hand domain on the N-terminal, which may regulate channel opening by Ca^{2+} ions (Zurborg et al., 2007). TRPA1 was previously reported to be permeable to both Na^{+} and Ca^{2+} ions, suggesting that it is non-selective cation channels (Story et al., 2003, Wang et al., 2008b). However, it has been recently shown to have greater calcium permeability than other ions, with P_{Ca}/P_{Na} of 0.8 (Karashima et al., 2010).

The TRPA1 protein is made up of approximately 1100 amino acids, with molecular size of 120-130 kDa. It is known to function as a homotetramer, composed of four identical TRPA1 subunits of TRPA1 proteins. The human TRPA1 gene consists of 27 exons and spans 55701 base pairs of the human chromosome 8q13, and is present in many vertebrates and invertebrates such as mouse, rat, dog, chicken, zebrafish, fruitfly and *Caenorhabditis elegans* (Nilius et al., 2012). Mammals are known to contain one TRPA1 gene, whilst other classes of the Animalia Kingdom contain multiple TRPA1 homologues (Nilius et al., 2012). All electrophile-sensitive TRPA1 is derived from a common ancestor of both vertebrates and invertebrate. Hence, the essential structures and properties of TRPA1 have been conserved for more than 500 million years (Kang et al., 2010).

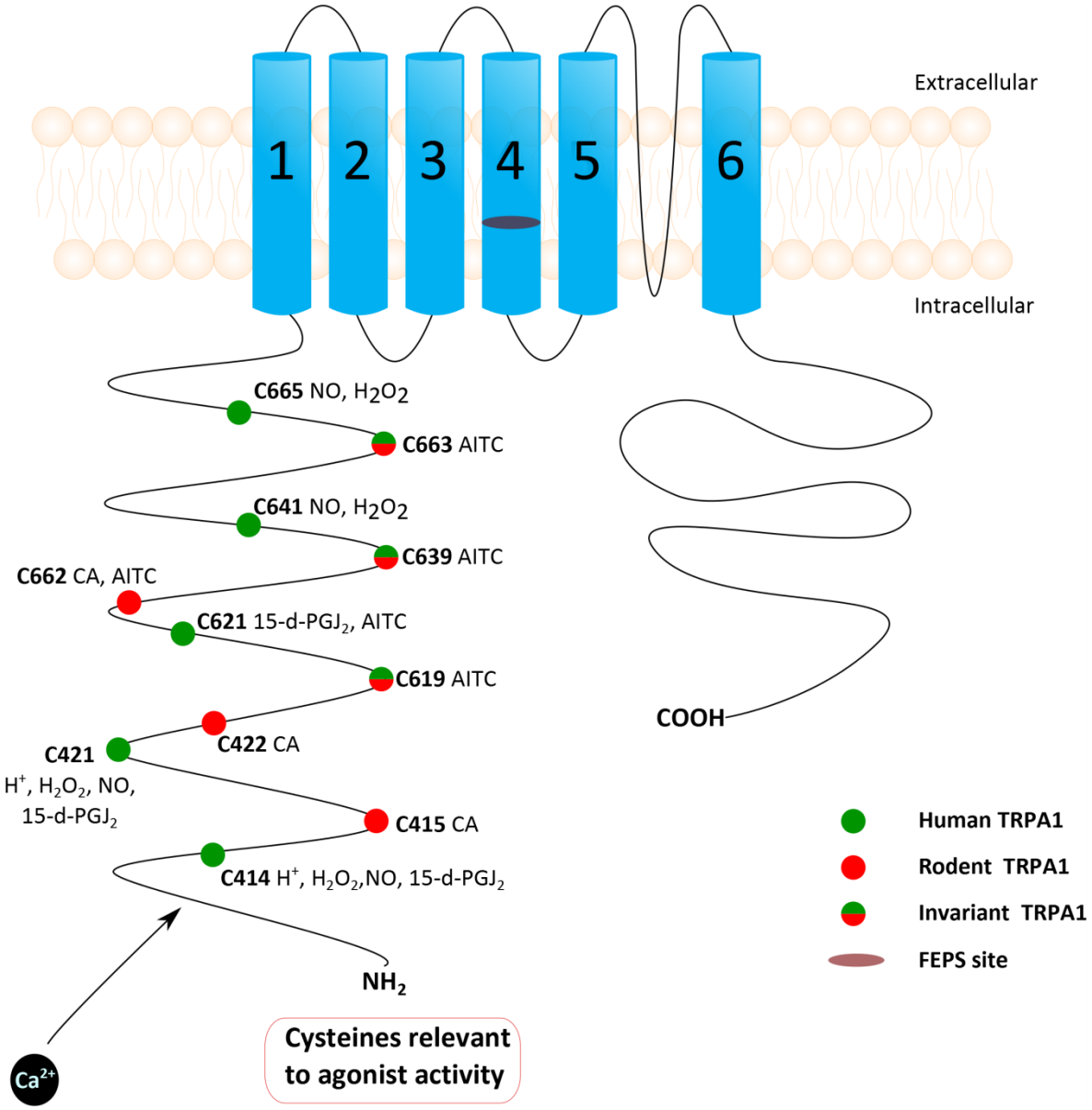

Figure 1.3 Structure and agonist activity of TRPA1 channelTRPA1 channel consists of six transmembrane domains and intracellular N- and C-terminus. The long cytoplasmic N-terminus has ankyrin repeat and EF-hand domains. Common agonists activate TRPA1 by covalent modification of cysteine residues located on the N-terminus of the channel. The schematic diagram summarises the identified residues important for the receptor activation for relevant species. Other putative binding/modulatory sites that regulate TRPA1 channel activity include calcium binding to the EF-hand domain and the familial episodic pain syndrome (FEPS) mutation. Diagram adapted from Bodkin & Brain (2010). Abbreviations: 15-d-PGJ_2, 15-d-prostaglandin J_2; AITC, allyl isothiocyanate, Ca^{2+}, calcium; CA, cinnamaldehyde; H_2O_2, hydrogen peroxide; NO, nitric oxide; TRPA1, transient receptor potential ankyrin-1.

1.3.2 Expression of TRPA1

TRPA1 was originally discovered in sensory neurons of DRG, trigeminal, vagal, jugular and nodose ganglion, and the inner ear (Bautista et al., 2005, Garcia-Anoveros and Nagata, 2007, Story et al., 2003). However, TRPA1 is now known to be expressed in multiple organs and tissues such as heart, small intestine, lung, skeletal, pancreas, brain and muscle (Stokes et al., 2006). The expression of TRPA1 has been demonstrated in the CNS, in neurons of the nucleus supraopticus and at presynaptic terminals to the magnocellular neurosecretory cells, and its activation has been shown to enhance glutamate release in the CNS (Yokoyama et al., 2011, Lee et al., 2012). TRPA1 expressed on astrocytes contribute to basal calcium levels and is involved in releasing signalling molecules such as D-serine into the extracellular space, further leading to N-methyl-D-aspartate (NMDA) receptor-dependent hippocampal long-term potentiation (Shigetomi et al., 2013). The role of TRPA1 in the CNS is to facilitate transmission of intense peripheral mechanical stimulus to the spinal cord (McGaraughty et al., 2010).

There is also evidence of TRPA1 being located in the ANS, where the sympathetic superior cervical ganglia was shown to express functional TRPA1 on cold-sensitive neurons (Smith et al., 2004). Additionally, TRPA1 is known to be widely expressed in peripheral tissues, as shown in mouse paw, sciatic nerve and spinal cord (Andrade et al., 2008). The most elegant discovery thus far has been the co-expression of TRPA1 in 60-75% of TRPV1-expressing sensory C-fibres, where approximately 97% of TRPV1-expressing neurons are C-fibres (Story et al., 2003, Kobayashi et al., 2005). TRPA1 and TRPV1 were shown to be co-immunoprecipitated in rat and mouse sensory neurons and TRPA1-TRPV1 expression system in Chinese Hamster Ovary (CHO) cells (Staruschenko et al., 2010). It was reported that the TRPA1-expressing population of neurons nearly always express TRPV1 (Bodkin and Brain, 2011) and hence, these findings suggest a possible interaction between the functional activity of the two channels, which will be discussed in Section 1.3.4.

Moreover, TRPA1 is also expressed in sensory neurons that do not express TRPV1 and skin cells other than neurons (Atoyan et al., 2009, Biro and Kovacs, 2009). TRPA1 is present in non-neuronal tissues such as endothelial cells isolated from rat cerebral arteries, and is localised to membrane projections approaching the underlying smooth muscle cells (Earley et al., 2009). Functional TRPA1 is also expressed on human keratinocytes and fibroblasts (Jain et al., 2011), and has been found to be co-localised with melanocyte marker pMel-17 in the basal layer of the epidermis (Atoyan et al., 2009). Positive immunostaining for TRPA1 protein was detected on the mouse epidermis (Denda et al., 2010b). There is also increasing evidence showing that TRPA1 is expressed on human dental pulp fibroblasts with a link to cold sensation and

mechanotransduction (El Karim et al., 2011). The role of cold in activating TRPA1 is currently a debatable issue in the literature and will be discussed more in sections 1.3.3.7, 1.3.8 and 1.4.

It is important to note that the protein expression of TRPA1 in mouse tissue over the last decade has been limited due to unavailability of a selective TRPA1 antibody, and the current evidence that TRPA1 mRNA or protein is expressed in a particular location needs to be further verified for functionality.

1.3.3 Endogenous and exogenous agonists of TRPA1

As TRPA1 is considered as a target for developing novel analgesic and anti-inflammatory drugs, understanding the pharmacology of this channel is important in the drug discovery and development research field. Interestingly, there are distinct pharmacological differences between the functional activity of human TRPA1 (hTRPA1) and rodent TRPA1 (rTRPA1). The pharmacology of the rhesus monkey TRPA1 (rhTRPA1) was demonstrated to be similar to the hTRPA1, whilst the rTRPA1 was shown to closely resemble mouse TRPA1 (mTRPA1) (Bianchi et al., 2012). Understanding the modulation of TRPA1 relies on studying the functional agonists' and antagonists' activities of the channel.

1.3.3.1 Pungent chemicals from vegetables and pollutants

Studies over recent years have identified a range of TRPA1 agonists, some of which include components of traditional medicines and irritants, which are electrophilic activators or non-electrophilic modulators. Electrophilic TRPA1 agonists act by modifying nucleophilic cysteine and lysine resides located on the N-terminal of TRPA1 (Bang and Hwang, 2009). Some of the exogenous agonists for TRPA1 include (1) isothiocyanates such as the pungent products from mustard oil, wasabi and horseradish (Bandell et al., 2004, Jordt et al., 2004), (2) methyl salicylate found in wintergreen oil (Bandell et al., 2004), cinnamaldehyde from cinnamon (Bandell et al., 2004), allicin and diallyl disulphide from garlic (Bautista et al., 2006, Macpherson et al., 2005), acrolein, which are α,β-unsaturated aldehydes in vehicle exhaust fumes and exhaust gas (Bautista et al., 2006, Andre et al., 2008, Simon and Liedtke, 2008) and Δ9 tetra-hydrocannabinol (Jordt et al., 2004, Patapoutian et al., 2003, Story et al., 2003, Nilius et al., 2012).

Mustard oil has been widely used as a pharmacological tool to study the presence of functional TRPA1 and neurogenic inflammation as it causes a dose-dependent release of substance P and CGRP from neuronal C-fibres (Louis et al., 1989, Grant et al., 2005). However, it has been reported to have poor TRPA1 selectivity due to its reactive nature (Bodkin and Brain, 2011).

There is evidence in the literature showing that mustard oil can activate porcine TRPV1 (Ohta et al., 2007). A recent study by Everaerts *et al.* showed that mustard oil has a bimodal effect on TRPA1, producing current inhibition at millimolar concentrations (Everaerts et al., 2010). This study also showed that mustard oil can stably activate mTRPA1 and hTRPV1 as well as TRPV1 receptors expressed on mouse sensory neurons. Furthermore, mustard oil induced TRPV1 stimulation and this response was potentiated by physiological temperatures (Everaerts et al., 2010). Mori *et al.* also showed that mustard oil increased intracellular calcium concentration in cells expressing TRPV1 in a dose-dependent manner (Mori et al., 2011). Overall, these studies provide evidence that mustard oil may have poor selectivity for TRPA1.

Cinnamaldehyde, an extract from cinnamon is used in traditional Chinese medicine to treat circulatory and inflammatory diseases (Yanaga et al., 2006) and is also known to cause neurogenic inflammation (Bodkin and Brain, 2011). Both mustard oil and cinnamaldehyde are highly lipophilic and can diffuse easily through the plasma membrane and rapidly activate TRPA1 (Cavanaugh et al., 2008). Cinnamaldehyde, as an electrophile can covalently modify specific cysteine residues via alkylative conjugate addition (Figure 1.3) (Sadofsky et al., 2011), but the exact mechanism is unknown. In hTRPA1, a small hydrophobic increase of the channel protein at primarily Cys619, Cys639 and Cys663, which are located between the last ankyrin repeated domain and segment 1, was shown to be sufficient to trigger robust channel opening (Hinman et al., 2006). In mTRPA1, the most reactive cysteine residues were Cys415 and Cys422, located in the 10^{th} and 11^{th} ankyrin repeat domains, and Cys622 found between the last ankyrin repeated domain and segment 1 of TRPA1 (Figure 1.3) (Macpherson et al., 2007).

1.3.3.2 Oxidants and metabolites of oxidative stress as TRPA1 activators

TRPA1 is also known as an oxygen sensor (Takahashi et al., 2011). The hypoxia inducible factor-1α is coupled with TRPA1 expression (Hatano et al., 2012), and TRPA1 is a critical sensor for both hypoxia and hyperoxia in vagal and sensory neurons (Takahashi et al., 2011). There is recent evidence showing that the pharmacological blockade of TRPA1 can cause a dose-dependent attenuation in hypoxic ventilator response (13% pure O_2 and 5% CO_2) (Pokorski et al., 2013). Products of oxidative stress that cause cysteine oxidation are known to be potential activators of TRPA1. High concentrations of endogenously-produced alkenal 4-ONE, an electrophilic compound produced by oxidative stress (Taylor et al., 2008) was also shown to activate TRPA1, although recent work from our group has shown that 4-ONE can also trigger TRPA1-independent effects that relate to oedema formation and pain (Graepel et al., 2011). Products of oxidative stress such as 4-hydroxynonenal (4-HNE), an α,β-unsaturated hydroxylalkenal have been previously shown to cause substance P and CGRP release *in vivo* by

activating N-terminal cysteine binding residues of TRPA1 (Trevisani et al., 2007), and these responses were absent in TRPA1 KO mice. Reactive oxygen species such as oxygen radicals and hydrogen peroxide (H_2O_2) are generally upregulated in inflammation and earlier studies have shown that they play an important role in the pathogenesis of inflammatory disease (Keeble et al., 2009). Interestingly, H_2O_2 has also been proposed as a TRPA1 activator and intraplantar (*i.pl.*) injection of H_2O_2 was previously shown to increase pain via a TRPA1-dependent mechanism (Andersson et al., 2008). These findings suggest that TRPA1 may be activated by endogenously derived metabolites of oxidative stress.

1.3.3.3 Gaseous mediators such as nitric oxide and H_2S activate TRPA1

Reactive nitrogen species like nitric oxide have also been shown to be potent activators of TRPA1. The endothelial tetrahydrobiopterin (BH_4) protein is an essential co-factor for nitric oxide production and can activate TRPA1 on DRG sensory neurons (Miyamoto et al., 2009). Recently, hydrogen sulphide (H_2S) was demonstrated to activate TRPA1 (Okubo et al., 2012, Ogawa et al., 2012, Andersson et al., 2012). The vasoactive H_2S was shown to evoke CGRP release from sensory neurons of isolated rat trachea in a TRPA1-dependent manner (Pozsgai et al., 2012). Furthermore, an H_2S donor sodium hydrogen sulphide (NaHS) was shown to activate TRPA1 expressed in CHO cells and stimulated DRG neurons isolated from TRPA1 WT but not TRPA1 KO mice (Andersson et al., 2012). Administration of NaHS (*i.pl.*) was also shown to evoke mechanical and cold hypersensitivities in TRPA1 WT but not TRPA1 KO mice *in vivo*(Andersson et al., 2012). All this evidence suggests that H_2S may mediate its effects via TRPA1 stimulation in the vasculature. Nevertheless, it is important to note that most of these studies used a high concentration of NaHS/H_2S and hence, this raises questions on the significance and relevance of the physiological changes mediated by these compounds.

1.3.3.4 Non-electrophilic TRPA1 agonist

As mentioned earlier, the majority of TRPA1 agonists are electrophilic and react by binding covalently to cysteine residues. Pfizer recently developed a non-reactive, non-volatile stable agonist PF4840154 for a safer and more robust screening assay to assess the pharmacology of TRPA1 channel (Ryckmans et al., 2011). This agonist can activate rTRPA1 and hTRPA1 selectively, as shown *in vitro* and *in vivo*. Our group demonstrated that PF4840154 induced licking-behaviours in a TRPA1-dependent manner *in vivo* (Ryckmans et al., 2011). Intriguingly, it remains unknown how a non-electrophilic agonist activates TRPA1 and if this relies on one or several selective binding sites, or if the compound enters the pore in the dilated mode (Nilius et al., 2011).

1.3.3.5 Modulation of TRPA1 by calcium and inflammatory mediators

Potent mediators are released from neurons during injury and inflammation; however the mechanisms of sensory neuron excitation remain largely unknown. TRPA1 can be activated or sensitised by other inflammatory mediators, in a mechanism involving G-protein coupled receptors (GPCRs) though second messenger signalling cascades. Bradykinin, serotonin and ATP can act on their respective GPCRs and indirectly activate TRPA1 (Bautista et al., 2006, Wang et al., 2008a). Bradykinin acts as an enhancer of TRPA1 by potentially activating the PLC pathway downstream of bradykinin2 receptor (B_2R) activation. This further leads to the breakdown of PIP_2 into DAG and IP_3, activating PKC and releasing calcium from internal stores, respectively. The PLC pathway regulates and activates TRPA1 via an unknown mechanism (Bautista et al., 2013) Thus, GPCR coupling can allow TRPA1 to increase its repertoire of both exogenous and endogenous ligands (Bautista et al., 2013).

Interestingly, studies by Wang *et al*. on whole cell recordings have recently demonstrated that modest increases in intracellular calcium, which correlates with cell stimulation, can activate TRPA1 channels. This potentiates agonist-induced TRPA1 currents, whilst larger elevations of intracellular calcium inactivate TRPA1. Wang and colleagues also identified key residues in the segment 5 to segment 6 linker of the TRPA1 channel, which control calcium permeability (Wang et al., 2008b). TRPA1 can also be directly activated by calcium by acting on residues on the EF-hand domain of the channel (Zurborg et al., 2007).

1.3.3.6 TRPA1 acts as a mechanosensor?

In contrast to acting as a chemosensor, TRPA1 has been reported to have mechanosensory properties and mediates nociception within the viscera in both normal and pathophysiological conditions (Brierley et al., 2011). Although several evidences from *in vivo* studies show a role for TRPA1 as a mechanosensor, TRPA1 has been speculated to be involved in the formation of mechanosensory complexes rather than solely mediating responses to mechanical stimuli (Nilius et al., 2012).

1.3.3.7 Cold activates TRPA1?

Lastly, but not least, cold temperatures (<17°C) can directly activate TRPA1 in heterologous expression systems (Story et al., 2003, Bandell et al., 2004). However, there is significant debate regarding the role of TRPA1 as a 'cold sensor' channel as studies from other groups failed to reproduce cold responsiveness in TRPA1 (Jordt et al., 2004, Nagata et al., 2005, Caspani and Heppenstall, 2009). Whilst there is increasing evidence from cellular and

behavioural studies in TRPA1 KO mice that TRPA1 is not required for acute cold-induced pain *in vivo* (Bautista et al., 2006), other groups have shown that pharmacological blockade of TRPA1 in primary sensory neurons can reverse cold-induced hyperalgesia caused by inflammation and nerve injury (Obata et al., 2005). The role of TRPA1 as a potential cold sensor will be discussed in section 1.3.8 and 1.4.

1.3.4 Transgenic mice and antagonists

As the availability of selective and potent TRPA1 antagonists is currently limited, most studies investigating the role of TRPA1 in pathological diseases have used TRPA1 KO mice, established in 2006 by two groups (Bautista et al., 2006, Kwan et al., 2006). Kwan *et al*. initially showed mice lacking functional TRPA1 were insensitive to oral supplementation of mustard oil, painful cold and mechanical stimuli (Kwan et al., 2006). Furthermore, the use of TRPA1 WT and KO mice showed that TRPA1 mediated inflammatory pain caused by bradykinin (Kwan et al., 2006). Although there is a difference in the method of TRPA1 gene deletion between both the strains of mice, there is a clear loss of functional TRPA1 (Story and Gereau, 2006). The TRPA1 KO mice derived from Kwan *et al.* were generated by replacing the exons encoding the S5 and S6 pore forming domains with a cassette containing an internal ribosome entry site, a human placental alkaline phosphatase gene and a polyadenylation sequence (Kwan et al., 2006). Hence, a TRPA1 transcript that cannot form a functional TRPA1 was produced. These mice are maintained on a mixed C57Bl/6J and B6129PF2/J background, and have been used in various publications from our group and others. On the other hand, the TRPA1 KO mice derived from Bautista *et al.* have their pore loop and much of their sixth transmembrane domain deleted (Bautista et al., 2006). These mice are maintained on a C57/BL6 background and are also used by many research groups. It is important to note that both strains are on a mixed genetic background and hence, this causes a problem when data are extrapolated to and from mouse models on a single background (Nilius et al., 2012).

As it is clear from several knock-down and KO studies that TRPA1 is involved in pain and inflammatory pathways, the development of pharmacological drugs to target this potential site may produce analgesic and anti-inflammatory effects (Defalco et al., 2010). Ruthenium red, a non-selective cation channel blocker, has been used in several studies to investigate the pharmacology of TRPA1. Ruthenium red not only interacts with the ligand binding site of TRP channels but also blocks the aqueous pore (Vriens et al., 2009), which will in turn prevent increase in intracellular cations. Camphor, the active ingredient of many balms, inhibited mustard oil-induced activation of TRPA1-expressing HEK293 cells (Sawada *et al*., 2007) but it was also shown to activate and desensitise TRPV1 (Xu *et al*., 2005). Studies in our laboratory

showed that camphor does not reduce 4-ONE induced mechanical hyperalgesia (Graepel, 2009) and hence, camphor is thought to be weak and non-selective TRPA1 antagonist.

McNamara *et al*. was the first to show that a substituted theophylline derivative HC-030031 blocked TRPA1-agonist formalin induced nociceptive responses (McNamara et al., 2007)*in vivo* whilst, Taylor-Clark *et al*. further showed that HC030031 inhibited TRPA1 agonists 15-Prostaglandins J_2 (15-PGJ_2)-induced responses *vitro*(Taylor et al., 2008). This compound is currently under preclinical investigation (Baraldi et al., 2010). HC030031 is non-electrophilic and hence, acts via non-covalent interaction with the TRPA1 channel (Nilius et al., 2012) and it was shown to inhibit both ally isothiocyanate (AITC)- or formalin-inward and outward currents rapidly and reversibly. Furthermore, HC030031 does not inhibit currents mediated by other TRP channels such as TRPV1, TRPV3, TRPV4 or NAV1.2 channels (McNamara et al., 2007). This finding highlights the high selectivity of HC030031 for TRPA1 and this compound will be widely used in the current project to characterise the role of TRPA1 in the peripheral vasculature *in vivo*.

AMG7160 belongs to the trichloro(sulfanyl)ethyl benzamide (TCEB) compound family and is also known to display differential pharmacology at rTRPA1. It marginally inhibits rTRPA1 activation by mustard oil while other TCEB compounds can act as partial agonists (Klionsky et al., 2007). Chembridge-5861528, also known as TCS5861528, is a newer derivative of HC030031 and was recently shown to reduce diabetic- and mustard oil induced mechanical hypersensitivity (Wei et al., 2009, Wei et al., 2010b, Wei et al., 2010a, Wei et al., 2013b, Wei et al., 2012, Wei et al., 2013a). Thus far, another oxime-derived compound A967079 has been reported to be the TRPA1 antagonist with the greatest affinity as it displays 1000-fold selectivity for TRPA1 when compared to other TRP channels and more than 150-fold selectivity over other 75 other ion channels, enzymes and G-protein coupled receptors. A967079 was shown to be effective in antagonising TRPA1 in human and rat cell lines *in vitro* and, in reducing spontaneous and mechanically evoked firing of spinal neurons in pain models of osteoarthritis *in vivo* (McGaraughty et al., 2010). Further studies showed that oral dosing of A967079 resulted in a significant decrease in nocifensive responses induced by the TRPA1 agonist AITC, osteoarthritic pain and cold allodynia produced by nerve injury in rats, without any changes in core body temperature or any side effects in terms of locomotor or cardiovascular responses (Chen et al., 2011).

Neuropathic pain is caused by highly effective chemotherapeutic agents, in cancer treatment with oxaliplatin and related drugs. A new compound ADM_09 was recently shown to revert oxaliplatin-induced neuropathic pain in rats by blocking TRPA1, without causing any

commonly associated negative side-effects, such as modifying normal behaviour, cardiotoxicity or toxicity towards astrocyte cell cultures. ADM_09 was further demonstrated to block both mTRPA1 and hTRPA1 persistently by binding to carnosine residue in a calcium-dependent manner and by forming disulphide bridge with lipoic acid residue (Nativi et al., 2013).

Furthermore, *in vitro* studies showed that the electrophilic oxime compound AP-18 attenuates mustard oil-induced nociceptive behaviour and Complete Freund's adjuvant (CFA)-induced mechanical hypersensitivity in TRPA1 WT but not KO mice (Defalco et al., 2010, Petrus et al., 2007, Fernandes et al., 2011). Some TRPA1 antagonists, including AP-18, have limitations such as short-acting and local application limitations. Nakatsuka *et al.* recently reported that AP18 was ineffective in inhibiting heterologously expressed frog TRPA1 (fTRPA1) and, neither heterologously nor endogenously fTRPA1 is sensitive to A967079 upon TRPA1 activation. The sites of the antagonistic action of A967079 is located on two specific amino acid residues located within transmembrane domain 5 of hTRPA1 (Nakatsuka et al., 2013). These new findings further highlight the difference in channel properties of TRPA1 in diverse animal species and hence, the identification and further understanding of molecular determinants for TRPA1 antagonists will help the new development of selective TRPA1 antagonists. It is evident that TRPA1 plays a significant role in inflammatory pain and may have a role in other systemic diseases and hence, the clinical development of novel and potent TRPA1 antagonists may be beneficial.

1.3.5 Receptor activity and desensitisation

Mustard oil and capsaicin administration are both well-known experimental models of inflammation. TRPA1 activation and sensitisation pathways have been suggested to be similar to those of TRPV1 (Nilius, 2007) and a few studies have reported that both receptors can cross-regulate each other's receptor activity and desensitisation (Ruparel et al., 2008, Salas et al., 2009). However, whilst repeated application of capsaicin causes desensitisation, Inoue *et al.* showed that repeated application of mustard oil creates consistent plasma extravasation in the mouse ear skin (Inoue et al., 1997). However, using calcium-imaging studies Anand *et al.* showed that repeated exposure to the TRPA1 agonist cinnamaldehyde produced desensitisation of primary cultured human DRG neurons (Anand et al., 2008). Pain sensations to mustard oil are also significantly delayed in atopic dermatitis patients after two mustard oil applications, as a result of functional sensory system desensitisation (Heyer et al., 1991). Therefore, agonist-based desensitisation therapies may potentially be useful in some inflammatory and painful conditions.

Capsaicin and mustard oil pre-treatment have both been shown to result in pharmacological and functional cross-desensitisation between TRPA1 and TRPV1 (Ruparel et al., 2008, Patacchini et al., 1990, Jacquot et al., 2005, Simons et al., 2004). TRPV1 activation by capsaicin has been shown to desensitise TRPA1 in nociception studies (Ruparel et al., 2008) and this is mediated by a calcium dependent pathway and PIP_2 depletion (Akopian et al., 2007). Capsaicin-gated massive calcium influx also activates calcium-dependent phospholipase C-δ (PLCδ) (Akopian et al., 2007) which further desensitises TRPA1 (Karashima et al., 2008). Interestingly, TRPA1 activation can also lead to TRPV1 desensitisation and this was suggested to be mediated by the calcineurin dependent pathway. Calcineurin is involved in dephosphorylating calmodulin-dependent protein kinase II (CAMKII) consensus sites located at the C-terminal of TRPV1 channel and this blocks ligand binding (Jung et al., 2004). Pre-incubation with lower concentrations of cinnamaldehyde was shown to enhance TRPV1-induced responses in rat DRG neurons, whilst high concentrations of cinnamaldehyde caused desensitisation to further TRPV1 stimulation (Anand et al., 2008). Akopian *et al.* reported that presence of TRPV1 regulates the magnitude of TRPA1 desensitisation, and in the absence of TRPV1, mustard oil induces receptor internalisation (Akopian et al., 2007). Therefore, consideration for both receptors may be necessary in any therapeutic developments.

It is interesting to note that the extensive co-expression of TRPA1 and TRPV1 in sensory neurons has been proposed to cause a potential functional interaction between the two channels, although the exact mechanisms and effects of this interaction are under debate. Salas *et al.* (2009) showed that mustard oil-gated currents exhibited faster kinetics activation in TRPA1-expressing than in TRPA1/TRPV1 co-expressing CHO cells *in vitro* (Salas et al., 2009). Salas *et al.* further proposed that there might be a down-regulation of TRPA1 expression in TRPV1 KO mice (Salas et al., 2009). However, TRPA1 KO mice have been shown to retain their responses to capsaicin (Macpherson et al., 2006, Aubdool, 2010) and TRPV1 KO mice have also been reported to retain their responses to mustard oil (Banvolgyi et al., 2004). Our recent study *in vivo* showed that TRPA1-mediated vasodilatation following topical application of mustard oil was significantly potentiated in TRPV1 KO mice or WT mice pre-treated with selective TRPV1 antagonist SB366791, when compared to TRPV1 WT mice or WT mice pre-treated with vehicle (Aubdool, 2010). This suggests that when TRPV1 and TRPA1 are both present, TRPV1 may regulate TRPA1-mediated responses induced by mustard oil. Studies investigating the interaction between TRPA1 and TRPV1 have relied on individual pharmacological approaches and to date there are no dual antagonist to selectively target TRPA1 and TRPV1.

In a recent review, Akopian *et al.* reported that mustard oil-induced responses leads to self-desensitisation of TRPA1 via two possible mechanisms which include (1) modification in the TRPA1 channel which needs time to recover and (2) internalisation of TRPA1 which further leads to decrease in TRPA1 activity (Akopian et al., 2007, Schmidt et al., 2009, Akopian, 2011). However, when TRPA1 and TRPV1 are co-expressed on the same sensory neuron, TRPV1 can inhibit the internalisation of the TRPA1 receptor, and thus, potentially preventing the second desensitisation mechanism (Akopian et al., 2007). It remains unknown if TRPA1-TRPV1 co-expression is exclusive in sensory neurons or if it also occurs in non-neuronal tissues. Future studies investigating TRPA1 and TRPV1 expression profiles and their interactions would provide details on the pharmacologic properties and function of these channels. If TRPV1 regulates the density of TRPA1 expression and functional activity, this will affect the responses of a TRPA1 agonist.

1.3.6 Vasodilator effects of TRPA1

There is increasing evidence in the literature showing that TRPA1 plays an important role in mediating inflammatory pain, but TRPA1 is also known to have a role in mediating vasorelaxant effects. Some of the agonists mentioned in section 1.3.3 have been used in studies to investigate the vascular effects of TRPA1. Bautista *et al.* was the first to show that TRPA1 channels are expressed in adventitial nerve fibres in the rat mesenteric arteries and demonstrated that they play a role in regulating the vascular tone in response to agonists such as mustard oil and allicin (Bautista et al., 2005). Interestingly, allicin has previously been shown to cause relaxation of *ex vivo* perfused feline mesenteric vessels via an unidentified mechanism (Mayeux et al., 1988), and also in isolated rat pulmonary arteries via induction of endothelial-derived nitric oxide production (Ku et al., 2002). Both these relaxation responses could perhaps now be attributed to TRPA1 as shown by Bautista *et al.* (2005). This TRPA1-mediated relaxation response in the phenylephrine pre-constricted mesenteric artery rings was shown to be dependent on CGRP release, but not TRPV1 activation (Bautista et al., 2005).

Following on from the evidence that mustard oil acts on TRPA1 (Jordt et al., 2004), our group used the mouse ear model to show that topical application of mustard oil (1%) induces vasodilatation via the release of neuropeptides such as CGRP and substance P (Grant et al., 2005). Grant *et al.* first developed the mouse ear model in our group, to allow simultaneous measurement of blood flow by laser Doppler flowmeter and oedema formation to characterise the mechanisms underlying neurogenic inflammation (Grant et al., 2002). Later studies by Pozsgai *et al*. from our group showed that mustard oil-induced vasodilatation was dependent on TRPA1 using transgenic mice (Pozsgai et al., 2010). Mustard oil was also demonstrated to

increase meningeal blood flow by acting TRPA1 and via the release of CGRP in rats (Kunkler et al., 2011). These findings highlight that there is increasing evidence in the literature showing CGRP release downstream of TRPA1 activation.

Functional TRPA1 was shown to be expressed on the endothelium of rat cerebral and cerebellar pial arteries, and Earley *et al*. showed that mustard oil caused vasodilation mediated by hyperpolarisation of the smooth muscle via myo-endothelial gap junctions (Earley et al., 2009). Experiments from Earley's laboratory failed to detect TRPA1 expression outside the cerebral circulation in sites such as the endothelium of rat mesenteric and renal interlobar arteries (Earley, 2012).

Our recent study using the mouse ear model showed that mustard oil-induced vasodilatation was enhanced in TRPV1 KO mice or CD1-mice pre-treated with a selective TRPV1 antagonist (Aubdool, 2010). However, our data here suggest that TRPV1 may be involved in regulating TRPA1-mediated responses induced by mustard oil. If mustard oil at a dose of 1% has non-specific effects apart from TRPA1, this raises the question on using mustard oil as a pharmacological agent to elucidate mechanisms underlying TRPA1-mediated responses and further, reinforces the requirement of a selective TRPA1 agonist.

A link between oxidative stress and TRPA1 has been previously proposed by earlier studies, as mentioned earlier (Trevisani et al., 2007). The lipid peroxidation product, 4-ONE was shown to activate TRPA1 in CHO cells *in vitro* (Andersson et al., 2008) and our group further investigated its effects on vasoactive responses *in vivo*. We showed that 4-ONE triggers unilateral mechanical hyperalgesia, oedema formation and vasodilatation in both a TRPA1-dependent and -independent manner (Graepel et al., 2011). 4-ONE-induced increase in blood flow was shown to be significantly reduced in the hindpaw of TRPA1 KO and α-CGRP KO mice, when compared to respective WT mice (Graepel et al., 2011). However, there was an increase in 4-ONE induced oedema formation and pain in TRPV1 KO mice. These results further suggested that 4-ONE might trigger TRPA1-independent effects in terms of plasma extravasation and pain sensitivity *in vivo* (Graepel et al., 2011).

More evidence of the role of TRPA1 in mediating vascular effects was recently shown by using the gaseous mediator H_2S. H_2S was demonstrated to mediate vasodilatation in pressurised mesenteric small arteries isolated from rats and this response was attenuated following the pre-treatment with capsaicin, a CGRP receptor antagonist Olcegepant or TRPA1 antagonist HC030031 (White et al., 2013). This response was shown to be dependent on sensory neuron activation but independent on nitric oxide or K_{ATP} channels (White et al., 2013). In the mouse

ear model, topical application of the H_2S donor NaHS (5%) was shown to mediate vasodilatation, which is dependent on TRPA1, as shown when the TRPA1 gene was deleted or pharmacologically blocked using HC030031 (Pozsgai et al., 2012). Furthermore, this response was shown to be unaffected in TRPV1 KO mice when compared to WT mice (Pozsgai et al., 2012). These findings highlight an important role in NaHS in activating TRPA1 and mediating vasoactive responses. However, it is important to note that intracolonic NaHS administration has been shown to evoke similar nociceptive effects in TRPA1 WT and KO mice and this finding suggests that the visceral pro-nociceptive effects of NaHS is independent of TRPA1 (Andersson et al., 2012). This further suggests that NaHS has TRPA1-independent effects, which requires further investigation.

As discussed here, it is clear that TRPA1-mediated responses may vary depending on the type of vascular beds or site of action. Although some compounds have been reported to activate TRPA1, further investigations have demonstrated that they also possess other unknown TRPA1-independent effects. The use of a selective TRPA1 agonist may answer this question and this will be discussed further in the next section focusing on cinnamaldehyde which has been documented to be a more selective TRPA1 agonist (Bodkin and Brain, 2011).

1.3.7 Vascular effects of cinnamaldehyde

Cinnamaldehyde has been reported to have good selectivity and potency towards TRPA1 (Bodkin & Brain, 2010). Several earlier studies have investigated the role of cinnamaldehyde in mediating cardiovascular responses, even before cinnamaldehyde was discovered to act on TRPA1. Harada & Yano (1975) showed that cinnamaldehyde caused a fall in blood pressure followed by respiratory stimulation and an increase in heart rate in anaesthetised dogs and guinea pigs. The mechanism of action here is unknown but it was suggested that this is mediated by cinnamaldehyde-induced vasodilatation in the peripheral vasculature (Harada and Yano, 1975). Using this previous knowledge, our group investigated the peripheral influence of TRPA1 in mediating cinnamaldehyde-induced cardiovascular responses. Indeed, injection (*i.v.*) of cinnamaldehyde induced a transient hypotensive response and decrease in heart rate, followed by a more sustained dose-dependent pressor response in WT which were all suppressed in TRPA1 KO mice (Pozsgai et al., 2010). Both the depressor and pressor responses were also shown to be dependent on α-adrenergic receptor activation (Pozsgai et al., 2010), suggesting a potential involvement of sympathetic nerve action. Indeed, there is earlier evidence showing an increase in plasma catecholamine levels following injection (*i.v.*) of cinnamaldehyde in anaesthetised dogs (Harada et al., 1982).

In terms of vascular effects, cinnamaldehyde was shown to induce relaxation in isolated pre-contracted rat aorta, which was impaired but not abolished when the endothelium was removed or following NOS inhibition (Yanaga et al., 2006). Xue *et al.* showed that cinnamaldehyde-induced relaxation was not dependent on nitric oxide, potassium channels or prostaglandins (Xue et al., 2011). It was shown that cinnamaldehyde dilates the vascular smooth muscle in an endothelium-independent manner and this may involve both calcium influx as well as release (Xue et al., 2011). It is important to note that these studies did not investigate the effects of TRPA1 inhibition on cinnamaldehyde-induced responses and it remains unknown whether TRPA1 is expressed in the smooth muscle cells of rat aorta. Investigation from Earley's laboratory have not detected any TRPA1 expression in the smooth muscle cell of rat cerebral resistance arteries (Earley, 2012).

However, later studies in our group showed that cinnamaldehyde-induced vasodilatation in mesenteric arterial rings were significantly less potent in TRPA1 KO than WT mice (Pozsgai et al., 2010). *In vivo,* administration cinnamaldehyde (*i.pl.*) was shown to increase blood flow in the paw skin of anaesthetised WT but not TRPA1 KO mice (Pozsgai *et al.,* 2010). It remains to be determined whether the activation of TRPA1 by cinnamaldehyde involved a neurogenic-dependent vasodilatation like other TRPA1 agonists *in vivo*.

Silva *et al.* investigated the mechanisms underlying topical cinnamaldehyde-induced oedema in the mouse ear and demonstrated that this response is dependent on TRPA1 stimulation and substance P release (Silva et al., 2011). The skin penetration for topical application of cinnamaldehyde has been shown to be about 55% (Silva et al., 2011, Bickers et al., 2005, Kasting et al., 1997). It is important to highlight that repeated applications of cinnamaldehyde did not cause desensitisation in terms of oedema formation (Silva et al., 2011).

Cinnamaldehyde has also been shown to have vascular effects in human studies. Cinnamaldehyde (10%) was shown to evoke significant changes in spontaneous pain and induced heat and mechanical hyperalgesia, with increase in neurogenic axon flare in the forearm of healthy participants (Namer et al., 2005). Topical application of cinnamaldehyde (1-10%) was shown to cause changes in Aδ-evoked potential amplitude, heat hypersensitivity and evoked pain in areas on the mid-volar forearm of healthy subjects (Roberts et al., 2011). It remains unknown whether cinnamaldehyde-induced responses in the cutaneous vasculature are dependent on TRPA1 in human. Nevertheless, topical application of cinnamaldehyde was demonstrated to accelerate skin permeability barrier recovery which was further delayed using the TRPA1 antagonist HC030031 (Denda et al., 2010b).

The exact nature of the downstream mechanism underlying cinnamaldehyde-induced responses in the vasculature *in vivo* is unknown. Therefore, my PhD project will investigate the mediators involved in mediating cinnamaldehyde-induced responses using the mouse ear model.

1.3.8 Is TRPA1 a thermosensor?

Temperature recognition remains critical for sensory perception and TRPA1 can be activated by cold temperatures, as mentioned earlier. However, the role of TRPA1 as a cold sensor has been a controversial issue in the literature and it remains unknown if TRPA1 is a receptor for noxious cold. Hence, this section will summarise all the current knowledge of cold as an activator of TRPA1.

1.3.8.1 Discovery of TRPA1 as a cold sensor

Using calcium imaging studies, it was clearly demonstrated that there was a rapid increase in calcium influx as the buffer is cooled from 17°C to 10°C, with the highest peak in calcium influx at 10-11°C in CHO cells transfected with TRPA1 but not untransfected cells (Story et al., 2003). The study conducted by Story *et al.* provided evidence that low temperature activates TRPA1 and they also clearly demonstrated that at higher temperatures (20-33°C), TRPA1-expressing cells failed to show any activation and changes in calcium influx. However, the other cold sensitive channel TRPM8, which was first identified through its sensitivity to cold and menthol *in vitro* (McKemy et al., 2002, Peier et al., 2002) was shown to be involved in this response. The majority of TRPM8-expressing cells responded and exhibited increased intracellular calcium at temperatures ranging from 19-24°C (Story et al., 2003). These findings correlated with previous results from Peier *et al.* (2002) suggesting that although both TRPM8 and TRPA1 respond to cold, the temperature threshold for TRPM8 is higher than TRPA1 (Peier et al., 2002, Story et al., 2003). The findings from Story *et al.* (2003) strongly suggested that TRPA1-expressing cells are majorly involved in detecting noxious cold stimulus due to its lower temperature threshold of activation, whilst TRPM8-expressing cells sense innocuous cold and their activation results in a pleasant cooling sensation. Interestingly, a population of sympathetic neurons derived from primary cultures of adult mouse superior cervical ganglia (SCG) neurons were shown to be sensitive to cold, when temperature was lowered from 25°C to 10°C, but not menthol. Furthermore, TRPA1 but not TRPM8 mRNA was detected in the sympathetic ganglia. It was suggested that cooling may directly affect sympathetic efferent activity (Smith et al., 2004) and the role of TRPA1 in mediating this response needs to be further validated. It is evident from these findings that both TRPA1 and TRPM8 are activated

by cold, but at different temperature thresholds and hence, more studies investigating cold may need to investigate the role of both receptors in cooling-induced responses.

1.3.8.2 Controversy surrounding TRPA1 as a cold sensor: an unresolved issue?

Following on from the previous finding, cold (9°C) was shown to activate TRPA1 using calcium-imaging studies in cultured rat DRG neurons (Bandell et al., 2004). Nevertheless, Jordt *et al.* showed that 96% of mustard oil-sensitive neurons did not respond to a cold stimulus (5°C) and the 4% cold-sensitive neurons also responded to the TRPM8 agonist menthol (Jordt et al., 2004). Further detailed analysis of the 4% cold-sensitive neurons showed that 95% of these neurons responded to menthol, whilst the other 5% showed no response to either cold or mustard oil. Cold (5°C) did not activate TRPA1-expressing HEK293 cells, although they showed responses to mustard oil. Hence this study showed the controversial finding that TRPA1 is unlikely to mediate cold sensitivity in cultured trigeminal neurons (Jordt et al., 2004). It is worth highlighting here that Jordt *et al.* investigated cold at a temperature of 5°C in particular which may not be dependent on TRPA1 activation or it could also be discrepancies between different assays. In addition, further studies in rat DRG neurons showed that menthol-insensitive neurons required stronger cooling for activation and were not stimulated by mustard oil and this study supported that TRPM8 rather than TRPA1 is involved in cold sensing at the temperature of 12°C (Babes et al., 2004).

The conflicting finding about the role of TRPA1 as a thermosensor following the finding by Jordt *et al.* led to the investigation of cold sensation *in vivo*. Obata *et al.* (2005) showed that (1) there was no overlap between TRPA1- and TRPM8-expressing sensory neurons, (2) CFA increases TRPA1 but not TRPM8 expression in TRK1-transforming tyrosine kinase protein (trkA)-expressing DRG neurons and (3) intrathecal administration of TRPA1 anti-sense oligode-oxynucleotide was shown to decrease cold-induced hyperalgesia in rats (Obata et al., 2005, Katsura et al., 2006). This study presented evidence to support the role of TRPA1 in mediating cold hyperalgesia.

The controversy surrounding the role of TRPA1 as a cold sensor was expected to resolve by the generation of TRPA1 KO mice, but interestingly the generation of TRPA1 KO mice from two different laboratories produced even more conflicting results. Kwan *et al.* showed that there was a decrease in cold (0°C) sensitivity or in acetone-induced evaporative cooling of TRPA1 KO mice in behavioural experiments as measured by paw withdrawal responses from a cold plate test (Kwan et al., 2006). It is worth noting here that these differences were only observed in female mice.

Nevertheless, *in vitro* studies using calcium imaging and primary cultured trigeminal neurons showed that there was no change in cold (6°C)-induced calcium influx between TRPA1 WT and KO mice. In both WT and TRPA1 KO mice, 16.7% of the trigeminal neurons were shown to be cold-sensitive and out of these, 78% are menthol-sensitive and 22% menthol-insensitive (Bautista et al., 2006). Furthermore, Bautista *et al.* demonstrated that there was no difference in cold sensation *in vivo* using similar tests as Kwan *et al.* (2006), where cold plate test investigated temperature from -10°C to 20°C and focussed on examining changes in hindpaw lifts and shivering (Bautista et al., 2006). No significant changes were observed in terms of acetone-induced flinches between TRPA1 WT and KO mice (Bautista et al., 2006).

Interestingly, Karashima *et al.* followed up the cold plate (0°C) study using TRPA1 WT and KO mice, on a similar genetic background to Bautista *et al.* (2006) and investigated the pain-behaviour in details. They found that the latency for the cold-induced first jump in the acute-cold response phase was significantly lower in TRPA1 KO mice of both sexes when compared to respective WT mice, and these responses were not observed when the cold plate was set at 10°C (Karashima et al., 2009). In another study, Sawada *et al.* addressed the controversial cold issue by showing that mTRPA1 responds to temperature lower than 18°C in primary cultured mouse DRG cells and HEK293 cells, in support with previous findings (Sawada et al., 2007). Furthermore, del Camino *et al.* illustrated clearly that mild cooling (10°C) markedly increases TRPA1 agonist AITC-evoked rTRPA1 currents and in the absence of this agonist, mild cooling or noxious cold only causes a slight increase in current amplitude *in vitro*(del Camino et al., 2010). A similar pattern of findings was shown *in vivo* where cold hypersensitivity was induced in WT mice but not TRPA1 KO mice by subcutaneous treatment of agonist 4-HNE. These results suggested that TRPA1 is a primary target of cold hypersensitivity in pathological situations that lead to generation of reactive oxygen species and pro-inflammatory activators of TRPA1, rather than cold detection (del Camino et al., 2010).

It is worth noting here that the reason why there is increasing controversial findings of TRPA1 as a cold sensor may be due to the temperature ranges investigated in the studies. Indeed, it was reported that the difference in preparation of TRPA1-expressing cells or stimulation protocol (different temperature and incubation time) might affect TRPA1-induced responses (Sawada et al., 2007, Sawada and Yamamoto, 1983).

1.3.8.3 Generation of TRPM8 KO and TRPA1/TRPM8 DKO

To be able to distinguish the cold-induced responses between TRPA1 and TRPM8, TRPM8 KO mice have been used in numerous studies. TRPM8 KO mice illustrated a large reduction in icilin- and menthol-induced responses in a number of cells, as assayed by calcium imaging studies (Bautista et al., 2007, Colburn et al., 2007, Dhaka et al., 2007). Using TRPM8 KO mice by Dhaka *et al.* yielded evidence showing that in primary cultured DRG neurons, cold (10°C) activates 14.9% of cold-sensitive neurons of WT mice and only 7.6% from TRPM8 KO mice (Dhaka et al., 2007). Behavioural studies further demonstrated that TRPM8 KO mice have severe behavioural deficits in response to cold stimuli when compared to WT mice and at cold temperature (16-20°C), both TRPM8 WT and KO mice show severe avoidance in a temperature gradient assay (Dhaka et al., 2007). Interestingly, it was also shown that at sub-zero centigrade temperature TRPM8 KO mice have normal nociceptive-like responses, further suggesting that another noxious cold receptor may be involved.

Since the generation of neither TRPA1 nor TRPM8 transgenic mice resolved the conflicting findings on cold sensation, it was sought that examining cold sensitivity in TRPA1 and TRPM8 double KO (DKO) mice was essential. Knowlton *et al.* showed that there was a dramatic reduction in the total number of cold-sensitive neurons in TRPM8 KO or TRPA1/TRPM8 DKO when compared to WT mice in calcium imaging studies using trigeminal ganglia neurons (Knowlton et al., 2010). Furthermore, no differences in responses were shown between TRPA1 WT and KO following cold challenge with a cooling gradient from 35°C to 9°C. It has been further suggested that TRPM8 expression may compensate for the lack of TRPA1 in TRPA1 KO mice and hence, the normal contribution of cold responses are observed. The other findings from Knowlton *et al.* studies include (1) behavioural studies which demonstrated that WT mice preferred warm temperatures over cold, whilst TRPM8 KO and TRPA1/TRPM8 DKO showed no preference, until the temperatures reached the extreme range (5°C), (2) cold mimetic icilin-nocifensive behaviours were absent in TRPM8 KO and TRPA1/TRPM8 DKO mice, but unchanged in TRPA1 KO mice when compared to WT mice and (3) neural activity was analysed by investigating the protein expression of immediate early gene *c-fos* following hindpaw stimulation with noxious cold (0°C), TRPM8 agonist menthol or icilin where *c-fos* expression was shown to be significantly decreased in TRPM8 KO and TRPA1/TRPM8 DKO, but unchanged in TRPA1 KO when compared to WT mice (Knowlton et al., 2010). This study using TRPA1/TRPM8 DKO provided evidence that TRPM8 rather than TRPA1 is the primary target for cold sensitivity.

1.3.8.4 Recent findings

Despite the increasing amount of studies aiming to resolve the conflicting results, there is now a wealth of papers recently supporting that cold activates TRPA1 directly. Interestingly, it was reported that genetic variations in TRPA1 contribute to individual variations according to gender in short duration cold pain sensitivity as observed in a European American cohort study (Kim et al., 2006). Moreover, a point mutation (N855S) in segment 4 transmembrane of TRPA1 has been reported to be linked with an autosomal-dominant familial episodic pain syndrome, characterised by upper body pain, which is triggered by fasting, cold and physical stress (Kremeyer et al., 2010). Kremeyer *et al.* also presented evidence of a possible role of TRPA1 in sensing cold, with enhanced currents observed following application of cold temperatures (12°C) in the mutant TRPA1 channel. The mutant channels were shown to be sensitive to the TRPA1 antagonist HC030031, further highlighting that the potential therapeutic role of TRPA1 antagonists in this pain syndrome (Kremeyer et al., 2010, Eid et al., 2008). Moreover, recent studies have demonstrated that TRPA1 may function to extend lifespan at cold but not warm temperatures, as a TRPA1-null mutant worm had a shorter lifespan than WT at 15°C and 20°C, and not 25°C (Xiao et al., 2013).

It is known from previous studies that reducing the whole body temperature of homeothermic mice by 0.3 to 0.5°C can extend longevity by 12% in male mice and 20% female mice (Conti et al., 2006), but it is currently unknown whether this is dependent on TRPA1. Recently, cold-induced longevity in worms was shown to be tissue specific as TRPA1 can function in both intestinal cells and neurons, but not muscle and hypodermal cells to modulate lifespan. This response is dependent on the activity of calcium, DAF-16 which is the primary transcription factor required for extending lifespan and protein kinase 2 (PKC-2) downstream of TRPA1 activation (Xiao et al., 2013). It remains unknown whether sensory neurons in and surrounding peripheral tissues, such as the skin, plays a role in mediating cold-induced longevity in a TRPA1-dependent manner.

Furthermore, although cold (<17°) as detailed in this section has been shown to activate TRPA1 in several *in vitro* and *in vivo* studies, the role of TRPA1 as a cold sensor in the peripheral vasculature is unknown. This will be further investigated in the current PhD project, and since there is earlier evidence to support that environmental cooling or local cold exposure can mediate changes in peripheral blood flow, this concept will be further discussed in Section 1.4.

1.4 The effects of cold in the vasculature

1.4.1 Physiological responses to cold

Cold exposure to the fingers, ears and toes is known to trigger a 'Hunting' reaction, which is usually observed over a period of 1h. It consists of a rapid decrease in skin temperature in the first few minutes during continuous immersion in ice-cold water and thereafter an increase in local skin temperature at 5-15 min following exposure during the rewarming phase. Cyclic phase of cooling and rewarming will follow, and Sir Thomas Lewis described this response as '*cold-induced vasodilatation*' (CIVD) (Lewis, 1930). A stylised "classic" reaction is illustrated in Figure 1.4 (Cheung and Daanen, 2012). The initial short-lived decrease in skin temperature is due to peripheral vasoconstriction which is a powerful mechanism required to reduce heat loss (Burton, 1955). This vasoconstriction phase is also known to be painful, and may be accompanied by 4-fold increase in respiratory frequency and tachycardia (Keatinge and Nadel, 1965, Leblanc et al., 1975).

The rewarming phase is where the blood vessels start to dilate, which increases both blood flow in the vasculature and local skin temperature. This phase is very important to prevent frostbite injury in extreme cold conditions. The skin temperature can rise by as much as 10°C. It is important to note that this response is frequently observed at low environmental temperatures (Burton, 1955) and may not be observed following severe cold exposure as local freezing would happen before CIVD has had time to develop even when the core body temperature is kept constant (Fox and Wyatt, 1962). In terms of responses in the finger, which is a site widely studied for CIVD it was earlier argued that the Hunting reaction is one of the four possible reactions of blood vessels to extreme cold exposure (Purkayastha et al., 1992). Hence, the other responses observed are (1) a continuous vasoconstriction state, (2) slow steady and continuous rewarming and (3) a proportional control form where the diameter of the blood vessel remains constant after the initial vasoconstriction phase following cold exposure (Purkayastha et al., 1992, Daanen, 2003).

However, later studies by Daanen (2001) showed that the Hunting reaction described by Lewis (1930) was observed in 210 out of 226 male subjects when the finger was immersed in ice water (Daanen, 2001) and hence, it was concluded that majority of the vascular responses to cold water finger immersion can be classified as the Hunting reaction. Strong cooling may decrease the skin temperature below a threshold for nerve conduction (7-8°C) (Vanggaard, 1975) and hence, no information from the periphery is transmitted to the CNS, leading to injury. Furthermore, as the core body temperature decreases the occurrence of CIVD decreases (Daanen and Van de Linde, 1992), which increases the likelihood of cold-induced injury in

hypothermic subjects as seen in soldiers during the extreme cold weather in World War I and II (Daanen, 1991).

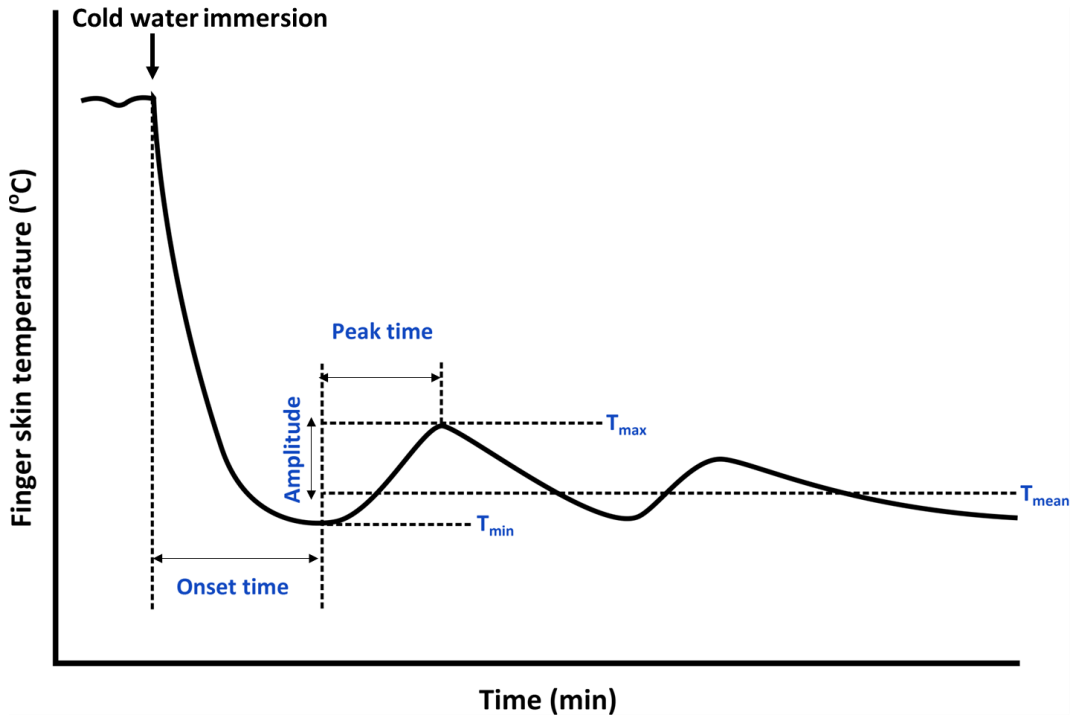

Figure 1.4 Parameters derived from a skin temperature profile of a subject's fingertip immersed in cold (5°C for 40 min) water. Finger skin temperature is the most commonly used measurement for cold-induced vasodilatation (CIVD), where a small thermocouple is attached to the palmar side of the distal phalanx with tape. The measured finger skin temperature during the active cooling period indicates the CIVD response occurring underneath the exposed cutaneous tissue. The changes in skin temperature are quantified using the terminologies (1) $\mathbf{T_{min}}$, lowest finger skin temperature before CIVD starts; (2) $\mathbf{T_{max}}$, highest finger skin temperature during CIVD; **onset time**, time from immersion to T_{min}; **amplitude**, difference between T_{min} and T_{max}; **peak time**, time interval between T_{min} and T_{max}; $\mathbf{T_{mean}}$, mean finger skin temperature over the immersion period, excluding the onset time. Diagram adapted from Daanen (2003).

1.4.2 Models of CIVD

Peripheral areas are preferred to study CIVD including elbows, knees, buttocks, palmar surfaces of the fingers, palms of the hands and the sole of the foot as all these sites generate reproducible responses of CIVD (Fox and Wyatt, 1962). In animal studies, the tail and paw are areas where the CIVD response is observed. Amongst all these sites, the skin itself plays an important role as a thermo-detector and the peripheral cold afferent nerve endings are found between the dermis and epidermis at approximately 150µm from the skin surface (Adair, 1999). Since the

1930s, various studies have investigated the mechanisms underlying CIVD as it is regarded as an effective protection against cold-induced injury. A prolonged exposure to wet cold can damage nerve and tissue, leading to pain and trenchfoot is a common example of a non-freezing cold injury (Daanen, 1991).

In a recent study, Lee *et al.* exposed the fingers of human subjects to cold (4°C) water for 30 min followed by a recovery period of 20 min. A normal pattern of the CIVD response was observed in terms of skin temperature and blood flow, with no change in rectal temperature or blood pressure parameters. However, there was an increase in finger pain sensation during the first 15 min of local cold exposure (Lee et al., 2013). The physiological responses to cooling are influenced by the exposure period or frequency and the medium of the cold exposure (air or water). The medium of the cold exposure can greatly affect the physiological responses to cold, where immersion in cold water (5-20°C) generates a greater CIVD responses than cold air (5-20°C) due to thermal conductivity, density and heat capacity (Kramer and Schulze, 1948). The Hunting reaction is not observed at a temperature greater than 15°C (Hirai et al., 1970, Lewis, 1930), and the optimal temperature for investigation is 5°C (Hirai et al., 1970). The cold water temperature used in most studies range from 0°C to 8°C, and earlier studies used ice (0°C) water with latest studies now focussing more on temperatures above 5°C which is known to generate less pain (Sendowski et al., 1997). The CIVD response is also known to be influenced by various factors including age, gender, physical fitness, mental stress, cold resistance training, diet, alcohol ingestion and tobacco smoking (Daanen, 2003).

The methods currently used to quantify the amount of vasodilatation following local cold exposure include indirect measurements of the diameter of blood vessels such as (1) strain gauge plethysmography, (2) laser Doppler flowmeter and (3) skin temperature (Daanen, 2003). The strain gauge plethysmography is the technique where a cuff is placed and inflated proximal to the measuring site where blood enter and gets trapped into the measured extremity. During this phase, there is a linear increase in the circumference as an indication of increase blood flow (Elkington, 1968).

The skin blood flow has a role in thermoregulation and is an important determinant of changes in the circulation following local cold exposure, and human skin blood flow is known to drop to nearly zero following whole body or local cooling and increase up to 8L/min (~60% cardiac output) in heat stress conditions (Charkoudian, 2010). The laser Doppler flowmeter is widely used to measure local skin blood flow, where the emitted laser light from an optic fibre probe is back scattered from moving red blood cells and creates a shift in frequency, known as the Doppler shift. There was debate in the literature regarding the penetration depth of the laser in

the skin (Daanen, 2003), but this has now been addressed with the development of new laser Doppler systems which is known to penetrate a depth of 1-2mm(Choi and Bennett, 2003). Moreover, a good relationship has been observed between laser Doppler flow and forearm blood flow (Johnson et al., 1984).

It is generally accepted that the skin temperature in the hands and digits is strongly correlated with cutaneous blood flow, although blood flow itself has a themoregulatory component mediated by 80-90% of AVAs (Figure 1.5) and a nutritional component mediated via 10-20% of the capillary system (Iwase et al., 2002, Niehof et al., 2006, Ruch et al., 2003). According to the CIVD literature, skin temperature has been the most widely used method to quantify changes in cutaneous blood flow responses following cold water immersion. This method relies on attaching a small thermocouple to the palmar side of the distal phalanx finger or the nail bed with a tape, and hence the temperature is a mixture reading of the finger skin temperature and the temperature of the surrounding cooling medium. The changes in skin temperature have been quantified using different terminologies as illustrated in Figure 1.4 (Daanen, 2003). It is important to note that the characteristics of the Hunting skin temperature response curve may be influenced by the ambient or core body temperature (Daanen et al., 1997), as a strong relationship has been demonstrated between body temperature and CIVD response (Daanen et al., 1997, Flouris and Cheung, 2009). Flouris *et al.* showed that oscillatory changes in finger blood flow in human subjects were related to core body temperature (Flouris et al., 2008).

Other factors include variability in water temperature and immersion depth, which can both influence the presence or magnitude of thermal adaptation. The surface area has also been suggested to have an influence, where a large cooled surface area may cause a greater cold stimulus (Cheung and Daanen, 2012).

The rabbit ear is another established model for studying control mechanisms such as vascular function, structure and control of cutaneous thermoregulatory blood flow, similar to those in human digital circulation (Grant, 1930, Grant, 1931). The rabbit ear model permits direct microvascular observations of AVAs (Pollock et al., 1997) and is known to exhibit cyclic increases and decreases in blood flow, as observed in the human digits (Grant, 1930, Grant, 1931). There was an overall reduction in blood flow and cutaneous perfusion in the ear similar to the responses observed in human studies, following a cold thermal stress (5-8°C for 10 min) in rabbit ears (Smith et al., 1994). This may be due to the similarities in digital and auricular vascular receptors and receptor subtypes. It is important to note that the ear microvasculature consists of the complex existence of α_1-, α_2-, and β-adrenergic receptors that may all be involved in inducing the biphasic vascular response of different adrenergic receptors.

The rat tail is also used as a model to investigate CIVD as it can develop some of the pathological conditions during and following cold exposure similar to observations in the human fingers and the rat tail demonstrates the cycles of CIVD during cold water exposure (Eide, 1976, Gardner and Webb, 1986). Thomas *et al.* further showed that cold induced alteration of cutaneous blood flow as assessed by laser Doppler flowmeter in the rat using a non-freezing cold injury model at a temperature of 1°C. The tail exhibits changes of loss of thermal sensitivity followed by enhanced thermal sensitivity and, can also manifest several characteristics of neural dysfunctions (Thomas et al., 1994).

The first *in vitro* model of the Hunting response was characterised by Gardner & Webb (1986) using isolated, perfused rat tail arteries in an organ bath when the arteries were cooled to 4-12°C. Cooling the bath caused a decrease in the flow of arteries and this was followed by a dilation phase. This response was further followed by flow oscillations of prolonged low flow and brief periods of high flow (Gardner and Webb, 1986). They showed that acute nerve denervation with 6-hydroxydopamine was able to block cooling-induced responses (Gardner and Webb, 1986). This method was later used by other studies to examine the mechanisms underlying cold-induced responses (Chotani et al., 2000).

Although CIVD has been extensively studied for >80 years, there are limitations in the clarity of reported primary studies in terms of protocols and definitions, and hence it is difficult to compare results across studies. Although understanding the CIVD nature is important and relevant clinically to protect against local cold-induced injury, the mechanisms underlying the CIVD response remain unclear or largely speculative and this will be discussed in the next section.

1.4.3 Mechanisms of CIVD

The mechanisms following local cold exposure was suggested to involve the generation of an action potentials in the peripheral cold fibre which release vasodilator substances from the peripheral nerve endings (Lewis, 1930). Lewis (1930) illustrated using denervation experiments that the CIVD response was dependent on an axon reflex. However, later studies questioned this theory as they failed to observe complete inhibition of CIVD in their experiments (Greenfield et al., 1951a, Keatinge, 1957, Keatinge, 1961), and this could have been as a result of the experimental set up. Hence, the proposed mechanisms for CIVD include (1) the involvement of axon reflex, (2) paralysis of the AVAs and the release of an unknown dilating substance in the blood (Aschoff, 1944), (3) blockade of the sympathetic nervous system or (4) effects of cold on the vascular smooth muscle activity (Shepherd et al., 1983, Gardner and Webb, 1986). Recent

evidence on CIVD in experiments using spinal cold stimulation suggest that spinal cord-induced cutaneous vasodilatation in the cooled (<25°C) hindpaw of rats is mediated via a reduction in efferent sympathetic activity or the activation of sensory nerves antidromically which releases vasodilators (Tanaka et al., 2003).

The next section will discuss the proposed mechanisms that are still subject to debate in further detail.

1.4.3.1 The involvement of axon reflex in CIVD

The axon reflex or antidromic vasodilatation theory consists of a reaction whereby cold stimuli can excite receptive endings of unmyelinated neurons in the skin and the evoked impulses are transmitted centrally and antidromically via the axon branches. This leads to an inhibition of the sympathetic nerve communication to the AVAs, and the release of vasoactive substances from the excited sensory nerve endings, which causes vasodilatation (Lewis, 1930, Hornyak et al., 1990). Lewis' theory was based on studies where it was clearly illustrated that CIVD was still present shortly after sympathectomy but completely absent after complete degeneration of peripheral nerves (Lewis, 1930).

Nevertheless, this theory has been questioned by other studies as Greenfield *et al.* observed that CIVD was present, although with reduced amplitude although in several patients without somatic innervation when compared to healthy subjects (Greenfield et al., 1951b). Furthermore, Daanen and Ducharme (2000) have used strong and painful electrical stimulation to evoke axon reflexes in the skin of a cold hand during the hunting reaction in human subjects. They showed a clear axon reflex in the warm hand but no observation of any axon reflex in the cold hand, as shown in experiments using laser Doppler flowmeter. Hence, it was suggested that axon reflex may not be the primary drive for CIVD (Daanen and Ducharme, 2000).

However, the early initial vasoconstriction following cold exposure is dependent on both intact sympathetic and sensory function, suggesting an involvement of an axon reflex (Johnson et al., 2005). This theory will be further investigated in the current PhD project by studying the role of neuropeptides in cold-induced vascular responses, as generation of axon-reflexes in the terminals of primary afferent neurons is known to release neuropeptides and induces vasodilatation.

1.4.3.2 The role of AVAs and the release of a dilator substance in CIVD

Blood vessels in the subcutis, also known as AVAs form a direct connection between arterial and the venous system and have been suggested to be involved in the underlying mechanisms mediating the CIVD response. In thermoneutral conditions, AVAs constrict 2/3 times per min causing rapid changes in blood flow (Figure 1.5). Following local cold exposure, AVAs dilate, resulting in blood flowing through this shunt and warming the tissue, playing an important role in thermoregulation. The 'Hunting response' in CIVD is thought to be due to the rhythmic relaxation and contraction of the strong muscular wall of the AVAs (Daanen, 1991). The number of AVA is not constant as it increases as local blood supply in the periphery increases and once, the stimulus is removed the number of AVAs decreases (Hale and Burch, 1960). Apart from having a role in thermoregulation, AVAs may also affect blood pressure and blood distribution as they are well distributed in the skin (Ciara, 1939, Hale and Burch, 1960).

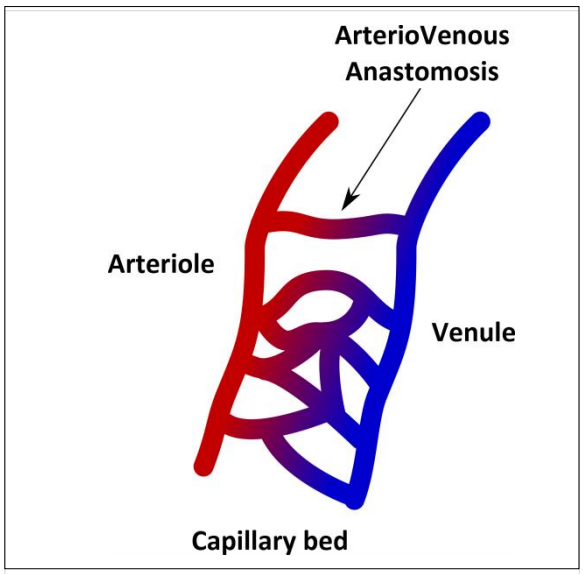

Figure 1.5 Schematic diagram illustrating arteriovenous anastomosis Arteriovenous anastomose (AVA), also known as 'shunt' regulate blood flow and is thought to be the primary mechanical regulator of cold-induced vascular response (CIVD). AVAs are relatively small vessels with a diameter of 10µm, which are present to connect the arteriole directly to a venule, before the arterioles break up into capillary beds. There are numerous AVAs in the ears and skin of mammals (Clara, 1959, Braverman, 1997).

CIVD has been suggested to be caused by the dilation of AVAs. Below a skin temperature of 35°C, AVAs constrict whilst below 21°C, AVAs remain closed to conserve heat (Edwards, 1967, Grant, 1931, Bergersen et al., 1997). AVA vasomotion has been suggested to be due to a dilating substance in the blood which is formed when the local temperature decreases under a certain threshold, and the increase in blood flow further washes the substance away (Aschoff, 1944). The concentration of the substance is thought to be dependent on the temperature of cold exposure and the vasodilatation is dependent on intact peripheral nerves. This further suggests that the vasodilating substance may be released from the peripheral nerves.

Interestingly, cooling has been shown to reduce adrenergic activation-induced contraction (Garcia-Villalon et al., 1992) and increase the release of the potent vasodilator nitric oxide in the endothelium of cutaneous blood vessel of rabbit ears, but not in deep arteries following

cholinergic stimulation (Fernandez et al., 1994). During the dilatation component of the CIVD response, it is known that the skin temperature starts to increase to return near to baseline values. Interestingly, nitric oxide has been shown to play an important role in sustained cutaneous vasodilation during prolonged local heating (Charkoudian, 2010, Kellogg et al., 1999). Local heat has been shown to cause shear-mediated nitric oxide release, which produces a vasodilatory response (Widmer et al., 2006). The nitric oxide synthase (NOS) enzymes, especially neuronal NOS (nNOS) and inducible NOS (iNOS) are known to be temperature sensitive and hence, the activity of NOS enzymes might be reduced by mild cooling (Venturini et al., 1999). Nitric oxide production was hypothesised to be enhanced by local cooling in the early non-adrenergic vasodilatation phase of CIVD and/or reduced during the non-adrenergic vasoconstriction phase (Yamazaki et al., 2006). Yamazaki *et al.* further showed that the initial phase of vasoconstriction observed following local cold exposure may be due to nitric oxide system inhibition, as shown in studies using the non-selective NOS inhibitor N-nitro L-arginine methyl ester (L-NAME). Pre-treatment with L-NAME was shown to reduce basal blood flow by reducing tonic nitric oxide production and reduce non-adrenergic vasoconstriction during prolonged cooling, without any major changes in non-adrenergic vasodilatation in the early phase of cooling (Yamazaki et al., 2006).

Furthermore, Hodges *et al.* showed that cooling (24°C)-induced responses in the skin of human subjects were similar in sites treated with L-NAME. The addition of nitric oxide with exogenous sodium nitroprusside to the L-NAME treated sites was demonstrated to restore cutaneous blood flow to its original baseline. Local cooling-induced vasoconstriction was absent in sites pre-treated with L-NAME without nitric oxide supplementation. These results showed that in addition to increased noradrenaline release, NOS inhibition play a role in driving the local cold exposure response (Hodges et al., 2006).

It may be worth highlighting that other vasodilator mediators in addition to nitric oxide may be involved in cold-induced vascular response, which currently needs further investigation and will be addressed in this current PhD project.

1.4.3.3 Role of adrenergic nerves in CIVD

The sympathetic nervous system can modulate blood flow. The cold pressor test, which involves the immersion of human subjects' hand in cold water, is known to cause a propounded physiological response, which includes activation of the sympathetic nervous system (Monahan et al., 2004, Victor et al., 1987, Robertson et al., 1979). The responses include an increase in arterial blood pressure and myocardial oxygen demand, which is linked to coronary

vasodilatation (Antony et al., 1994, Dubois-Rande et al., 1995). Sympathetic stimulation has been previously shown to alter the CIVD response but it also appears to be influenced by local cooling, independently of the general sympathetic stimulation (Sendowski et al., 2000).

Eliminating the sympathetic drive is known to be hard to accomplish without adverse side effects in humans and hence, Smits *et al.* investigated the role of the sympathetic system in rat paws using a spared nerve injury model (SNI) and complete sciatic lesion (CSL) model (Smits et al., 2013a). In that study, there were no changes in the CIVD reaction patterns between CSL, SNI and sham-operated rats. This implies that the vascular control may function without peripheral nerve innervation and perhaps, local factors such as norepinephrine have more influence (Smits et al., 2013a).

The theory suggests that there is a decrease in norepinephrine release from adrenergic nerve endings. Using the *in vitro* model of CIVD, Gardner and Webb showed that CIVD did not occur in the rat tail when norepinephrine was continuously perfused, leading to vasoconstriction which suggests that CIVD may only be achieved by reducing transmitter release from adrenergic nerve endings (Gardner and Webb, 1986). Earlier studies by Keatinge (1961) showed that following ice-water immersion, CIVD was still present in the index fingers of human subjects pre-exposed to ionophoresis of adrenaline (Keatinge, 1961). This suggests that a major cause of cold-induced vasodilatation is impairment or loss of vascular response to constrictor hormones at near freezing point, and a higher concentration of adrenaline is required to cause maximal contraction of the blood vessels.

In human fingers, cooling was shown to augment α_2-adrenergic but suppresses α_1-adrenergic vasoconstriction to noradrenaline, whereas warming produces the opposite effects (Freedman et al., 1992). Using isolated saphenous veins of the dog, Rusch *et al.* showed that cooling (10-20°C) depresses venous smooth muscle contractility and between the temperature 5 and 10°C the adrenergic neurotransmission was interrupted (Rusch et al., 1981). This data provides more evidence showing that the continued affinity for noradrenaline combined with neurotransmitter inhibition, which may allow the cutaneous veins to constrict during severe cold exposure (Rusch et al., 1981).

The local cooling vasoconstrictor response is known to be dependent on intact noradrenergic cutaneous active vasoconstrictor nerves (Johnson et al., 2005). The pharmacological blockade of neurotransmitter release from sympathetic vasoconstrictor nerves using bretylium reversed the initial phase of local cooling-induced vasoconstriction into a vasodilatation response in the cutaneous vasculature (Johnson et al., 2005, Pergola et al., 1996, Pergola et al., 1993).

Furthermore, the pharmacological blockade of α- and β-adrenergic receptors was also shown to reverse cooling-induced vasoconstriction as cooling continues (Johnson et al., 2005). It is well established that there is a decrease in the release of norepinephrine with an increased sensitivity of noradrenergic receptors following local cold exposure and this results in a reduction in blood flow and tissue temperature. This may lead to reduce noradrenergic neurotransmission and as a consequence, there is an increase in blood flow (Gardner and Webb, 1986, Daanen, 2003, Ji et al., 2007).

1.4.3.4 Vascular smooth muscle activity

The vasoconstrictor response following local cold treatment is necessary to reduce heat loss, and usually results from a reflex increase in sympathetic output, with the release of noradrenaline and a direct increase in noradrenaline activity on adrenergic receptors. Earlier evidence suggests that the smooth muscle activity induced by the simulation of α-adrenergic receptors may be depressed or even abolished when the tissue temperature is reduced to low levels and a nervous blockade occurs, leading to a vasodilatation response (Folkow et al., 1963, Shepherd et al., 1983). Several studies by Keatinge *et al.* showed that low tissue temperature enhances vasoconstriction and below a certain threshold, this inhibited contractility by interfering with the crossbridge formation (Keatinge, 1970, Keatinge, 1980). Hence, increased blood flow to the finger and raised skin temperature during CIVD are dependent on smooth muscle cells relaxation (Bergersen et al., 1999).

Following on from this earlier evidence, studies by Bailey focussing on the Rho effector, Rho kinase have further aided us to understand the mechanism underlying cold-induced vasoconstriction in the vascular smooth muscle cells (Bailey et al., 2005). Rho belongs to the Ras family of small GTP-binding proteins and is known to cycle between a GDP-bound inactive state and a GTP-bound active state, and regulate actin/myosin-dependent processes in the vascular smooth muscle cells (Somlyo and Somlyo, 2003). Smooth muscle myosin ATPases are activated by actin after phosphorylating regulatory myosin light chains (MLC) by a calcium-calmodulin-dependent MLC kinase (MLCK). Conversely, smooth muscle myosin ATPases are inactivated after dephosphorylating MLC by a calcium-independent MLC phosphatase (MLCP) mechanism. Rho kinase is known to inhibit MLCP, increasing MLC phosphorylation and causing vascular smooth muscle contraction, and this mechanism is widely known to be present in various vascular beds (Somlyo and Somlyo, 2003).

Moderate cooling to 28°C was shown to generate mitochondrial reactive oxygen species and activate the Rho kinase, which further enables translocation of the silent α_{2C}-adrenergic

receptors to the plasma membrane and increase calcium sensitivity of the contractile response, in cutaneous arteries from mouse tail arteries (Bailey et al., 2004, Bailey et al., 2005) and equine digital veins (Zerpa et al., 2010b, Zerpa et al., 2007, Zerpa et al., 2010a). Interestingly, 17β-oestradiol was shown to increase α_{2C}-adrenergic receptors expression and selectively increased cold-induced amplification of α_{2C}-adrenergic receptors induced constriction in isolated mice tail arteries (Eid et al., 2007). This finding in turn suggests that there is an increase in cold-induced vasoconstriction activity under oestrogen-replete conditions that may be an important mechanism in studying Raynaud's phenomenon. Raynaud's phenomenon is characterised by excessive reduced blood flow in response to local cold exposure and it is more common in female than male subjects (Roustit et al., 2011).

It is evident from these findings that VSMC play an important role in cold-induced vasoconstriction, which is known to cause local vascular injury. The current PhD project will use this known mechanism to evaluate if TRPA1 may drive this cold-induced vasoconstrictor response in the vasculature via the involvement of α_{2C}-adrenergic receptors.

1.4.4 Recent research advances and future direction of cold-induced responses

Spinal cord stimulation in patients with peripheral vascular diseases such as ischemic leg pain can result in beneficial pain relief effects and this is largely secondary to increase in blood flow in the lower extremities (Linderoth et al., 1995). However, the mechanisms underlying this response remain unknown but Linderoth *et al.* speculated that there is a reduction in efferent sympathetic activity and/or activation of sensory nerves antidromically, which in turn releases vasodilators (Linderoth et al., 1995, Linderoth et al., 1991, Linderoth et al., 1992, Linderoth et al., 1994). Skin temperature has been suggested to have an effect on the mechanisms underlying spinal cord stimulation nerve (Tanaka et al., 2003).

Interestingly, spinal cold stimulation-induced cutaneous vasodilatation in the cooled (<25°C) hindpaw of rats at 60% motor threshold was shown to be mediated by CGRP, as shown in experiments using the CGRP receptor antagonist $CGRP_{8-37}$. CGRP was released via antidromic stimulation of the sensory nerves only rather than activation of the sympathetic nerve (Tanaka et al., 2003). This results overall suggest that both nerves are involved in the cold-induced response but greatly depends on the level of cutaneous sympathetic activity. The contraction phase is probably caused by stimulation of α-adrenergic receptors in the smooth muscle wall and the relaxation may be caused by a nervous blockade of the sympathetic system. In contrast, spinal cold stimulation-induced cutaneous vasodilatation in the moderate cooled (25-28°C) hindpaw of rats at 60% motor threshold moderate was predominantly mediated via sensory

afferent fibres. This is one of the first pieces of scientific evidence showing the important role of the humoral mediator CGRP in cold-induced responses, and this will be further investigated in the current PhD project.

The earlier section focussed on the role of CIVD, which is the blood flow responses observed during active local cooling period. Interestingly, other studies have also investigated the dynamic vascular responses following the active cooling period, which is generally believed to be characterised as rewarming (Smits et al., 2013b). However, this remains a debatable issue in the literature. The clear difference between the Hunting response in CIVD and rewarming is that the Hunting response consists of a cyclic oscillation in blood flow induced by vasoconstrictionand vasodilatation that occurs in extremities on cold exposure (Lewis, 1930), whilst rewarming consists of a vasodilator response which stabilises for $\pm$ 10 min, without any observations of either vasodilation or vasoconstriction for up to 20 min (Ruijs et al., 2009, Hu et al., 2012). Rujis *et al.* showed that following cold (14-15°C) stress testing in median or ulnar nerve injury patients, there was an active rewarming phase due to vasodilatation after cold exposure, and this active rewarming is disturbed in patients with peripheral nerve injury (Ruijs et al., 2009). In rats, Hu *et al.* showed that following cold (0°C) stress, which consisted of immersing both hindpaws in cold water for 5 min, there was a rapid decrease in blood perfusion, which eventually returned to basal level at about 10 min following the cold stress (Hu et al., 2012).

As detailed above, it is evident that there are clear different patterns in blood flow responses during and following the active cooling period, and hence, understanding the mechanisms underlying the phenomenon of both responses is important. Indeed, it is clear from the information summarised in this chapter that cold-induced vascular response is complex and involves an integrated system with the involvement of both sensory and sympathetic nervous system. No studies to date have directly investigated all the proposed theory in one specific cold model in the peripheral vasculature *in vivo* and hence, this thesis will address this issue and investigate the mechanism underlying cold-induced vascular response, with a potential link to TRPA1.

1.5 Aims

The aims of this PhD project were to determine the role of TRPA1 in the regulation of vascular blood flow, and to investigate the signalling mechanisms underlying TRPA1-mediated vasodilatation. It is hypothesised that cinnamaldehyde and cold activate TRPA1 in the peripheral vasculature to mediate changes in blood flow.

The specific aims of this project are to:

1. Utilise a murine ear model to investigate the effects of an exogenous TRPA1 agonist cinnamaldehyde in quantitative terms of blood flow responses in studies using genetically modified mice and pharmacological inhibitors.

2. Investigate the mechanisms underlying TRPA1-dependent vascular mechanisms especially relative to cinnamaldehyde, using a pharmacogenetic approach in the mouse ear model.

3. Develop and characterise a local acute model of cold-induced vascular response *in vivo* in the mouse hindpaw to measure cutaneous blood flow and skin temperature.

4. Investigate the involvement of TRPA1, sensory nerves, sympathetic nerves and reactive oxygen species in cold-induced vascular response, in terms of blood flow responses in the mouse hindpaw using genetically modified mice and pharmacological inhibitors.

5. Investigate the roles of TRPA1, CGRP, adrenergic receptors, superoxide and Rho-kinase signalling in mediating the vasoconstrictor or vasodilator component of the cold-induced vascular response.

Chapter 2 – Materials & Methods

Chapter 2 – Materials & Methods

2.1 Animals

All experiments were conducted in accordance with the UK Home Office Animals (Scientific Procedures) Act, 1986 and were approved by the King's College London Animal Care and Ethics Committee. Male and Female CD1 mice (20-30g, 8-12 weeks of age) were purchased from Charles River, UK. Mice were housed in in groups of up to 5 animals in a climatically controlled environment (22 ± 2°C), on a 12 hour light (7am-7pm)/dark (7pm-7am) cycle, with free access to a normal diet and water *ad libitum*. A range of transgenic mice was utilised and their details are documented in section 2.2. Mice of both genders were used for characterisation studies with cinnamaldehyde and analysed for gender differences. No differences were observed between gender, as shown in Figure 3.1B. Male mice were used for all studies investigating cold-induced vascular responses. Transgenic mice were sex- and age-matched with their respective WT mice.

Anaesthesia for non-recovery procedures was induced by an intraperitoneal (*i.p.*) injection of a combination of ketamine (75 mg/kg) (Vetlar, Pfizer) and medetomidine (1mg/kg) (Domitor, Pfizer) in saline. A surgical level of anaesthesia was maintained throughout procedures and assessed by the absence of a withdrawal reflex upon pinching of a hindpaw or the tail.

27G needles were used for intravenous (*i.v.*) injection, 25G needles for *i.p.* and subcutaneous (*s.c.*) injection, and 30G (BD Micro-Fine insulin syringes, 0.3ml) for intraplantar (*i.pl*) injection into the hindpaw. At the end of experiments, mice were euthanised by cervical dislocation, a recognized schedule 1 method.

2.2 Generation of transgenic mice

2.2.1 Generation and genotyping of TRPA1 KO mice

TRPA1 WT and KO mice were gifted by Professor Stuart Bevan (King's College London, UK). TRPA1 KO mice were generated by replacing the exons encoding the 5th and 6th transmembrane domain including the interconnecting pore loop which contains the selectivity filter of TRPA1 with a cassette containing an internal ribosome entry site (IRES) and a human placental alkaline phosphatase gene (PLAP) and a polyadenylation sequence as described previously by Kwan *et al.* (Kwan et al., 2006). Since a truncated product of the TRPA1 gene may still be present and cause unwanted side effects, an endoplasmic reticulum (ER) retention signal encoded by the amino acid sequence KDEL and a stop codon were placed in the frame with the exon before the IRES PLAP cassette (Kwan et al., 2006). Any potential product translated from the TRPA1 gene was sequestered by the endoplasmic reticulum. The vector was then transfected into a

mouse embryonic stem cell line where they were injected in blastocysts to generate male chimeric mice. These mice were mated with C57BL/6J or B6129PF2/J to produce heterozygote animals, which were subsequently intercrossed (Kwan et al., 2006).

Genotyping of the mice was carried out using endpoint polymerase chain reaction (PCR). Genomic DNA was extracted from ear punches or tail snips using commercially available REDExtract-N-AMPTM Tissue PCR kit (Sigma Aldrich, UK) and PCR was performed on the TRPA1 gene or the cassette using the following primers (Euofins Scientific, Europe). The PCR reaction mixture was made up as illustrated in table 2.1.

TRPA1 WT forward: 5'-TCC TGC AAG GGT GAT TGC GTT GTC TA-3'
TRPA1 WT reverse: 5'-TCA TCT GGG CAA CAA TGT CAC CTG CT-3'
TRPA1 KO forward: 5'-CCT CGA ATC GTG GAT CCA CTA GTT CTA GAT-3'
TRPA1 KO reverse: 5'-GAG CAT TAC TTA CTA GCA TCC TGC CGT GCC-3'

A thermal cycler (PTC-225 Peltier Thermal Cycler, MJ Research, USA) was used to denature the DNA and activate the Taq polymerase for 2 min at 94°C, then 34 cycles of 94°C for 30s, 64°C for 30s, 68°C for 30s were used to amplify the gene of interest. The amplified product was then held at 4°C until visualised and analysed by gel electrophoresis on an agarose gel (1.8% w/v, Sigma Aldrich) in tris/borate/ethylenediaminetetraacetic acid (TBE; Biorad, UK) with images captured under an ultraviolet (UV) camera (Syngene, G-Box). WT bands are located at 310bp and TRPA1 KO bands at 200bp. Both bands are present in heterozygous animals.

Component	**Volume per reaction (µl)**
TRPA1 WT forward (10µM)	0.4
TRPA1 WT reverse (10µM)	0.4
TRPA1 KO forward (10µM)	0.4
TRPA1 KO reverse (10µM)	0.4
Genomic DNA sample	4
REDExtract-N-AMP PCR Readymix™	10

Table 2.1 Endpoint PCR reaction mixture listillustrating the different constituents and volumes required per sample for TRPA1 genotyping.

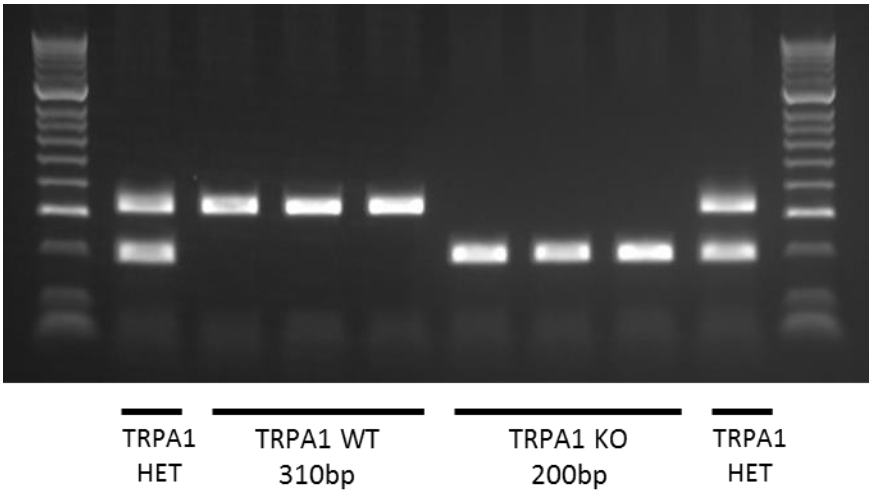

Figure 2.1 Agarose gel illustrating the location of TRPA1 WT and KO DNA. A DNA ladder, shown both on the right and left of the gel was used to determine the size of the bands. The heterozygote genomic DNA displays a band at both the WT (310bp) and KO (200bp) bands.

2.2.2 Generation and genotyping of TRPV1 KO mice

TRPV1 WT and KO mice were gifted by Merck, Sharpe and Dohme (The Neuroscience Research Centre, Essex, UK). The TRPV1 KO mice were generated by deleting the exon encoding part of the 5th and all of the 6th putative transmembrane domains of the TRPV1 channel, together with the pore-loop region. This was replaced with the phosphoglycerine kinase-neomycin (pGK-neo) gene as previously described (Caterina et al., 2000). The TRPV1 gene is known to be located on the somatic chromosome (11B3). The construct was electroporated into 129X1/SvJ-derived JM1 embryonic stem cells and injected into C57BL/6J blastocysts. The resulting chimeric animals were crossed to C57BL/6J female mice to produce heterozygote animals, which were subsequently intercrossed. Matings between TRPV1 heterozygous mice can produce offsprings with the expected Mendelian distributions of gender and genotype. TRPV1 KO mice were shown to be fertile, viable and largely indistinguishable from WT littermates, without observed differences in general appearance, gross anatomy, body weight, locomotion and overt behaviour (Caterina et al., 2000).

Genotyping of the mice was carried out using endpoint PCR. Genomic DNA was extracted from ear punches or tail snips using commercially available REDExtract-N-AMPTM Tissue PCR kit (Sigma Aldrich, UK) and PCR was performed on the TRPV1 gene or the cassette using the following primers (Euofins Scientific, Europe). The PCR reaction mixture was made up as illustrated in table 2.2.

TRPV1 WT forward: 5'-CGA GGA TGG GAA GAA TAA CTC ACT G-3'
TRPV1 WT reverse: 5'-GGA TGA TGA AGA CAG CCT TGA AGT C-3'
Neomycin forward: 5'-TTT TGT CAA GAC CGA CCT GTC C-3'
Neomycin reverse: 5'-CCC TCA GAA CTC GTC AAG AAG-3'

A thermal cycler (PTC-225 Peltier Thermal Cycler, MJ Research, USA) was used to denature the DNA and activate the Taq for 14.5 min at 95°C, then 35 cycles of 95°C for 45s, 60°C for 60s, 72°C for 60s, and the final elongation at 72°C for 60s were used to amplify the gene of interest. The amplified product was then held at 4°C and analysed by gel electrophoresis on an agarose gel (1.8% w/v, Sigma Aldrich) in TBE (Biorad, UK) with images captured under a UV camera (Syngene, G-Box). WT bands are located at 188bp and neomycin bands at 700bp, which is found in the disrupted gene in the TRPV1 KO mice.

Component	**Volume per reaction (µl)**
TRPV1 WT forward (5µM)	2
TRPV1 WT reverse (5µM)	2
Neomycin forward (5µM)	2
Neomycin reverse (5µM)	2
Genomic DNA sample	5
REDExtract-N-AMP PCR Readymix™	10

Table 2.2 Endpoint PCR reaction mixture list illustrating the different constituents and volumes required per sample for TRPV1 genotyping.

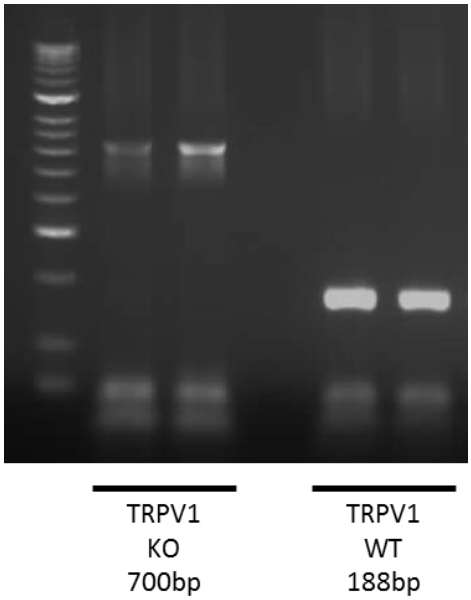

Figure 2.2 Agarose gel illustrating the location of TRPV1 WT and KO DNA. A DNA ladder, shown on the left of the gel was used to determine the size of the bands. Bands for TRPV1 WT at 188bp and KO at 700bp, representing the neomycin cassette.

2.2.3 Generation and genotyping of TRPM8 KO mice

TRPM8 WT and KO mice were gifted by Professor Stuart Bevan (King's College London, UK). The TRPM8 KO mice were generated by designing a targeting vector to replace 569bp of the genomic sequence within exons 13 and 14, encoding amino acids 594-661 within the presumptive cytoplasmic amino-terminal domain of the targeted gene with a neomycin cassette. In addition to removing the coding information, a stop codon was introduced before and a frameshift after the deleted segment (Bautista et al., 2007). TRPM8 WT (C57BL/6) and KO littermates were bred from heterozygotic mice, and matings between heterozygous animals generated siblings with normal characteristics with the Mendelian distributions for gender and genotype. The resulting TRPM8 KO mice were normal in overall appearance and viability, without any differences in core body temperature (Bautista et al., 2007).

The genotyping of the mice was carried out using endpoint PCR. Genomic DNA was extracted from ear punches or tail snips using commercially available REDExtract-N-AMPTM Tissue PCR kit (Sigma Aldrich, UK) and PCR was performed on the TRPM8 gene or the cassette using the following primers (Euofins Scientific, Europe). The PCR reaction mixture was made up as illustrated in table 2.3.

TRPM8 WT forward: 5'-CCT TGG CTG CTG GAT TCA CAC AGC-3'
TRPM8 WT reverse: 5'-GCT TGC TGG CCC CCA AGG CT-3'
Neomycin forward: 5'-TTT TGT CAA GAC CGA CCT GTC C-3'
Neomycin reverse: 5'-CCC TCA GAA CTC GTC AAG AAG-3'

A thermal cycler (PTC-225 Peltier Thermal Cycler, MJ Research, USA) was used to denature the DNA and activate the Taq polymerase for 3 min at 94°C, then 35 cycles of 94°C for 30s, 68°C for 60s, 72°C for 60s, and the final elongation at 72°C for 2 min were used to amplify the gene of interest. The amplified product was then held at 4°C until visualised and analysed by gel electrophoresis on an agarose gel (1.8% w/v, Sigma Aldrich) in TBE (Biorad, UK) with images captured under a UV camera (Syngene, G-Box). WT bands are located at 426bp and neomycin bands at 500bp which is found in the disrupted gene in the TRPM8 KO mice.

Component	**Volume per reaction (µl)**
TRPM8 WT forward (20µM)	0.6
TRPM8 WT reverse (20µM)	0.6
Neomycin reverse (20µM)	0.6
Genomic DNA sample	2
REDExtract-N-AMP PCR Readymix™	10

Table 2.3 Endpoint PCR reaction mixture list illustrating the different constituents and volumes required per sample for TRPM8 genotyping.

2.2.4 Generation and genotyping of TRPV4 KO mice

TRPV4 WT and KO mice were gifted by Dr Andrew Grant (King's College London, UK). The TRPV4 KO mice were generated by excising exon 12 of the TRPV4 gene, which codes for the pore-loop and adjacent transmembrane domains 5 and 6. This exon was flanked by *loxP* genetic elements and an adjacent neomycin selection cassette was inserted, followed by another *loxP* sites (Liedtke and Friedman, 2003). The targeting vector was electroporated into RW4 embryonic stem cells and the resulting chimeras were bred with C57BL/6 mice. Heterozygous TRPV4 mice were intercrossed to generate TRPV4 KO mice (Liedtke and Friedman, 2003). Matings between TRPV1 heterozygous mice can produce offsprings with the expected Mendelian distributions of gender and genotype. TRPV4 KO mice were shown to be fertile, viable and largely indistinguishable from WT littermates, without observed differences in

general appearance, gross anatomy, body weight, locomotion and overt behaviour (Liedtke and Friedman, 2003).

The genotyping of the mice was carried out using endpoint PCR. Genomic DNA was extracted from ear punches or tail snips using PCR extraction mixture containing Go-Taq polymerase, Go-Taq buffer, 10mM nucleotides (Promega, UK) and PCR was performed on the TRPV4 gene or the cassette using the following primers (Sigma Aldrich, UK). Primers specific for the flanking regions of the exon 12 were used to identify the genotype of the mice.

The PCR reaction mixture was made up as illustrated in table 2.4.

Long TRPV4 WT forward: 5'-CAT GAA ATC TGA CCT CTT GTC CCC-3'
Long TRPV4 WT reverse: 5'-TTG TGT ACT GTC TGC ACA CCA GGC-3'
Short TRPV4 WT forward: 5'-AGG GCG ATA AGC ATG TTC AAC AGG-3'
Short TRPV4 WT reverse: 5'-TGC ACC AAC ATG AAG GTC TGT GAC G-3'

A thermal cycler (PTC-225 Peltier Thermal Cycler, MJ Research, USA) was used to denature the DNA with different cycle temperature profiles for the long and short transcripts. For the long transcript, Taq polymerase is activated for 5 min at 94°C, then 10 cycles of denaturation at 94°C for 30s, annealing at 68°C for 90s and 72°C for 2 min, another 20 cycles of 94°C for 30s, 68°C for 90s and extension at 72°C for 2.5 min, followed by a final extension at 72°C for 10 min; and for the short transcript, Taq polymerase is activated for initial heating at 94°C for 5 min, 35 cycles of denaturation at 94°C for 30s, annealing at 65°C for 1 min and extension at 72°C for 1 min followed by final extension at 72°C for 10 min. The amplified product was then held at 4°C until visualised and analysed by gel electrophoresis on an agarose gel (1.8% w/v, Sigma Aldrich) in TBE (Biorad, UK) with images captured under a UV camera (Syngene, G-Box). WT bands are located at 251bp (short transcript) and at 2.1Kb (long transcript), and KO bands are located at 1.1Kb (long transcript) without any band for the short transcript.

Component	**Volume per reaction (µl)**
Long TRPV4 WT forward (100µM)	0.08
Long TRPV4 WT reverse (100µM)	0.08
Short TRPV4 WT forward (100µM)	0.08
Short TRPV4 WT reverse (100µM)	0.08
Genomic DNA sample	2
Extraction PCR mix	18

Table 2.4 Endpoint PCR reaction mixture list illustrating the different constituents and volumes required per sample for TRPV4 genotyping.

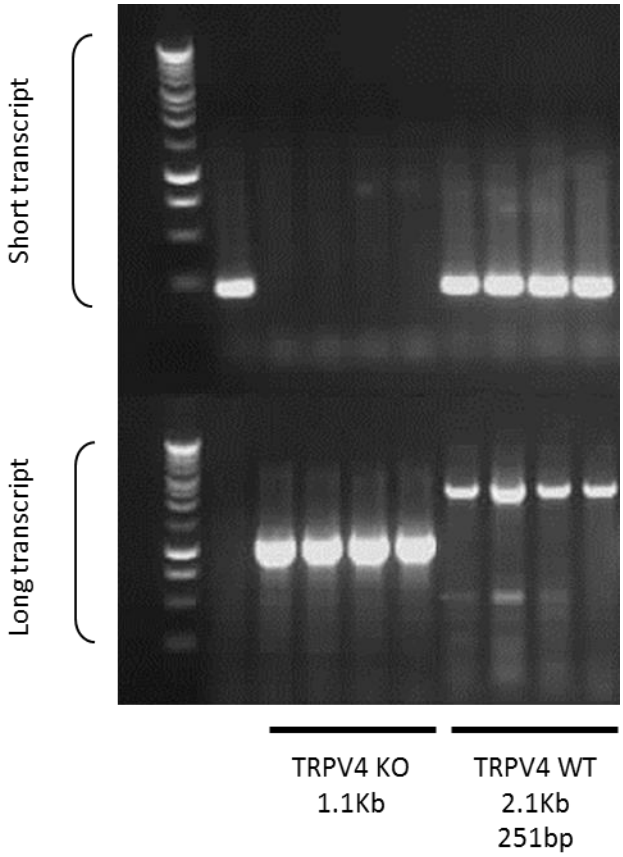

Figure 2.3 Agarose gel illustrating the location of TRPV4 WT and KO DNA. A DNA ladder, shown on the left of the gel was used to determine the size of the bands. Bands for TRPV4 WT are at 251bp (short transcript) and 2.1Kb (long transcript), and TRPV4 KO are at 1.1Kb (long transcript).

2.2.5 Generation and genotyping of α-CGRP KO mice

α-CGRP WT and KO mice were gifted by Dr Anne-Marie Salmon (Institute Pasteur, France). The α-CGRP KO mice were generated by disrupting exon 5 of the calcitonin/ αCGRP gene which is specific for α-CGRP and replaced by a cassette containing lacz/CMV/neomycin resistance genes (Salmon et al., 1999). The targeting construct was electroporated into HM1 ES cells and four clones were selected and injected into C57B1/h6 blastocysts. Following germline passage, heterozygous α-CGRP mice were obtained after crossing with the C57BL/6 strain. Heterozygous animals were interbred to generate α-CGRP WT, KO and heterozygous mice (Salmon et al., 1999). Matings between α-CGRP heterozygous mice can produce offsprings with the expected Mendelian distributions of gender and genotype. α-CGRP mice displayed normal growth and behavioural characteristics, and have been previously shown to demonstrate anti-nociceptive behaviour challenged by morphine (Salmon et al., 1999).

The genotyping of the mice was carried out using endpoint polymerase chain reaction (PCR). Genomic DNA was extracted from ear punches or tail snips using commercially available REDExtract-N-AMPTM Tissue PCR kit (Sigma Aldrich, UK) and PCR was performed on the αCGRP gene or the cassette using the following primers (Eurofins Scientific, Europe). The PCR reaction mixture was made up as illustrated in table 2.5.

Primer A: 5'-CCC CTA ATG GCC TTG TGA TTG-3'
Primer B: 5'-ACC TCC TGA TCT GCT CAG CAG-3'
Primer D: 5'-GAT GGG CGC ATC GTA ACC CGT-3'

A thermal cycler (PTC-225 Peltier Thermal Cycler, MJ Research, USA) was used to denature the DNA and activate the Taq polymerase for 5 min at 94°C, then 35 cycles of 94°C for 30s, 56°C for 30s, 72°C for 60s, and the final elongation at 72°C for 7 min were used to amplify the gene of interest. The amplified product was then held at 4°C and analysed by gel electrophoresis on an agarose gel (1.8% w/v, Sigma Aldrich) in TBS (Biorad, UK) with images captured under a UV camera (Syngene, G-Box). WT bands are located at 290bp and KO bands at 420bp. Both bands are present in heterozygous animals.

Component	**Volume per reaction (µl)**
Primer A (10µM)	2
Primer B (10µM)	2
Primer D (10µM)	2
Genomic DNA sample	4
REDExtract-N-AMP PCR Readymix™	10

Table 2.5 Endpoint PCR reaction mixture list illustrating the different constituents and volumes required per sample for CGRP genotyping.

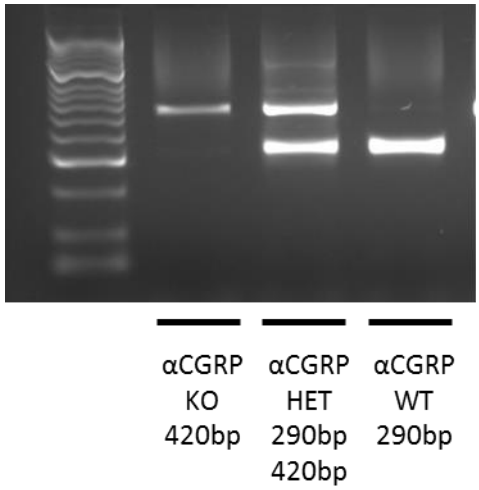

Figure 2.4 Agarose gel illustrating the location of α-CGRP WT and KO DNA. A DNA ladder, shown on the left of the gel was used to determine the size of the bands. Bands for αCGRP WT at 290bp, KO at 420bp and αCGRP HET at 290bp and 420bp.

2.2.6 Generation and genotyping of NOX4 KO mice

NADPH oxidase 4 (NOX4)WT and KO mice were gifted by Prof Ajay Shah (King's College London, UK). The NOX4 KO mice were generated by targeted deletion of the translation initiation site, and exons 1 and 2 of the gene. A 5' murine NOX4 genomic DNA fragment was isolated from a 129sv DNA BAC library and used to generate a targeting construct containing exons 1 and 2 `flanked by *loxP* sites, a negative-selection diptheria toxin A cassette and a positive selection neomycin cassette flanked by Flippase Recognition Target sites. The targeting construct was electroporated into 129sv embryonic stem cells, recombinant clones. Heterozygous mice generated from the germline chimeras were bred with C57BL/6 Cre-deletor mic and Flp-deletor mice to generate heterozygous KO mice. NOX4 KO mice were generated by intercrossing progeny and backcrossed with C57BL/6 mice (Zhang et al., 2010). NOX4 KO mice displayed normal growth and behavioral characteristics.

The genotyping of the mice was carried out using endpoint PCR. Genomic DNA was extracted from ear punches or tail snips using commercially available REDExtract-N-AMPTM Tissue PCR kit (Sigma Aldrich, UK) and PCR was performed on the NOX4 gene or the cassette using the following primers (Euofins Scientific, Europe). The PCR reaction mixture was made up as illustrated in table 2.6.

Primer A: 5'-GTT GCT GGC TTC TGC TTC TT-3'
Primer B: 5'-AAG CTT CCG ATT CCC ATT CT-3'
Primer D: 5'-CTT TGT GTG GTT GCT TAG GAG A-3'

A thermal cycler (PTC-225 Peltier Thermal Cycler, MJ Research, USA) was used to denature the DNA and activate the Taq polymerase for 2 min at 95°C, then 35 cycles of 95°C for 30s, 60°C for 30s, 72°C for 30s, and the final elongation at 72°C for 8 min were used to amplify the gene of interest. The amplified product was then held at 4°C until visualised and analysed by gel electrophoresis on an agarose gel (1.8% w/v, Sigma Aldrich) in TBE (Biorad, UK) with images captured under a UV camera (Syngene, G-Box). WT bands are located at 543bp and KO bands at 190bp. Both bands are present in heterozygous animals.

Component	**Volume per reaction (µl)**
Primer A (10µM)	0.5
Primer B (10µM)	0.5
Primer D (10µM)	0.5
Genomic DNA sample	1
REDExtract-N-AMP PCR Readymix™	12.5

Table 2.6 Endpoint PCR reaction mixture listillustrating the different constituents and volumes required per sample for NOX4 genotyping.

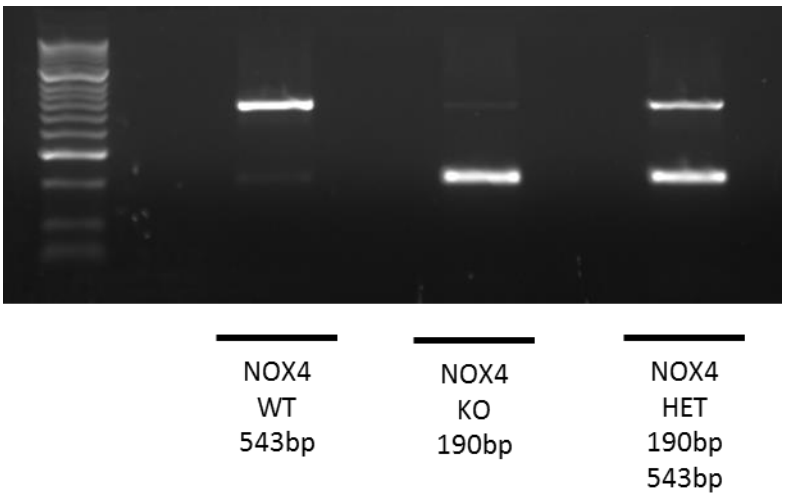

Figure 2.5 Agarose gel illustrating the location of NOX4P WT and KO DNA. A DNA ladder, shown on the left of the gel was used to determine the size of the bands. Bands for NOX4 WT at 543bp, KO at 190bp and NOX4 HET at 190bp and 543bp.

2.3 Measurement of cutaneous blood flow

Cutaneous blood flow in the mouse was assessed using a non-invasive two-channel laser Doppler flowmeter (FloLab satellite and server, Moor Instruments, UK) connected to a PowerLab data acquisition system, which measures blood flow at a single point of the blood vessel (ADInstruments, UK) (Grant et al., 2005, Grant et al., 2004) or Full-Field Laser Perfusion Imager (FLPI) (MoorFLPI, Moor Instruments, UK) which assesses blood flow in larger areas such as the whole ear or hindpaw (Starr et al., 2008, Graepel et al., 2011). Both techniques have been used widely in various basic and clinical studies as a diagnostic screening tool and to explore the microvascular control mechanisms within the cutaneous vasculature (Humeau et al., 2007a, Humeau et al., 2007b). For all blood flow measurements recorded in this study, mice were anaesthetised with ketamine and medetomidine.

For the laser Doppler flowmeter, each fibre optic VP5 probe (Moor Instruments, UK) was fixed in position over the skin with a normal laboratory manipulator by clamping onto a black acetal shank, and placed 2-3mm directly over the surface skin of each ear of the anaesthetised mouse. To ensure that measurements are consistent and comparable, each probe was placed on a blood vessel branching from the ear artery, approximately at the same point in both ears. Baseline measurements for a 5 min period ensured stability and similar flux readings from both ears (Grant et al., 2002). The laser Doppler blood flowmeter was equipped with dual channels thereby allowing simultaneous measurement of a vehicle-treated site (contralateral ear) and cinnamaldehyde-treated site (ipsilateral ear) (Figure 2.6).

The ear is known as an excellent site to study the microvascular changes, with its simplicity, low cost and high reproducibility for microcirculatory responses. The laser Doppler technique consists of the physical principle governing the behaviour of all harmonic waves known as the Doppler effect as described by Christian Johann Doppler and the set-up is summarised in figure 2.6. The Doppler probes direct a laser beam to the skin surface via optical fibres than run through the probe head. The laser penetrates the skin tissue to approximately 1mm depth and is reflected back to the probe head by the optically dense red blood cells in the cutaneous vasculature (Figure 2.6) (Vongsavan and Matthews, 1993). The reflected light has two components, where the first portion consists of light returning from stationary objects with a similar frequency as the transmitted lights, and the second portion is the reflected light off a moving object such as red blood cell and thus, undergoes a frequency shift, as dictated by the Doppler effect (Powers and Frayer, 1978, Choi and Bennett, 2003). The resultant mixing of these two frequencies of reflected light produces a “beat frequency” which is further analysed by the laser Doppler machine to generate an indirect measure of red blood cell velocity in form of a flow-related variable unit called “flux”. Flux is defined as the product of moving red cells

in a given volume and the mean net velocity of their movement (Choi and Bennett, 2003, Nilsson et al., 1980). Vasodilatation allows a greater number of red blood cells to flow at a greater speed through the laser beam thus flux increases linearly with vasodilatation. The flowmeter was calibrated weekly according to the manufacturer's instructions, using a flux standard from Moor Instruments, a suspension of polystyrene microspheres in water that move according to the rules of Brownian motion to ensure standardisation of recordings (Vongsavan and Matthews, 1993).

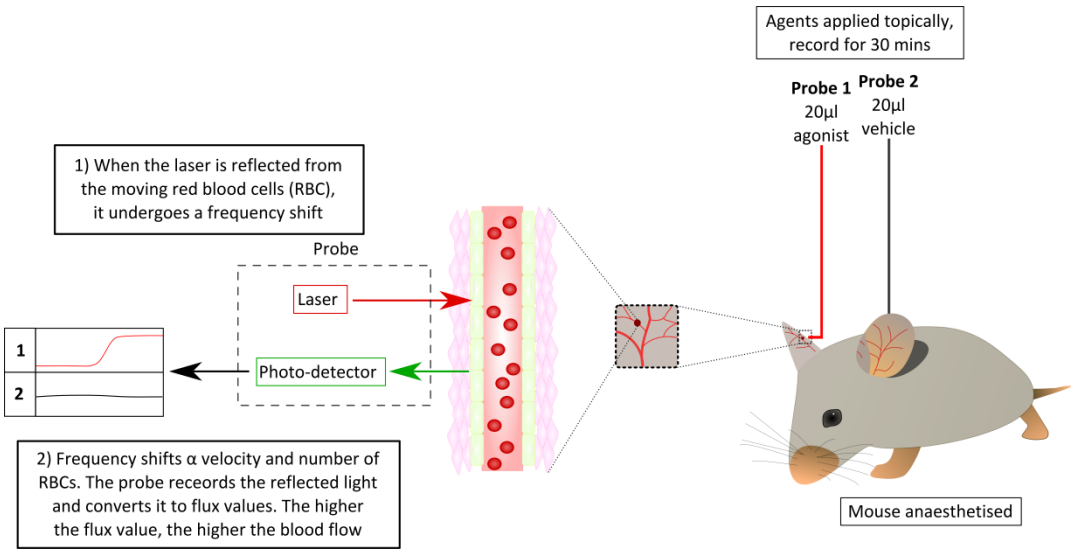

Figure 2.6 Schematic representation of the experimental set-up showing the laser Doppler flowmeter and probes, which contain the optical fibres for blood flow monitoring.

For the FLPI recordings, anaesthetised mice were placed under the scanner with the plantar aspect of the hindpaws facing upwards. The scanner was mounted 30cm above the skin surface and the exposure time of the camera was set up at 8.3ms for all experiments. The flux values were calculated from the selected rectangular regions of interest (ROI) of the whole hindpaw skin surface.

Images were collected every 1 min for up to 10 min pre-treatment, representing baseline and for up to 30 min post-treatment. Blood flow traces were created by the image processing software MoorFLPI measurement V3.0 (Moor Instruments Ltd, UK) at regular intervals of 4s. The FLPI measures to a maximum depth of approximately 1mm in skin, measuring mainly superficial blood flow and images blood vessels at the tissue surface. Laser speckle uses a random interference pattern produced by the coherent addition of scattered laser light with slightly

different path lengths. When the skin surface tissue under the scanner is illuminated with a diverging infrared beam, this penetrates the tissue to ~1mm depth, producing a granular or speckle pattern of different colours, depending on the variations in blood flow imaged by a CCD camera integrated into the scanner (Dunn et al., 2001). Both the temporal and spatial intensity variations of this pattern is known to contain information about the motion of the scattering particles and quantitative flow information. The intensity fluctuation of the speckle pattern is known to be more rapid in areas of increased blood flow. Speckle imaging has been reported to be used for accurate, high-resolution imaging of real-time assessment of dermal tissue and skin blood flow and is very simple to implement, requiring only a standard CCD camera and laser (Dunn et al., 2001).

In this study, both the laser Doppler flowmeter and laser speckle imaging were used to measure blood flow responses. Comparison studies examining the similarities and differences between both techniques have shown that there was a high correlation (R^2=0.98) in cerebral blood flow measurements in adjacent areas (Dunn et al., 2001). Measurements of flux changes in response to various treatments were made over a defined set period of 5-10 min baseline recording pre-treatment and 30 min recording post-treatment using both techniques as (Pozsgai et al., 2010).

2.4 Treatment protocols

2.4.1 Cinnamaldehyde-induced blood flow

Cinnamaldehyde was diluted in vehicle (10% DMSO in ethanol) to give a final solution of 1, 10 or 30% cinnamaldehyde and a total volume of 20µl was applied topically to the ipsilateral ear (10µl on each side of the ear). The contralateral ear was treated in a similar fashion with 20µl of vehicle, serving as a control. 10% cinnamaldehyde was shown to generate reproducible blood flow responses in preliminary studies as shown in Chapter 3 and hence, was used in subsequent experiments. This dose of cinnamaldehyde was used in previous studies evaluating the physiological effects of TRPA1 activation in humans and shown to evoke significant spontaneous pain, induced heat and mechanical hyperalgesia, cold hyperalgesia and a neurogenic axon reflex reaction (Namer et al., 2005). Blood flow was measured at baseline in the anaesthetised mice for 5-10 min and the blood flow measurement recordings were paused. Cinnamaldehyde (10%) or vehicle was applied topically on the ear and blood flow was subsequently measured for 30 min. Special care was taken not to move the mouse or probes throughout the procedure. All experiments using cinnamaldehyde administration were conducted using laser Doppler flowmetry and images were captured using the FLPI for two sets of experiment (Figure 3.1C and 3.2C).

2.4.2 Capsaicin-induced blood flow

Capsaicin was diluted in vehicle (100% ethanol) to give a final solution of 10mg/ml and a total volume of 20µl was applied topically to the ipsilateral ear (10µl on each side of the ear). The contralateral ear was treated in a similar fashion with 20µl of vehicle, serving as a control. This dose of capsaicin was shown to generate reproducible blood flow responses in previous studies (Grant et al., 2002, Starr et al., 2008) and hence, was used in this study. Blood flow was measured at baseline in the anaesthetised mice for 5-10 min, followed by the topical administration of capsaicin or vehicle on the ear and blood flow was then measured for 30 min (Grant et al., 2002). All experiments using capsaicin administration were conducted using laser Doppler flowmetry.

2.4.3 Mustard oil-induced blood flow

Mustard oil was diluted in vehicle (Paraffin oil) to give a final solution of 1% solution and a total volume of 20µl was applied topically to the ipsilateral ear (10µl on each side of the ear). The contralateral ear was treated in a similar fashion with 20µl of vehicle, serving as a control. This dose of mustard oil was shown to generate reproducible blood flow responses in previous studies (Grant et al., 2005, Fernandes et al., 2011) and hence, was used in this study. Blood flow was measured at baseline in the anaesthetised mice for 5-10 min, followed by the topical administration of capsaicin or vehicle on the ear and blood flow was then measured for 30 min(Grant et al., 2005). All experiments using capsaicin administration were conducted using laser Doppler flowmetry.

2.4.4 Cold-induced vascular responses

Previous studies have provided evidence that TRPA1 may be activated by cold (<17°C), as discussed in chapter 1. Using the TRPA1 KO mice on a similar genetic background to the ones used in our current study, Andersson *et al.* showed that cold stimuli-induced responses were significantly reduced in TRPA1 KO when compared to WT mice (Andersson et al., 2008). In this study, a model was designed to study the effects of brief local cold exposure on vascular blood flow in the hindpaw of mice using the FLPI.

Mice were anaesthetised with ketamine and medetomidine, and placed in a ventral position on a heating mat, maintained at a constant temperature of 36°C. Each hindpaw of the mouse was selected as ROI and cutaneous blood flow was assessed using the FLPI. A baseline measurement was taken for 5 min. The mouse was subsequently removed from the heating mat and the ipsilateral paw was exposed up to the level of the joint between the tibia and the calcaneum to cold water (10°C) for 5 min. In one set of experiment, the ipsilateral paw was

immersed in warm water (26°C) for 5 min. The contralateral hindpaw was left untreated at room temperature (~22°C). Hence, this protocol allowed the simultaneous assessment of blood flow responses in the cold-treated and control paws in the same mouse which minimised the influence of external factors such as the temperature of the cooling medium. Following cold water immersion, the hindpaw was dried using soft tissue paper and the mouse was placed back in its previous position with little adjustments to ROI. Care was taken to ensure that the animal was re-positioned within 1 min following the end of cold treatment and blood flow was recorded for 30 min. It is important to note here that no blood flow measurements were taken during the cold water immersion period. However, in some experiments, the skin surface temperature was measured during the cold water immersion phase (section 2.5). Mice were placed on a heating mat throughout the blood flow measurement procedure. All the experiments studying cold-induced vascular responses were conducted using the FLPI, focussing on the blood flow in the whole area of the hindpaw.

The response to cooling consisted of an initial reduction in flux, in keeping with vasoconstriction, followed by a slow developing sustained increased flux, consistent with vasodilatation. This whole response observed following treatment is termed "*cold-induced vascular response*", and is different from the Hunting response observed in previous published CIVD studies, where blood flow responses are assessed during the treatment period. Hence, in this study blood flow is being assessed before the treatment (at baseline) and after treatment (in the recovering/rewarming phase).

As discussed earlier in chapter 1, there are many factors such as age, core body temperature, ambient temperature, gender and stress that influence cold-induced blood flow or skin temperature responses (Flouris and Cheung, 2009, Daanen, 2003). All these parameters were taken into consideration in this protocol as all experiments were conducted with (1) young aged mice (8-12 weeks), (2) core body temperature was regulated by using a heating mat which also prevents the occurrence of reflex vasoconstriction in the untreated contralateral hindpaw following cold-water immersion of the ipsilateral hindpaw, (3) the ambient temperature was always kept ~22°C, (4) male mice were used for all studies although preliminary studies showed no difference in cold-induced vascular response between male and female WT mice and (5) care was taken to minimise handling stress prior to beginning the experiment.

Results are expressed as (1) arbitrary flux units measured as area under the recorded flux (response curve) vs time for the entire recording period of 30 min following cold treatment or (2) as a measure of maximum % decrease in blood flow from baseline to 2 min following cold treatment and maximum % increase in blood flow from 2 min to 30 min following cold treatment. Data analysis and representation will be further discussed in section 2.8.

2.5 Measurement of skin temperature

2.5.1 Skin surface temperature

Mice were anaesthetised with ketamine and medetomidine, as described previously and placed in a prone position where their legs and tails were stretched out onto a heating blanket and allowed to rest for 5 min. A skin surface temperature sensor was secured via a fine wire (T200KC Digitron Instrumentation, UK) on the mouse hindpaw and baseline skin surface temperature readings were recorded for 5 min at 1 min interval. Following baseline recordings, the mouse hindpaw was then immersed in cold water (10°C) for 5 min, where the skin surface temperature was continuously measured at each minute interval. Following the local cooling treatment, the mouse hind-paw was dried and changes in hind-paw skin surface temperature were monitored for 30 min at 1 min intervals. Time '0 min' represents the end of the cold treatment after the cold-treated hindpaw has been dried.

2.5.2 Subcutaneous temperature

Mice were anaesthetised with ketamine and medetomidine, as described previously and placed in a prone position, where their legs and tails were stretched out onto a heating blanket and allowed to rest for 5 min. The temperature sensitive microchip transmitter (idENTICHIP, Biothermo, UK) was implanted *s.c.* in the mouse ventral hindpaw following a small incision in the skin (~0.5 cm), which was sutured in a discontinuous pattern using 4-0 coated VICRYL™ suture (Ethicon, Johnson & Johnson, UK). Special care was taken to avoid bleeding due to blood vessel damage. Mice were monitored for the next 15 min. Baseline subcutaneous temperature readings were recorded for 5 min at 1 min intervals using a pocket reader (RE6016; Companion animal radio-frequency identification (RFID) microtransponder system; Destron Fearing, Minnesota, USA). Following baseline recordings, the mouse hindpaw was then immersed in cold water (10°C) for 5 min, where the skin *s.c.* temperature was continuously measured at each minute interval. Following the local cooling treatment, the mouse hind-paw was dried and changes in hind-paw skin subcutaneous temperature were monitored for 30 min at 1 min intervals. Time '0 min' represents the end of the cold treatment after the cold-treated hindpaw has been dried.

The temperature microchip transmitter consists of a built-in thermometer unit that is powered through an electromagnetic field generated by the pocket reader using unique digital identification numbers. The specified temperature of this reader is 24-50°C. Time '0 min' represents the end of the cold treatment after the cold-treated hindpaw has been dried.

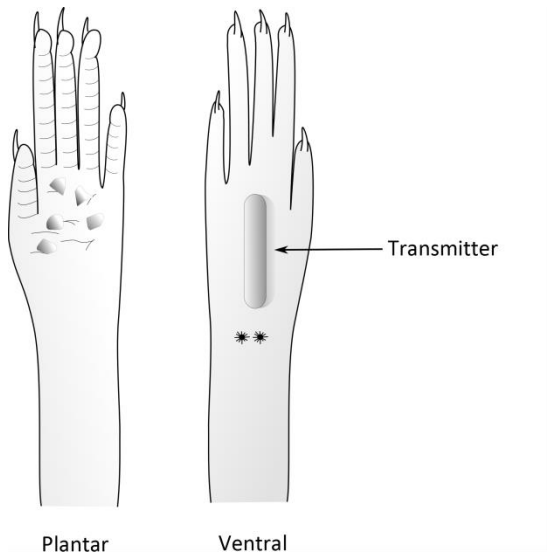

Figure 2.7 Schematic diagram illustrating the position of the temperature sensitive transmitter. The temperature sensitive microchip transmitter (idENTICHIP, Biothermo, UK) was inserted subcutaneously on the ventral side of the anaesthetised mouse hindpaw. **represents the suture sites.

2.6 Drugs administered to mice

Table 2.7 List of doses of drugs with their respective vehicle that were administered to mice. All drugs were prepared fresh on the day of use. Volume of drugs administered for intravenous (*i.v.*) and subcutaneous (*s.c*) are 5µl/g, intraperitoneal (*i.p.*) is 10µl/g and intraplantar (*i.pl.*) is 50µl/paw.

Drug	Dose	Route of administration	Vehicle	Source	References
1400W	3mg/kg or10mg/kg	*i.v.*	saline	Sigma Aldrich	(Raimura et al., 2013)
AMTB	10mg/kg	*i.p.*	10% DMSO in saline	Gifted: Prof.Bevan, UK	(Lashinger et al., 2008)
AMG9810	50mg/kg	*i.p.*	2% DMSO in saline	Sigma Aldrich	(Gavva et al., 2005)
Apocynin	20mg/kg	*i.v.*	saline	Sigma Aldrich	(Starr et al., 2008)
BIBN4096BS	0.3mg/kg	*i.v.*	saline	Tocris	(Starr et al., 2008)
Catalase	25000U/kg	*i.v.*	saline	Sigma Aldrich	(Starr et al., 2008)
Capsaicin	10mg/ml	Topical (20µl)	ethanol	Sigma Aldrich	(Grant et al., 2002, Starr et al., 2008, Grant et al., 2005)
$CGRP_{8-37}$	400nmol/kg	*i.v.*	saline	Sigma Aldrich	(Grant et al., 2002, Starr et al., 2008)
Cinnamaldehyde	10%	Topical (20µl)	10% DMSO in ethanol	Sigma Aldrich	(Namer et al., 2005)
Deferoxamine	25mg/kg	*i.p.*	saline	Sigma Aldrich	(Starr et al., 2008)
EMLA	2.5% lidocaine + prilocaine	Topical (5min)	N/A	Sigma Aldrich	(Hodges et al., 2007)
Glibenclamide	20mg/kg	*i.v.*	saline	Sigma Aldrich	(Buckingham et al., 1989)

Guanethidine	30mg/kg	*s.c.*	saline	Sigma Aldrich	(Honda et al., 2007)
HC030031	100mg/kg	*i.p.*	10% DMSO in saline	Tocris	(McNamara et al., 2007)
Indomethacin	20mg/kg 5mg/kg	*i.v./* *s.c.*	0.05% /5% $NaHCO_3$ in saline	Sigma Aldrich	(Starr et al., 2008)
JP1302	3µg/kg	*s.c.*	saline	Sigma Aldrich	(Sallinen et al., 2007)
Lidocaine	2%	*i.pl.*	saline	Sigma Aldrich	(Moini Zanjani and Sabetkasaei, 2010)
L-NAME	15mg/kg	*i.v.*	saline	Sigma Aldrich	(Starr et al., 2008)
Mustard-Oil	1%	Topical (20µl)	Paraffin oil	Sigma Aldrich	(Grant et al., 2005, Fernandes et al., 2011)
N-acetylcysteine	300mg/kg	*i.p.*	saline	Sigma Aldrich	(Zwingmann and Bilodeau, 2006)
Phentolamine	5mg/kg	*i.p.*	saline	Sigma Aldrich	(Koganezawa et al., 2006)
Ruthenium Red	3mg/kg	*i.p.*	saline	Sigma Aldrich	(Cordova et al., 2011)
SB366791	5mg/kg	*i.p.*	2% DMSO in saline	Sigma Aldrich	(Aubdool, 2010)
SMTC	10mg/kg	*i.v.*	saline	Tocris	(Gozal et al., 1996)
SR140333	480nmol/kg	*i.v.*	saline	Gifted: Dr X.Emonds-Alt, France	(Grant et al., 2002, Starr et al., 2008)
Superoxide Dismutase	25000U/kg	i.v.	saline	Sigma Aldrich	(Starr et al., 2008)
TCS5861528	10mg/kg	*i.p.*	2% DMSO in saline	Tocris	(Wei et al., 2009)
TEA	6mg/kg	*i.v.*	saline	Sigma Aldrich	(Inokuchi et al., 2003, Starr et al., 2008)

TEMPOL	30mg/kg	*i.v.*	saline	Sigma Aldrich	(Starr et al., 2008)
Y27632	5mg/kg	*i.p.*	saline	Sigma Aldrich	(Buyukafsar et al., 2006)
Yohimbine	10mg/kg	*s.c.*	saline	Sigma Aldrich	(van Oene et al., 1984)

2.7 Molecular Biology

2.7.1 Measurement of gene expression using Real-Time Polymerase Chain Reaction (RT-PCR)

2.7.1.1 RNA isolation and purification

Total RNA was extracted and purified from samples (DRG, ear and hindpaw footpad) from treated and untreated mice, using the Qiagen Microarray RNA extraction kit (Qiagen, UK) in accordance with the manufacturer's instructions. Unlike DNA, RNA is very easily and rapidly degraded by RNAses and hence, all tissue samples were quickly excised using RNAse/DNAse free consumables and stored in 500µl RNA*later* solution (Applied Biosystems, Life Technologies Ltd, Paisley, UK) for a minimum of 24h at 4°C, followed by long-term storage at -80°C until required. Consumables were made RNAse-free using the RNA decontamination solution RNAse ZAP (Invitrogen, UK).

The extraction kit used the QIAzol reagent to induce phase separation by centrifuging the tissue homogenate in a solution contained water-saturated phenol and chloroform, producing an upper aqueous phase and a lower organic phase (Chomczynski and Sacchi, 1987); the nucleic acids such as RNA are separated into the upper phase whilst proteins and other debris are separated into the lower organic phase.

Tissue sample was placed into a microcentrifuge tube containing QIAzol reagent (1ml) and 5mm stainless steel beads and, was further homogenised in a Tissue Lyser II LT (2-5 min, 30Hz) using the 'bead-milling' method for homogenization whilst ensuring sterility. Chloroform (200µl, Sigma, UK) was then added before being centrifuged to initiate phase-separation and the homogenate was further centrifuged (12000g, 15 min, 4°C). The resulting precipitated RNA was sequentially purified and eluted with the silica-based spin columns for RNA extraction using ethanol (70% in RNA/DNA free water) and wash buffers (phosphate buffers: RW1 and RPE which enable nucleic acids to bind to a silica membrane and, excess ethanol and unwanted cellular contents such as protein/DNA to be washed away). Following this step, the total RNA (30-50µl) was eluted in nuclease-free water and stored at -80°C until reverse transcription, within 6 months of collection.

2.7.1.2 Measurement of RNA quality

RNA concentration and purity were determined using the Nanodrop 1000 spectrophotometer (Thermoscientific, UK) by measuring absorbance at 260nm (A_{260}) and the concentration calculated based on the assumption that 1 unit at A_{260} corresponds to 40µg/ml RNA. The ratio of absorbance at 260 and 280 (A_{260}/A_{280}) values provide a measurement for RNA purity with

respect to protein contaminants measured at 280nm; and (2) A_{260}/A_{230} values as an indication for ethanol and guanidine contamination which is absorbed at 230nm. An overall ratio close to 2 (1.8-2.2) suggests good purity (Bustin et al., 2009).

2.7.1.3 Reverse Transcription

Isolated total RNA (500ng) was first transcribed into cDNA using the High Capacity RNA to complementary DNA (cDNA) kit (Applied Biosystems, UK), as per manufacturer's instructions. Total RNA was aliquoted in nuclease free water (9µl) to produce the required concentration, where 20x RT buffer (10µl) and 20x Buffer mix (1µl) was added to the mixtures. Samples were then reverse transcribed using a thermal cycler (DNA Engine Tetrad 2 Peltier Thermal Cycler) at 37°C for 60 min, 95°C for 5 min and held at 4°C for a minimum of 5 min. The cDNA was stored at -20°C until used in qRT-PCR. Samples that underwent reverse transcription without the active enzyme were used as negative control.

2.7.1.4 Quantitative RT-PCR

Real time PCR amplification was performed using cDNA samples obtained through reverse transcription using a SyberGreen based PCR mix (Sensi-Mix, SYBR-green no ROX, Bioline, UK). Briefly, a 10µl reaction mix consisted of SYBR Green (5µl), 0.5µl of each primer (stock concentration of 10µM) for the target gene, nuclease free water (2µl) and cDNA (2µl).

Target genes were amplified using a 3 step program in a real time PCR thermocycler (Rotor-Gene 6000, Qiagen) under the following conditions: (1) the polymerase enzymes were first activated by heating samples to 95°C for 10 min, (2) then subjected to 40 cycles of 95°C for 10s to separate strands, 57°C for 15s to anneal primers and 72°C for 10s to amplify products, (3) and finally melt at 68-90°C. Details of primers used and their respective PCR products are summarised in table 2.1. Target gene expression was expressed as copies/µl, expression values, and standardised to the reference genes GAPDH and β-actin, as these genes are expressed at a constant level across various conditions. Efficiency of the PCR reaction was assessed by examining the melt curves for each reaction to exclude primer-dimer formation and to ensure that only one product was amplified. Using the GeNorm v1.2 software, a normalisation factor was obtained, based on the geometric mean of the reference genes included (Vandesompele et al., 2002). qRT-PCR was performed on all samples at the same time in order to regulate the experimental conditions tightly for direct comparison and minimising experimental errors such as degradation of standards, variations in sample preparations, and the efficiency of the reverse transcription and PCR amplification.

Target Gene	Primer Sequence	Accession number	Product length (base pairs)
α-CGRP	F: AGCAGGAGGAAGAGCAGGA R: CAGATTCCCACACCGCTTAG	NM_007587.2	71
β-CGRP	F: CCTGCAGGCCTGAGTCAC R: GGCATGGTGAGTTCAACTTTATG	NM_0540843.2	64
TAC-1	F: AAGCCTCAGCAGTTCTTTGG R: TCTGGCCATGTCCATAAAGA	NM_009311.2	100
TRPA1	F: AGGTGATTTTTAAAACATTGCTGAG R: CTCGATAATTGATGTCTCCTAGCAT	NM_177781.4	168
eNOS	F: GACCCTCACCGCTACAACAT R: GTCCTGGTGTCCAGATCCAT	NM_008713.4	62
iNOS	F: CCTGGTACGGGCATTGCT R: GCTCATGCGGCCTCCTT	NM_010927.3	90
nNOS	F: GACTGATGGCAAGCATG R: GCCCAAGTAGAGCCATCTG	NM_008712.2	87
GAPDH	F: GGTCATCCCAGAGCTGAACG R: TTGCTGTTGAAGTCGCAGGA	NM_008084.2	210
β-actin	F: CACAGCTTCTTTGCAGCTCCTT R: TCAGGATACCTCTCTTGCTCT	NM_007393.3	250

Table 2.8: List of genes and their primer sequences with amplicon size (base pairs) used for qRT-PCR. Working solutions were diluted 1 in 10 from the primer stocks, and all primers were purchased from Sigma, UK. F: forward, R: reverse.

2.7.2 Tissue protein quantification by chemiluminescent Western blotting

2.7.2.1 Preparation of tissue samples

Tissue (mouse ear or footpad) were snapfrozen in liquid nitrogen and samples were stored at -80°C. Tissues were then homogenised in 700µl of sodium-dodecyl sulphate (SDS) lysis buffer (50mM Tris base pH6.8, 10% glycerol and 2% SDS) supplemented with 0.02% protease inhibitor cocktail (4-(2-aminoethyl) benzenesulfonyl fluoride, pepstain A, bestatin, E-64, leupeptin and aprotinin) and phosphatase inhibitor (1 tablet/10ml; PhosSTOP; Roche, UK) in a microcentrifuge tube containing 5mm stainless steel beads by the Tissue Lyser II LT(2-5 min, 30Hz). Tissue homogenates were centrifuged at 13,000rpm for 15min at 4°C to separate supernatant containing the protein from tissue debris and fat. Supernatant was collected and stored at -20°C.

2.7.2.2 Determination of protein concentration

The Lowry copper-based protein assay method was employed to determine the protein concentration of the total protein lysates (Lowry et al., 1951). This assay is based on the 'biuret reaction' where proteins, regardless of composition, form a coloured chelate complex with cupric ions in alkaline conditions. Both are maximally sensitive when samples concentrations are diluted as necessary to be similar to those of standards (Sapan et al., 1999).

The conventional Lowry protein assay method was employed (Lowry et al., 1951) using the BioRAD Reagent A + Reagent B kit (Bio-Rad, UK). To generate the standard curve, bovine serum albumin (BSA, 5µl of 0.1-2 mg/ml) was dissolved in double distilled water (ddH_2O). Samples were diluted (1:10) in ddH_2O, if too concentrated. Both standards and samples were loaded in duplicate to clear wells in a 96-well plate, and incubated with 25µl of reagent A and 200µl of reagent B. The plate was then shaken briefly and incubated at room temperature for 15 min, following which absorbance was read at 750nm on a micro-titer reader (SpectraMAX 190, using the SOFTmaxPRO software, version 3.13, Molecular Devices Corporation, California, USA). Protein standard curves were generated by expressing the mean optical density (OD) values obtained at 750nm relative to known protein concentration from BSA standards. Protein standards with a correlation coefficient of $R^2 > 0.995$ were accepted and used to determine protein concentration.

A blank of ddH_2O allowed for removal of background absorbance. Furthermore, the reducing agents in the lysis buffer used for tissue homogenisation are highly reactive with cupric ions and hence, a small volume of SDS lysis buffer was diluted in ddH_2O (1:10) and protein concentration was determined.

2.7.2.3 Equalisation of protein loading and SDS-PAGE

Following protein quantification, 30µg of protein was measured and reduced using 10% 2-Mercaptaethanol (2-ME) and 0.2% bromophenol blue (BPB, sample dye). Protein samples were denatured further at 95°C for 5 min. Protein samples along with a pre-stained protein ladder, were loaded on to designated lanes of a pre-set SDS-PAGE gel for separation by electrophoresis. The gel consisted of a lower "resolving" gel [10% polyacrylamide; composition: 3ml of 30% acrylamide (National Diagnosics, UK); 2.25ml of 0.5M Tris-HCl-pH8.8; 3.75ml of ddH_2O; 45µl of 10% APS (ammonium persulfate) and 15µl Tetramethylethylenediamine (TEMED)] and an upper "stacking" gel [5% of polyacrylamide; composition: 1.75ml ddH_2O, 750µl Tris-HCl-pH6.8, 500µl of 30% acrylamide, 25µl of 10% APS, and 10µl TEMED], which was made on the day of use and allowed to set prior to protein loading. The final concentration of acrylamide within the gel determines the protein separation achieved. 12% acrylamide gel allows for protein separation at MW 20-60kDa; 10% gel for MW of 60-100kDa; and 8% gel for MW >100kDa.

SDS-PAGE gels were run in "running" buffer [composition: 10% Tris-glycine buffer (BioRad, USA), 0.5% of 20% SDS-pH7.2 (National Diagnostics)] in ddH_2O) at 150V for approximately 1.5-2h.

2.7.2.4 Transfer of separated proteins to PVDF membrane and immunoblotting

Following separation of proteins, the gels and protein blotting membranes (pore size 0.45µM, binding capacity: 80-100µg/cm^2, Biorad, USA) were allowed to equilibrate in transfer buffer (10% Tris-Glycine buffers (Biorad, USA), 15% methanol (Fisher Scientific, UK) in ddH_2O). Polyvinyldiene difluoride (PVDF) membrane was activated in methanol for 5s and all three components were assembled in the semi-dry electrophoretic transfer equipment (Biorad, USA). The separated proteins were then electro-transferred onto the PVDF membrane and equilibrated in transfer buffer at 20V for 2h, using semi-dry electrophoretic transfer equipment.

The membrane was blocked with 5% skimmed milk powder in PBS 0.01% Tween or 5% BSA in Tris Buffered saline (TBS) 0.01% Tween at room temperature for 1h, to prevent non-specific binding. Membranes were subsequently washed using PBS/TBS 0.01% Tween for 30 min to remove residual blocking solution and left to incubate with primary antibody at 4°C overnight. Primary antibodies were diluted in PBS/Tween 0.1% or PBS/Tween 0.1% consisting of 3% BSA. Membranes were subsequently incubated with appropriate species-specific horseradish peroxidase (HRP) conjugated secondary antibody (1:2000 in 3% milk in PBS/0.1% Tween) for 1h at room temperature. Membranes were subjected to washing with PBS/TBS 0.01% Tween

for 15min once, followed by three 5-min washes, after primary and secondary antibody incubations.

For chemiluminescence detection, the membrane was incubated with 1ml ECL substrate solution (Milipore, UK) for 60 sec and developed in the G-Box gel documentation system (Syngene Ingenius Biosystems), with images captured using Syngene 2D gel imaging software. Densitometric analysis was conducted using Image J analysis software version 1.32 (NIH, USA), which quantifies protein band intensity based on peak area. Amount of eNOS, p-MLC, total MLC and nitrotyrosine were expressed relative to the reference protein β-actin, as a ratio in arbitrary densitometry units.

For detection of protein with similar MW, membranes were stripped of bound primary antibody prior to probing by incubation with diluted antibody stripping solution (1x of ReBlot Plus, Millipore, UK) for 15 min at room temperature. Membranes were subsequently washed with 5% skimmed milk in TBS Tween 0.01% by three 5 min washes to allow the bound antibody to be stripped from the membranes and secondary antibody was incubated for 1h at room temperature. Membranes were visualised for any bands using chemiluminescence detection, as described above.

Primary antibody	Species	Dilutent	Dilution	Molecular Weight (kDa)	Manufacturer	Catalogue number
eNOS	Rabbit	3% BSA in PBS 0.1% Tween	1:500	133	SantaCruz	C-20, SC-654
Total MLC	Rabbit	3% BSA in TBS 0.1% Tween	1:500	18	CellSignaling	3672
p-MLC (Ser19)	Rabbit	3% BSA in TBS 0.1% Tween	1:500	18	CellSignaling	3671
Nitrotyrosine	Mouse	3% BSA in PBS 0.1% Tween	1:500	Various	Abcam	Ab61392
β-actin	Mouse	3% BSA in PBS 0.1% Tween	1:2000	42	Sigma	A1978

Table 2.9 Primary antibody dilutions for immunoblotting.

Secondary antibody	Species	Dilutent	Dilution	Manufacturer	Catalogue number
Rabbit	Goat	3% BSA in PBS 0.1% Tween	1:2000	Millipore	AP132P
Mouse	Goat	3% BSA in TBS 0.1% Tween	1:2000	Millipore	AP124P

Table 2.10 Secondary antibody dilutions for immunoblotting.

2.7.3 Measurement of noradrenaline concentration using Enzyme-Linked Immunosorbant Assay (ELISA)

2.7.3.1 Preparation of tissue samples

Mice hindpaw footpads were collected at 2 min and 30 min following local cold (10°C) water treatment in TRPA1 WT and KO mice and immediately snap-frozen in liquid nitrogen before being stored at -80°C until processing. Tissue was homogenised using RIPA lysis buffer [composition of 1% NP-40, 0.1% SDS, 50mM Tris-HCl, 150mM NaCl, 0.5% Sodium Deoxycholate, 1mM EDTA; pH7.4] (Sigma-Aldrich, UK) containing protease inhibitors (1tablet/50 ml, Roche Diagnostics, UK). Tissue homogenates were then centrifuged at 13,000 rpm for 15 min at 4°C to separate supernatant containing the protein from tissue debris and fat. Supernatant was collected and kept on ice until it was used.

2.7.3.2 ELISA assay

Noradrenaline concentrations were measured using a commercially available noradrenaline ELISA kit (RE59261; IBL International, Hamburg, Germany), based on the sandwich principle. Briefly, 20µl of tissue lysates and standards (0-500 ng/ml) and controls (high and low concentration of noradrenaline samples) were added to the extraction plates and incubated for 30 min. Thus, noradrenaline was extracted using a cis-diol-specific affinity gel, acylated and then derivatised enzymatically.

Following extraction, bound noradrenaline (25µl) was eluted from all samples using the release buffer (0.1M HCl and colour indicator) and transferred to a 96-well ELISA plate. This stage used the competitive ELISA microtiter plate format where the antigen is bound to the solid phase of the microtiter plate. The derivatised standards, controls, samples of interest and the solid phase bound analyte compete for a fixed number of anti-serum binding sites. Following the procedure when the system is in equilibrium, free antigen and antigen-antiserum complexes are removed by washing, and the antibody bound to the solid phase is detected by an anti-rabbit IgG conjugated to peroxidase where this enzyme catalyses the substrate TMB. 50µl of noradrenaline antiserum was incubated with all samples at room temperature for 2h on an orbital shaker and the plates were thoroughly washed with diluted washing buffer and 100µl of enzyme conjugate was added into each well, and incubated for 1h at room temperature. Following a series of washes, the substrate solution pNPP (200µl) was incubated at room temperature for 40min and the reactions were subsequently stopped by adding pNPP stop solution (50µl). The optical density of each well was measured at an absorbance of 405nm by the microtiter plate reader and a standard curve was plotted using the provided standards in the commercial kits. Both positive and negative controls were assayed to determine accuracy of the

extraction and ELISA. A standard curve for the noradrenaline concentrations was plotted to determine the concentrations of the unknown samples. Noradrenaline concentrations were then normalised to the tissue protein content of each sample, as determined by Lowry copper-based protein assay (previously described in section 2.6.2.2).

2.7.4 Measurement of CGRP concentration using Enzyme-Linked Immunosorbant Assay (ELISA)

2.7.4.1 Preparation of tissue samples and peptide extraction

Mice ears were collected at 30 min following vehicle (10% DMSO in ethanol) or cinnamaldehyde (10%) treatment, and hindpaw footpads were collected at 30 min following local cold (10°C) water treatment in WT mice and immediately snap-frozen in liquid nitrogen before being stored at -80°C until processing. Tissue was homogenised using 5ml/g lysis buffer (10mM Tris, pH7.4) and centrifuged at 13,000 rpm for 15 min at 4°C to separate supernatant containing the protein from tissue debris and fat. Supernatant was collected, acidified with equal amount of buffer A (TFA, 1% trifluoroacetic acid, Phoenix Pharmaceuticals Inc, USA) and further centrifuged at 10,000 rpm for 20 min at 4°C. Following centrifugation, the supernatant was loaded on an equilibrated SEP-Pak C18 cartridge (Millipore) and equilibration was performed by washing once with buffer B (1ml) and three times with buffer A (3ml). The peptides were further eluted with buffer B (3ml) and collected into a 5ml tube, evaporated to dryness overnight using a freeze dryer.

2.7.4.2 ELISA assay

CGRP concentrations were measured using a commercially available CGRP ELISA kit (Rat/Mouse; EIA1 Kit; Phoenix Pharmaceuticals Inc, USA), which measures both α- and β-CGRP, based on the sandwich principle. Briefly, extracted peptides were dissolved in 250µl RIA buffer.

Briefly, 50µl of tissue lysates and standards (0-100 ng/ml) and positive control were added to the immunoplate, which is pre-coated with the secondary antibody with the non-specific binding sites blocked. This was followed by the addition of 25µl of the primary CGRP antibody and biotinylated peptide. The plate was left to incubate at room temperature for 2h, where the secondary antibody can bind to the Fc fragment of the primary antibody whose Fab fragment will be completely bound by both the biotylated peptide and peptide standards and/or targeted peptides in the samples. The immunoplate was subsequently washed four times using 1x assay buffer (350µl/well) and 100µl of streptavidin-horseradish peroxidase (SA-HRP) solution was added to catalyse the substrate solution and left to incubate for 1h at room temperature.

Following the procedure, the immunoplate was further washed several times and the substrate solution TMB (100µl) was added and left to incubate at room temperature for 1h. The reactions were subsequently stopped by adding 2M HCl (100µl/well) and the optical density of each well was measured at an absorbance of 450nm and a standard curve was plotted using the provided standards in the commercial kit. A positive control (provided in the kit) was assayed to determine accuracy of the extraction and ELISA. A standard curve for the CGRP concentrations was plotted to determine the concentrations of the unknown samples. CGRP concentrations were then normalised to the tissue protein content of each sample, as determined by Lowry copper-based protein assay (previously described in section 2.6.2.2). Although cross-reactivity occurs with all the forms of CGRP (78.6% with CGRPII rat and 20.1% human) and to a certain degree with CGRP from other species (100% with rat and 15.1% with human), it is not cross-reactive with closely related peptides such as calcitonin (0%) and amylin (<0.01%).

2.7.5 Measurement of superoxide levels using Lucigenin

Superoxide release from fresh skin samples was measured by chemiluminescence using lucigenin as a probe (Fernandes et al., 2013, Guzik and Channon, 2005). Mice ears were collected at 30 min following vehicle (10% DMSO in ethanol) or cinnamaldehyde (10%), and hindpaw footpads were collected at 2 min and 30 min following local cold (10°C) water treatment in TRPA1 WT and KO mice and added in an Eppendorf tube each containing 100µl of modified Kreb's buffer (composition: 131mM NaCl, 5.6mM KCl, 25mM $NaHCO_3$, 1mM $NaH_2PO_4 \cdot H_2O$, 5mM glucose, 5mM HEPES, 100µM L-arginine, 2.5mM $CaCl_2$, 1mM $MgCl_2$ and 100µM NADPH) and kept on ice. 100µl of Krebs' buffer containing lucigenin (bis-N-methylacridinium nitrate; 10mM) and NADPH (500µM; Sigma-Aldrich, UK) was added to the samples in the presence or absence of superoxide dismutase (SOD; 50U/ml; Sigma-Aldrich) and left to incubate at room temperature in the dark for 5 min. Chemiluminescence was recorded after 4 min using a GloMax 20/20 luminometer (Promega, UK). Tissue protein concentration of each sample was also determined using Lowry copper-based protein assay (previously described in section 2.6.2.2). Results are expressed as the difference in the relative light units per mg of protein in the presence and absence of SOD after subtraction of background luminescence.

2.7.6 Measurement of H_2O_2 using Amplex Red

H_2O_2 levels were measured by the Amplex Red H_2O_2/Peroxidase Assay kit (Invitrogen, UK) (Keeble et al., 2009). Mouse ears were collected at 30 min following vehicle (10% DMSO in ethanol) or cinnamaldehyde (10%) treatment, and hindpaw footpads were collected at 30 min following local cold (10°C) water treatment in WT mice, snap frozen in liquid nitrogen and stored at -80°C until assayed. Tissues were homogenised in a phosphate buffer (0.05M $NaPO_4$,

pH 7.4, 1ml/sample) containing sodium azide (0.01M) to inhibit catalase activity in the samples. The homogenates were centrifuged at 4°C for 10 min at 10,000 rpm and the supernatants were filtered through Millipore tubes (0.5µM pore diameter) by centrifugation at 4°C for 2 min at 10,000 rpm. 100µl of sample and H_2O_2 standard (0-40 µM) were added in each well of a 96-well plate, followed by an addition of 100µl of solution containing 0.05M $NaPO_4$ (pH7.4), HRP (0.2U/ml), and Amplex Red reagent (10-acetyl-3,7-dihydroxyphenoxazine; 25.7 µg/ml) and left to incubate for 2h at 37°C. Absorbance was read at 560nm by the microtiter plate reader and the readings obtained for samples incubated in the absence or presence of Amplex Red reagent were compared to a H_2O_2 standard curve (0-40 µM). Tissue protein concentration of each sample was also determined using Lowry copper-based protein assay (previously described in section 2.6.2.2). Results are expressed as the difference between samples incubated in the presence or absence of Amplex Red (µM) and normalised to the protein content (µM/L/mg).

2.8 Experiment design and analysis

Most of the experiments will involve four groups. I have therefore used power analysis for a two-way ANOVA design, using previous published data from the mouse ear model and hindpaw vasculature investigating neurogenic vasodilatation (Graepel et al., 2011, Grant et al., 2005, Pozsgai et al., 2010, Aubdool, 2010). For confidence at the 0.05 (5%) with power at 0.8% (80%) and the effect size of medium (0.75), a minimal size groups of n=8 is recommended.

Results are expressed as mean ± standard error of the mean (S.E.M.) unless otherwise stated. Statistical analysis was performed using two-way ANOVA (analysis of variance) followed by Bonferroni *post hoc* tests or unpaired student's t-test by the GraphPad Prism software version 6.0. P values < 0.05 were considered statistically significant.

2.8.1 Cinnamaldehyde-induced blood flow data analysis

The typical response to cinnamaldehyde involves an initial gradual increase in blood flow, which stays constant over the recording period, as a result of sustained vasodilatation. Blood flow data to cinnamaldehyde-induced responses was expressed as area under the recorded flux vs. time trace for the entire recording period (30 min) following topical treatment (Figure 2.8).

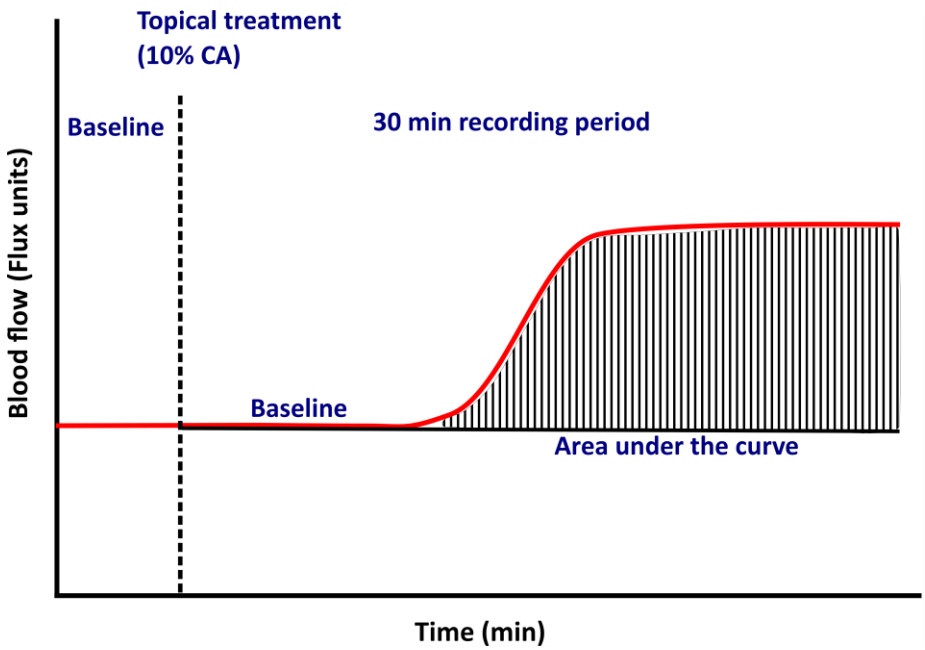

Figure 2.8 Representative trace demonstrating the time-course for a blood flow response following the topical administration of cinnamaldehyde to the mouse ear. Baseline blood flow was measured for 5 min, cinnamaldehyde (10%, CA) was administered topically on the mouse ear and blood flow resumed for another 30 min. Data was analysed as mean area under the response curve (shaded area) in the 30 min following treatment.

2.8.2 Cold-induced vascular response data analysis

The typical response to local cooling (10°C) in the mouse hindpaw involves a rapid, transient decrease in blood flow from baseline followed by an increase in blood flow to return to baseline levels to maintain the normal function of the vasculature. Figure 2.9 summarises the temperature profile of this response and the parameters derived to analyse this response. In this study, blood flow data to cold-induced vascular responses was expressed as

(1) Area under the response curve (recorded flux vs. time trace) for the entire recording period (30 min) following the cold treatment when the cold-treated hind paw was dried. Area under the curve (AUC) was calculated using GraphPad Prism software 6.0, with set baseline value following cold water immersion.

(2) Net vasoconstriction which was the % change in blood flow at ~2 min following local cold water immersion from baseline. This was calculated from the recorded flux values (arbitrary units) at ~2 min following local cold water immersion and recorded flux values at baseline.

(3) Net vasodilatation which was the % change in blood flow at 30 min from ~2 min following local cold water immersion. This was calculated from the recorded flux values at 30 min and ~2 min following local cold water immersion.

In naïve conditions for a normal response, if there is, for example, a 50% decrease in blood flow from baseline (net vasoconstriction), this will be followed by approximately a 50% increase in blood flow to near basal levels (net vasodilatation). Hence, the magnitude of vasoconstriction directs the vasodilatation phase.

If a pharmacological antagonist reduces the vasoconstrictor phase, this will in turn requires less vasodilatation to return blood flow to baseline. However, some drugs may have an effect on the net vasodilatation phase and hence, in these situations the net vasoconstriction will be the same as in normal conditions, with a reduction in the vasodilator component of the cold-induced vascular response. In these experiments, blood flow does not return to baseline following the local cold-induced vasoconstriction, as shown for example in Figure 5.2.

The mathematical calculations used to derive net vasoconstriction and vasodilatation are as follows:

$$Net\ vasoconstriction = \frac{(Peak\ vasoconstriction - Baseline)}{Baseline} \times 100\%$$

$$Net\ vasodilatation = \frac{(Peak\ vasodilatation - Peak\ vasoconstriction)}{Peak\ vasoconstriction} \times 100\%$$

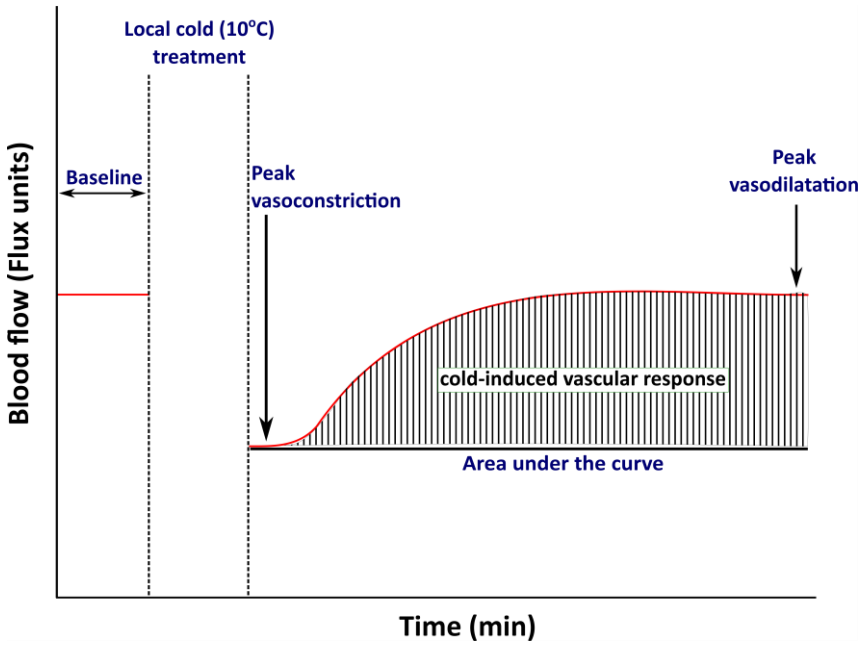

Figure 2.9 Representative trace demonstrating the time-course blood flow responses to local cold (10°C) water immersion in the mouse hindpaw. Baseline blood flow was measured for 5 min, the ipsilateral paw was immersed in cold water for 5 min, and blood flow was subsequently measured for 30 min post cooling. Parameters derived from this blood flow profile response are (1) **Baseline**, mean blood flow flux value during the 5 min recording before local cold water immersion, (2) **Peak vasoconstriction**, the lowest blood flow value which is usually at 2 min following local cold exposure, (3) **Peak vasodilatation**, the highest blood flow value which is usually when the blood flow returns to baseline following the initial cold-induced vasoconstriction response. Cold-induced vascular response represents the total vascular changes happening in the mouse hindpaw for 30 min following cold water immersion and these data are analysed as area under the response curve (shaded area), expressed as blood flow ($x10^3$ flux units).

Chapter 3 – Investigating cinnamaldehyde-induced vasodilatation

Chapter 3 – Investigating cinnamaldehyde-induced vasodilatation

3.1 Introduction

The skin is a thermoregulatory site, with an extensive and well-developed microcirculation (Braverman, 2000). The mouse ear model has been previously used in this laboratory to investigate neurogenic vasodilatation after topical application of the TRPV1 agonist capsaicin (Grant et al., 2002, Starr et al., 2008) and the TRPA1 agonist mustard oil (Grant et al., 2005, Pozsgai et al., 2010). The external ear itself is known as a useful organ to study cutaneous vascular reactivity as its anatomical structures including AVAs and nerves, are well represented to study the physiology and pharmacology of vascular neuroeffector systems (Eghianruwa and Eyre, 1991, Kalsner, 1972). The major divisions of the ear consist of the outer, middle and inner ear, and the cranial VIII nerve. The outer ear is typically used to investigate peripheral mechanisms. The mouse ear is innervated by the sensory nerves from the cervical spinal levels (C2-C4) and motor neurons from the facial nucleus, which project to the medullary somatosensory nuclei (MSN) in the brainstem (Holstege et al., 1977). The cranial nerve VIII contains afferent fibres, which target the sensory epithelia of the inner ear. The neurons in the rostral ventrolateral medulla (RVLM) of the brainstem have been implicated in controlling the ear pinna blood flow (Blessing and Nalivaiko, 2000).

As discussed previously in chapter 1, cinnamaldehyde (10%) has also been demonstrated to induce heat and mechanical hyperalgesia in human forearm (Namer et al., 2005), but it remains unknown whether this response is dependent on TRPA1. Recent studies from this group using laser Doppler flowmetry have shown that cinnamaldehyde (*i.pl.*) in mice triggered a significant increase in blood flow which was significantly reduced in TRPA1 KO mice (Pozsgai et al., 2010).

The aim of this PhD project was to investigate the mechanisms underlying TRPA1-mediated vasodilatation in the mouse ear model using pharmacological inhibitors and genetically modified mice. Cinnamaldehyde was chosen as it was previously reported to be a selective TRPA1 agonist (Bandell et al., 2004, Bodkin and Brain, 2011). It is hypothesised that cinnamaldehyde activates TRPA1 selectively and causes vasodilatation via the release of the neuropeptides CGRP and substance P, and may also involve generation of reactive oxygen species.

3.1.1 Brief methods

Using the non-invasive two-channel laser Doppler flowmeter, cinnamaldehyde-induced vascular responses were studied, as detailed in Chapter 2 (section 2.4). Briefly, skin blood flow was measured concomitantly in both ears of mice anaesthetised with ketamine (75mg/kg) and medetomidine (1mg/kg). A probe, allowing blood flow to me measured precisely at one point in the ear skin ($1mm^2$ and to 1-2mm depth) was placed on each ear and a baseline reading was obtained. Cinnamaldehyde (10%) was topically applied to the ipsilateral ear and vehicle (10% DMSO in ethanol) to the contralateral ear. Blood flow recordings were taken for 30 min and data was collected as arbitrary flux units, which are proportional to blood flow.

Initial studies investigated cinnamaldehyde-induced blood flow responses in both male and female CD1 WT mice, and all subsequent further experiments were conducted in male CD1 mice. All the blood flow results presented in this chapter are derived from laser Doppler flowmeter and expressed as AUC, as detailed in section 2.8.Some images were captured using the FLPI for two sets of experiments (Figure 3.1C and 3.2C).A range of pharmacological inhibitors was used to investigate the mediators involved in mediating cinnamaldehyde-induced vasodilatation (section 2.6).

Ear tissue samples were collected at 30 min following cinnamaldehyde or vehicle treated of WT mice and *ex vivo* analysis was conducted to investigate CGRP levels using ELISA, superoxide release using Lucigenin assay, H_2O_2 generation using AMPLEX RED assay, mRNA gene expression using qRT-PCR as well as eNOS and nitrotyrosine protein expression using western blotting (section 2.7).

3.2 Results

3.2.1 Characterisation of cinnamaldehyde-induced vasodilatation in the mouse ear model

Cinnamaldehyde (1-30%, 20µl) or vehicle (10% DMSO in ethanol, 20µl) was applied topically to the ears of male or female CD1 mice (n=5) and caused an increase in blood flow, which was significant at 3% and 10% as compared to respective vehicle-treated ears (Figure 3.1A). A dose of 10% cinnamaldehyde generated reproducible results, with a gradual increase in blood flow at 10 min onwards following topical application (Figure 3.1C-D) which remained constant for the 30 min duration recording period. This dose was chosen for subsequent studies to investigate the mechanisms underlying this vasodilatation. Interestingly, this chosen dose was used previously on human forearm (Namer et al., 2005) and shown to sensitise the C fibre-mediated noxious heat withdrawal, as shown by a significant reduction in the withdrawal latency (Dunham et al., 2010). Additionally, there was no change in cinnamaldehyde-induced vasodilatation between male and female CD1 mice (n=5, Figure 3.1B).

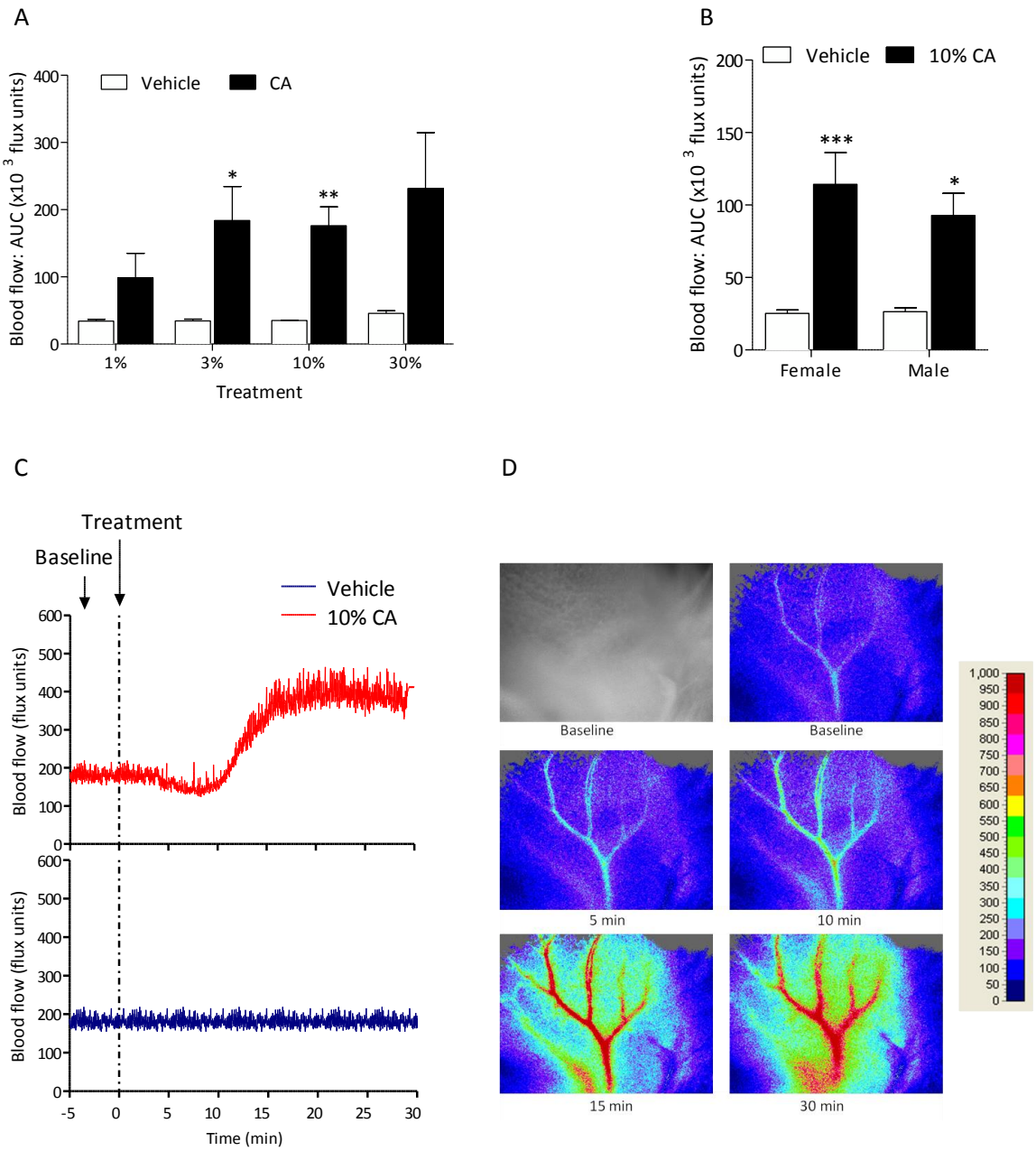

Figure 3.1 Effects of cinnamaldehyde (CA) on blood flow responses in the ears of CD1 mice using laser Doppler techniques.
Blood flow (x 10^3 flux units) in mouse ears following topical application of 20µl cinnamaldehyde (1-30%) or vehicle (10% DMSO in ethanol). Results recorded over 30 min and shown as mean + S.E.M. A) Effects of 1% to 30% of cinnamaldehyde on peripheral blood flow in male CD1 mice (n=5), B) No gender differences in 10% cinnamaldehyde-mediated vasodilatation in the peripheral vasculature (n=5), C) Representative traces of blood flow responses assessed by laser Doppler flowmeter vs. time trace at baseline and following topical application of 10% cinnamaldehyde. An upward deflection is proportional to an increase in blood flow, D) Representative images as observed by the Full-Field Laser Perfusion Imager alongside grey/black scale 'photo' image showing blood flow recorded at baseline and over 30 min for cinnamaldehyde-treated ear in male in CD1 mouse. *p<0.05, **p<0.01, ***p<0.001 compared to respective vehicle-treated ears of CD1 mice using Student's t test or 2-way ANOVA followed by the Bonferroni *post hoc* test.

3.2.2 Role of TRPA1 in cinnamaldehyde-induced blood flow

The non-selective cation channel blocker ruthenium red (3mg/kg, *i.p.*, 30 min) was initially used to investigate the role of TRP channels in mediating cinnamaldehyde-induced vasodilatation. There was a significant attenuation in blood flow responses following cinnamaldehyde application compared to control pre-treated group ($p<0.05$, n=4-5, Figure 3.2A). The role of TRPA1 was subsequently investigated using TRPA1 WT and KO mice. As shown by the representative image, cinnamaldehyde-induced vasodilatation was significantly decreased in TRPA1 KO as compared to WT mice ($p<0.001$, n=4, Figure 3.2B-C). The non-selective calcium-operated potassium channel blocker tetraethylammonium chloride (TEA) was administered at 6mg/kg (*i.v.*, 5 min) and was demonstrated to significantly decrease cinnamaldehyde-induced vasodilatation compared to control pre-treated group ($p<0.001$, n=3, Figure 3.2D).

TRPA1 antagonists were used to further confirm the role of TRPA1 in this response and surprisingly, the TRPA1 antagonist TCS5861528 (10mg/kg, *i.p.*, 30 min) failed to block the cinnamaldehyde-induced vasodilatation (Figure 3.3A) to a similar level as seen previously in the TRPA1 KO mice (Figure 3.2B). TCS5861528 at this current dose was previously shown to attenuate mechanical hypersensitivity in diabetic rats *in vivo* and to inhibit the ability of TRPA1 agonist (mustard oil and 4-HNE) to induce calcium influx in human TRPA1 transfected HEK cells using calcium imaging studies (Wei et al., 2009).

The selectivity of TCS5861528 for TRPA1 and TRPV1 channels were further characterised in this mouse model. Topical application of the TRPA1 agonist mustard oil caused a significant increase in blood flow as compared to vehicle-treated ear ($p<0.001$, n=3) in the control group, as expected and this is in agreement with previous findings (Aubdool, 2010). However, pre-treatment with TCS5861528 significantly reduced mustard oil induced vasodilatation ($p<0.01$, n=3-4, Figure 3.3B) but not to a lesser degree than that previously shown in TRPA1 KO mice (Pozsgai et al., 2010).

The TRPV1 agonist capsaicin induced a significant increase in blood flow, as expected and this is in agreement with previous findings (Aubdool, 2010). Interestingly, this response remains unchanged with pre-treatment of TCS5861528 (Figure 3.3C). The data here suggests that although TCS5861528 acts on TRPA1 and not TRPV1, at the dose of 10mg/kg it does not inhibit cinnamaldehyde-induced vasodilatation.

The role of TRPA1 in mediating cinnamaldehyde-induced vasodilatation was further confirmed using the well-characterised TRPA1 antagonist HC030031 (100mg/kg, *i.p.*) (McNamara et al., 2007). Cinnamaldehyde-induced vasodilatation was inhibited in WT mice pre-treated with HC030031 as compared to control groups (n=4-5, $p<0.001$, Figure 3.3D). It may be worth

highlighting here that although the dose of HC030031 is 10-fold higher than TCS5861528, it has been previously characterised in several studies and shown to be selective for TRPA1, as discussed earlier in chapter 1. These results highlight the role of TRPA1 in mediating cinnamaldehyde-induced vascular responses.

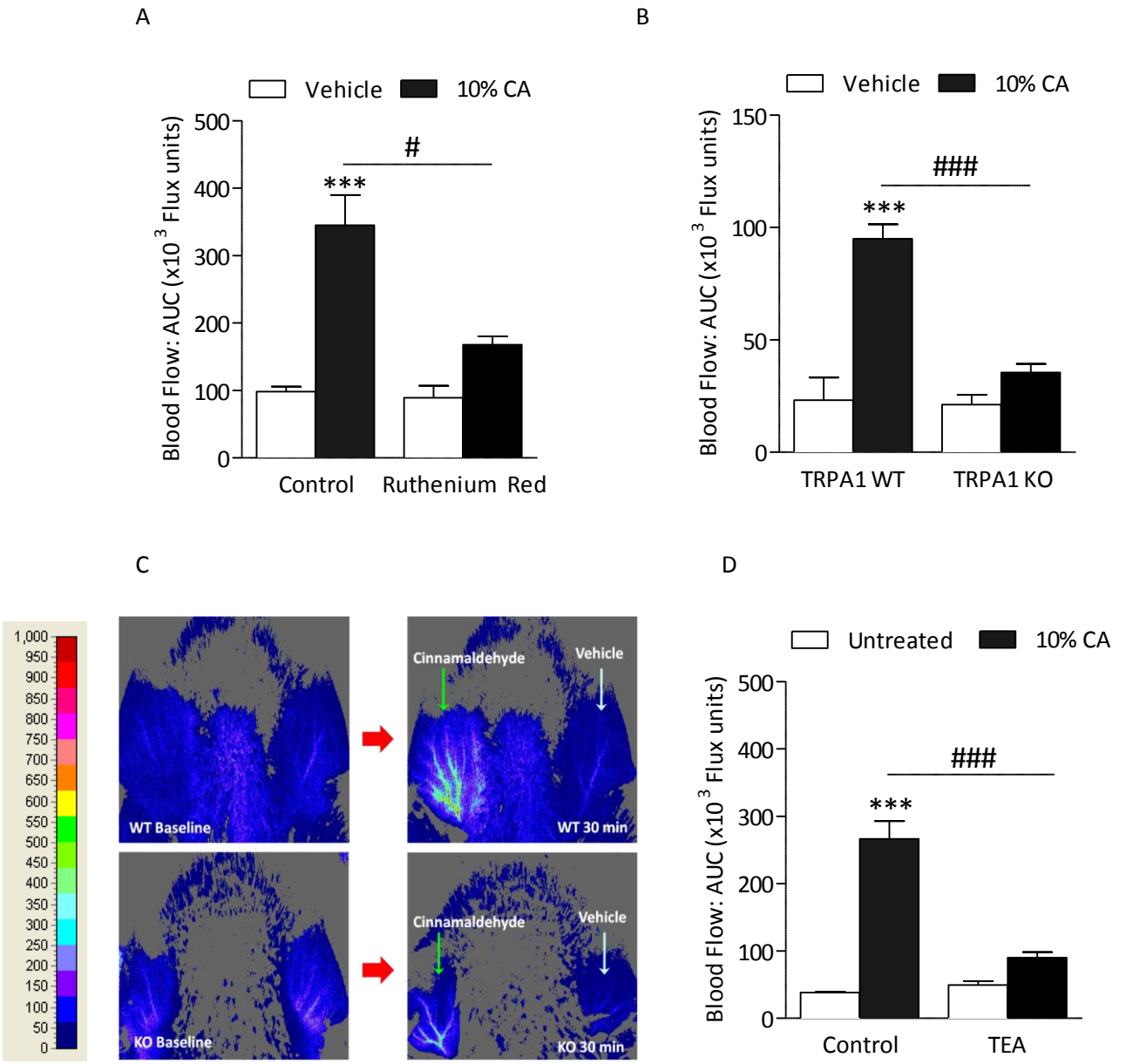

Figure 3.2 Role of TRPA1 in cinnamaldehyde-induced vasodilatation

Blood flow (x 10^3 flux units) in mouse ears following topical application of cinnamaldehyde (CA, 10%) or vehicle (10% DMSO in ethanol) using laser Doppler techniques. Results recorded over a 30 min period and shown as mean ± S.E.M. **A**) Effects of pre-treatment of the non-selective cation channel blocker Ruthenium Red (3mg/kg, *i.p.*, n=4) or control (saline, *i.p.*, n=5) on cinnamaldehyde-induced vasodilatation in male CD1 mice using laser Doppler flowmeter, **B**) Cinnamaldehyde-induced vasodilatation in the ears of male TRPA1 WT and KO mice (n=4),**C**) Representative images as observed by the Full-Field Laser Perfusion imager where blood flow was recorded at baseline and 30 min post application in male TRPA1 WT and KO mouse and **D**) Effects of pre-treatment of tetraehylammonium (TEA, 6mg/kg, *i.v.*, n=3) or control (saline, *i.v.*, n=3) on cinnamaldehyde-induced vasodilatation in the ears of CD1 mice using laser Doppler flowmeter. ***p<0.001, compared to respective vehicle-treated, #p<0.05, ###p<0.001 compared to CA-treated ears of CD1 mice using 2-way ANOVA followed by Bonferroni *post hoc* test.

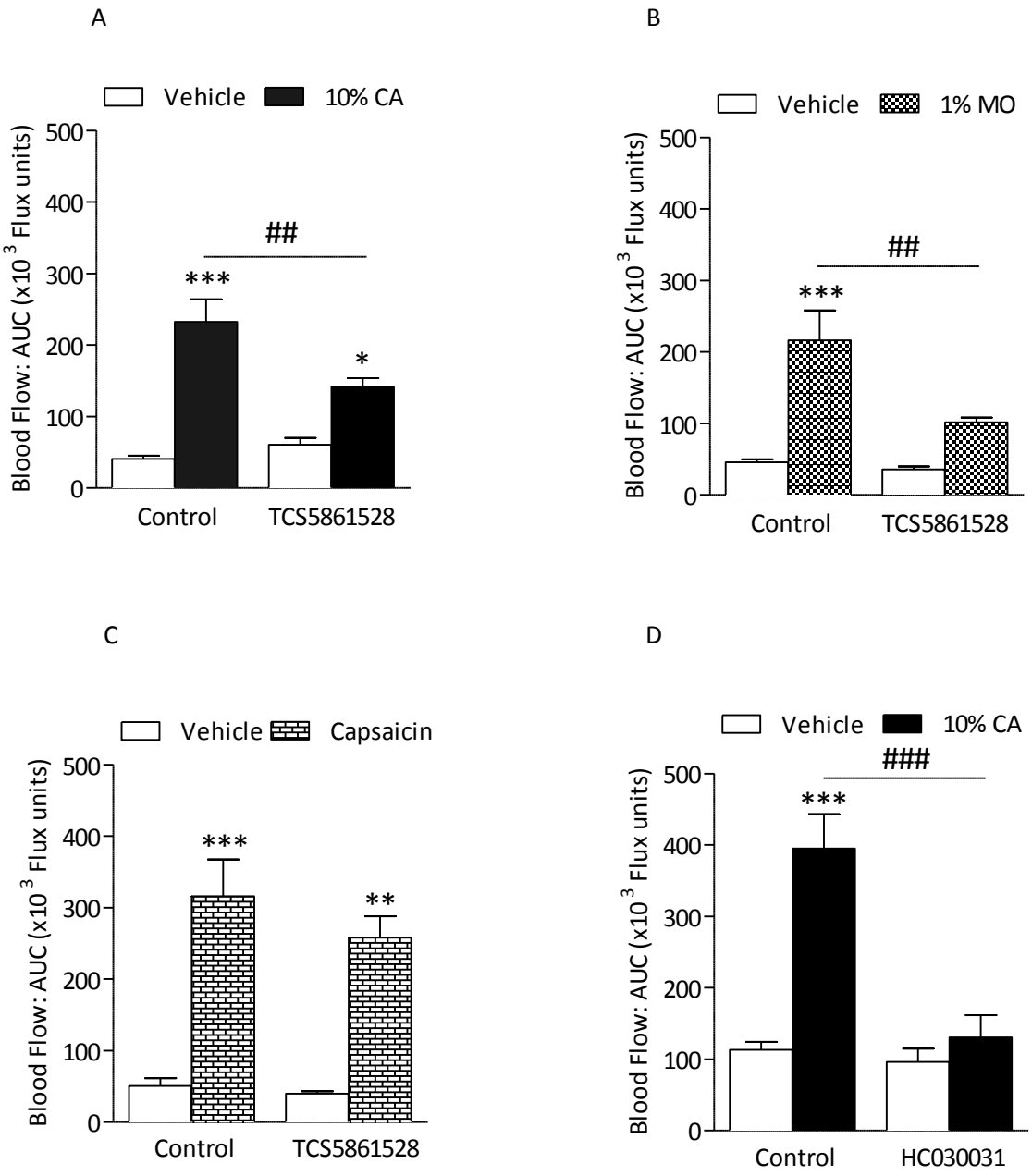

Figure 3.3 Effects of TRPA1 antagonists on cinnamaldehyde (CA)-induced blood flow responses in the peripheral vasculature

Blood flow (x 10^3 flux units) in mouse ears following topical application of cinnamaldehyde (CA), mustard oil (MO) or capsaicin using laser Doppler techniques. Results recorded over 30 min period and shown as mean ± S.E.M. Effects of pre-treatment with the TRPA1 antagonist TCS5861528 (10mg/kg, *i.p.*, 30 min) or control (2% DMSO in saline,*i.p.*, 30 min) in male CD1 mice ears following topical application of 20µl of **A**) cinnamaldehyde (10%) or vehicle (10% DMSO in ethanol) (n=5), **B**) mustard oil (1%) or vehicle (paraffin oil) (n=4-5) and **C**) capsaicin (200µg) or vehicle (ethanol) (n=3-4). **D**) Cinnamaldehyde-induced vasodilatation after the pre-treatment with the TRPA1 antagonist HC030031 (100mg/kg, *i.p.*, 30 min) or control (10% DMSO in saline) in male TRPA1 WT mice (n=4-5). **p<0.01, ***p<0.001 compared to respective vehicle-treated, ##p<0.01, ###p<0.001 compared to CA-treated ears of mice using 2-way ANOVA followed by Bonferroni *post hoc* test.

3.2.3 Role of other TRP channels in cinnamaldehyde-induced vasodilatation

The possible contributions of other TRP channels such as TRPV1 and TRPM8 to cinnamaldehyde-induced vasodilatation were investigated in genetically modified mice. TRPA1 receptors have been previously shown to be co-expressed with TRPV1 in sensory neurons where I recently demonstrated that the TRPA1 agonist mustard oil-induced vasodilatation is potentiated in TRPV1 KO mice or WT mice pre-treated with the TRPV1 antagonist SB366791 compared to mice pre-treated with control (Aubdool, 2010). There was no significant change in cinnamaldehyde-induced increase in blood flow in the ears of WT and TRPV1 KO mice ($n=5$, $p>0.05$, Figure 3.4A).

The potential involvement of the cold-sensitive TRPM8 channels was also investigated in cinnamaldehyde-induced vasodilatation using the TRPM8 antagonist AMTB (10mg/kg, *i.p.*). This dose was previously shown to antagonise TRPM8 in volume-induced rhythmic bladder contraction studies in anaesthetized rat (Lashinger et al., 2008). Our results show that there was no significant difference in cinnamaldehyde-treated ears in AMTB-treated WT mice compared to control-treated WT mice ($n=5$, $p>0.05$, Figure 3.4B).

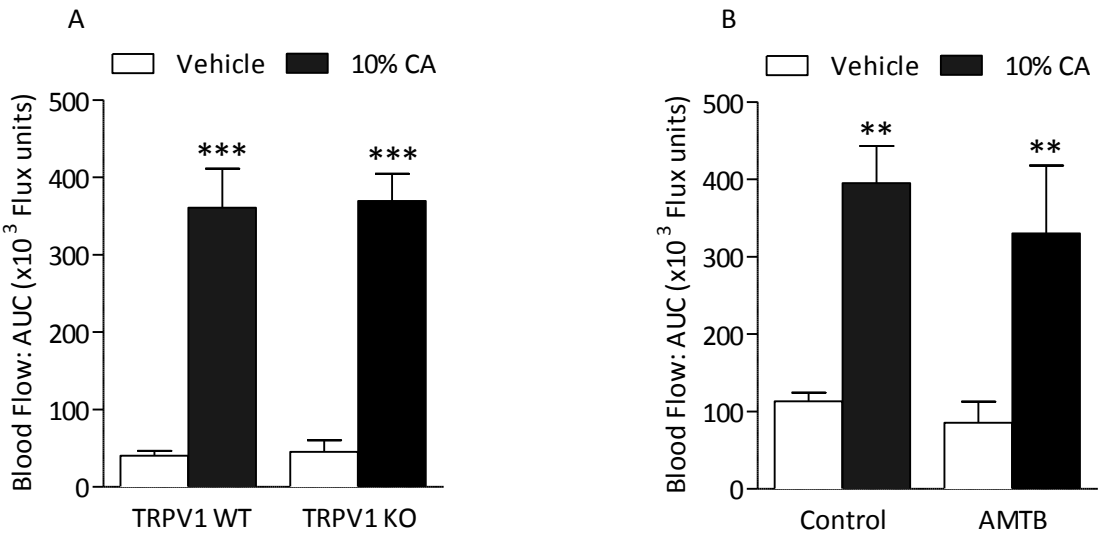

Figure 3.4 Role of other TRP channels in cinnamaldehyde-induced vasodilatation
Blood flow (x 10^3 flux units) in mouse ears following topical application of 20µl cinnamaldehyde (CA, 10%) or vehicle (10% DMSO in ethanol) using laser Doppler techniques. Results recorded over a 30 min period and shown as mean ± S.E.M. Cinnamaldehyde-induced vasodilatation in the ears of **A**) TRPV1 WT and KO mice (n=5) and **B**) in male CD1 mice pre-treated with the TRPM8 antagonist AMTB (10mg/kg, *i.p.*, 30 min) or control (10% DMSO in saline, *i.p.*, 30 min) (n=5). **p<0.01, ***p<0.001 compared to respective vehicle-treated ears using 2-way ANOVA followed by Bonferroni *post hoc* test.

3.2.4 Role of neuropeptide CGRP and substance P in cinnamaldehyde-induced vasodilatation

Both CGRP and substance P are vasodilator neuropeptides and their role in mediating neurogenic vasodilatation has been well established (Aubdool and Brain, 2011). Their contribution in mediating cinnamaldehyde-induced vasodilatation was investigated in WT mice. Co-administration of the CGRP receptor antagonist $CGRP_{8-37}$ and the NK_1 receptor antagonist SR140333 caused a significant decrease in cinnamaldehyde-induced vasodilatation as compared to control-treated mice ($n=4$, $p<0.001$, Figure 3.5A). The data presented here suggest that both neuropeptides may be involved in cinnamaldehyde-induced blood flow responses. This evidence led to investigating whether both neuropeptides are equally involved in inducing cinnamaldehyde-induced vasodilatation in gene expression and blood flow studies. At 30 min following topical treatment of cinnamaldehyde (10%), there was a significant decrease in the mRNA expression of the TAC-1 gene, which encodes substance P when compared to vehicle-treated ears ($n=5$, $p<0.05$, Table 3.1). However, there was no significant change in cinnamaldehyde-induced blood flow responses in SR140333-treated WT mice compared to control-treated WT mice ($n=4$, $p>0.05$, Figure 3.5B), suggesting that substance P may not be involved in this response.

CGRP protein levels were investigated using ELISA in cinnamaldehyde-treated and vehicle-treated ear samples at 30 min following topical application. There was a significant decrease in CGRP levels in cinnamaldehyde-treated compared to vehicle-treated ear tissue homogenates of WT mice ($n=6$, $p<0.01$, Figure 3.6). However, analysis of CGRP gene expression demonstrated that α-CGRP mRNA expression was significantly increased in cinnamaldehyde-treated compared to vehicle-treated ears ($n=6$, $p<0.05$, Table 3.1). There was an increase in β-CGRP mRNA gene expression in cinnamaldehyde-treated as compared to vehicle-treated ears ($n=6$, $p<0.05$, Table 3.1). Furthermore, there was a significant decrease in cinnamaldehyde-induced vasodilatation in α-CGRP KO mice compared to α-CGRP WT mice ($n=3$, $p<0.01$, Figure 3.5C) and a similar trend was observed in CGRP8-37-treated WT mice compared to control-treated WT mice ($n=5$, $p<0.001$, Figure 3.5D).

As CGRP has been shown to mediate vasodilatation by stimulating adenylyl cyclase, increasing cAMP, which further activates PKA and opens K_{ATP} channels (Quayle et al., 1994), the role of K_{ATP} channels in cinnamaldehyde-induced vasodilatation was investigated. Cinnamaldehyde-induced increase in blood flow was significantly reduced WT mice pre-treated with the K_{ATP} channels blocker glibenclamide (20mg/kg) compared to control-treated WT mice ($n=4$-6, $p<0.001$, Figure 3.5E). The data here suggests that CGRP release downstream of TRPA1 activation may activate K_{ATP} channels and lead to a myogenic-mediated hyperpolarisation-induced neurogenic vasodilatation.

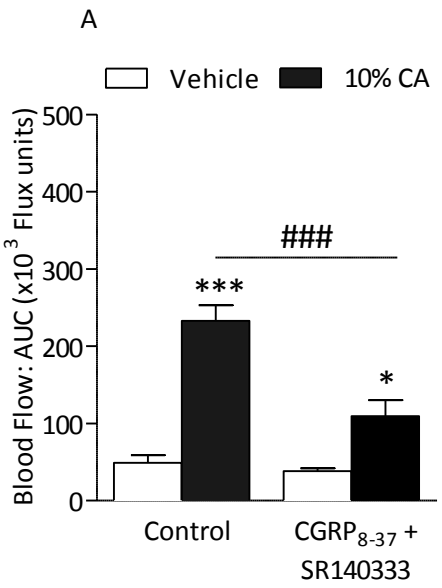
A
Vehicle
10% CA
Blood Flow: AUC (x10 3 Flux units)
500
400
300
200
100
0
###
***
*
Control
CGRP8-37 + SR140333

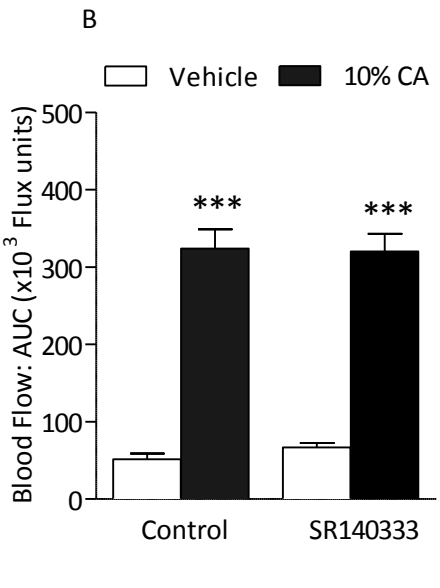
B
Vehicle
10% CA
Blood Flow: AUC (x10 3 Flux units)
500
400
300
200
100
0
***
***
Control
SR140333

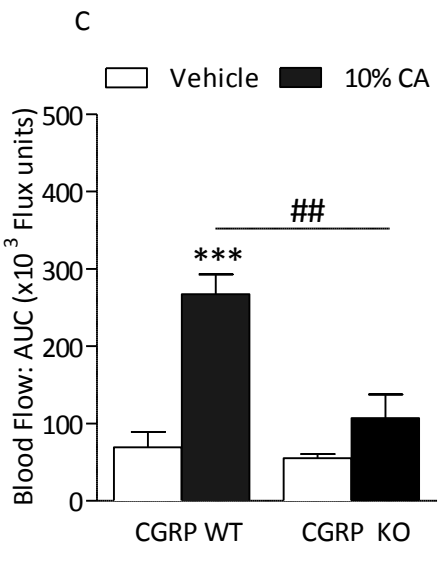
C
Vehicle
10% CA
Blood Flow: AUC (x10 3 Flux units)
500
400
300
200
100
0
##
***
CGRP WT
CGRP KO

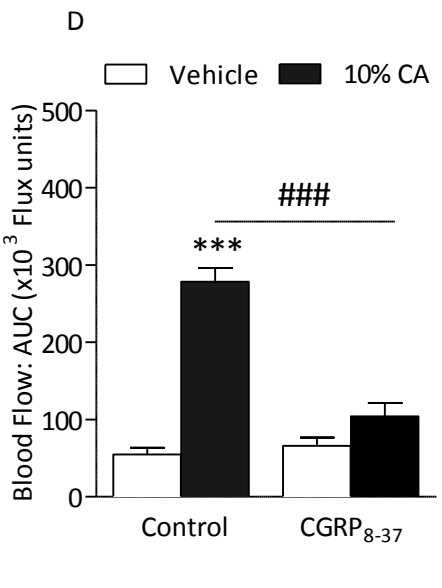
D
Vehicle
10% CA
Blood Flow: AUC (x10 3 Flux units)
500
400
300
200
100
0
###
***
Control
CGRP8-37

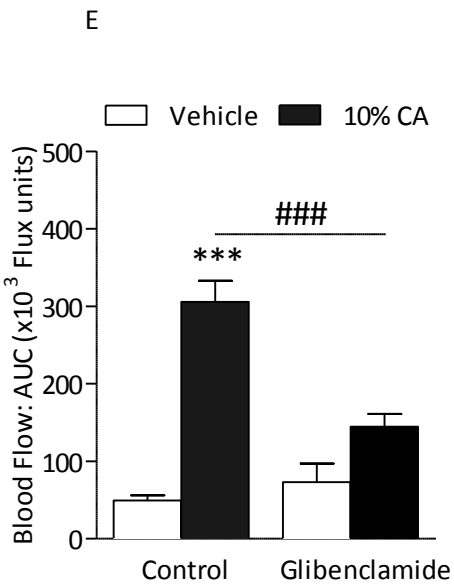
E
Vehicle
10% CA
Blood Flow: AUC (x10 3 Flux units)
500
400
300
200
100
0
###
***
Control
Glibenclamide

Figure 3.5 Role of neuropeptides in cinnamaldehyde (CA)-induced vasodilatation
Blood flow (x 10^3 flux units) in mouse ears following topical application of 20µl cinnamaldehyde (CA, 10%) or vehicle (10% DMSO in ethanol) using laser Doppler techniques. Results recorded over a 30 min period and shown as mean ± S.E.M. Cinnamaldehyde-induced vasodilatation in the ears of male CD1 mice pre-treated with **A**) a combination of the selective CGRP receptor antagonist $CGRP_{8-37}$ (400nmol/kg, *i.v.*, 5min) and neurokinin-1 receptor antagonist SR140333 (480nmol/kg, *i.v.*, 5min) (n=4) or control (0.01% BSA in saline, n=4) and **B**) with SR140333 alone or respective control (saline) (*i.v.*, 5min, n=5), **C**) Cinnamaldehyde-induced responses in male α-CGRP WT and KO mice (n=3). Effects of pre-treatment of **D**) $CGRP_{8-37}$ alone or respective control (0.01% BSA in saline) (*i.v.*, 5min, n=5) and **E**) ATP-sensitive potassium (K_{ATP}) channels blocker enclamide (20mg/kg, *i.v.*, 5 min, n=4) or respective control (10% DMSO in saline, *i.v.*, 5 min, n=6) in male CD1 mice. ***p<0.001 compared to respective vehicle-treated ears, ##p<0.01, ###p<0.001 compared to CA-treated ears using 2-way ANOVA followed by Bonferroni *post hoc* test.

		Treatment	
Gene	**Sample (n)**	**Vehicle**	**10% CA**
α-CGRP	6	22.6 ± 8.6	484 ± 250.3*
β-CGRP	6	11552 ± 1846	21416 ± 5378
TAC-1	5	202.5 ± 80.0	49.3 ± 11.5*

Table 3.1 Expression of neuropeptides mRNA in cinnamaldehyde (CA)-treated ear samples using RT-qPCR. mRNA expression of α-CGRP, β-CGRP and the substance P marker TAC-1 at 30 min following topical application of cinnamaldehyde or vehicle (10% DMSO in ethanol) in the mouse ear. Results are expressed as copy numbers per sample normalised to GAPDH and β-actin (n=5-6). *p<0.05 compared to respective vehicle-treated ears of CD1 mice using Student's *t* test.

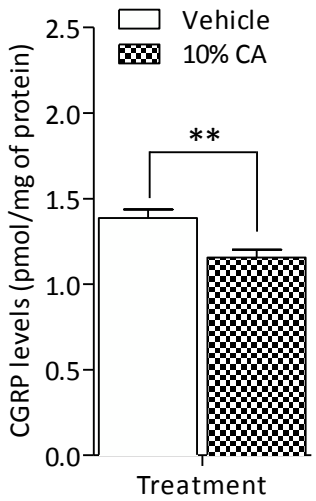

Figure 3.6 Effects of cinnamaldehyde (CA) treatment on CGRP protein levels Ear tissues from male CD1 mice were harvested at 30 min following topical application of cinnamaldehyde (CA, 10%) or vehicle (10% DMSO in ethanol). Total CGRP levels were determined using ELISA and normalised to mg of tissue protein. Results are expressed as pmol/mg of tissue protein and denotes mean ± S.E.M, n=6. **p<0.01 compared to respective vehicle-treated ears of CD1 mice using Student's *t* test.

3.2.5 Role of prostaglandins in cinnamaldehyde-induced vasodilatation

The role of the mediator prostaglandins was investigated using the non-selective cyclooxygenase inhibitor indomethacin, at two different doses. Cinnamaldehyde-induced vasodilatation was not significantly affected by pre-treatment with indomethacin at 20mg/kg (*i.v.*) or at 5mg/kg (*s.c.*) compared to control-treated group ($p>0.05$, $n=3$, Figure 3.7A-B), suggesting that prostaglandins are not involved in cinnamaldehyde-induced vasodilatation.

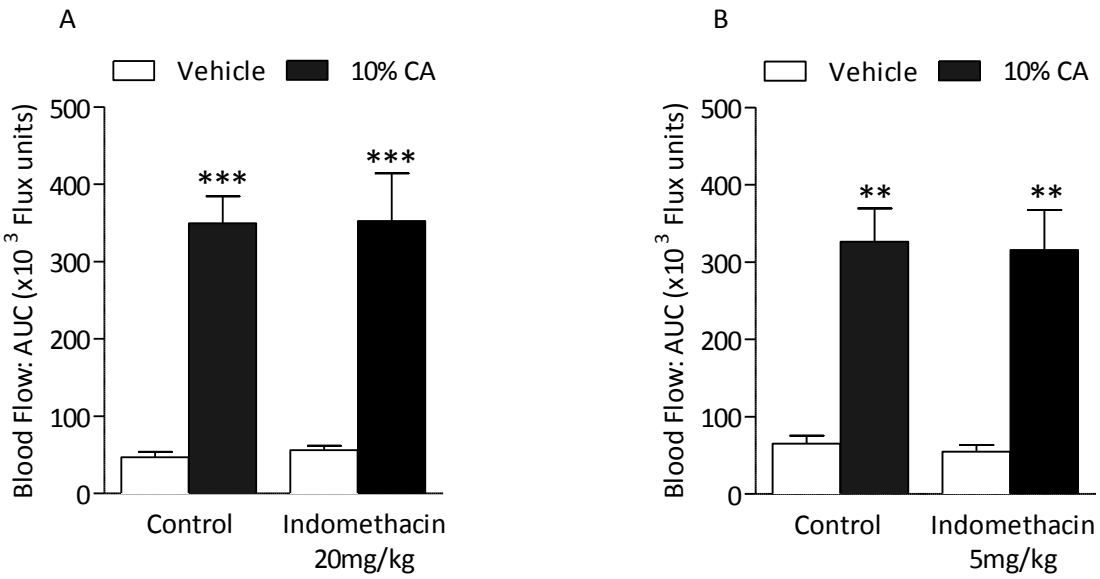

Figure 3.7 Role of prostaglandins in cinnamaldehyde (CA)-induced vasodilatation
Blood flow (x 10^3 flux units) in mouse ears following topical application of 20µl cinnamaldehyde (CA, 10%) or vehicle (10% DMSO in ethanol) using laser Doppler techniques. Results recorded over a 30 min period and shown as mean ± S.E.M. Cinnamaldehyde-induced vasodilatation in the ears of male CD1 mice pre-treated with the cyclo-oxygenase inhibitor indomethacin at **A**) 20mg/kg or control (0.05% $NaHCO_3$ in saline) (*i.v.*, 5 min, n=3) and **B**) 5mg/kg or control (5% $NaHCO_3$ in saline) (*s.c.*, 30 min, n=3). **p<0.01, ***p<0.001 compared to respective vehicle-treated ears using 2-way ANOVA followed by Bonferroni *post hoc* test.

3.2.6 Role of nitric oxide in cinnamaldehyde-induced vasodilatation

Using the non-selective NOS inhibitor L-NAME (15mg/kg, *i.v.*, 5 min), I investigated the role of the classic vasodilator nitric oxide was investigated in cinnamaldehyde-induced vasodilatation. Pre-treatment with L-NAME caused a significant decrease in cinnamaldehyde-induced vasodilatation as compared to control-treated group (n=4, $p<0.01$, Figure 3.8A). I further investigated if L-NAME can inhibit the residual responses shown in CD1 mice pre-treated with neuropeptide CGRP and substance P NK1 receptor antagonists (Figure 3.5A). A combination treatment of the neuropeptide receptor antagonists $CGRP_{8-37}$ and SR140333 with L-NAME significantly reduced the cinnamaldehyde-induced vasodilatation as compared to control-treated group (Figure 3.8B).

Using the selective inducible NOS (iNOS) inhibitor 1400W and the neuronal NOS (nNOS) inhibitor SMTC, the role of specific NOS isoforms was investigated in cinnamaldehyde-induced vasodilatation. Pre-treatment with the iNOS inhibitor 1400W (3mg/kg, *i.v.*) alone did not affect cinnamaldehyde-induced vasodilatation compared to control-treated group (n=9, Figure 3.8C). Furthermore, pre-treatment with 1400W in combination with the neuropeptide receptor antagonists did not abolish the cinnamaldehyde-induced vasodilatation (n=6-7, Figure 3.8D), suggesting that nitric oxide derived from iNOS does not participate in this response. However, pre-treatment with the nNOS inhibitor SMTC (10mg/kg, *i.v.*) alone significantly decreased cinnamaldehyde-induced vasodilatation as compared to control-treated group (n=6-7, $p<0.001$, Figure 3.8E). Pre-treatment with SMTC in combination with the neuropeptide receptor antagonists inhibited cinnamaldehyde-induced vasodilatation in comparison to control-treated groups (n=4-6, $p<0.001$, Figure 3.8F). This suggests that nNOS-derived nitric oxide participates in this response. Due to unavailability of a selective eNOS inhibitor, the mRNA and protein expression of eNOS was investigated in cinnamaldehyde-treated ear tissue samples at 30 min following topical application and compared to vehicle-treated samples. As shown in Figure 3.9A, there was a significant increase in eNOS mRNA copies in cinnamaldehyde-treated samples compared to vehicle. However, there was no change in total eNOS protein expression between cinnamaldehyde- and vehicle-treated samples (Figure 3.9B and C).

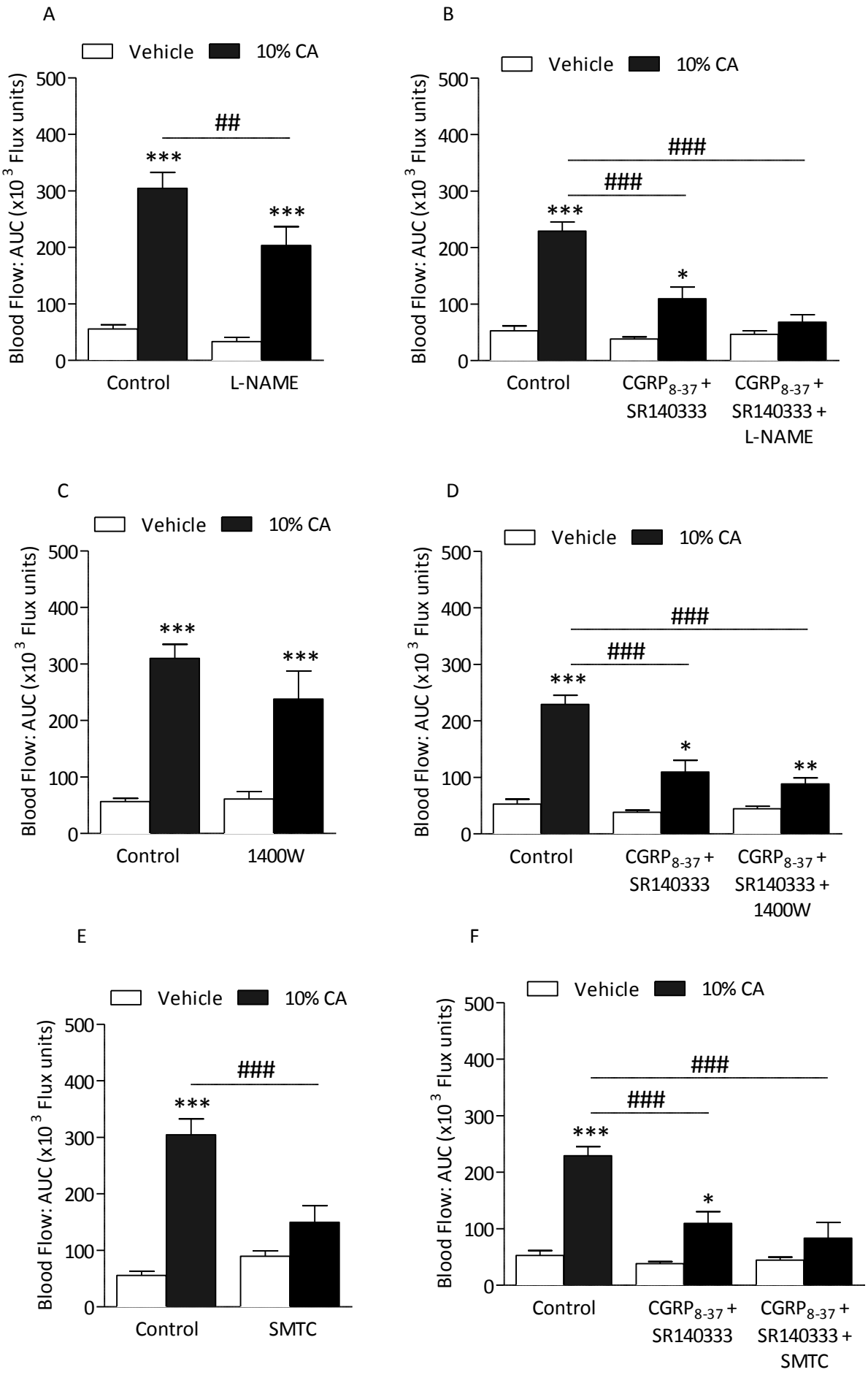
A
Vehicle
10% CA
Blood Flow: AUC (x10 3 Flux units)
500
400
300
200
100
0
##
***
***
Control
L-NAME
B
Vehicle
10% CA
Blood Flow: AUC (x10 3 Flux units)
###
###
***
*
Control
CGRP8-37 + SR140333
CGRP8-37 + SR140333 + L-NAME
C
Vehicle
10% CA
Blood Flow: AUC (x10 3 Flux units)
***
***
Control
1400W
D
Vehicle
10% CA
Blood Flow: AUC (x10 3 Flux units)
###
###
***
*
**
Control
CGRP8-37 + SR140333
CGRP8-37 + SR140333 + 1400W
E
Vehicle
10% CA
Blood Flow: AUC (x10 3 Flux units)
###
***
Control
SMTC
F
Vehicle
10% CA
Blood Flow: AUC (x10 3 Flux units)
###
###
***
*
Control
CGRP8-37 + SR140333
CGRP8-37 + SR140333 + SMTC

Figure 3.8 Role of nitric oxide in cinnamaldehyde (CA)-induced vasodilatation
Blood flow (x 10^3 flux units) in mouse ears following topical application of 20µl cinnamaldehyde (CA, 10%) or vehicle (10% DMSO in ethanol) using laser Doppler techniques. Results recorded over a 30 min period and shown as mean ± S.E.M. Male mice were pre-treated with nitric oxide synthase (NOS) inhibitor alone or in the presence of a combination of the selective CGRP receptor antagonist $CGRP_{8-37}$ (400nmol/kg, *i.v.*, 5min) and the neurokinin-1 receptor antagonist SR140333 (480nmol/kg, *i.v.*, 5min) (n=4) or respective control (0.01% BSA in saline, n=4). Cinnamaldehyde-induced vasodilatation in the ears of male CD1 mice pre-treated with **A**) and **B**) non-selective nitric oxide synthase inhibitor L-NAME (15mg/kg, *i.v.*, 5min, n=6) or control (saline, *i.v.*, 5min, n=5) alone in the presence of $CGRP_{8-37}$ and SR140333 (n=4-5), **C**) and **D**) iNOS inhibitor 1400W (3mg/kg, *i.v.*, 5min, n=9) or control (saline, *i.v.*, 5min, n=9) with or without $CGRP_{8-37}$ and SR140333 (n=4-7), **E**) and **F**) nNOS inhibitor SMTC (10mg/kg, *i.v.*, 5min, n=7) or control (saline, *i.v.*, 5min, n=6) with or without $CGRP_{8-37}$ and SR140333 (n=4-6). *p<0.05, **p<0.01, ***p<0.001 compared to respective vehicle-treated ears, ##p<0.01, ###p<0.005 using 2-way ANOVA followed by Bonferroni *post hoc* test.

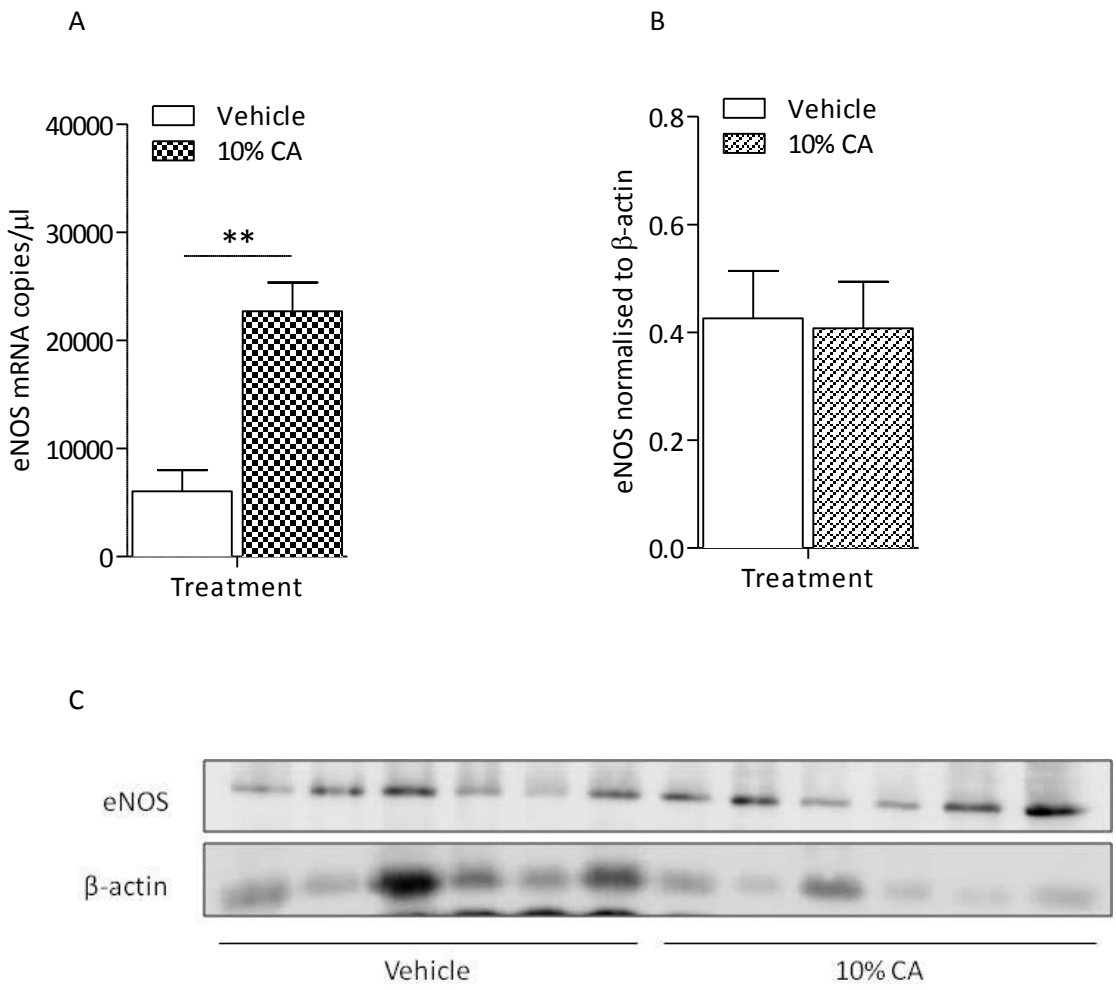

Figure 3.9 Effects of cinnamaldehyde (CA) on total eNOS expression. Ear tissues from male CD1 mice were harvested at 30 min following topical application of cinnamaldehyde (CA, 10%) or vehicle (10% DMSO in ethanol). **A**) mRNA expression of eNOS following topical application of CA or vehicle in the mouse ear tissues. Results are expressed as copy numbers per sample normalised to GAPDH and β-actin (n=4 per group), **B**) eNOS protein expression was determined by immunoblotting and **C**) analysed by densitometry relative to the loading control β-actin. Data denotes mean ± S.E.M, n=6. Data was analysed by using Student's *t* test.

3.2.7 Role of reactive oxygen species in cinnamaldehyde-induced vasodilatation

Our results thus far demonstrate clearly that both neuropeptides and nitric oxide mediate vasodilatation downstream of TRPA1 activation. Previously, a link between neurogenic-induced blood flow responses and reactive oxygen species generation was established in our group (Starr et al., 2008) and hence, I further investigated the role of reactive oxygen species in cinnamaldehyde-induced vasodilatation. Using the reactive oxygen species scavenger N-acetylcysteine (300mg/kg, *i.p.*), It was shown that there was a significantly decrease in cinnamaldehyde-induced vasodilatation compared to control-treated group ($n=6$, $p<0.001$, Figure 3.10A). This dose of N-acetylcysteine was previously shown to inhibit xylene-induced neurogenic plasma extravasation (Sandor et al., 2009). I further investigated whether the source of reactive oxygen species generation using the NADPH oxidase (NOX) inhibitor apocynin (Starr et al., 2008). Apocynin (20mg/kg, *i.v.*, 5min) has been previously shown to significant decrease TRPV1-mediated neurogenic vasodilatation in the mouse ear model (Starr et al., 2008). Pre-treatment with apocynin was able to significantly decrease cinnamaldehyde-induced responses as compared to the control-treated group ($n=6$-7, $p<0.01$, Figure 3.10B), indicating that reactive oxygen species being generated by NOX play a role in mediating this vasodilatation.

There are several isoforms of NOX and I further investigated the role of NOX4, which was recently demonstrated to generate superoxide downstream of TRPV1 and nNOS activation (Ito et al., 2013). Topical application of cinnamaldehyde induced a significant increase in blood flow compared to vehicle-treated ears in NOX4 WT mice ($n=4$, $p<0.01$, Figure 3.10C), and this remains unchanged in NOX4 KO mice, suggesting that NOX4 is not involved in generating reactive oxygen species in this model.

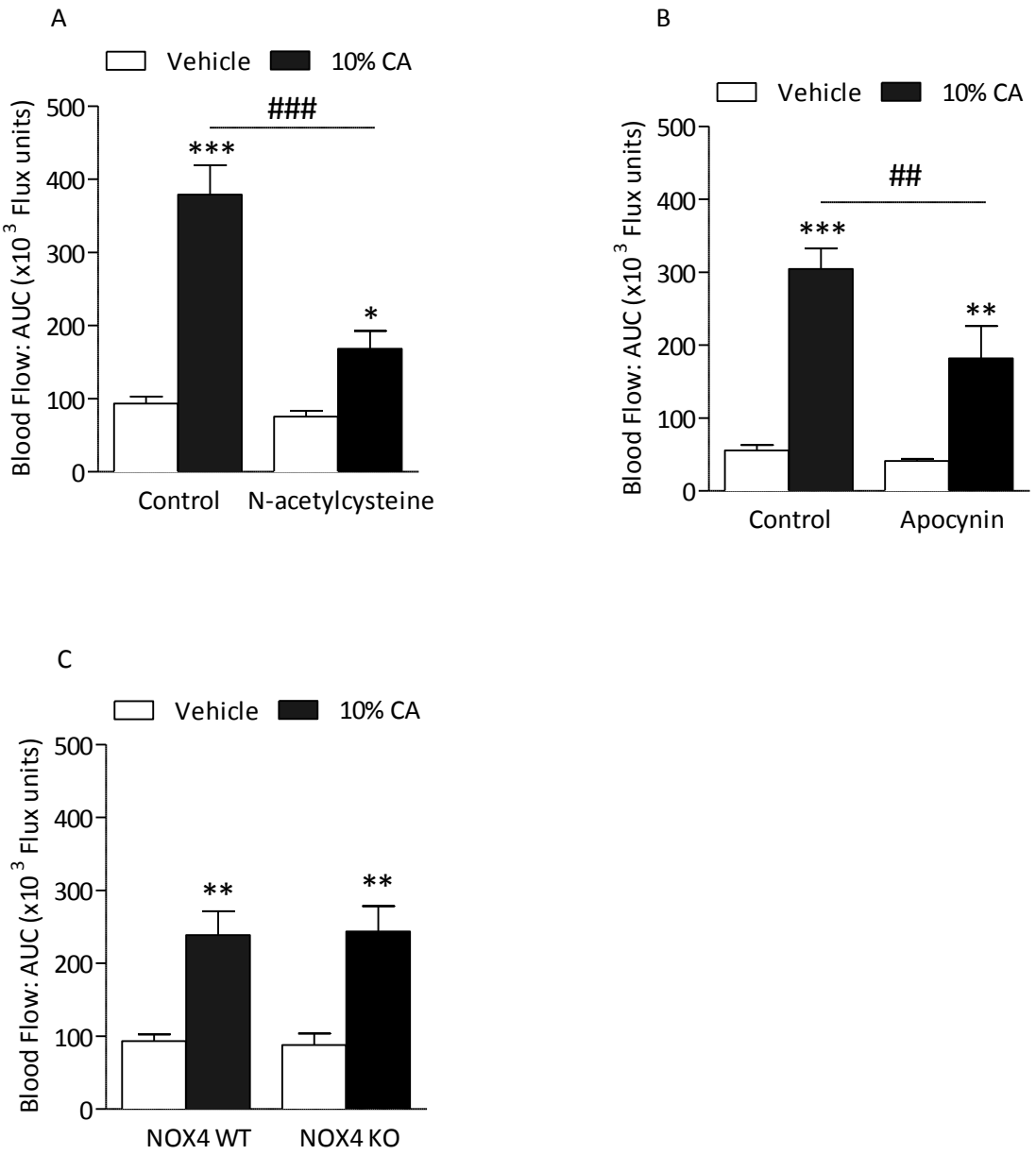

Figure 3.10 Role of reactive oxygen species in cinnamaldehyde (CA)-induced vasodilatation

Blood flow (x 10^3 flux units) in mouse ears following topical application of 20µl cinnamaldehyde (CA, 10%) or vehicle (10% DMSO in ethanol) using laser Doppler techniques and FLPI. Results recorded over a 30 min period and shown as mean ± S.E.M. Cinnamaldehyde-induced vasodilatation in the ears of male CD1 mice pre-treated with **A**) reactive oxygen species scavenger N-acetylcysteine (300mg/kg, *i.p.*, 30 min, n=6) or control (saline, *i.p.*, 30 min, n=6), **B**) NADPH oxidase inhibitor apocynin (20mg/kg, *i.v.*, 5 min, n=7) or control (saline, *i.v.*, 5 min, n=6). **C**) Cinnamaldehyde-induced vasodilatation in the ears of NOX4 WT and KO mice (n=4). **p<0.01, ***p<0.001 compared to respective vehicle-treated ears, ##p<0.01, ###p<0.005 using 2-way ANOVA followed by Bonferroni *post hoc* test.

3.2.8 Role of hydrogen peroxide (H_2O_2) and catalase in cinnamaldehyde-induced vasodilatation

The role of reactive oxygen species in cinnamaldehyde-induced vasodilatation was further investigated in this study. Pre-treatment with SOD and the H_2O_2 scavenger catalase have been previously shown to reduce capsaicin-induced neurogenic vasodilatation *in vivo* (Starr et al., 2008). In this study, co-treatment of catalase and SOD caused a significant reduction in cinnamaldehyde-induced vasodilatation when compared with responses in the presence of the deactivated enzymes (n=3-6, $p<0.01$, Figure 3.11A). The roles of H_2O_2 and superoxide were further investigated using individual treatment of each pharmacological inhibitor alone.

Administration of catalase alone caused no significant change in cinnamaldehyde-induced vasodilatation (n=4, $p>0.05$, Figure 3.11B). Furthermore, there was no change in H_2O_2 levels between vehicle- and cinnamaldehyde-treated ear tissue samples at 30 min following topical treatment (n=12, $p>0.05$, Figure 3.11C).

Administration of SOD alone proved to be remarkably ineffective in inhibiting cinnamaldehyde-induced vasodilatation (n=3, $p>0.05$, Figure 3.11D). Chemiluminescence was used to detect superoxide levels in the vascular tissue and surprisingly, there was a significant decrease in superoxide levels in cinnamaldehyde-treated when compared to vehicle-treated ear samples at 30 min following topical treatment (n=10, $p<0.05$, Figure 3.11E). The ineffectiveness of SOD in this study could be due to its lack of ability to cross the plasma membrane and hence, the role of superoxide was further investigated using the membrane permeable SOD mimetic tempol. Tempol proved to be remarkably effective at reducing cinnamaldehyde-induced vasodilatation as compared to control-treated group (n=6, $p>0.001$, Figure 3.11F).

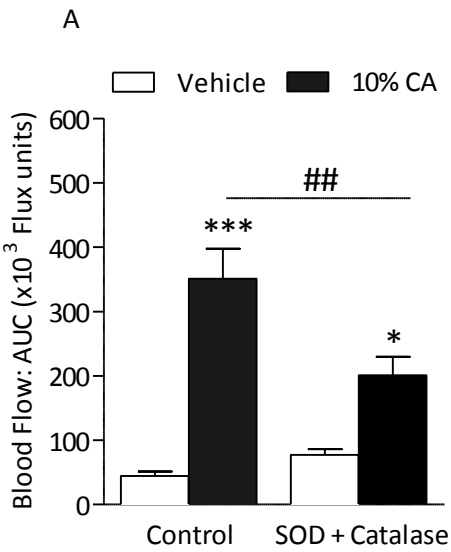
A
Vehicle
10% CA
Blood Flow: AUC (x10 3 Flux units)
600
500
400
300
200
100
0
##
***
*
Control
SOD + Catalase

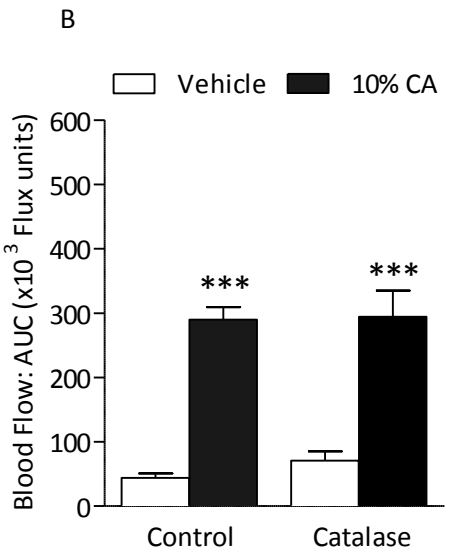
B
Vehicle
10% CA
Blood Flow: AUC (x10 3 Flux units)
600
500
400
300
200
100
0
***
***
Control
Catalase

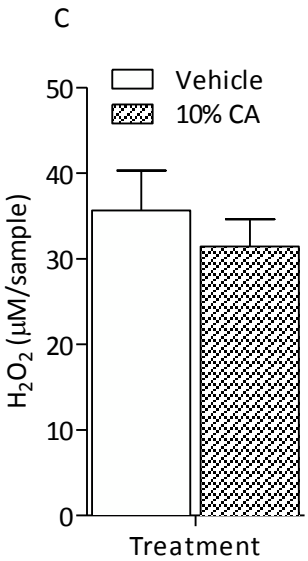
C
Vehicle
10% CA
H2O2 (µM/sample)
50
40
30
20
10
0
Treatment

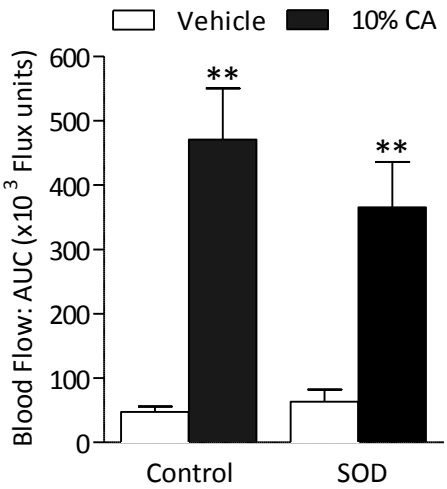
D
Vehicle
10% CA
Blood Flow: AUC (x10 3 Flux units)
600
500
400
300
200
100
0
**
**
Control
SOD

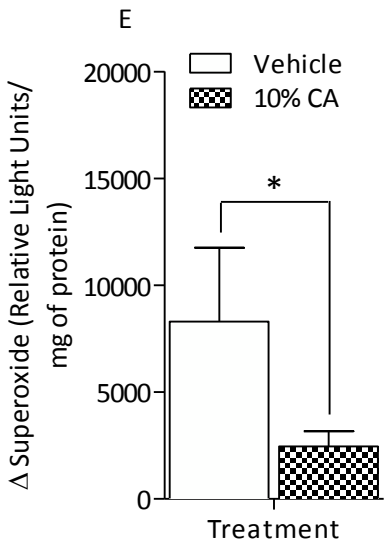
E
Vehicle
10% CA
Δ Superoxide (Relative Light Units/ mg of protein)
20000
15000
10000
5000
0
*
Treatment

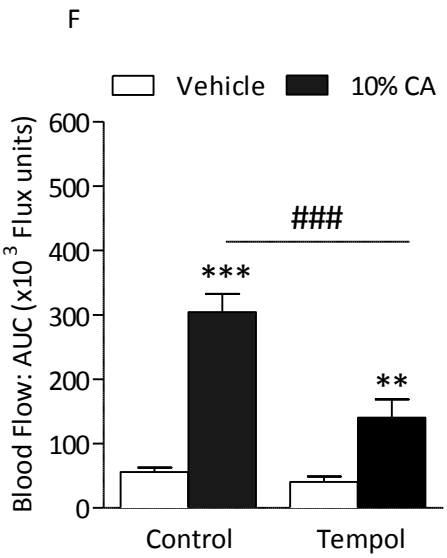
F
Vehicle
10% CA
Blood Flow: AUC (x10 3 Flux units)
600
500
400
300
200
100
0
###
***
**
Control
Tempol

Figure 3.11 Role of hydrogen peroxide (H_2O_2) and catalase in cinnamaldehyde-induced vasodilatation

Blood flow (x 10^3 flux units) in male CD1 mouse ears following topical application of 20µl cinnamaldehyde (CA, 10%) or vehicle (10% DMSO in ethanol) using laser Doppler techniques. Results recorded over a 30 min period and shown as mean ± S.E.M. Cinnamaldehyde-induced vasodilatation in the ears of mice pre-treated with **A**) a combination of superoxide dismutase (SOD, 25000U/kg) and catalase (25000U/kg) or control (denatured SOD and catalase enzyme at 95°C for 20 min, *i.p.*, n=6) and **B**) catalase alone (25000U/kg, *i.p.*, n=3) or respective control (denatured catalase enzyme at 95°C for 20 min, *i.p.*, n=4). **C**) H_2O_2 levels in vehicle or CA-treated ear tissues at 30 min following topical treatment in mice as measured by the AMPLEX RED assay (n=12). **D**) Cinnamaldehyde-induced vasodilatation in the ears of mice pre-treated with SOD alone (25000U/kg, *i.p.*, n=3) or respective control (denatured SOD enzyme at 95°C for 20 min, *i.p.*, n=3). **E**) Superoxidelevels in vehicle or CA-treated ear tissues at 30 min following topical treatment in mice (n=10), as measured by Lucigenin assay (n=10). **F**) Cinnamaldehyde-induced vasodilatation in the ears of mice pre-treated with SOD mimic tempol (30mg/kg) or respective control (saline, *i.v.*, n=6). *p<0.05, **p<0.01, ***p<0.001 compared to respective vehicle-treated ears, ##p<0.01, ###p<0.005 using 2-way ANOVA followed by Bonferroni *post hoc* test.

3.2.9 Role of hydroxyl radicals and nitrotyrosine in cinnamaldehyde-induced vasodilatation

Hydroxyl radicals, which are generated from H_2O_2, formation is dependent on the catalysis by ferrous iron and has been previously shown to be involved in CGRP-mediated neurogenic relaxation (Norisue et al., 1997). I further investigated the role of hydroxyl radicals by using the iron chelator deferoxamine. Pre-treatment of deferoxamine was shown to significantly decrease cinnamaldehyde-induced vasodilatation when compared to control-treated group ($n=6$, $p<0.001$, Figure 3.12).

Our previous results in this study have shown that both nitric oxide and superoxide are two mediators that are involved in mediating cinnamaldehyde-induced increase in blood flow. Nitric oxide is known to react with superoxide to produce peroxynitrite (Beckman and Koppenol, 1996), which can mediate vasodilatation *in vivo*(Graves et al., 1998). Intracellullar peroxynitrite can interact with nitrate proteins such as tyrosine residues to form 3-nitrotyrosineand hence, increased nitrotyrosine levels are commonly used as a marker of the participation of peroxynitrite. Total nitrotyrosine protein levels were measured in this study and were found to be significantly increased in ear tissue samples treated with cinnamaldehyde when compared to vehicle-treated samples following a 30 min of topical application ($n=6$, $p<0.001$, Figure 3.13 A-B).

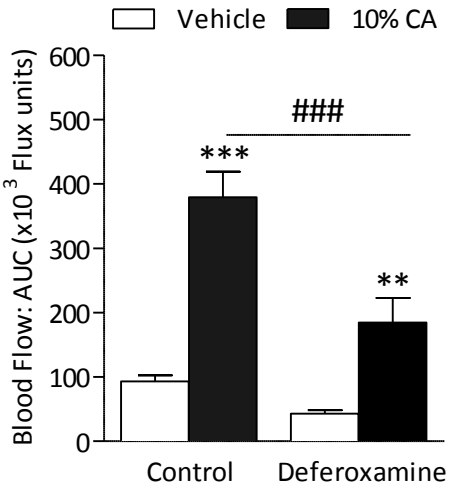

Figure 3.12 Role of hydroxyl radicals in cinnamaldehyde-induced vasodilatation
Male CD1 mice were pre-treated with iron chelator deferoxamine (25mg/kg, *i.p.*, 30 min, n=6) or control (saline, *i.p.*, 30 min, n=6) and blood flow (x 10^3 flux units) was measured for 30 min following topical application of 20µl cinnamaldehyde (CA, 10%) or vehicle (10% DMSO in ethanol) using laser Doppler techniques. Results are shown as mean $\pm$ S.E.M. **p<0.01, ***p<0.001 compared to respective vehicle-treated ears, ###p<0.005 using 2-way ANOVA followed by Bonferroni *post hoc* test.

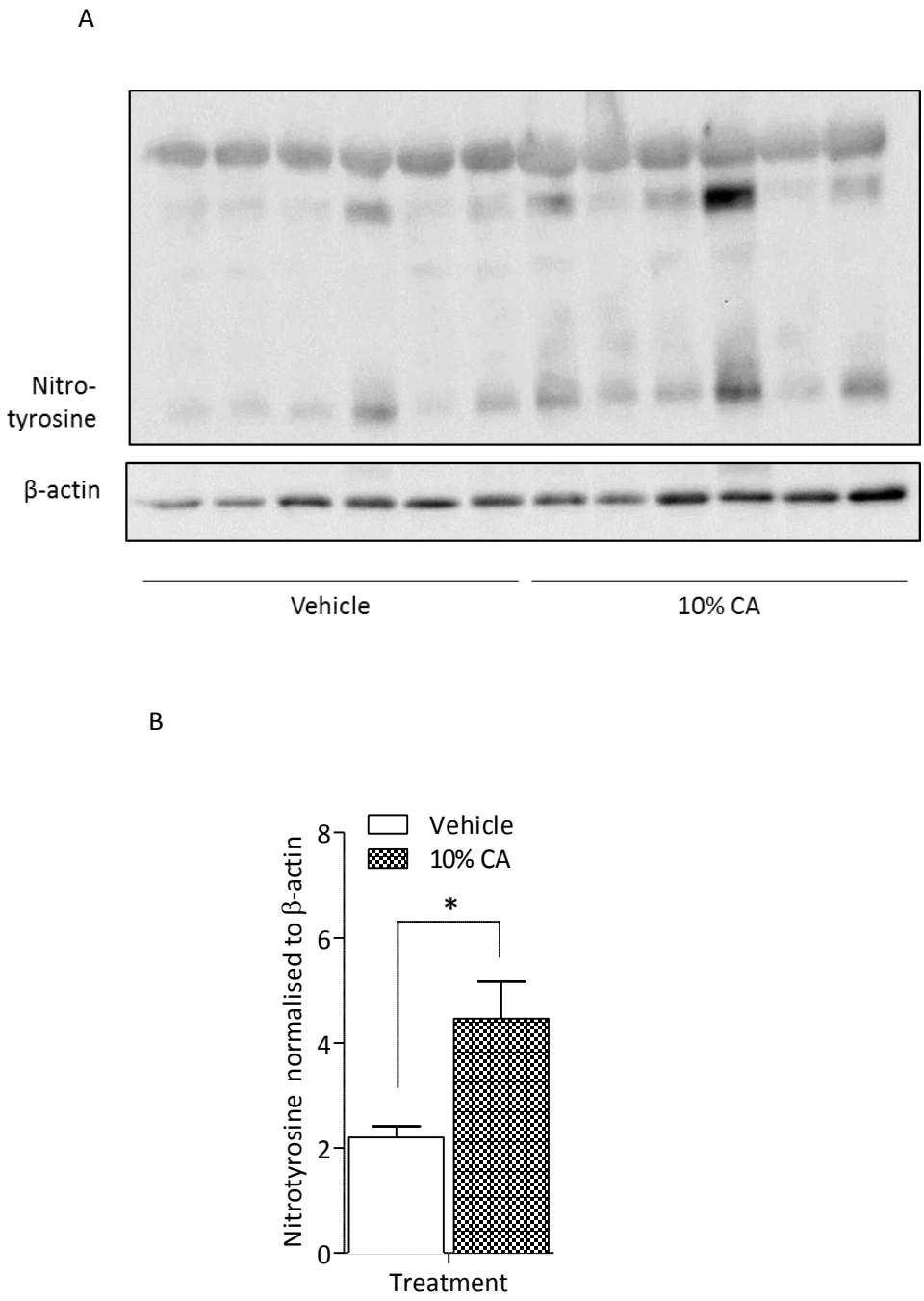

Figure 3.13 Effects of cinnamaldehyde (CA) on total nitrotyrosine expression. Ear tissues from male CD1 mice were harvested at 30 min following topical application of cinnamaldehyde (CA, 10%) or vehicle (10% DMSO in ethanol). **A**) nitrotyrosine protein expression was determined by immunoblotting and **B**) analysed by densitometry relative to the loading control β-actin. Data denotes mean ± S.E.M, n=6. *p<0.05 compared to respective vehicle-treated ears of CD1 mice using Student's *t* test.

3.3 Discussion

This chapter examined the *in vivo* effects of cinnamaldehyde, a proposed TRPA1 agonist on peripheral blood flow. I hypothesised that activation of TRPA1 channels, which are widely expressed on sensory nerve fibres, would lead to vasodilatation in the peripheral vasculature. Initial studies confirmed that topical application of cinnamaldehyde to the mouse ear caused an increase in blood flow, which was dependent on TRPA1 channels but not TRPV1 or TRPM8 channels. I showed that the cinnamaldehyde-induced blood flow responses are dependent on the release on the microvascular vasodilator CGRP but not substance P. This chapter also provides novel evidence indicating that nNOS-derived nitric oxide and reactive oxygen species mediates the vasodilator response to TRPA1 activation by cinnamaldehyde.

3.3.1 Cinnamaldehyde-induced vasodilatation is dependent on TRPA1

Cinnamaldehyde, the main component of cinnamon oil is commonly used and is regarded as the most selective TRPA1 agonist (Bandell et al., 2004). In this chapter, I show that topical application of cinnamaldehyde (10%) induced an increase in blood flow in the mouse ear model. Since there was no difference in cinnamaldehyde-induced vasodilatation between male and female CD1 mice, male CD1 mice were used throughout the study to minimise animal use, which is in line with the application of the 3R's in animal research.

Interestingly, topical cinnamaldehyde (10%) has been previously demonstrated to elicit burning pain and induce heat allodynia as well as an axon reflex flare reaction on the forearm of healthy subjects (Namer et al., 2005). Additionally, Namer *et al.* showed that cinnamaldehyde induced an increase in superficial blood flow 10 min after topical application and this correlates with the blood flow responses observed in this study.

The selectivity of cinnamaldehyde for TRPA1 was further investigated using various TRP channels antagonists and transgenic mice. Ruthenium red, a non-selective cation channel blocker, has been previously used *in vitro* and *in vivo* to block TRPA1 and TRPV1 channels. Ruthenium red has been previously shown to block the TRPA1 agonist mustard oil-induced contraction of the rat bladder at micromolar concentrations (Patacchini et al., 1990) and mustard oil-induced calcium influx in cultured rat sensory neurons (Jordt et al., 2004). In this study, I chose to investigate the effects of ruthenium red at 3mg/kg, which was previously shown to reduce the nociception induced by *i.pl.* injection of menthol *in vivo* (Cordova et al., 2011). Pre-treatment with ruthenium red was effective in reducing cinnamaldehyde-induced vasodilatation, suggesting an involvement of non-selective cation channels in this study.

The involvement of TRPA1 in cinnamaldehyde-induced blood flow increase was further investigated using pharmacological blockade of TRPA1 channel activity and in mice where the TRPA1 gene was deleted. In this study, cinnamaldehyde-induced vasodilatation was significantly reduced in TRPA1 KO mice. These data suggest that cinnamaldehyde selectively activates TRPA1 and this supports earlier findings of Pozsgai *et al*. (2010) in our laboratory who showed that the vasodilator effect induced by cinnamaldehyde was inhibited in the paw skin of anaesthetised TRPA1 KO mice.

The effects of another TRPA1 antagonist TCS5861528 (also known as Chembridge-5861528), a new derivative of HC030031 was investigated in the cinnamaldehyde-induced blood flow responses. Systemic administration of TCS5861528 (10mg/kg twice daily for a week) has previously been shown to significantly attenuate mechanical-induced withdrawal responses in diabetic and control groups of rats (Wei et al., 2009). In our study, I demonstrated that pre-treatment with TCS5861528 (10mg/kg) significantly decreased cinnamaldehyde-induced vasodilatation but the response was not completely inhibited. Thus, I further verify the selectivity of TCS5861528 (10mg/kg) in blocking the responses to a different TRPA1 agonist mustard oil or activating other TRP channels such as TRPV1.

Mustard oil has been previously shown to mediate peripheral vasodilatation in the mouse ear model in a TRPA1-dependent manner as demonstrated in TRPA1 KO mice (Pozsgai et al., 2010). The results here correlate with previous findings, demonstrating clearly that mustard oil mediated an increase in ear blood flow compared to control-treated group and interestingly, these responses were significant reduced in the TCS5861528-treated group. However, in the TCS5861528-treated group, mustard oil-treated ears had a slightly higher ear blood flow as compared to vehicle-treated ears, albeit not significant. TCS5861528 has been previously shown to antagonise AITC-induced responses in human TRPA1-transfected HEK-293 cells ($IC_{50,}$ 42µM) (Wei et al., 2009) and in rat TRPA1-transfected HEK-93 cells (IC_{50}, 230 nM) (Wei et al., 2010a). It remains to be determined whether a higher dose of TCS5861528 would be more effective in inhibiting both mustard oil- and cinnamaldehyde-induced vasodilatation *in vivo*.

Moreover, to assess whether TCS5861528 acts on TRPV1, capsaicin-induced vasodilatation was determined in a separate group of mice pre-treated with TCS5861528 or its respective control. The TRPV1 agonist, capsaicin increases peripheral blood flow as shown previously in our group (Grant et al., 2002, Starr et al., 2008) and this response was unaffected by the pre-treatment with TCS5861528. Interestingly, previous studies by Wei *et al.* have demonstrated that TCS5861528 at a dose of 100µM had no TRPV1 channel agonism or antagonism (Wei et al., 2010a). Hence, although TCS5861528 was not effective in inhibiting cinnamaldehyde-

induced vasodilatation in this study, these evidences suggest that TCS5861528 at a dose of 10mg/kg does not activate or block TRPV1 receptors *in vivo*.

The properties of TCS5861528 were first characterised by Wei *et al. in vitro* using human TRPA1-transfected HEK-293 cells where it was compared to the prototype TRPA1 antagonist HC030031. HC030031 was shown to antagonise TRPA1 induced responses induced by 4-HNE and AITC in a concentration-dependent manner, with IC_{50} values of 42μM and 48μM, respectively whilst TCS5861528 was shown to have a greater affinity for TRPA1 channels with IC_{50} values of 14μM and 19μM (Wei et al., 2009). I further tested the TRPA1 antagonist HC030031 that is known to block activation of TRPA1 by 15-PGJ_2 and reduce activation by mustard oil *in vitro*(Taylor-Clark et al., 2008). HC030031 has been previously shown to inhibit formalin-induced flinching in rats (McNamara et al., 2007) and TRPA1 agonist PF4840154-induced licking behaviours in CD1 mice (Ryckmans et al., 2011). Pre-treatment with HC030031 in this study significantly suppressed cinnamaldehyde-induced vasodilatation, similar to the inhibition observed in TRPA1 KO mice. Although previous studies have shown that TCS5861528 has a greater affinity for TRPA1 than HC030031 *in vitro* (Wei et al., 2009), our results provide clear evidence that at the dose utilised, TCS5861528 did not completely block cinnamaldehyde-induced vasodilatation, when compared to experiments using HC030031. From our findings using TRPA1 KO mice and the selective TRPA1 antagonist HC030031, I can confirm that cinnamaldehyde activates TRPA1 to increase blood flow in the ear skin. Furthermore, effective doses of the calcium-activated potassium channel blocker TEA was shown to significant reduce cinnamaldehyde-induced vasodilatation, supporting the role of calcium in the TRPA1-mediated vasodilator response in the mouse ear. TEA administered at 6mg/kg is known to give a plasma concentration of approximately 0.5mM, with no change in systemic arterial blood pressure and was previously shown to inhibit neurogenic vasodilatation in human forearm (Inokuchi et al., 2003).

It is also known that TRPA1 is co-expressed in approximately 60-75% of all TRPV1-positive sensory neurons under normal conditions (Story et al., 2003, Kobayashi et al., 2005), suggesting a potential interaction between the two channels, although the potential mechanisms and effects of this interaction is under debate. Salas *et al*. (2009) showed that mustard oil-gated currents exhibited faster kinetics activation in TRPA1-expressing than in TRPA1/TRPV1 co-expressing CHO cells *in vitro*. Our recent study *in vivo* showed although TRPV1-mediated vasodilatation is not affected by deletion of TRPA1 gene, but TRPA1-mediated vasodilatation by mustard oil is significantly potentiated when TRPV1 channels are blocked using the TRPV1 antagonist SB366791 in TRPV1 KO mice (Aubdool, 2010). Therefore, it was suggested that a potential link between receptor function and TRPV1 might be involved in regulating TRPA1 receptor-

mediated responses. However, our results here showed that TRPV1 gene deletion did not affect cinnamaldehyde-induced vasodilatation in the peripheral vasculature. It remains to be determined whether these responses are present when TRPV1 channels are pharmacologically blocked. These results provide evidence that cinnamaldehyde does not activate TRPV1 channels.

It has been reported that the co-expression between TRPA1 and TRPM8 was rare, where 3.3% of neuronal profiles displayed both TRPA1 and TRPM8 (Kobayashi et al., 2005). Functional interactions between these two channels have been speculated, as they are both cold sensors. The TRPM8 channel blocker AMTB was shown to inhibit TRPM8 agonist icilin-induced calcium influx *in vitro* and also shown to significantly attenuate reflex responses to noxious urinary bladder distension (Lashinger et al., 2008). I further investigated the role of TRPM8 in cinnamaldehyde-induced increase in blood flow. Pre-treatment with AMTB was not effective in suppressing cinnamaldehyde-induced vasodilatation. Thus, this study confirms that cinnamaldehyde does not activate TRPM8.

3.3.2 Cinnamaldehyde-induced vasodilatation is dependent on neuropeptide CGRP and neuronal-derived nitric oxide

Capsaicin and mustard oil are both known to produce their inflammatory effects by activation of sensory C-fibres, which mediate the release of neuropeptides such as substance P, and CGRP from the nerve terminals (Lembeck and Holzer, 1979, Lundberg et al., 1985, Brain et al., 1985). There is previous evidence from our group demonstrating that capsaicin and mustard oil-induced vasodilatation depends on the release of both CGRP and substance P (Grant et al., 2005). TRPA1 channels are expressed on sensory neurons, which also express TRPV1, CGRP and substance P (Jordt et al., 2004) and in this study, I investigated whether these neuropeptides are involved in TRPA1-mediated vasodilatation induced by cinnamaldehyde using pharmacological blockade of both CGRP and NK_1 receptors.

Co-treatment with the NK_1 receptor antagonist SR140333 and CGRP receptor antagonist $CGRP_{8-37}$ significantly reduced cinnamaldehyde-induced blood flow responses. The doses of SR140333 and $CGRP_{8-37}$ were chosen based on previous studies in the group showing that both inhibitors can inhibit substance P-induced and CGRP-induced vasodilatation, respectively in the mouse ear model (Grant et al., 2002, Grant et al., 2005, Starr et al., 2008). This finding suggests that both neuropeptides are released following TRPA1 activation by cinnamaldehyde and this finding is similar to Engel *et al.* (2011) who demonstrated that 2,4,6-trinitrobenzene sulfonic acid (TNBS) induced TRPA1-dependent release of substance P and CGRP in colonic sensory neurons (Engel et al., 2011). However, in this study these responses were not completely

blocked, as there was a small but significant increase in blood flow in cinnamaldehyde-treated ears as compared to vehicle-treated ears of mice pre-treated with both SR140333 and $CGRP_{8-37}$. This finding led us to investigate the treatment of SR140333 and $CGRP_{8-37}$ alone on cinnamaldehyde-induced vasodilatation.

Surprisingly, SR140333 pre-treatment did not inhibit cinnamaldehyde-induced blood flow responses and this result suggests that substance P may not be involved in these responses. This finding does not correlate to previous findings in our group where substance P has been shown to mediate TRPA1 agonist mustard oil induced neurogenic vasodilatation (Grant et al., 2005, Pozsgai et al., 2010). Moreover, systemic injection of mustard oil activates TRPA1 and increases substance P content in the peritoneal fluid of rat (Trevisan et al., 2013) and substance P release from sensory neurons through p38 phosphorylation in mice hindpaw (Nakamura et al., 2012). However, in the case for cinnamaldehyde although it activates TRPA1 selectively, its vasodilatation is not dependent on the release of substance P. Electrophysiology studies on rat DRG neurons showed that there may be more nerves expressing CGRP than substance P as substance P was mainly found in 53% of C-fibres and 21% of Aδ-fibres, with poor expression on Aα/β-fibres (n=80), whilst CGRP was mainly found in 46% of C-fibres and 38% of Aδ-fibres, with increased expression (17%) on Aα/β-fibres (n=73) (Lawson et al., 1993). It would be interesting to investigate the proportion and subtypes of nerves expressing TRPA1 with both neuropeptides to determine why substance P may not be involved in cinnamaldehyde-induced vasodilatation.

The role of CGRP in cinnamaldehyde-induced vasodilatation was investigated using either genetic deletion or the pharmacological blockade of CGRP receptors. Several TRPA1 agonists have been shown to stimulate CGRP release from spinal cord, oesophagal sensory neurons, rat hindpaw skin and DRG neurons (Qin et al., 2008, Ruparel et al., 2008, Trevisani et al., 2007). It was unknown if TRPA1-mediated vasodilatation induced by cinnamaldehyde is dependent on CGRP in the mouse ear model. Our study addresses this by clearly showing that pre-treatment with $CGRP_{8-37}$ or in α-CGRP KO mice, there was a marked decrease in cinnamaldehyde-induced increase in blood flow responses in the mouse ear model. I also demonstrated that cinnamaldehyde treatment could significantly increase α-CGRP mRNA expression at 30 min following topical treatment. There was also an increase in β-CGRP mRNA expression but interestingly; I demonstrated a significant decrease in CGRP levels in cinnamaldehyde-treated when compared to vehicle-treated ear tissue samples. It remains unknown whether there was an increase in α-CGRP at an earlier time point or at the 30 min treatment time-point; CGRP levels are higher in the plasma than tissue. Kunkler *et al.* (2011) have also shown that other TRPA1 agonists and environmental irritants can release CGRP from dissociated rat trigeminal ganglia

neurons (Kunkler et al., 2011). This finding overall increases the evidence of CGRP release downstream of TRPA1 activation in different tissues and vascular beds.

The results in this study suggest that CGRP is the primary neurogenic vasodilator involved in cinnamaldehyde-induced vasodilatation in the peripheral vasculature and further reflect that different TRPA1 agonists may have specific vasodilator mechanisms depending on the site of action. CGRP-induced vasodilatation has been reported to be due to either a direct effect on the vascular smooth muscle or indirect effect mediated through vascular endothelium, as discussed in chapter 1 (Smillie and Brain, 2011). I showed in this study that pre-treatment with the K_{ATP} channel blocker glibenclamide suppressed cinnamaldehyde-induced vasodilatation in the mouse ear. Interestingly, this data is in contrast with Yanaga *et al.*findings who previously reported that vasorelaxant effects of cinnamaldehyde were independent of glibenclamide-sensitive K_{ATP} channels in isolated rat aorta (Yanaga et al., 2006). However, here I show that K_{ATP} channels are involved in cinnamaldehyde-mediated vasodilatation in the ear vessels *in vivo* where consequently, it is possible that cinnamaldehyde may activate TRPA1 on sensory neurons and release CGRP which mediates vasodilatation by opening K_{ATP} channels on the vascular smooth muscle cells.

Since pharmacological blockade with the neuropeptide receptor antagonists was not able to completely inhibit cinnamaldehyde-induced vasodilatation, I investigated the other mediators and pathways that may be involved in the residual vasodilator effects. There is reported evidence that nitric oxide-mediated vasodilatation is dependent on activation and opening of K_{ATP} channels (Armstead, 1996). Moreover, CGRP itself can bind on its receptor complex on endothelial cells where it increases eNOS activity, mediated through a cAMP-PKA dependent pathway, leading to increased nitric-oxide production (Edvinsson et al., 1985, Brain and Grant, 2004). Intrabrachial infusion of CGRP was shown to result in a dose-dependent and reproducible forearm vasodilator response, which is dependent on the release of nitric oxide (de Hoon et al., 2003). There are other studies showing that CGRP-induced vasodilatation is independent of nitric oxide (Brain et al., 1993, Kawasaki et al., 1988, Klede et al., 2003). Using the previous findings, I investigated if nitric oxide produced downstream of CGRP-mediated pathway may play a role in cinnamaldehyde-induced vasodilatation and this was further investigated in this study using the non-selective nitric oxide synthase (NOS) inhibitor L-NAME. Pre-treatment with L-NAME showed a marked decrease in blood flow responses to cinnamaldehyde and further experiments investigated the pharmacological blockade of NOS together with neuropeptide receptor antagonists, where cinnamaldehyde-induced vasodilatation was completely abolished. There was no change in baseline blood flow after pre-treatment with

these pharmacological inhibitors. This provides further evidence that both neuropeptide and nitric oxide are involved in this response.

In the present study, I sought to investigate the source of nitric oxide synthase by using selective inhibitors to the different isoforms of nitric oxide synthase. In this study, CGRP has been shown to play an important role in cinnamaldehyde-induced increase in blood flow response and interestingly, CGRP can interact with receptors on the vascular endothelial cell to increase the production of cAMP which further stimulates nitric oxide production. This process here has been suggested to involve a direct effect of protein kinase A (PKA) on eNOS. Nitric oxide diffuses into the adjacent vascular smooth muscle cells and activates guanylate cyclase, which leads to relaxation (Brain and Grant, 2004). I demonstrated that there was no change in total eNOS protein in the ear following cinnamaldehyde treatment when compared to vehicle treatment, suggesting that nitric oxide is not being derived from eNOS. However, it remains unknown if there were any changes in phosphorylated eNOS or NOS activity.

I further demonstrated that there was an increase in nNOS mRNA that may contribute to an increased endogenous production of nitric oxide which contributes to peripheral vasodilatation. The present study demonstrates clearly that SMTC, a more specific nNOS inhibitor, but not the iNOS selective inhibitor 1400W, antagonised cinnamaldehyde-induced vasodilatation. Upon activation under certain inflammatory conditions, iNOS is known to be expressed by many cell types including vascular smooth muscles and endothelial cells, which are relevant to our study (Griffith and Stuehr, 1995, Forstermann and Kleinert, 1995). Interestingly, our data showed that intravenous injection of 1400W did not significantly affect the baseline blood flow. This finding is in agreement with recent published findings reporting that 1400W (3mg/kg, *i.v.*) caused no effects at baseline or on capsaicin-induced hyperaemic response in gastric mucosa in rats *in vivo* (Raimura et al., 2013). 1400W was chosen as an iNOS inhibitor as it is 5000-fold more selective for iNOS than eNOS (Garvey et al., 1997) and the two doses studied in this study have been previously used in rats and shown to selectively target iNOS (Patel et al., 2004, Cheng and Pang, 2004). SMTC at the chosen dose was previously shown to selectively target nNOS *in vivo* in studies using conscious rats (Gozal et al., 1996).

Our finding here strongly suggests that sensory neurons that contain nNOS may release nitric oxide following TRPA1 stimulation by cinnamaldehyde. An interaction between CGRP and nitric oxide in gastric vasodilatation through sensory neurons has been previously reported (Chen and Guth, 1995). There is also evidence showing that numerous TRPV1-immunoreaactive axons express nNOS (Raimura et al., 2013) but it remains unknown whether the nerves innervating the ear blood vessels express both TRPA1 and nNOS. However, an interaction between nitric oxide and CGRP has been previously speculated, where NO has been

suggested to act on sensory neurons to release CGRP which further diffuses to smooth muscle to mediate vasodilatation (Wei et al., 1992, Akerman et al., 2002). Keratinocytes and endothelial cells are known to release nitric oxide during inflammation and are thought to be in close proximity to sensory nerve endings (Cals-Grierson and Ormerod, 2004, Lowenstein et al., 1994).

Moreover, results from Miyamoto *et al*. (2009) suggest that endogenous levels of nitric oxide are able to activate TRPV1 and TRPA1 and increase pain behavioural responses (Miyamoto et al., 2009). Cinnamaldehyde acts on TRPA1 channels and increase intracellular calcium and an elevation in calcium has been previously reported to be important in activating calcium-dependent nNOS (Moncada et al., 1997). Thus, in this study I are providing evidence that neuronally-derived nitric-oxide plays an important role in the vasodilator response induced by cinnamaldehyde which is possibly being released downstream of TRPA1 activation. It is also evident in this study that the NO-dependent component in cinnamaldehyde-induced vasodilatation exists when CGRP receptors are antagonised.

3.3.3 Prostaglandins do not mediate cinnamaldehyde-induced vasodilatation

The role of other endothelial-derived mediator prostaglandins was investigated in cinnamaldehyde-induced responses *in vivo*. Prostacyclin is known to activate adenyl cyclase and elevate cyclic adenosine monophosphate levels to relax blood vessels (Martin et al., 1985). Interestingly, treatment of the cyclooxygenase inhibitor, indomethacin was shown not to inhibit TRPV1-mediated vasodilatation in mice (Starr et al., 2008). However, there is evidence in the literature suggesting the metabolites of prostaglandins D2, 15-deoxy-$\Delta^{12,14}$-prostaglandins J_2 ($15dPGJ_2$) can activate heterologously expressed hTRPA1 in human embryonic kidney cells and in a subset of chemosensitive mouse trigeminal neurons (Taylor-Clark et al., 2008). 15-d-PGJ_2 is generated during oxidative stress in inflammation and has also been shown to evoke inward currents and an increase in intracellular calcium in TRPA1-expressing CHO cells (Andersson et al., 2008). This study showed that indomethacin had no effect on cinnamaldehyde-induced vasodilatation. These results suggest that cyclo-oxygenase pathway may not be involved in inducing vasodilator effects of cinnamaldehyde.

3.3.4 Investigating the involvement of reactive oxygen species TRPA1-mediated vasodilatation

Reactive oxygen species are known to play an important physiological role in regulating vascular tone but can also cause vascular reactivity and vascular inflammation in pathological conditions. A potential link between cinnamaldehyde and reactive oxygen species production

has been established in previous cancer studies. Cinnamaldehyde is thought to have skin sensitising properties at high concentration (mM) but at low concentration, it was documented to inhibit secretion of interleukin-1β and tumor necrosis factor-α within lipopolysaccharide stimulated macrophages (Chao et al., 2008). Ka *et al*. (2003) showed that cinnamaldehyde treatment can induce reactive oxygen species production in human leukeumia promyelocytic cells and this is blocked by the antioxidant N-acetylcysteine (Ka et al., 2003). Moreover, cinnamaldehyde treatment increased reactive oxygen species production, which was blocked by vitamin E in human hepatoma PLC/PRF/5 cells (Wu et al., 2004).

In this study, cinnamaldehyde-induced vasodilatation was significantly reduced in mice pre-treated with N-acetylcysteine suggesting that there may be a potential link between TRPA1-mediated responses and increase in radical species generation. N-acetylcysteine is known to act as a precursor to glutathione, which is a powerful antioxidant and free radical scavenger. Interestingly, cinnamaldehyde contains an α,β-unsaturated carbonyl moiety which functions as a potent Michael reaction acceptor and causes endogenous antioxidant glutathione depletion (Cernuda-Morollon et al., 2001, Heiss et al., 2001, Rossi et al., 2000). These earlier findings may explain the inhibitory effects of N-acetylcysteine on cinnamaldehyde-induced vasodilatation. N-acetylcysteine scavenges radicals by reactions with the thiol group in the molecule (Aruoma et al., 1989) and hence, NAC may react with cinnamaldehyde-reactive electrophilic group and interfere with its ability to activate TRPA1. Thus, further experiments using more selective reactive oxygen species pathway modulators were used to elucidate the role of reactive oxygen species in cinnamaldehyde-induced vasodilatation.

One possible source of reactive oxygen species in cellular signalling is NOX (Li and Shah, 2004) and interestingly, pre-treatment with the NOX inhibitor apocynin was able to partially decrease cinnamaldehyde-induced vasodilatation. This dose was also previously shown to inhibit TRPV1 agonist capsaicin-induced vasodilatation (Starr et al., 2008). Here, it is possible that the NOX enzymes may be one of the sources of reactive oxygen species generation in cinnamaldehyde-induced vasodilatation. I investigated the possible role of NOX4 in cinnamaldehyde-induced vasodilatation as a link between nNOS and NOX4 was previously reported by Ito et al. (2013). I sought to investigate whether NOX4 may be involved in TRPA1-mediated vasodilatation and interestingly, there was no change in cinnamaldehyde-induced vasodilatation between NOX4 WT and KO mice. This finding suggests that NOX4 itself is not involved in mediating this vasodilatation but it remains unknown whether other isoforms of NOX such as NOX2 plays a role.

I further investigated the role of superoxide dismutase (SOD) and catalase, which enhances the catalysis of superoxide and H_2O_2, respectivelyin cinnamaldehyde-induced vasodilatation. Co-

treatment with SOD and catalase showed a significant decrease in the blood flow responses induced by cinnamaldehyde, showing the potential role of both mediators. This cocktail administration of SOD and catalase have also been previously shown to be effective in improving survival and minimising cell damage in the canine ischemia-reperfusion injury model (Jolly et al., 1984) and in capsaicin-mediated vasodilation (Starr *et al.*, 2008). To further confirm the potential role of superoxide and H_2O_2 in cinnamaldehyde-induced vasodilatation, I investigated the effects of separate administrations of SOD and catalase. Interestingly, pre-treatment with catalase alone had no effects in affecting cinnamaldehyde-induced vasodilatation and there was also no marked change in H_2O_2 between vehicle- and cinnamaldehyde-treated ear samples. A similar trend was demonstrated with the single treatment of SOD which had no effects in cinnamaldehyde-induced vasodilatation but surprisingly, I found that the level of superoxide release in cinnamaldehyde-treated samples was significantly less than vehicle-treated ear tissue samples at 30 min following treatment. It remains unknown how the level of superoxide is changed at earlier time points. Since there was a decrease in superoxide levels, I further investigated this using a cell-permeable SOD mimic tempol which increases catalysis of superoxide to undergo antioxidant pathway rather than SOD which may have poor permeability, further limiting their bioavailability and activity. Pre-treatment with tempol was shown to significantly decrease the cinnamaldehyde-induced vasodilatation, suggesting that tempol may be more potent in inhibiting the redox signalling in this response. Overall, in this study it seems like single treatment of SOD and catalase alone may not be sufficient to inhibit all the reactive oxygen species whereas co-administration of SOD and catalase increases the rate of superoxide conversion into H_2O and O_2.

A study by Ka *et al.* (2003) showed cinnamaldehyde to induce reactive oxygen species signalling by increased mitochondrial permeability transition in cancer HL-60 cell lines, where the mitochondrial membrane becomes more permeable resulting in mitochondrial damage and superoxide release due to incomplete oxygen generation during the electron transport chain (Ka et al., 2003). It is possible that cinnamaldehyde may induce reactive oxygen species production independently of TRPA1 in the sensory nerves to potentiate TRPA1 activation. The production of mitochondrial superoxide species in the spinal cord has also been shown to cause persistent pain, which was reduced by tempol and phenyl-N-*tert*-butylnitrone, a potent free radical scavenger (Kim et al., 2008). Another study has also supported the role of systemic administration of tempol to attenuate pain symptoms in inflammatory pain model (Khattab, 2006). Hence, there are possibilities that cinnamaldehyde-mediated TRPA1 activation may lead to increased reactive oxygen species production in the sensory nerves, which could further potentiate TRPA1 activation in the nerve terminals.

The superoxide species released can undergo 2 pathways: 1) redox signalling or 2) react with NO produced by nNOS resulting in peroxynitrite production. Peroxynitrite species can react with saturated fatty acids and the product directly and selectively activate TRPA1 (Taylor-Clark *et al.,* 2009) highlighting the possibility of the involvement of this peroxidation product in CA-sustained vasodilation response. This is consistent with the earlier finding in this study that inhibition of nNOS with SMTC was shown to reduce cinnamaldehyde-induced vasodilatation suggesting a role of peroxynitrite as one of the potential endogenous TRPA1 agonists to potentiate cinnamaldehyde-induced vasodilator response. Since an increase in nitrotyrosine levels have been reported to show the participation of peroxynitrite (Halliwell, 1997), I further investigated the effects of cinnamaldehyde treatment on total nitrotyrosine levels. In our study, I demonstrated an increased level of total nitrotyrosine protein expression in cinnamaldehyde-treated compared to vehicle-treated ear tissue samples. This finding suggests the possible interaction between superoxide and nNOS-derived nitric oxide, which may produce peroxynitrite following cinnamaldehyde treatment, but it remains unknown whether this response is dependent on TRPA1.

The role of hydroxyl radicals and oxidative stress was also investigated in the cinnamaldehyde-mediated vasodilatation. Excess H_2O_2 may be converted into oxidative stress molecules, such as hydroxyl radicals in the presence of transition metals, such as iron (Li & Shah, 2004). Deferoxamine (an iron chelator) significantly reduced cinnamaldehyde-induced vasodilation, suggesting the role of hydroxyl radicals and oxidative stress in this response. Andersson *et al.,* (2008) suggested that hydroxyl radicals may mediate TRPA1 activation of H_2O_2 in the sensory neurons, further supporting the potential role of reactive oxygen species in potentiating TRPA1 activation in the sensory nerves. However, Xue and colleagues (2011) have also shown cinnamaldehyde to induce vasodilation in rats' aorta, suggesting a vascular-dependent pathway of CA-mediated vasodilation. Prasad & Bharadwaj (1996) showed hydroxyl radicals to cause vasodilation *in vitro*, which may highlight the potential role of cinnamaldehyde in mediating vascular-dependent reactive oxygen species production and vasodilation or the reactive oxygen species production may be mediated downstream of CGRP, as proposed for capsaicin-mediated vasodilation (Starr et al., 2008). Currently, the *in vivo* mouse ear model does not allow us to distinguish the main site where reactive oxygen species is produced and I have not established the major source of reactive oxygen species production in the cinnamaldehyde-mediated vasodilation. Further studies are required to elucidate the role of other superoxide sources, such as mitochondria (inhibited by thenoyltrifluoroacetone), cytochrome P450 and xanthine oxidase (inhibited by allopurinol) (Li & Shah, 2004) in cinnamaldehyde-mediated neurogenic vasodilation. It remains unknown whether the generation of reactive oxygen species is TRPA1- and sensory nerve- dependent and hence, further investigation is required.

3.4 Conclusion

The results in this chapter highlight the selectivity of cinnamaldehyde to activate TRPA1 and increase blood flow in the peripheral vasculature and investigated the signalling mechanisms underlying TRPA1-depdendent vasodilatation. The findings are summarised in Figure 3.14. Using a combination of genetically modified mice and pharmacological inhibitors, I demonstrated the relative contribution of the vasoactive neuropeptide CGRP, but not substance P to this response, highlighting the involvement of a neurogenic component. Moreover, it was clearly demonstrated that cinnamaldehyde-induced vasodilatation is independent of cyclooxygenase-derived products such as prostaglandins but dependent on nNOS-derived nitric oxide. This is the first study to illustrate a link between TRPA1 activation and nNOS-derived nitric oxide production in the peripheral vasculature. Previous work has shown a crucial role for reactive oxygen species in mediating neurogenic-induced vasodilatation, downstream of CGRP and NK_1 receptors activation (Starr et al., 2008). In the current study, I also introduce the concept that reactive oxygen species, such as superoxide, hydroxyl radicals and peroxynitrite play a pivotal role in TRPA1-dependent vasodilation, possibly downstream of CGRP. The source of reactive oxygen species remains unknown and requires further investigation (Figure 3.15). TRPA1-mediated vasodilatation involving reactive oxygen species may be important in understanding neurogenic inflammation in different pathophysiological conditions such as migraine or ischemic damage.

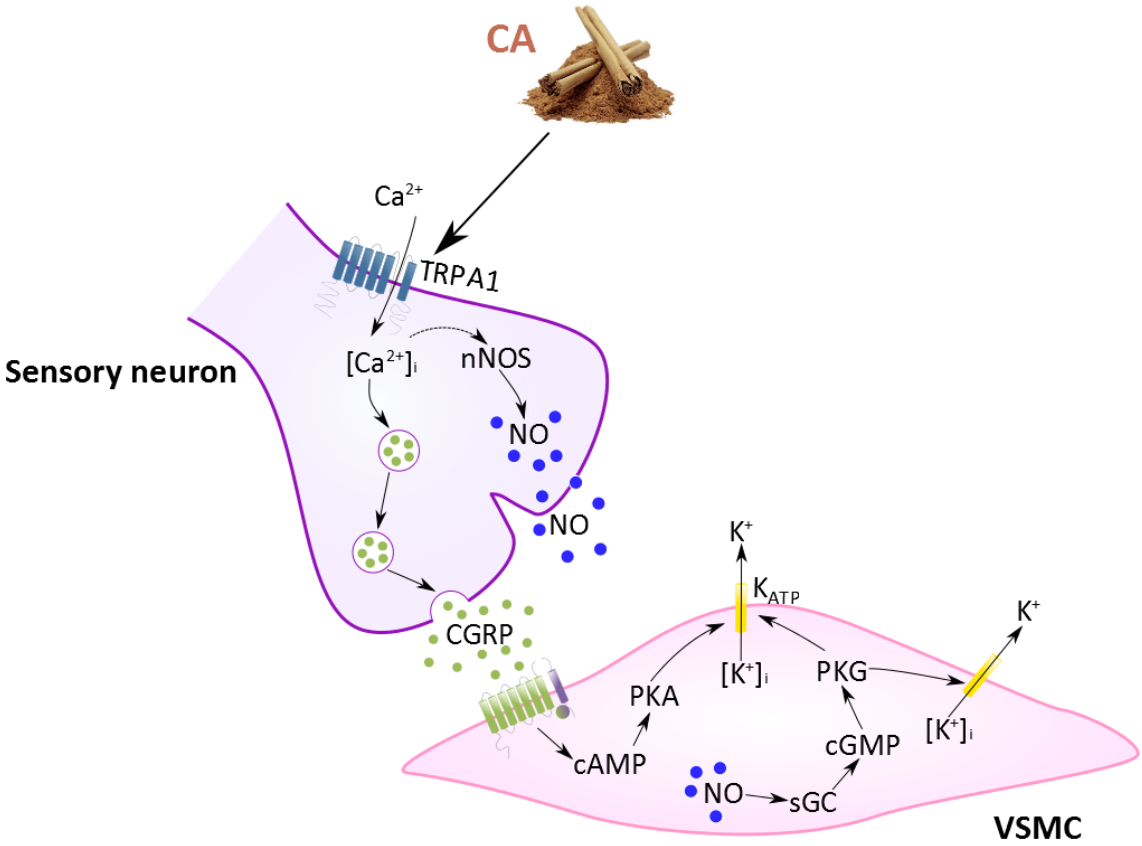

Figure 3.14 Signalling mechanisms underlying TRPA1-dependent vasodilatation by exogenous agonist cinnamaldehyde. The diagram summarises the signalling pathways involved in mediating cinnamaldehyde-induced vasodilatation in the peripheral vasculature. Cinnamaldehyde activates TRPA1 and causes stimulation of nerve endings from primary afferent neurons. This releases the neuropeptide CGRP and nNOS-derived nitric oxide to mediate an increase blood flow in the vasculature. CGRP acts on CGRP receptor complex; CRLR and RAMP1 to induce an increase in intracellular cAMP via adenylyl cyclase and cAMP further phosphorylate PKA and open K_{ATP} channels to mediate relaxation. Nitric oxide acts on stimulating sGC to subsequently form cGMP, activating PKG which causes reuptake calcium and opens potassium channels, leading to hyperpolarization of the membrane and further relaxing the VSMC. Abbreviations: CA, Cinnamaldehyde; cAMP,cyclic adenosine monophosphate; cGMP,cyclic guanosine monophosphate; CGRP, calcitonin gene-related peptide; $ONOO^-$, peoxynitrite; NO, nitric oxide; nNOS, neuronal nitric oxide; K_{ATP}, ATP-sensitive potassium;PKA, protein kinase A; PKG, protein kinase G; sGC, soluble guanylyl cyclase; TRPA1, transient receptor potential ankyrin-1; VSMC, vascular smooth muscle cell.

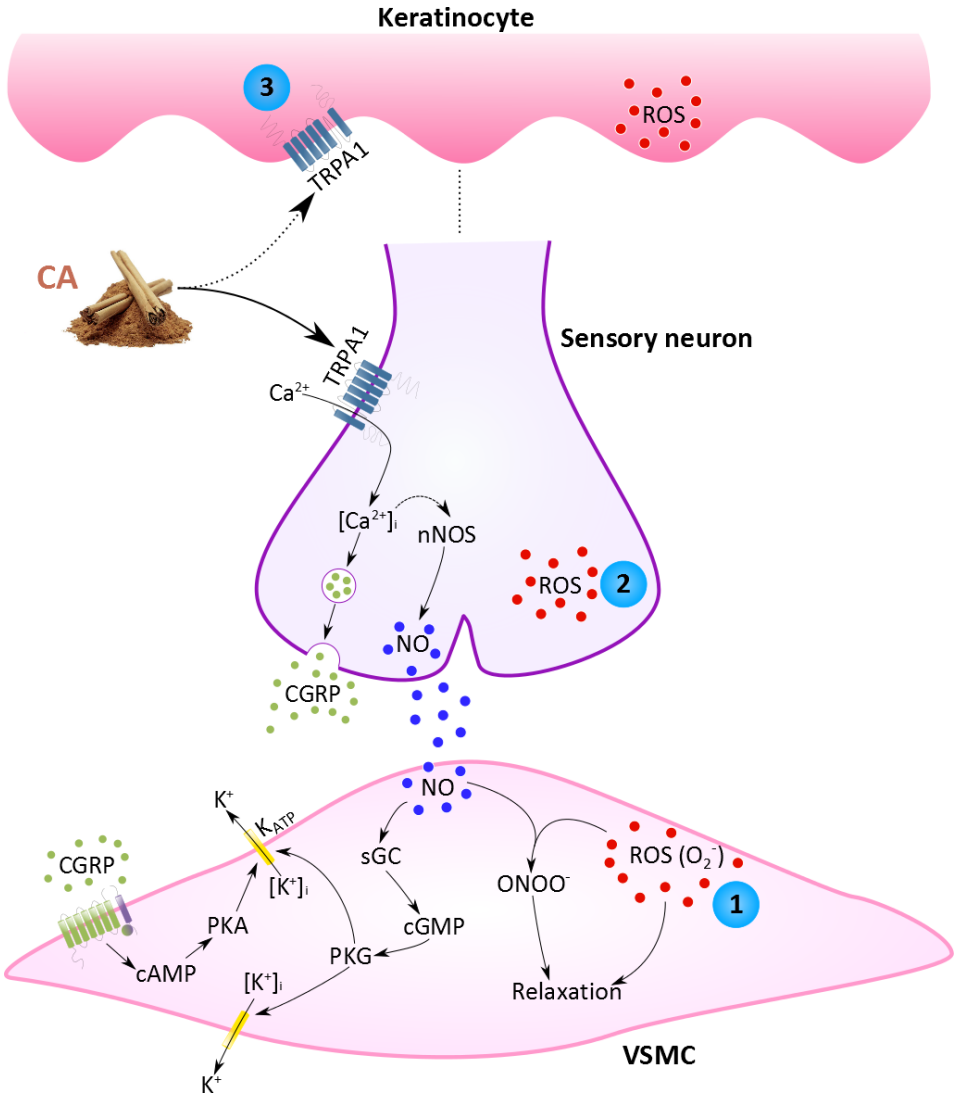

Figure 3.15 Proposed signalling mechanisms and sources of ROS involved in TRPA1-dependent vasodilatation by exogenous agonist cinnamaldehyde. The diagram summarises the reactive oxygen species (ROS) signalling pathways involved in mediating cinnamaldehyde-induced vasodilatation in the peripheral vasculature. ROS may be produced (1) in the VSMC downstream of neuropeptide CGRP receptor activation. ROS such as superoxide can react with nitric oxide to produce peroxynitrite, leading to relaxation of VSMC; (2) directly in the sensory neurons or (3) release by the keratinocytes following activation of TRPA1. Abbreviations: CA, Cinnamaldehyde; cAMP,cyclic adenosine monophosphate; cGMP,cyclic guanosine monophosphate; CGRP, calcitonin gene-related peptide; $ONOO^{-}$, peoxynitrite; NO, nitric oxide; nNOS, neuronal nitric oxide; PKA, protein kinase A; PKG, protein kinase G; ROS, reactive oxygen species; sGC, soluble guanylyl cyclase; TRPA1, transient receptor potential ankyrin-1; VSMC, vascular smooth muscle cell.

Chapter 4 – Investigating cold-induced vascular responses

Chapter 4 – Investigating cold-induced vasodilatation

4.1 Introduction

In the previous chapter, the role of TRPA1 in the peripheral vasculature was investigated using an exogenous TRPA1 agonist which was shown to cause vasodilatation and I investigated the detailed mechanisms underlying this response *in vivo.* I sought to further use this knowledge and investigate if a similar mechanism exists when TRPA1 is activated using a different stimulus, a local cold challenge. Since its discovery, TRPA1 has been reported to be a cold sensor (Story et al., 2003) and several studies have investigated its role in cold-induced hyperalgesia. However, this remains a controversial issue with a host of conflicting evidence as there are other thermo-sensitive TRP channels such as TRPM8, TRPV4 and TRPV1. Furthermore, a role of TRPA1 in the vascular response to cold has not been previously investigated. Zhou *et al.* recently reported only 15.3% of airway receptors in the lower respiratory tract of rat could respond to cold (8°C) in a TRPA1-dependent manner and these receptors can be activated by TRPM8 agonist menthol (Zhou et al., 2011). Several studies have investigated the role of both TRPM8 and TRPA1 in cold-induced responses (Namer et al., 2008, Knowlton et al., 2011, Gentry et al., 2010, Knowlton et al., 2010). The conflicting evidence may be due to the different cooling temperature parameters and profiles investigated in these studies. Additionally, both TRPM8 and TRPA1 are cold-sensors and hence, there is increased probability that both channels are activated in these studies. It is unknown whether there is an interaction between these two channels.

It is well established from human studies that at an environmental temperature of 10°C or less, CIVD occurs to reduce the risk of local cold-induced injury (Daanen, 2003), as discussed in chapter 1. CIVD consists of a competition between mechanisms under central control, such as closing of blood vessels to retain body heat and local mechanisms, such as opening of blood vessels to avoid local cold-induced injury (Daanen, 2003). The exact mechanisms underlying this CIVD phenomenon remain unknown, although a few theories including the axon reflex (Hornyak et al., 1990, Ji et al., 2007) and sympathetic nerve (Gardner and Webb, 1986) have been proposed, as discussed in chapter 1. When this project was initiated, there was a lack of *in vivo* models to study acute cold responses in the peripheral vasculature. Therefore, the aim of this study was to design an acute local cold model in mouse that responded similarly to earlier human findings. This would then be used to investigate the mechanisms underlying the cold-induced vascular responses *in vivo*, using a non-freezing temperature (10°C), which is hypothesised to selectively target the temperature window of TRPA1.

4.1.1 Brief methods

Using the FLPI, cold-induced vascular responses were studied, as detailed in Chapter 2 (section 2.4). Briefly, skinblood flow was measured concomitantly in the whole area of both hindpaw of male mice anaesthetised with ketamine (75mg/kg) and medetomidine (1mg/kg). Following baseline measurement for 5-10 min, the mouse was subsequently removed from the heating mat and the ipsilateral paw was exposed up to the level of the joint between the tibia and the calcaneum to cold water (10°C) for 5 min. In one set of experiment, the ipsilateral paw was immersed in warm water (26°C) for 5 min. The contralateral hindpaw was left untreated at room temperature (~22°C). Hence, this protocol allowed the simultaneous assessment of blood flow responses in the cold-treated and control paws in the same mouse. Following treatment, the hindpaw was dried as detailed in section 2.4.4 and blood flow measurement was resumed for 30 min using the FLPI.

All the experiments studying cold-induced blood flow responses were conducted using FLPI in male mice. The response to cooling consisted of an initial reduction in flux, in keeping with vasoconstriction, followed by a slow developing sustained increased flux, consistent with vasodilatation. This whole response observed following treatment is termed "*cold-induced vascular response*" in this chapter. Data was recorded as flux arbitrary units and in this chapter, data was analysed as AUC from time '0 min' following treatment (cold water immersion and drying of hindpaw) to 30 min recording, as detailed in section 2.8.2.A range of pharmacological inhibitors was used to investigate the mediators involved in mediating cold-induced vascular responses (section 2.6).

Skin subcutaneous and surface temperature was measured in the hindpaw at baseline and following local cold treatment. Skin surface temperature was also monitored during the active cooling period, as detailed in section 2.5. Hindpaw tissue samples were collected at 30 min following local cold treatment and *ex vivo* analysis was conducted to investigate superoxide release using Lucigenin assay, H_2O_2 generation using AMPLEX RED assay and mRNA gene expression using qRT-PCR (section 2.7).

4.2 Results

4.2.1 Characterisation of cold-induced vascular response in the mouse hindpaw

In this chapter, I describe the development of a new model to investigate the effects of local cooling on blood flow responses in the mouse hindpaw. Previous studies have looked at different methods such as using thermocouples attached to the skin (Daanen, 2003), immersing tail or limb in stirred ice water or using modified peltier cooling elements to cool the ventral side of the hindpaw (Kusters et al., 2010). In our model, the ipsilateral paw of the anaesthetised mouse was immersed in 10°C water for 5 min whilst the contralateral paw remained untreated and skin temperature or blood flow were recorded following treatment. Unfortunately, it was impossible to measure blood flow during the cooling period where the paw was immersed in cold water. However, this non-invasive set-up enabled responses in both hindpaws to be measured simultaneously for a period afterwards, where the ipsilateral hind-paw is treated with cold and the contralateral hindpaw of the same mouse acts as control. The technique also allowed simultaneous bilateral assessment of cold-induced vascular response following treatment in the ipsilateral hindpaw, as well as monitoring any potential reflex vasoconstriction in the untreated contralateral hindpaw of the mice.

Both the ipsilateral and contralateral hindpaws showed similar baseline blood flow (Figure 4.1A-B). Figure 4.1A illustrates the time course of blood flow measurement at baseline and following treatment. Following the 5 min immersion in 10°C water, the blood flow of the ipsilateral treated hindpaw rapidly declined and this phase represents the transient vasoconstriction of the vascular response and minimal changes were observed in the untreated contralateral paw (Figure 4.1A-B). A maximum drop in blood flow is observed after approximately 2 min of blood flow measurement in the cold-treated hindpaw (Figure 4.1A-B). Cold-induced vasoconstriction is not regarded as a generalised response as it only occurs in the cold-treated hindpaw. The mechanisms underlying the constrictor response will be further detailed in chapter 5. Blood flow then gradually returns to baseline, as shown by the recording over the 30 min period (Figure 4.1A). This phase is referred to in this chapter as vasodilatation and the exact nature of this response, i.e. whether it is rewarming or a direct vasodilator nature is discussed in chapter 5 and 6.

The changes in skin temperature were also monitored and are shown in Figures 4.1C and D. There was a rapid drop in both skin surface and subcutaneous temperature following the local cold treatment in the ipsilateral hindpaw, with no changes observed in the untreated contralateral hindpaws (n=3-6). The subcutaneous temperature of the hindpaw decreased to a

reading of 24°C, which was the minimum temperature that the implanted temperature microchips could detect (Figure 4.1C).

By comparison, the skin surface temperature of the hindpaw was measured during the active cooling period when the hindpaw was immersed in cold water and the temperature decreased to approximately 15°C (Figure 4.1D), as measured by the attached skin surface temperature wire thermometer.. Both the skin surface and subcutaneous temperature of the cold-treated ipsilateral hindpaw was shown to return to basal temperature 10-12 min following treatment. No changes in temperature were observed in the untreated contralateral paws throughout the measurement period that followed treatment. The changes in hindpaw blood flow responses appear to play a role in maintaining a constant peripheral cutaneous temperature, confirming the role of cutaneous skin blood flow in peripheral temperature homeostasis. The blood flow responses over the 30 min recording period were quantified using area under the curve, from 0 min, immediately after cold treatment to 30 min following treatment, as described in chapter 2. Cold (10°C) water immersion for 5 min caused a significant increase in the cold-induced vascular response when compared to untreated hindpaw or hindpaw treated at 26°C (Figure 4.1E).

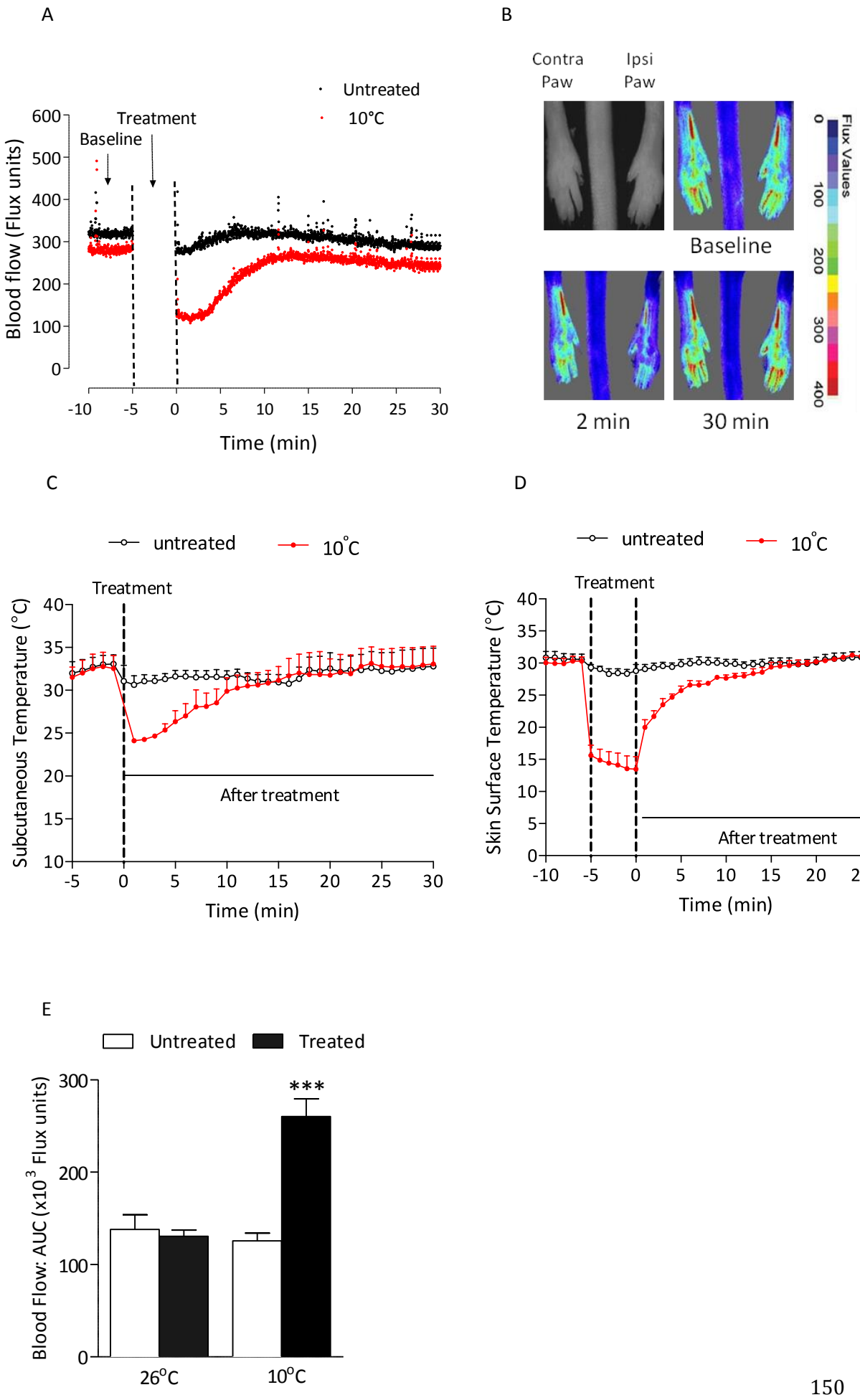
A
Untreated
10°C
Treatment
Baseline
Blood flow (Flux units)
Time (min)
B
Contra Paw
Ipsi Paw
Baseline
2 min
30 min
Flux Values
C
untreated
10°C
Treatment
After treatment
Subcutaneous Temperature (°C)
Time (min)
D
untreated
10°C
Treatment
After treatment
Skin Surface Temperature (°C)
Time (min)
E
Untreated
Treated
***
Blood Flow: AUC (x10³ Flux units)
26°C
10°C

Figure 4.1 Characterisation of cold-induced vascular response in the hindpaw of CD1 mice using Full-field Laser Perfusion Imager.

Blood flow responses in mouse ipsilateral hindpaw following cold water (10°C) immersion while the contralateral hindpaw remains untreated. Results recorded over 30 min following treatment **A**) Representative traces of blood flow responses assessed by Full-Field Laser Perfusion Imager vs. time trace at baseline and following local cold challenge of mouse hindpaw. An upward deflection in the trace is proportional to an increase in blood flow, **B**) Representative images as observed by the Full-Field Laser Perfusion Imager alongside grey/black scale 'photo' image showing blood flow recorded at baseline and over 30 min for cold-treated hindpaw in male CD1 mouse, **C**) Effects of local cold challenge on subcutaneous skin temperature in hindpaw of CD1mice as measured using subcutaneously implanted temperature sensors (n=3). Subcutaneous temperature was measured at baseline (-5 to 0 min) and following local cold treatment (0 to 30 min),**D**) Effects of local cold challenge on skin surface temperature in hindpaw of CD1 mice as measured using a surface temperature wire thermometer on the hindpaw (n=6). Skin surface temperature was measured at baseline (-10 to -5 min), during local cold treatment (-5 to 0 min) and following treatment (0-30 min),**E**) Blood flow ($\times 10^3$ flux units) measured over 30 min period following local water treatment at 10°C (n=4) and 26°C (n=7), with respective control (untreated ipsilateral hindpaw) and expressed as area under the curve (AUC). Results are shown as mean $\pm$ S.E.M. ***$p<0.001$ compared to respective untreated hindpaw of mice using Student's *t* test.

4.2.2 Role of TRPA1 in cold-induced vascular response

I next investigated if this cold-induced vascular response observed to 10°C cooling is dependent on TRPA1 *in vivo* in mice. As shown in the representative trace, following cold immersion there was a decrease in blood flow which returned back to baseline over the 30 min period in TRPA1 WT mice hindpaw, but this response was completely absent in TRPA1 KO hindpaw (Figure 4.2A) and no change was observed in the untreated paw. A similar trend was observed whilst assessing the cold-induced vascular response, which was inhibited in the TRPA1 KO mice when compared to WT mice ($p<0.001$, n=9-12, Figure 4.2B). Our results illustrate that both the vasoconstrictor and vasodilator components of the cold-induced vascular responses are inhibited in the TRPA1 KO mice, and the role of TRPA1 in cold-induced vasoconstriction will be further discussed in chapter 5.

To confirm the role of TRPA1, I further used the TRPA1 antagonist HC030031, which was previously shown in chapter 3 to significantly decrease cinnamaldehyde-induced vasodilatation. Pre-treatment with HC030031 (100mg/kg, *i.p.*) caused a marked decrease in cold-induced vascular responses when compared to control-treated group ($p<0.001$, n=8-10, Figure 4.2C). However, there seems to be a residual response to cold-water immersion in the hindpaws of mice pre-treated with HC030031, albeit this remaining response is not significant. I also observed no change in blood flow responses when the hindpaw was immersed in 26°C warm water and therefore this experiment acts as a positive control (n=4, Figure 4.2D).

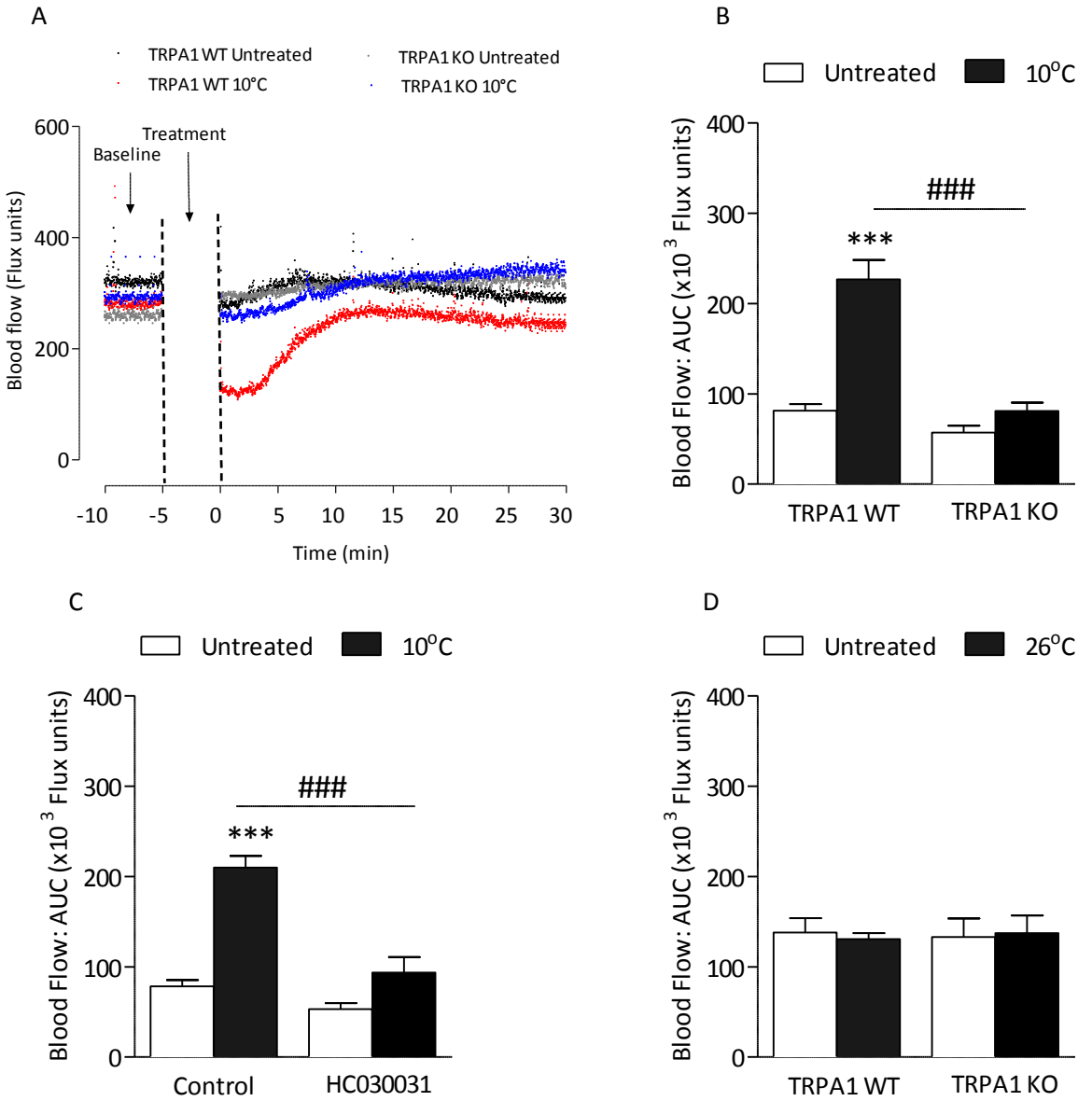

Figure 4.2 Cold-induced vascular response is dependent on TRPA1 in the peripheral vasculature

Blood flow responses in mouse ipsilateral hindpaw following cold water (10°C) immersion and contralateral hindpaw remains untreated using Full-Field Laser Perfusion Imager (FLPI). Results recorded over 30 min following treatment **A**) Representative traces of blood flow responses assessed by FLPI vs. time trace at baseline and following local cold challenge in TRPA1 WT and KO mouse. An upward deflection in the trace is proportional to an increase in blood flow. Blood flow ($\times 10^3$ flux units) measured over 30 min period following local water treatment at 10°C with respective control (untreated ipsilateral hindpaw) and expressed as area under the curve (AUC) in **B**) TRPA1 WT and KO mice (n=9-12) and in **C**) WT mice pre-treated with the TRPA1 antagonist HC030031 (100mg/kg, *i.p.*, 30 min, n=8) or control (10% DMSO in saline, *i.p.*, 30 min, n=10). **D**) Blood flow responses following local water treatment at 26°C with respective control (untreated ipsilateral hindpaw) in TRPA1 WT and KO mice (n=4). Results are shown as mean ± S.E.M. ***p<0.001, compared to respective untreated, ###p<0.001 compared to cold-treated hindpaw of mice using 2-way ANOVA followed by Bonferroni *post hoc* test.

4.2.3 Role of other thermosensitive TRP channels in the cold-induced vascular response

With the increasing conflicting evidence suggesting that TRPA1 is not the primary sensor of cold, I sought to investigate the potential role of the other thermosensitive TRP channels in the cold (10°C)-induced vascular responses. I previously showed in chapter 3 that TRPV1 does not have a role in influencing the TRPA1 agonist cinnamaldehyde-induced vasodilatation. Since it is known that TRPA1 is co-expressed on TRPV1-expressing sensory neurons, I investigated whether TRPV1 can potentially interact with TRPA1 and play a role in cold-induced vascular responses. As expected there was no significant change in cold-induced vascular responses between WT and TRPV1 KO mice ($p>0.05$, n=5-7, Figure 4.3A). This finding was further confirmed in mice pre-treated with the TRPV1 antagonists SB366791 and AMG9810, where there was no change in cold-induced changes in blood flow responses. I further confirm that TRPV1, known as a thermo-sensor for noxious heat does not play a role in cold-induced vasodilatation, despite its presence on sensory nerves ($p>0.05$, n=5-7, Figure 4.3B-C).

The thermosensitive channel TRPV4 has been reported to be activated at a temperature range of 25 to 34°C (Guler et al., 2002, Watanabe et al., 2002). The cold-induced blood flow responses were unaltered in TRPV4 KO mice, when compared to WT mice, which indicates lack of involvement of this channel (n=3, Figure 4.3D). This finding suggests that local cold (10°C) treatment does not activate TRPV4. There is an unclear understanding of the role of TRPM8 which is also expressed on sensory neurons and is proposed to be activated at a temperature between 10°C and 25°C (Knowlton et al., 2010, Almeida et al., 2012). Interestingly, cold-induced vascular responses were significantly reduced in TRPM8 KO mice when compared to WT mice ($p<0.05$, n=5, Figure 4.3E), but not to the same extent observed in the TRPA1 KO mice (Figure 4.2B). A similar trend in cold-induced vascular responses was observed in CD1 mice pre-treated with the selective TRPM8 antagonist AMTB (10mg/kg) when compared to control-treated group ($p<0.05$, n=4-9, Figure 4.3F).

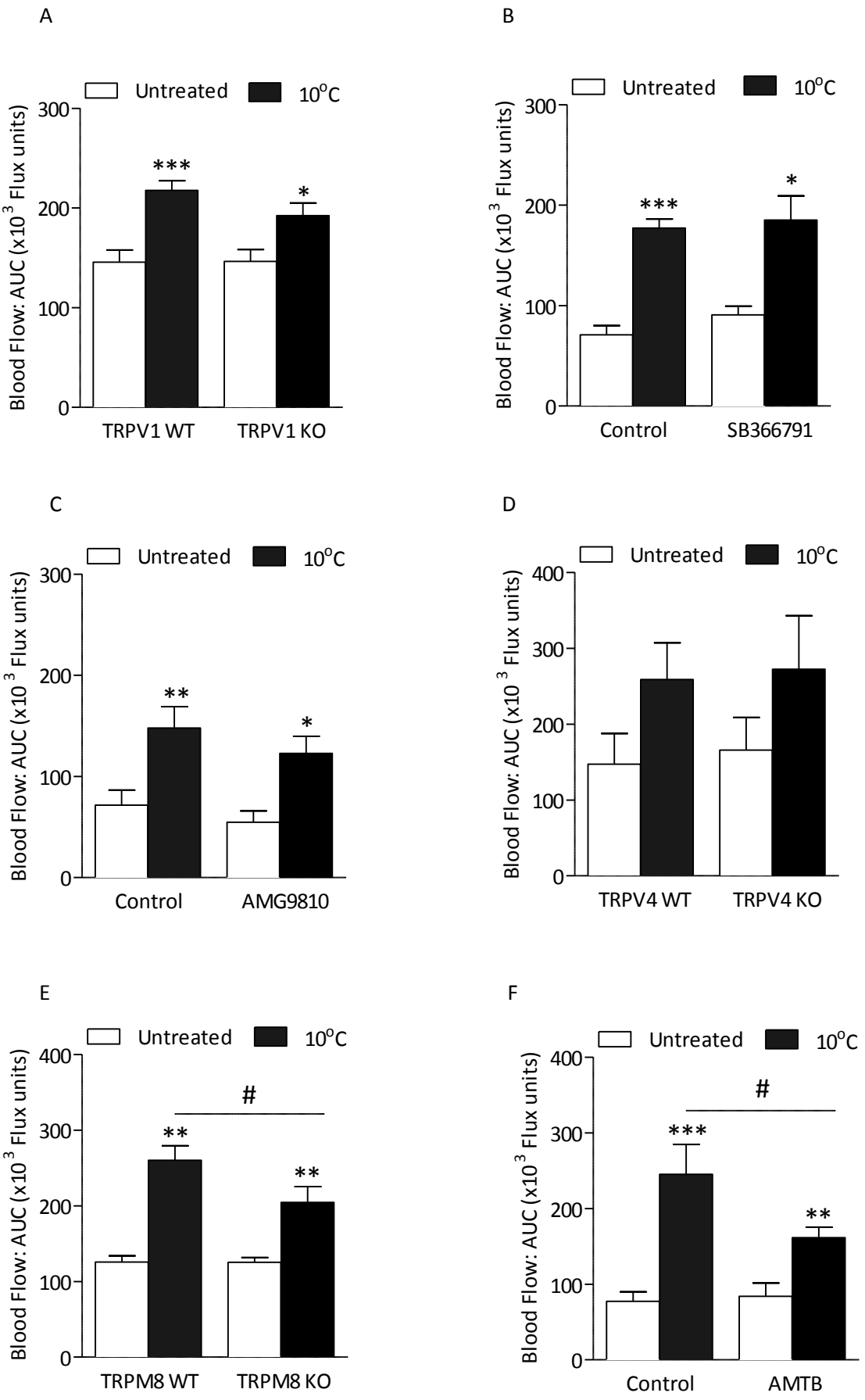
A
Untreated
10°C
Blood Flow: AUC (x10 3 Flux units)
300
200
100
0
***
*
TRPV1 WT
TRPV1 KO
B
Untreated
10°C
Blood Flow: AUC (x10 3 Flux units)
300
200
100
0
***
*
Control
SB366791
C
Untreated
10°C
Blood Flow: AUC (x10 3 Flux units)
300
200
100
0
**
*
Control
AMG9810
D
Untreated
10°C
Blood Flow: AUC (x10 3 Flux units)
400
300
200
100
0
TRPV4 WT
TRPV4 KO
E
Untreated
10°C
Blood Flow: AUC (x10 3 Flux units)
400
300
200
100
0
#
**
**
TRPM8 WT
TRPM8 KO
F
Untreated
10°C
Blood Flow: AUC (x10 3 Flux units)
400
300
200
100
0
#
***
**
Control
AMTB

Figure 4.3 The role of thermosensitive TRP channels in cold-induced vascular response in the peripheral vasculature

Blood flow (x 10^3 flux units) in mouse hindpaw following cold water (10°C) immersion while the contralateral hindpaw remains untreated using FLPI. Blood flow (× 10^3 flux units) recorded over 30 min following treatment and expressed as area under the curve (AUC). **A**) Effects of local cold challenge in TRPV1 WT (n=7) and KO (n=8) mice, **B**) Effects of TRPV1 antagonist SB366791 (5mg/kg, *i.p.,* 2h, n=7) and control (2% DMSO in saline) in CD1 mice (n=7), **C**) Effects of the TRPV1 antagonist AMG9810 (50mg/kg, *i.p.*, 30 min, n=5) and control (2% DMSO, 5% Tween-80 in saline) in CD1 mice (n=5), Effects of local cold challenge in **D**) TRPV4 WT and KO mice (n=3), **E**) TRPM8 WT and KO mice (n=5) and **F**) WT mice pre-treated with the TRPM8 antagonist AMTB (10mg/kg, *i.p.*, 30 min, n=4) or control (2% DMSO in saline, n=9). Results are shown as mean ± S.E.M. *p<0.05, **p<0.01, ***p<0.001 compared to respective untreated, ##p<0.01 compared to cold-treated hindpaw of mice using 2-way ANOVA followed by Bonferroni *post hoc* test.

4.2.4 Role of sensory neurons and neuropeptides in cold-induced vascular responses

Previous studies in our group have shown that TRPA1-mediated vasodilatation induced by TRPA1 agonists mustard oil and 4-ONE are dependent on the release of neuropeptides in the periphery (Grant et al., 2005, Graepel et al., 2011). Furthermore, I have increasing evidence in chapter 3 showing that the TRPA1 agonist cinnamaldehyde also increases blood flow responses in a CGRP/substance P-dependent manner. Hodges *et al.* (2007) demonstrated that sensory neurons play a role in cold-induced responses as the blockade of the sensory nerves using local anaesthesia was shown to decrease local prolonged cooling-induced cutaneous vascular conductance in humans (Hodges et al., 2007). It remains unknown whether sensory neurons have a role in an acute local cold treatment. I investigated the role of sensory neurons in our cold model by initially using local anaesthesia. The local pharmacological blockade of the sensory neurons using topical administration of EMLA, which is a combination of lidocaine and prilocaine was shown to have no significant effect in decreasing cold-induced vascular response when compared to control ($p>0.05$, n=3-5, Figure 4.4A). This finding was further investigated using a different administration of the local anaesthetic. Administration of the sodium channel blocker lidocaine (*i.pl.*) only was further shown to cause a significant decrease in cold-induced vascular response when compared to control-treated groups ($p<0.01$, n=5, Figure 4.4B). It is worth highlighting that pre-treatment with lidocaine also caused a decrease in baseline blood flow and in blood flow responses in the untreated contralateral hindpaw (Figure 4.4B).

TRPA1 is known to be expressed on sensory neurons and it is evident from our study that TRPA1 can act as a vascular cold sensor at low temperature (10°C). I hypothesised that if sensory neurons have a role in influencing cold-induced blood flow responses, these effects may be mediated by the release of neuropeptides following the activation of TRPA1 by cold (10°C). This concept was investigated in pharmacogenetic studies. I first provide clear evidence that the pharmacological blockade of both neuropeptide CGRP and NK_1 receptors using $CGRP_{8-37}$ and SR140333, respectively caused a marked decrease in cold-induced vascular response when compared to control (n=8, $p<0.001$, Figure 4.4C). This finding suggests that both neuropeptides may have a role in cold-induced vascular response, in agreement to previous findings with the TRPA1 agonist cinnamaldehyde in chapter 3. The contribution of each neuropeptide in this response was further investigated, where interestingly I showed that both neuropeptides contributed to cold-induced vascular responses. Our results showed that pre-treatment with SR140333 alone was sufficient to cause a significant decrease in cold-induced blood flow responses ($p<0.001$, n=7-8, Figure 4.4D) and a similar pattern was observed in the group pre-treated with $CGRP_{8-37}$ alone ($p<0.01$, n=7, Figure 4.4E). I also investigated the effects of the

non-peptide CGRP receptor antagonist BIBN4096BS on the potential CGRP-induced responses in the local cold model. This antagonist is more stable and has been shown to be an effective and selective antagonist in the mouse (Doods et al., 2000, Grant et al., 2004). Pre-treatment with BIBN4096BS caused a similar decrease in cold-induced vascular responses as $CGRP_{8-37}$, when compared to control-treated group ($p<0.01$, n=9, Figure 4.4F).

To further confirm the role of the neuropeptide CGRP in this model, I investigated the effects of local cold (10°C) treatment for 5 min in α-CGRP WT and KO mice. Local cold (10°C) water treatment caused a significant increase in blood flow responses when compared to the untreated hindpaw in CGRP WT mice, but surprisingly there was no significant decrease in cold-induced vascular responses between α-CGRP WT and KO mice ($p>0.05$, n=5, Figure 4.5A). This finding does not correlate to the previous results with CGRP receptor antagonists and hence, I further investigated the expression of α-CGRP, β-CGRP, and TRPA1 mRNA in α-CGRP WT and KO mice**.** I showed that α-CGRP KO mice expressed no copies of α-CGRP mRNA in DRG samples, but surprisingly there was a significant increase in β-CGRP and TRPA1 mRNA levels in the α-CGRP KO mice when compared to WT mice ($p<0.01$, n=3, Figure 4.5 B-D). To investigate the role of β-CGRP in the cold-induced vascular responses, α-CGRP KO mice were pre-treated with BIBN40964BSwhich would be expected to antagonise the potential effects of β-CGRP on CGRP receptors in the α-CGRP KO mice. Interestingly, I demonstrated that cold-induced vascular responses were shown to be significantly reduced in α-CGRP KO pre-treated with BIBN4096BS when compared to control ($p<0.01$, n=5, Figure 4.5D).

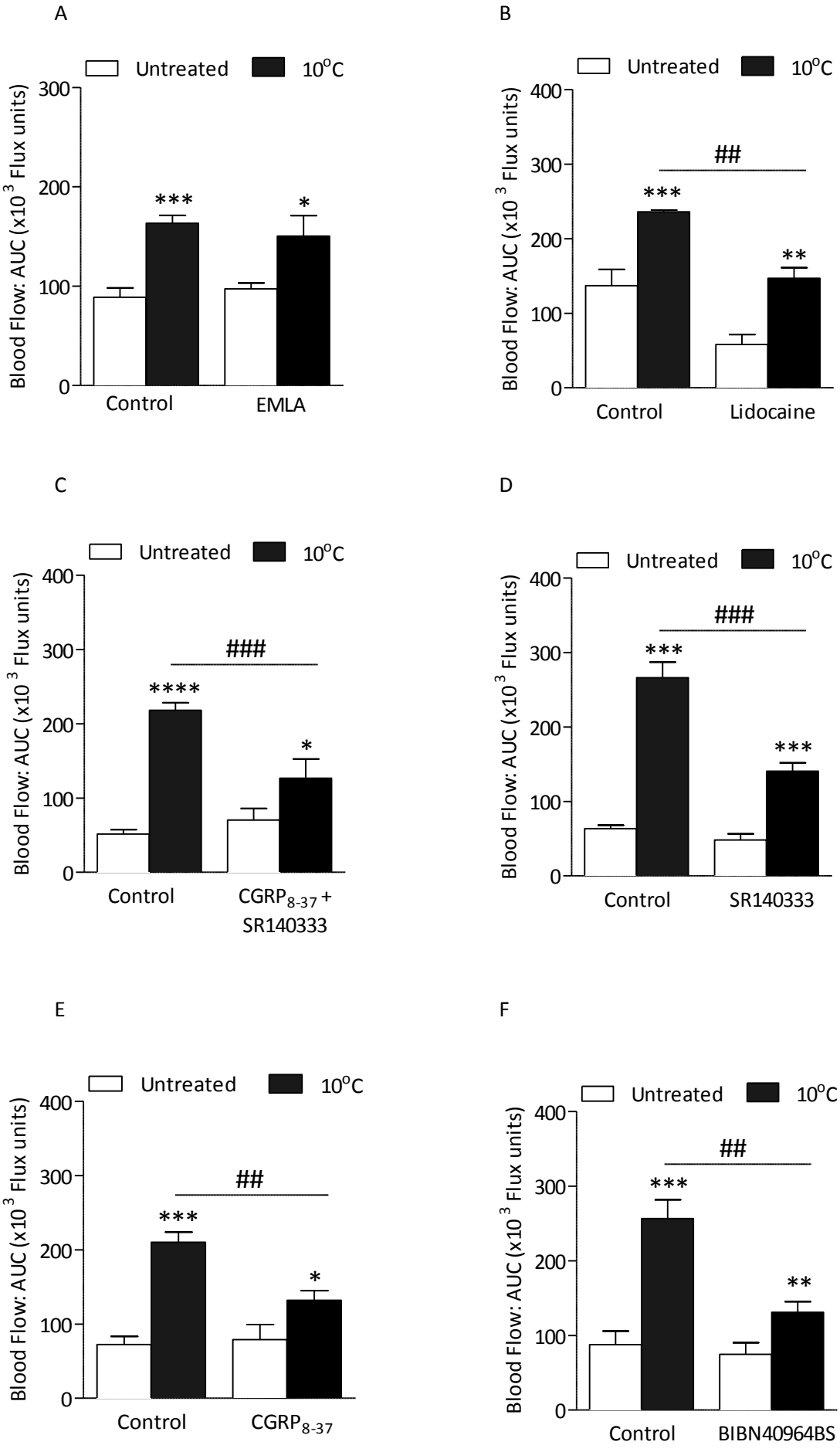
A
Untreated
10°C
Blood Flow: AUC (x10 3 Flux units)
300
200
100
0
***
*
Control
EMLA
B
Untreated
10°C
Blood Flow: AUC (x10 3 Flux units)
400
300
200
100
0
##
***
**
Control
Lidocaine
C
Untreated
10°C
Blood Flow: AUC (x10 3 Flux units)
400
300
200
100
0
###
****
*
Control
CGRP8-37 + SR140333
D
Untreated
10°C
Blood Flow: AUC (x10 3 Flux units)
400
300
200
100
0
###
***
***
Control
SR140333
E
Untreated
10°C
Blood Flow: AUC (x10 3 Flux units)
400
300
200
100
0
##
***
*
Control
CGRP8-37
F
Untreated
10°C
Blood Flow: AUC (x10 3 Flux units)
400
300
200
100
0
##
***
**
Control
BIBN40964BS

Figure 4.4 The cold-induced vascular response is partially dependent on neuropeptides in the peripheral vasculature

Blood flow responses in mouse ipsilateral hindpaw following cold water (10°C) immersion while the contralateral hindpaw remains untreated using FLPI. Blood flow ($\times 10^3$ flux units) recorded over 30 min following treatment and expressed as area under the curve (AUC). Cold-induced vascular responses in the hindpaw of CD1 mice pre-treated with **A**) EMLA (2.5% lidocaine and 2.5% prilocaine, topical, 5min, n=3) or untreated (n=5), **B**) local sensory neuron blockade using the sodium channel blocker lidocaine (2% in saline, *i.pl*., 5min, n=5) or control (saline, *i.pl.*, 5 min, n=5), **C**) a combination of the selective CGRP receptor antagonist $CGRP_{8-37}$ (400nmol/kg, *i.v.*, 5min) and the neurokinin-1 receptor antagonist SR140333 (480nmol/kg, *i.v.*, 5min) (n=8) or control (0.01% BSA in saline, n=8), **D**) with SR140333 alone or respective control (saline) (*i.v.*, 5min, n=7-8), **E**) $CGRP_{8-37}$ alone or respective control (0.01% BSA in saline) (*i.v.*, 5min, n=7), **F**) CGRP receptor antagonist BIBN40946S alone (0.3mg/kg, *i.v.*, 5 min, n=9) or respective control (saline, *i.v.*, 5 min, n=10). Results are shown as mean ± S.E.M. *p<0.05, **p<0.01, ***p<0.001, ****p<0.0001 compared to respective untreated, ##p<0.01, ###p<0.001 compared to cold-treated hindpaw of mice using 2-way ANOVA followed by Bonferroni *post hoc* test.

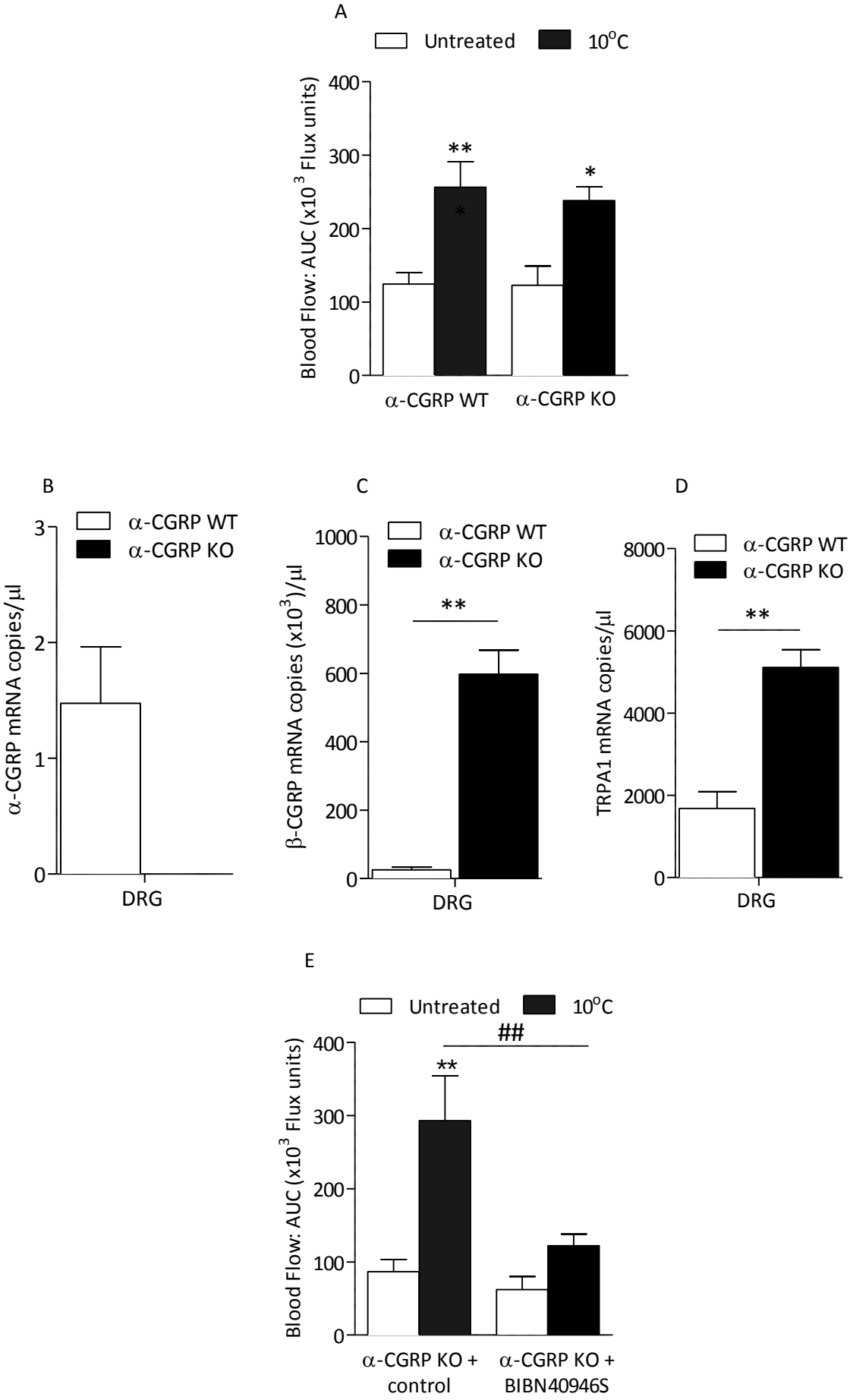
A
Untreated
10°C
Blood Flow: AUC (x10 3 Flux units)
400
300
200
100
0
**
*
*
α-CGRP WT
α-CGRP KO
B
α-CGRP WT
α-CGRP KO
α-CGRP mRNA copies/µl
3
2
1
0
DRG
C
α-CGRP WT
α-CGRP KO
β-CGRP mRNA copies (x10³)/µl
1000
800
600
400
200
0
**
DRG
D
α-CGRP WT
α-CGRP KO
TRPA1 mRNA copies/µl
8000
6000
4000
2000
0
**
DRG
E
Untreated
10°C
Blood Flow: AUC (x10 3 Flux units)
400
300
200
100
0
##
**
α-CGRP KO + control
α-CGRP KO + BIBN40946S

Figure 4.5 The cold-induced vascular response is dependent on β-CGRP in the peripheral vasculature

Blood flow responses in mouse ipsilateral hindpaw following cold water (10°C) immersion while the contralateral hindpaw remains untreated using FLPI. Blood flow ($\times 10^3$ flux units) recorded over 30 min following treatment and expressed as area under the curve (AUC). **A**) Cold-induced vascular responses in the hindpaw of α-CGRP WT and KO mice (n=5). Expression of **B**) α-CGRP, **C**) β-CGRP and **D**) TRPA1 mRNA in cold (10°C)-treated DRG samples using qRT-PCR. Samples were collected at 30 min following treatment in the anaesthetised mice and results are expressed as copy numbers per sample normalised to GAPDH and actin (n=3). **D**) Cold-induced vascular responses in the hindpaw of α-CGRP KO mice pre-treatment with CGRP receptor antagonist BIBN40946S alone (0.3mg/kg, *i.v.*, 5 min, n=5) or respective control (saline, *i.v.*, 5 min, n=5). Results are shown as mean $\pm$ S.E.M. *p<0.05, **p<0.01 compared to respective untreated, ##p<0.01 compared to cold-treated hindpaw of mice using 2-way ANOVA followed by Bonferroni *post hoc* test or Student's t-test.

4.2.5 Effects of indomethacin in cold-induced vascular responses

Following on from the evidence that neuropeptides have a role in cold-induced vascular responses, I further investigated the role of other established vasodilators such as prostaglandins. Prostaglandins have previously been reported to activate TRPA1 in HEK cells (Taylor-Clark et al., 2008) and *in vivo* to induce pain (Materazzi et al., 2008). Furthermore, Franz previously showed that prostaglandins are involved in modulating vasomotor tone, as measured by changes in foot-pad temperature during cold exposure (0°C) in domestic cats (Franz, 1985). I investigated the role of prostaglandins in cold-induced vascular responses in this study using the non-selective cyclo-oxygenase inhibitor indomethacin. I showed that pre-treatment with indomethacin had no significant effects in suppressing the cold-induced vascular responses ($p>0.05$, $n=10$-12, Figure 4.6).

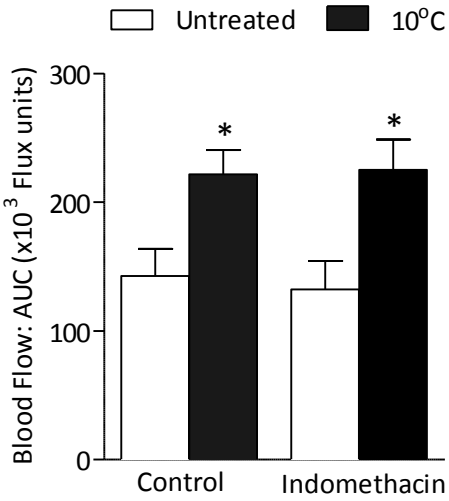

Figure 4.6 Cold-induced vascular response is independent of prostaglandins in the peripheral vasculature

Blood flow responses in mouse ipsilateral hindpaw following cold water (10°C) immersion while the contralateral hindpaw remains untreated using FLPI. Blood flow ($\times 10^3$ flux units) recorded over 30 min following treatment and expressed as area under the curve (AUC). Cold-induced vascular responses in the hindpaw of CD1 mice pre-treated with non-selective cyclooxygenase inhibitor indomethacin (5mg/kg, *s.c.*, 60 min, n=10) or control (5% $NaHCO_3$ in saline, *s.c.*, 60 min, n=12). Results are shown as mean $\pm$ S.E.M. *$p<0.05$ compared to respective untreated hindpaw of mice using 2-way ANOVA followed by Bonferroni *post hoc* test.

4.2.6 Role of nitric oxide and neuropeptides in cold-induced vascular responses

Our results thus far have shown that local cold (10°C) exposure for 5 min induced a cold-induced vascular response which is dependent on the activation of TRPA1 and I further showed that neuropeptides play an important role in the vasodilator component of the responses. Neuropeptides are known to be released following the stimulation of sensory neurons. It is interesting to note that in this study, the pharmacological blockade of the neuropeptide receptors caused a significant decrease in TRPA1-mediated vascular responses with both TRPA1 agonists cinnamaldehyde and cold (10°C). However, there remains a residual effect and as shown in chapter 3 this is mediated by nitric oxide for cinnamaldehyde-induced vasodilatation but it remains unknown whether nitric oxide is involved in cold-induced vascular responses. It is known from several previous human studies that cold exposure and shear stress can increase eNOS activation at 28°C and decrease eNOS activation at 4°C (Binti Md Isa et al., 2011). Furthermore there is also evidence showing that cooling has time-dependent effects on nitric oxide production in cutaneous and deep arteries of rabbit (Fernandez et al., 1994). Thus, I investigated the role of nitric oxide in the cold-induced vascular responses using pharmacological inhibitors.

Pre-treatment with the non-selective NOS inhibitor L-NAME was shown to cause a significant decrease in cold-induced vascular responses compared to control groups ($p<0.01$, n=7-10, Figure 4.7A). This highlights that nitric oxide may play a role in the cold-induced vascular responses mediated by TRPA1. Furthermore, pre-treatment with a combination of neuropeptide receptor antagonists and L-NAME was shown to completely abolish the cold-induced vascular response ($p<0.0001$, n=8, Figure 4.7B). This highlights an important role of both neuropeptides and nitric oxide in the cold-induced vascular response. I previously showed that nNOS was involved in cinnamaldehyde-induced vasodilatation in chapter 3 and hence, I further investigated the source of NOS for the generation of nitric oxide in the cold-induced responses. I initially investigated the possible role of iNOS by using the selective iNOS inhibitor 1400W. Interestingly, pre-treatment with the iNOS inhibitor 1400W at two different doses (1 and 3mg/kg) was shown to significantly reduce cold-induced vascular responses ($p<0.01$, n=5-7, Figure 4.7C) and this suggests an important role of iNOS-derived nitric oxide in the cold-induced blood flow responses. Pre-treatment with the selective nNOS inhibitor SMTC was shown to significantly decrease cold-induced vascular responses when compared to control treated groups ($p<0.0001$, n=6-7, Figure 4.7D). Furthermore, I clearly showed that the cold-induced vascular responses were completely abolished in CD1 mice pre-treated with a

combination of $CGRP_{8-37}$, SR140333 and SMTC when compared to control ($p<0.0001$, n=7-9, Figure 4.7E).

The expression of the 3 isoforms of NOS mRNA was investigated in the hindpaw and DRG tissue samples at 30 min following the local cold treatment of the hindpaw. Interestingly, I found that there was no significant change in eNOS, iNOS and nNOS mRNA expression between cold-treated hindpaw or DRG tissue samples when compared to their respective untreated tissue samples in WT mice ($p>0.05$, n=4-5, Table 4.1).

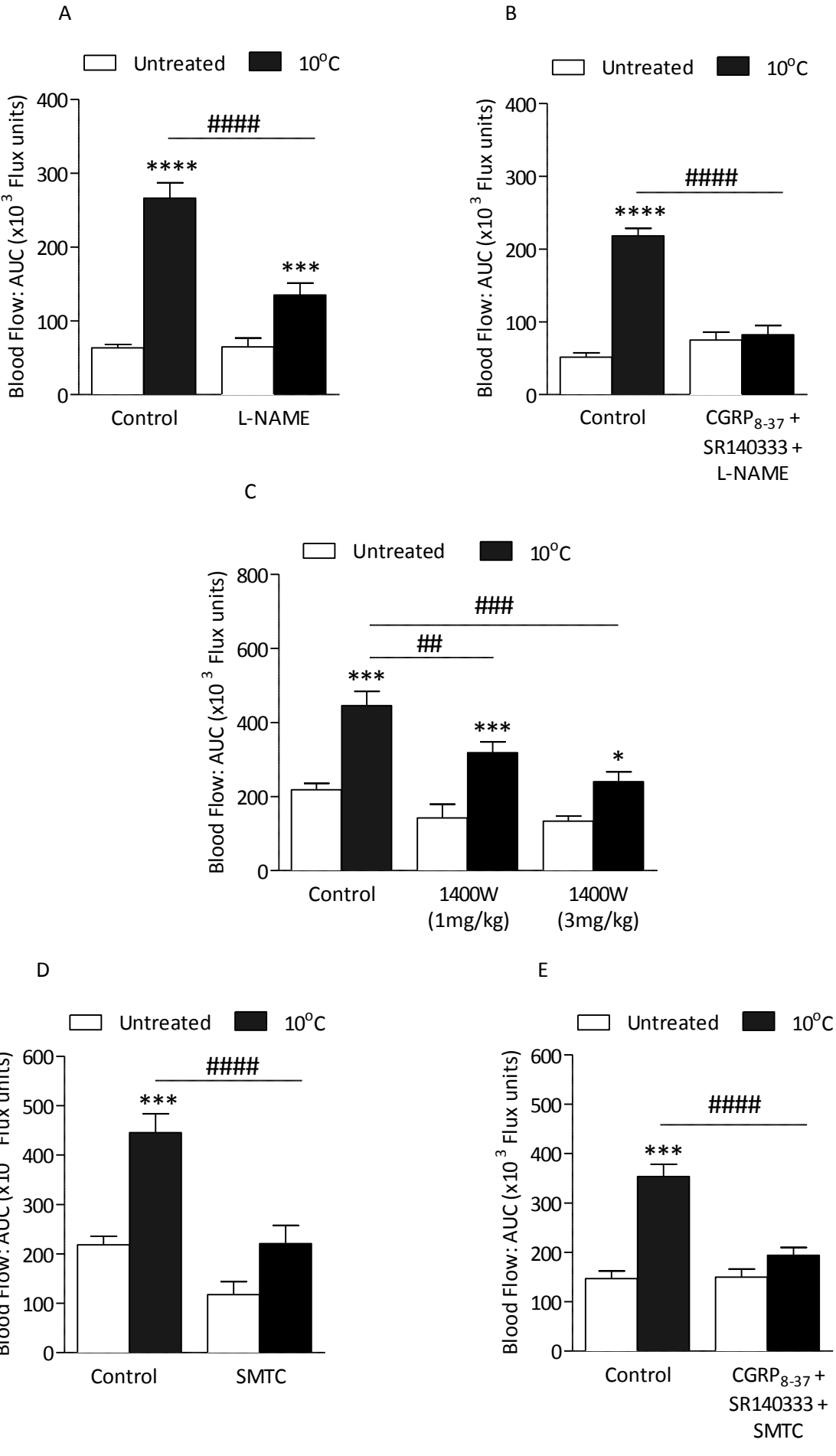
A
Untreated
10°C
Blood Flow: AUC (x10 3 Flux units)
400
300
200
100
0
####
****
***
Control
L-NAME
B
Untreated
10°C
Blood Flow: AUC (x10 3 Flux units)
400
300
200
100
0
####
****
Control
CGRP8-37 + SR140333 + L-NAME
C
Untreated
10°C
Blood Flow: AUC (x10 3 Flux units)
800
600
400
200
0
###
##
***
***
*
Control
1400W (1mg/kg)
1400W (3mg/kg)
D
Untreated
10°C
Blood Flow: AUC (x10 3 Flux units)
600
500
400
300
200
100
0
####
***
Control
SMTC
E
Untreated
10°C
Blood Flow: AUC (x10 3 Flux units)
600
500
400
300
200
100
0
####
***
Control
CGRP8-37 + SR140333 + SMTC

Figure 4.7 Cold-induced vascular response is dependent on nitric oxide and neuropeptides in the peripheral vasculature

Blood flow responses in mouse ipsilateral hindpaw following cold water (10°C) immersion while the contralateral hindpaw remains untreated using FLPI. Blood flow ($\times 10^3$ flux units) recorded over 30 min following treatment and expressed as area under the curve (AUC). Cold-induced vascular responses in the hindpaw of CD1 mice pre-treated with **A**) and **B**) non-selective nitric oxide synthase inhibitor L-NAME (15mg/kg, *i.v.*, 5min, n=7) or control (saline, *i.v.*, 5min, n=10) alone in the presence of $CGRP_{8-37}$ and SR140333 (n=8), **C**) selective iNOS inhibitor 1400W (1mg/kg or 3mg/kg, i.*v.*, 5min, n=5-7) or control (saline, *i.v.*, 5min, n=7), **D**) and **E**) nNOS inhibitor SMTC (10mg/kg, *i.v.*, 5min, n=6) or control (saline, *i.v.*, 5min, n=7) with or without $CGRP_{8-37}$ and SR140333 (n=7-9). Results are shown as mean $\pm$ S.E.M. ***p<0.001, ****p<0.0001 compared to respective untreated, ##p<0.01, ###p<0.001, ####p<0.0001 compared to cold-treated hindpaw of mice using 2-way ANOVA followed by Bonferroni *post hoc* test.

Gene	Plantar Skin		DRG	
	Untreated	Cold (10°C)	Untreated	Cold (10°C)
eNOS	107294 ± 29808	65408 ± 36425	45329 + 14100	59691 + 4547
iNOS	267.4 ± 36.14	245.5 ± 26.5	223.8 ± 12.1	291.9 ± 15.7
nNOS	715.4 ± 83.1	892.9 ± 301.9	1368 ± 205.3	1643 ± 277.7

Table 4.1 Expression of NOS mRNA in cold (10°C)-treated DRG and paw samples using RT-qPCR. mRNA expression of eNOS, iNOS and nNOS at 30 min following treatment in the anaesthetised mouse. Results are expressed as copy numbers per sample normalised to GAPDH and actin (n=4-5). Data was analysed using Student's *t* test.

4.2.7 Role of reactive oxygen species in cold-induced vascular responses

There is clear evidence in the previous chapter that TRPA1-mediated vasodilatation induced by cinnamaldehyde is dependent on the generation of reactive oxygen species such as hydroxyl radicals, superoxide and nitrotyrosine. Furthermore, there is evidence in the literature showing that *in vitro*, cold (4°C) treatment can induce the release of reactive oxygen species, mostly hydroxyl radicals (Rauen and de Groot, 1998), and cooling the mouse tail artery was shown to cause a rapid increase in reactive oxygen species in vascular smooth muscle cells (Bailey et al., 2005). I sought to investigate the role of reactive oxygen species in our cold model, by focusing on the reactive oxygen species scavengers or inhibitors, which were shown to reduce cinnamaldehyde-induced vasodilatation in chapter 3.

Pre-treatment with reactive oxygen species scavenger N-acetylcysteine showed no significant change in cold-induced vascular responses when compared to control ($p>0.05$, n=4, Figure 4.8A). The genetic deletion of NOX4 also had no effects in altering cold-induced blood flow responses, as shown in NOX4 WT and KO mice (n=5-7, Figure 4.7B) and this suggests that reactive oxygen species are not generated by NOX4. Interestingly, I demonstrated that pre-treatment with SOD and H_2O_2 scavenger catalase was remarkably ineffective in suppressing cold-induced vascular response in CD1 mice when compared to control (n=4, Figure 4.8C). There were no significant changes in H_2O_2 or superoxide levels between cold-treated and untreated hindpaw tissue samples collected at 30 min following treatment ($p>0.05$, n=6, Figure 4.8D-E).

I demonstrated that pre-treatment with SOD mimetic tempol resulted in a significant decrease in cold-induced blood flow responses when compared to control-treated groups ($p<0.01$, n=4, Figure 4.8F). Although hydroxyl radicals have been previously reported to be involved in cold-induced effects, I demonstrated that pre-treatment with the iron chelator deferoxamine was ineffective in causing significant changes in cold-induced vascular responses ($p>0.05$, n=4, Figure 4.8G).

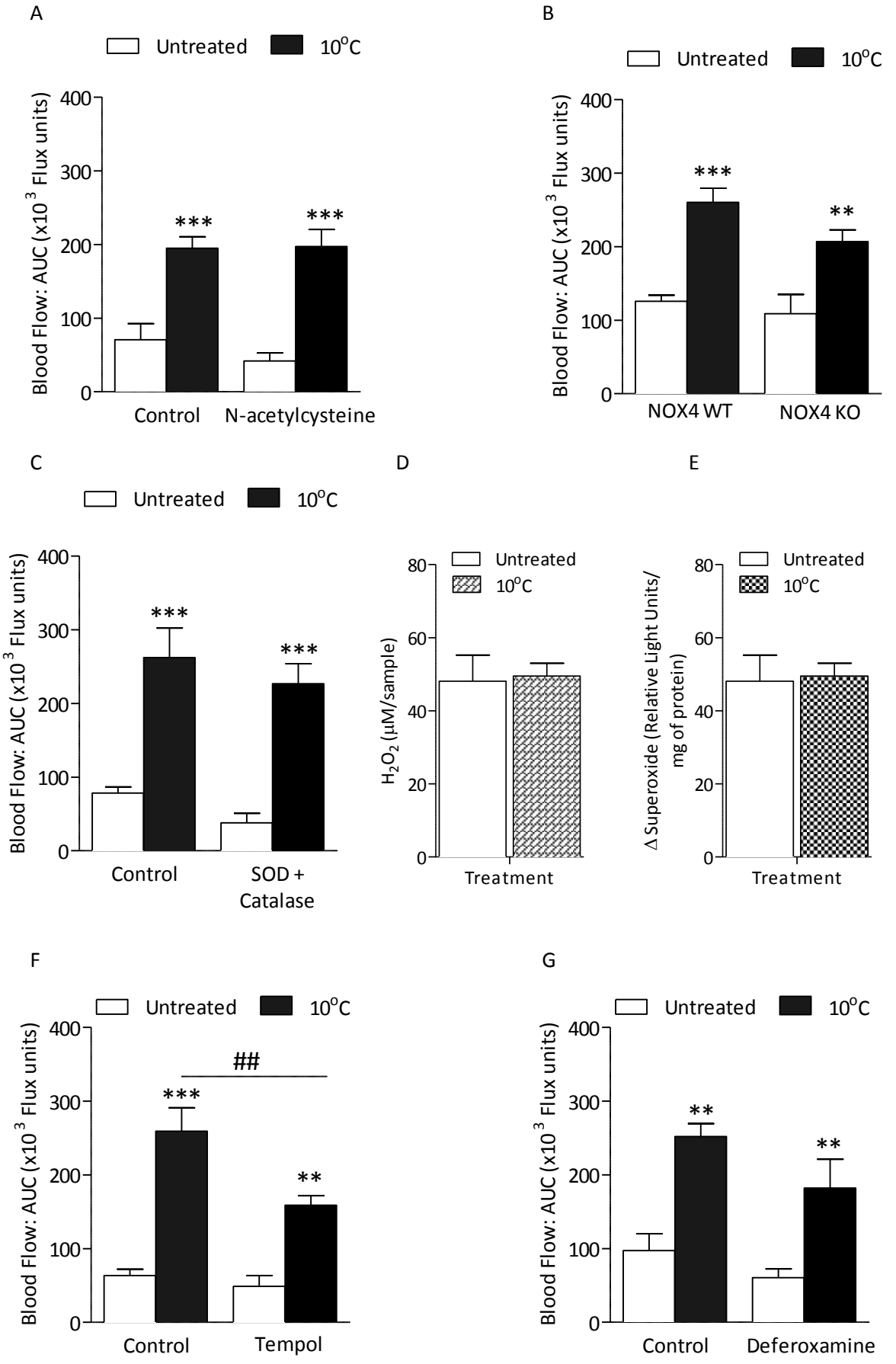
A
Untreated
10°C
Blood Flow: AUC (x10 3 Flux units)
400
300
200
100
0
***
***
Control
N-acetylcysteine
B
Untreated
10°C
Blood Flow: AUC (x10 3 Flux units)
400
300
200
100
0
***
**
NOX4 WT
NOX4 KO
C
Untreated
10°C
Blood Flow: AUC (x10 3 Flux units)
400
300
200
100
0
***
***
Control
SOD + Catalase
D
Untreated
10°C
H2O2 (µM/sample)
80
60
40
20
0
Treatment
E
Untreated
10°C
Δ Superoxide (Relative Light Units/ mg of protein)
80
60
40
20
0
Treatment
F
Untreated
10°C
Blood Flow: AUC (x10 3 Flux units)
400
300
200
100
0
##
***
**
Control
Tempol
G
Untreated
10°C
Blood Flow: AUC (x10 3 Flux units)
400
300
200
100
0
**
**
Control
Deferoxamine

Figure 4.8 Cold-induced vascular response is dependent on reactive oxygen species in the peripheral vasculature

Blood flow responses in mouse ipsilateral hindpaw following cold water (10°C) immersion while the contralateral hindpaw remains untreated using FLPI. Blood flow ($\times 10^3$ flux units) recorded over 30 min following treatment and expressed as area under the curve (AUC). Cold-induced vascular responses in the hindpaw of **A**) CD1 mice pre-treated with reactive oxygen species scavenger N-acetylcysteine (300mg/kg, *i.p.*, 30 min, n=4) or control (saline, *i.p.*, 30 min, n=4), **B**) NOX4 WT and KO mice (n=5-7) and **C**) CD1 mice pre-treated with a combination of superoxide dismutase (SOD, 25000U/kg) and catalase (25000U/kg) or control (denatured SOD and catalase enzyme at 95°C for 20 min, *i.p.*, n=4), **D**) H_2O_2 levels in untreated or cold-treated hindpaw skin tissues at 30 min following treatment in mice as measured by AMPLEX RED assay (n=6), **E**) Superoxide levels in untreated or cold-treated hindpaw skin tissues at 30 min following topical treatment in mice, as measured by Lucigenin assay (n=6). Cold-induced vascular responses in the hindpaw of CD1 mice pre-treated with **F**) SOD mimic TEMPOL (30mg/kg) or respective control (saline, *i.v.*, n=4), **G**) iron chelator deferoxamine (DFO, 25mg/kg, *i.p.*, 30 min, n=4) or control (saline, *i.p.*, 30 min, n=4). Results are shown as mean $\pm$ S.E.M. **p<0.01, ***p<0.001 compared to respective untreated, ##p<0.01 compared to cold-treated hindpaw of mice using 2-way ANOVA followed by Bonferroni *post hoc* test.

4.3 Discussion

This chapter examined the *in vivo* effects of local cold immersion, a proposed model of activating TRPA1 in the mouse hindpaw by analysing the total overall change in blood flow from baseline following cold treatment. Hence, the term 'cold-induced vascular response' is used to define the changes in blood flow for 30 min following cold treatment in this chapter. The next chapter will concentrate on the vasoconstrictor response of the cold-induced vascular response. I hypothesised that the cold-induced vascular response would consist of an initial phase of vasoconstriction followed by vasodilatation where the blood flow returns to baseline. Initial studies confirmed this hypothesis and further showed that this response was dependent on TRPA1, with a potential involvement of TRPM8, which warrants further investigation. The other thermosensitive channels such as TRPV1 and TRPV4 do not play a role in this cold-induced vascular response. I further demonstrated that this response is dependent on the release of both neuropeptides CGRP and substance P. Similar to my previous findings with cinnamaldehyde in chapter 3, this chapter also provides novel evidence that nNOS-derived NO and superoxide may mediate the vasodilator response to TRPA1 activation by cold.

4.3.1 Characterisation of cold-induced vascular response in the peripheral vasculature

Previously, Brain *et al.* showed that a brief local cold exposure in humans fingers can trigger a vasodilator response which is important in protecting against cold-induced injury (Brain et al., 1990). This protective phenomenon of the cold-induced vascular response is important and used as a diagnostic tool in quantitative sensory-testing for patients suffering from peripheral vascular diseases such as diabetes and Raynaud's disease (Brain et al., 1990, Kusters et al., 2010). It has been shown that Raynaud's patients have an increased vasoconstrictor response to cold (Brain et al., 1990, Charkoudian, 2003). Local cold exposure using cold air (28°C to 5°C) was shown to reduce blood flow and skin temperature of mice hindpaws, with the biggest decrease in responses at 5°C, but it was reported that more reproducible results are derived at 10°C (Honda et al., 2007). It is worth highlighting here that the cold-induced vascular response in this study is different from previous reported CIVD or Hunting reaction. The latter is a cyclic regulation of blood flow during prolonged cooling of exposed areas such as hands, feet and nose (Lewis, 1930, Leblanc et al., 1975, Daanen, 2003) and this will be discussed more fully in the General Discussion (chapter 6). In this study, I presented an acute model consisting of local treatment for 5 min where blood flow is assessed following treatment and measured for 30 min. I observed a 'single' biphasic vascular response, where there is a transient vasoconstriction following the local treatment and this response is followed by a vasodilatation phase which brings blood flow back to baseline, without any changes in the untreated paw. Interestingly,

Thomas *et al.* showed that the increase in blood flow in the cold-induced vasodilatation phase did not reach the same level to the baseline blood flow in human subjects (Thomas et al., 1994). It is important to note that in our current cold model, blood flow returns to baseline over the course of recording for 30 min following treatment, which is important to protect against local cold-induced injury.

CIVD has been reported to vary within and between subjects as it is influenced by several factors such as core body temperature, ambient temperature, gender, age and stress (Daanen, 2003). Thus, in order to reduce variability in our study, all these parameters were taken into consideration and kept constant. Skin temperature remains an important measured parameter in cold studies and I observed a rapid decrease in skin temperature following the local treatment, which returned to baseline temperature over the 30 min period recording. This highlights that in our acute cold model, the mice hindpaw blood flow is able to recover completely from the cold-induced vasoconstriction. Previous studies by Kusters *et al.* have shown that the temperature of the rats hindpaws declined rapidly when paws were cooled by the peltier elements in a water bath below than 5°C, but the skin temperature in their study does not return to baseline (Kusters et al., 2010).

CIVD as reported in other studies consist of continuous blood flow fluctuations, vasoconstriction and vasodilatation which are usually recorded during the treatment period itself (Daanen, 2003). Since prolonged vasoconstriction results in tissue damage, the vasodilatation phase is important to prevent cold-induced injury and maintain healthy blood flow to the periphery (Daanen, 2003). In cold studies, the magnitude of the vasodilatation has been reported to rely on the core body temperature and warmth of the skin, as well as the external ambient temperature and time of the day the experiments are taken place. These observations correlate with previous findings by Daanen (2003) and can affect reproducibility of CIVD. Lack of vasodilatation or excessive vasoconstriction in response to cold can cause prolonged tissue hypoxia and in extreme cold conditions, or as evident in Raynaud's phenomenon, can result in cyanosis and may lead to gangrene (Block and Sequeira, 2001). Although the hunting reaction or CIVD is not observed in our model, the cold-treated hindpaw does not remain in a vasoconstricted state. There is a recovery phase where the vessel returns to a normal or dilating state allowing blood to flow back and prevent any local vessel injury. This reproducible response observed over the 30 min following treatment is referred as the 'cold-induced vascular response' throughout this study. This response is selective at 10°C as no changes in blood flow responses were found at a higher temperature (26°C) which is equivalent to the room temperature and serves as a control. This chapter used various pharmacological blockers and

transgenic mice to investigate the mediators involved in the cold-induced vascular response to characterise the model.

4.3.2 The role of TRPA1 in cold-induced vascular response in the peripheral vasculature

I provide novel evidence that the cold-induced vascular response in the periphery after 10°C water immersion is dependent on TRPA1, as shown clearly in TRPA1 KO mice and mice pre-treated with the TRPA1 antagonist HC030031. This finding provides evidence that cold temperature at 10°C activates TRPA1, which supports previous *in vitro* findings discussed in chapter 1. Story *et al.* showed that there is a rapid increase in calcium influx when the buffer is cooled from 17°C to 11°C, with the highest peak influx at 11°C in CHO cells transfected with mTRPA1, but not untransfected cells (Story et al., 2003). El Karim *et al.* have also shown that pre-treatment with HC030031 can block cold (12 $\pm$ 2°C)-induced calcium increase in cultured human dental pulp fibroblasts (El Karim et al., 2011). Furthermore, it was previously shown that TRPA1 KO mice displayed significantly increased paw withdrawal latencies when placed on a cold plate at 10°C when compared to TRPA1 WT mice (Andersson et al., 2008). With the controversy surrounding the role of TRPA1 as a thermo-sensor or thermo-regulator, our current study provides new evidence of TRPA1 as a vascular cold (10°C) sensor in the periphery.

I subsequently investigated the role of other thermo-sensitive TRP channels by initially targeting the heat and warm TRP channels, TRPV1 and TRPV4 respectively. As expected, TRPV1 was shown to play no role in influencing cold-induced vascular responses *in vivo* using TRPV1 KO mice. This finding was confirmed using WT mice pre-treated with TRPV1 antagonist SB366791, at a dose previously shown to have an effect in TRPV1-mediated nociceptive effects (Fernandes, 2011a). Interestingly, this dose was previously shown to have no significant effects on TRPV1 agonist capsaicin-induced vasodilatation in the mouse ear model (Fernandes, 2011a). TRPV1 channels have a polymodal activation profile where they can be activated by noxious heat, changes in protons and endogenous ligands, where interestingly there are different classes of antagonists which block different and not all modes of activation (Alawi and Keeble, 2010). I further investigated the role of the high selective TRPV1 antagonist AMG9810, which is known to block all modes of TRPV1 activation (Gavva et al., 2005). Our results showed that the pharmacological blockade of TRPV1 had no effect on cold-induced vascular responses, confirming that TRPV1 is not involved in this cold model.

Following on from the heat sensor TRPV1, I investigated the potential role of TRPV4, which is activated by warm temperatures (~25°C) (Guler et al., 2002, Watanabe et al., 2002) and has been suggested to play a role in thermosensation. Cold treatment was shown to reduce TRPV4

expression in tongue and muscle, without any change in skin and hence, it was further suggested that TRPV4 in the skin may act as an environmental thermosensor (Nagai et al., 2012). I investigated the role of TRPV4 in our cold model. I showed clearly that there was an increase in cold-induced vascular response following cold treatment (10°C) for 5 min in the treated hindpaw of WT mice when compared to the contralateral untreated hindpaw, and interestingly the deletion of the TRPV4 gene has no effect on these responses. Indeed, other studies have also demonstrated there was no change in core body temperature between TRPV4 WT and KO mice following a cold stress where mice were exposed to 4°C for 150 min in a cold room (Liedtke and Friedman, 2003). Altogether, these findings suggest that TRPV4 is not involved in cold-induced responses.

The findings that TRPV1 and TRPV4 play no role in influencing cold-induced vascular responses agree well with earlier published thermal characteristics of these channels and strengthen our findings that TRPA1 is acting as a vascular cold sensor at 10°C *in v*ivo. The next aim of this study was to investigate the role of the cold sensor TRPM8 which is known to be expressed in approximately 10% of primary afferent sensory neurons. There is presently an unclear understanding of the role of the thermo-TRP channels associated with cooling. However, there is an increasing amount of evidence showing that TRPM8 is sensitive to environmental cool temperatures below 25°C (Zholos, 2010, McKemy et al., 2002) and mediates deep body cooling which is associated with cutaneous vasoconstriction (Almeida et al., 2012). The evidence thus far suggests that TRPM8 is potentially involved in thermoregulation as TRPM8 antagonists cause a change in core body temperature in mice and rats (Almeida et al., 2012) but its role in mediating local cold-induced responses remains unknown. On the other hand, TRPA1 may not be tonically active as TRPA1 antagonists were demonstrated to have no effect in altering core body temperature in mice (Chen et al., 2011, Fernandes, 2011b). This suggests that TRPA1 may be more involved in local thermosensation. Indeed, a recent study by Knowlton *et al.* has demonstrated *in vivo* how the importance of TRPM8 overrides TRPA1 in cold detection in a study that was restricted to neural and behavioral experiments (Knowlton et al., 2010). It is important to note here that the study by Knowlton *et al.* was restricted to temperatures of 5-30°C. Based on these evidences, I investigated the role of TRPM8 in our acute cold set up model in the vasculature.

Here, I have explored the possibility of an interaction between TRPA1 and TRPM8 in our cold model, focusing on 10°C and the cutaneous vasculature. Our data showed clearly that the pharmacological blockade or genetic deletion of TRPM8 caused a significant decrease in the cold-induced vascular responses, but to a lesser extent compared to the pharmacological

blockade or genetic deletion of TRPA1. This evidence is in disagreement with recent findings by Knowlton *et al.* (2013) who showed that the selective ablation of TRPM8 neurons *in vivo* induced a loss of sensitivity to both innocuous and noxious cold (Knowlton et al., 2013). It is important to note here that innocuous cold consists of experiments where the surface skin temperature is reduced to 17°C following application of acetone whilst noxious cold consisted of investigating nociceptive behaviours when the mice were placed on a cold plate at 0°C (Knowlton et al., 2013). Nonetheless, as shown previously in chapter 3, the exogenous TRPA1 agonist cinnamaldehyde-mediated vasodilatation remained unchanged in the presence of the TRPM8 antagonist AMTB. Hence, I proposed that TRPM8 is not the primary vascular cold sensor at 10°C but may partially be involved in mediating the vascular response as the tissue warms up during recovery. Indeed, further investigation is required to understand the role of TRPM8 in mediating cold-induced vascular responses in our local cold model. Nevertheless, it is clear from our results that the TRPA1 channel is involved in the all phases of the cold-induced vascular response.

4.3.3 The role of sensory neuron in the cold-induced vascular responses

It is well established that mechanosensitive Aδ- and C-fibres innervating the hairy and glabrous skin are polymodal and sensitive to changes in temperatures (Simone and Kajander, 1996, Simone and Kajander, 1997, Cain et al., 2001). The role of sensory neurons themselves in cold-induced responses has been studied since the early 1930s (Lewis, 1930). It is known that these responses are controlled neurally as cold-induced vasoconstriction was shown to be reduced in the nerve injured paw (Kusters et al., 2010). Nevertheless, the mechanism underlying cold-induced responses is still debatable. Whilst some studies have shown that axon reflexes do not occur in cold induced vasodilatation (Daanen and Ducharme, 2000), other studies have shown that sensory nerve blockade prevents local skin cooling-induced vasoconstriction (Johnson et al., 2005, Pergola et al., 1993, Thompson-Torgerson et al., 2007, Yamazaki et al., 2006). It has also been suggested that local cooling can stimulate the vasoconstrictor nerves via a sensory-dependent manner, which relies on a direct communication to the sympathetic nervous system (Johnson et al., 2005).

Moreover, most of the studies investigating the role of thermosensitive TRP channels in relation to cold have been performed on DRG or trigeminal neurons, and this highlights that there is a link between cold and sensory neuron in detecting of cold stimulus. Although it is well-established that TRPA1 is widely expressed on sensory neurons, there is also increasing evidence of the presence of TRPA1 on non-neuronal cells such as keratinocytes, endothelial

cells and in sympathetic ganglia (Tsutsumi et al., 2010, Denda et al., 2010a, Earley, 2012, Smith et al., 2004). The mechanism underlying the activation of non-neuronal TRPA1 is currently not well understood. From our previous study in chapter 3, our data suggests that the sensory neurons play an important role in TRPA1-mediated vascular response as I showed clearly that activation of TRPA1 by cinnamaldehyde induced a neurogenic vasodilatation. Therefore, in this study I tested whether sensory nerves are required for the cold-induced vascular responses.

Our results showed that pre-treatment with local anaesthetic EMLA topically had no effect on the cold-induced vascular responses. This is in disagreement with previous studies where application of EMLA topically was shown to reverse the initial vasoconstrictor responses associated with slow local cooling in human subjects (Hodges et al., 2007). A possible limitation from our experiments could be that EMLA, when applied topically was not given sufficient time (5min) for absorption and significant blockade of local sensory neuron. Hence, this experiment was followed by investigatingthe injection (*i.pl.*) of lidocaine on cold-induced vascular responses. I observed that pre-treatment with lidocaine caused a significant decrease in cold-induced vascular responses when compared to control. Interestingly, there was also a decrease in the untreated paw of the lidocaine pre-treated group, but this difference did not reach statistical significance level. Previous studies have also reported conflicting evidence about the effects of lidocaine on altering sensory function and epidermal nerve fibre density, where pressure pain and thresholds for cold-induced pain were not affected by the application of a lidocaine (5%) patch in healthy skin (Wehrfritz et al., 2011). Although our findings here suggest that the sensory neuron may have a role in the cold-induced blood flow responses, further studies are required to establish a link between local anaesthesia and cold-induced responses.

To further investigate the role of sensory neurons in the cold-induced vascular responses, I sought to investigate the role of the mediators released downstream of TRPA1 activation. The vasodilator phase of a cold-induced vascular response is thought to be dependent on the release of neuropeptides such as CGRP and substance P but these theories are yet to be investigated directly (Charkoudian, 2003, Tew et al., 2011). It was previously shown that CGRP and substance are co-transported from the DRG and CGRP was suggested to have a modulatory effect on substance P (Gibbins et al., 1985). Our study illustrated clearly that both neuropeptides CGRP and substance P play a role in the cold-induced vascular response and interestingly, the pharmacological blockade of both the CGRP receptors and NK_1 receptors was not sufficient to completely inhibit the cold-induced vascular responses. This data is in agreement with our

previous findings in chapter 3, thus showing that TRPA1 activation causes a neurogenic-dependent vasodilatation using both cold and cinnamaldehyde.

The role of substance P itself in cold-induced responses has not been widely studied, but it is well established that it is a potent vasodilator (Brain and Cox, 2006). Here, I show clearly that substance P has a role in mediating blood flow changes following a local cold treatment. An interaction between sympathetic-mediated noradrenaline responses and non-sympathetic vasodilation was previously hypothesised and this is thought to involve substance P (Lewis, 1930, Ochoa et al., 1993) and the temporal changes in blood flow response is thought to reflect the duration of actions of these neurotransmitters. Ochoa *et al.* suggested that both neurotransmitters are released simultaneously from the sensory neurons post-cold stimulation to maintain vasodilatation, resulting in the re-warming phase (Ochoa et al., 1993). Furthermore, it was previously suggested that substance P-induced vasodilatation is dependent on endothelium-derived nitric oxide, as shown in human coronary, forearm vessels and skin (Tagawa et al., 1997, Klede et al., 2003). The role of nitric oxide in cold-induced vascular response will be further discussed in section 4.3.5.

Local cooling (<25°C) was previously shown to alter neural mechanisms leading to changes in peripheral vasodilatation by spinal cord stimulation in the hindpaw in experiments using $CGRP_{8-37}$(Tanaka et al., 2003). Cold-induced vascular responses were clearly shown to be dependent on CGRP, because blockade of CGRP receptors with the antagonists $CGRP_{8-37}$ and BIBN4096BS has a significant decrease on the magnitude of the blood flow responses. Unexpectedly, I found that there was no change in cold-induced vascular responses between α-CGRP WT and KO mice and this result highlights clearly that α-CGRP may not be involved in mediating the blood flow changes in our cold model. Interestingly, cooling of the rat cranial dura matter was previously shown to induce an increase in blood flow independent of CGRP (Holom et al., 2008). It is important to note that CGRP is not a single peptide but consists of 2 separate peptides (α-CGRP and β-CGRP), which are both expressed in the DRG (Schutz et al., 2004). α-CGRP primary sensory neurons have been shown to contribute to thermoregulation and cold detection and interestingly, cold sensation was shown to be enhanced following the ablation of α-CGRP neurons in adult mice (McCoy et al., 2013). This enhancement was reported to be independent of the number of TRPM8-expressing DRG neurons or an increase in the number of cold-receptive fields (McCoy et al., 2013). I did not observe an enhancement in cold-induced vascular responses in the α-CGRP KO mice when compared to WT mice, but interestingly there was an upregulation of β-CGRP and TRPA1 mRNA expression in the DRG of α-CGRP KO mice compared to WT mice. It is important to note here that these samples

were collected at 30 min following cold treatment, but a similar pattern of β-CGRP mRNA expression was previously reported in naïve α-CGRP WT and KO mice (Smillie, 2012). It is possible that these changes may be due to compensatory changes in the KO mice, as a result of the α-CGRP gene deletion. However, this is in disagreement with previous findings by Schutz *et al.* (2004) who showed that there was no change in β-CGRP mRNA expression in the DRG between naïve α-CGRP WT and KO mice, on a similar genetic background (Schutz et al., 2004).

Further to our data presented here with regards to the CGRP receptor antagonists and α-CGRP KO mice, I hypothesised that β-CGRP may play an influential role in the blood flow responses. To test this possibility, I investigated the effects of BIBN4096BS in the α-CGRP KO mice and I showed clearly that the cold-induced vascular response was subsequently significantly decreased, to a similar extent shown with WT mice pre-treated with the CGRP receptor antagonists. Both isoforms of CGRP have been reported to have approximately equipotent biological activities (Sams et al., 1999); although they are distributed differently in tissues. Whilst α-CGRP is known to be found predominantly on sensory neurons and CNS, β-CGRP is known to be predominant in enteric nerves and the pituitary gland. There is also evidence now to show that keratinocytes which express the CGRP receptor components; CRLR, RAMP1 and RCP, also express β-CGRP (Hou et al., 2011). Our results highlight the important role of β-CGRP in mediating cold-induced vascular responses in the periphery. It remains unknown in our model whether β-CGRP is released from the keratinocytes or sensory neurons. However, a key role for keratinocytes in sensory transduction has been suggested (Lumpkin and Caterina, 2007) as these cells are in intimate contact with the sensory nerves. Although cooling has been shown to evoke a calcium influx response with pharmacological characteristics consistent with TRPA1 activation (Tsutsumi et al., 2010), a role for keratinocytes in the vascular response to cooling has not to our knowledge been considered. Altogether, in this study I can conclude that cold-induced vascular induced by TRPA1 activation is dependent on substance P and β-CGRP.

4.3.4 The role of prostaglandins in the cold-induced vascular responses

Our results thus far show that there remains a residual response following the pharmacological blockade of both the sensory neuropeptide receptor antagonists and hence, this suggests that other mediators may be involved in this cold model. Cold-induced vasodilatation was previously reported to occur as a result of depressed vascular smooth muscle activity and increase in vasodilator compounds (Folkow et al., 1963). Arachidonic acid metabolites have been proposed to have vasoactive properties and the role of prostaglandins in cinnamaldehyde-

induced vasodilatation was investigated previously in chapter 3. During re-establishment of blood flow into the vessels following cold-induced vasoconstriction, cyclooxygenase pathways have been reported to produce prostaglandins, which alter vascular reactivity (Hamberg et al., 1975, Harlan and Harker, 1981).

I found that indomethacin had no effect on cinnamaldehyde-induced responses. Similarly, pre-treatment with indomethacin had no effects on altering cold-induced vascular responses in our model and hence, this suggests that cyclooxygenase products may not be involved in this response. The role of prostaglandins has previously been studied and Ormerod *et al.* (1988) showed that when the arms of normal subjects were challenged in cold water (10°C) for 5 min, there was an increase in PGD_2 levels in the serum (Ormerod et al., 1988). Furthermore, indomethacin has also been shown to inhibit cold-induced changes in cat hind-feet following local cold water (0°C) exposure (Franz, 1985). Nevertheless, in our cold model at 10°C, indomethacin had no effect in affecting cold-induced vascular responses and hence, our results indicate no role of prostaglandins in this model in the vasculature.

4.3.5 The role of nitric oxide in the cold-induced vascular responses

The vasoactive substance nitric oxide was previously shown in chapter 3 to have a prominent role in mediating TRPA1-mediated vasodilatation induced by topical cinnamaldehyde in the peripheral vasculature. As discussed in chapter 1, animal studies have shown that both the neuropeptides CGRP and substance P-induced vascular responses may be mediated via the generation of secondary vasodilator mediators such as nitric oxide (Clough, 1999, Weidner et al., 2000, Clough and Church, 2002, Klede et al., 2003). I further investigated the role of nitric oxide in the cold-induced vascular responses using selective pharmacological inhibitors of the different isoforms of NOS, as used previously in chapter 3. Although, nitric oxide has been previously shown to participate in cold-induced vasodilatation (as discussed in chapter 1), the direct link between nitric oxide and cold-induced responses remains missing with conflicting evidence in the literature. Garcia-Villalon *et al.* (1992) showed that cooling can increase the availability of eNOS in the rabbit ear artery and inhibits adrenergic receptor agonist-induced contraction *in vitro* (Garcia-Villalon et al., 1992, Garcia-Villalon et al., 1995). However, other studies showed that stepwise cooling (37 to 4°C)-induced relaxation of rat aortic smooth muscle was independent of a neural or nitric oxide mechanism (Mustafa and Thulesius, 2001). Interestingly, the NOS enzymes have been previously reported to be temperature sensitive (Venturini et al., 1999) and L-NAME pre-treatment was shown to decrease cooling (4°C)-induced vascular conductance in the human skin (Yamazaki et al., 2006).

Following on from these previous studies, I investigated the effects of NOS inhibition in our cold model and showed that pre-treatment with L-NAME was able to significantly decrease the cold-induced vascular responses. A similar pattern was shown in chapter 3 for studies with cinnamaldehyde. Additionally, pre-treatment with L-NAME and neuropeptide receptor antagonists $CGRP_{8-37}$ and SR140333 was able to abolish the cold (10°C)-induced blood flow responses in the hindpaw of WT mice. It is worth highlighting here that these drugs have been used previously to study neurogenic vasodilatation (Starr et al., 2008) and in this study, there is no change in baseline blood flow following pre-treatment of antagonists or in the untreated paws. Nevertheless, previous studies have shown that functional NOS control the basal vascular tone in intact human skin (Yamazaki et al., 2006). Altogether here, I provide novel and clear evidence that these mediators are involved in mediating TRPA1-induced blood flow responses in the peripheral vasculature.

In terms of the cold model, our results show that NO is partially responsible in mediating blood flow responses following local skin cold treatment at 10°C. To further characterise the role of NO, I investigated the effects of iNOS and nNOS inhibition using 1400W and SMTC respectively, at a dose previously used for investigating the mechanisms underlying cinnamaldehyde-induced vasodilatation in chapter 3. Unexpectedly, I observed a significant reduction in cold-induced vascular responses in 1400W-treated mice when compared to control and these findings suggest that iNOS-derived NO plays a role in this response. It remains unknown in our study how iNOS-derived NO is released as resting cells are known to express little or no iNOS. However, Nisoli *et al.* showed that iNOS synthesis is induced in brown adipose fat (BAT) cells in response to β-adrenergic receptors activation and an increase in cAMP production (Nisoli et al., 1997). It would be interesting to investigate whether local cold exposure induces the expression of iNOS in BAT and potentially play a role in our acute cold model.

Interestingly, there is also evidence showing that the activation of CGRP receptors by CGRP can stimulate iNOS gene expression via a MAPK pathway in trigeminal ganglion glial cells (Vause and Durham, 2009). It is evident from our results that CGRP plays a prominent role in the cold-induced vascular responses but it remains unknown if CGRP release downstream of TRPA1 activation by the cold stimulus would have an effect on iNOS expression in the peripheral vasculature in an acute treatment. As shown previously in Chapter 3, pre-treatment with 1400W did not have an effect on cinnamaldehyde-induced vasodilatation. Hence, this implies that iNOS-derived NO is not a mechanism exclusive to TRPA1 activation but is downstream to cold activation. The source of iNOS is unknown in our study but cold exposure

at -4°C for 3 min has been shown to cause vasoconstriction where leukocytes becomes trapped in the microvasculature (Bourne et al., 1986) and the total number of adherent neutrophil cells were shown to be greatest on cooling at 10°C *in vitro,* which impairs local microcirculation in cold (Nash et al., 2001). In the rewarming phase, it was suggested that the activated cells are released into the systemic circulation (Nash et al., 2001) and if so, it would be interesting to determine whether leukocytes are a potential source of iNOS in our model.

Furthermore, selective inhibition of nNOS was shown to partially decrease TRPA1-mediated vasodilatation by cinnamaldehyde. The aim of the current study was to determine whether nNOS-derived NO is involved in the cold-induced vascular response, using a dose previously used in chapter 3 in studies with cinnamaldehyde. Our study revealed that pre-treatment with SMTC caused a significant decrease in blood flow at baseline and this correlates to previous findings by Melikian *et al.* who also showed a similar pattern in the forearm of normal subjects. This dose does not affect the eNOS-mediated vasodilatation elicited by acetylcholine, substance P or shear stress(Melikian et al., 2009). All these findings further strengthen the role of nNOS in regulating normal vessel tone *in vivo.* Moreover, I showed that cold-induced vascular responses were significantly reduced in the presence of SMTC, to a greater extent than treatment with L-NAME or 1400W alone. These results provide novel *in vivo* evidence that nNOS-dependent local release of nitric oxide modulates blood flow responses following activation by cold (10°C) treatment in the peripheral vasculature. Hence, the question which arises from our evidence is whether nitric oxide is being released from the sensory neuron itself following TRPA1 activation by cold or via other potential pathways as nNOS is now known to be expressed in several smooth muscle cell and endothelial cells (Boulanger et al., 1998, Bachetti et al., 2004).

In fact, pre-treatment with a combination of the neuropeptide receptor antagonists and SMTC was able to inhibit the cold-induced blood flow responses, with no significant change in the untreated hindpaw when compared to control groups. A link between nNOS/nitric oxide and CGRP has been speculated in previous studies and interestingly, nNOS was shown to be co-localised with the CRLR, RAMP2 and RAMP3 in rat DRG neurons (Wang et al., 2013). There is also evidence showing that 82% of TRPA1-expressing myenteric neurons also express NOS in mice (Poole et al., 2011) but it remains to be determined whether nNOS and CGRP are found in TRPA1-expressing sensory neurons innervating the blood vessels in the hind-paws. Our group has previously shown that the nNOS inhibitor 7-nitroindazole has no effects on CGRP-induced vasodilation in the rat cutaneous vasculature, however it was clearly shown that the stimulation of the saphenous nerve releases nitric oxide and causes neurogenic-dependent vascular changes (Kajekar et al., 1995). Interestingly, nitric oxide has been previously suggested

to act on sensory neurons to release CGRP, which further relaxes smooth muscle (Wei et al., 1992, Akerman et al., 2002).

It is clear from this study that nitric oxide participates in this response, however it remains to be determined in which phase is nitric oxide involved in the cold-induced blood flow responses. Previous studies have speculated that the vasoconstriction phase is dependent on an increase in noradrenaline release and decrease in both NOS activity and other processes occurring downstream of NOS (Hodges et al., 2006). The role of eNOS in our model is unclear. Previously, it was shown that cold exposure (4°C) alone was not able to significantly change eNOS expression in bovine aortic endothelial cells (BAEC) *in vitro* but required the presence of shear stress (Binti Md Isa et al., 2011). The findings from the present study suggests that (1) both neuropeptides and nitric oxide are potentially released from the sensory neuron following TRPA1 activation by cold and/or (2) nitric oxide may stimulate CGRP release from sensory neuron, and mediate the cold-induced vascular responses.

4.3.6 The role of reactive oxygen species in the cold-induced vascular responses

Several studies have investigated the effects of whole body cooling on generating reactive oxygen species such as superoxide by mitochondria calcium, whereby nitric oxide plays a permissive role in reaction with superoxide (Kevin et al., 2003, Camara et al., 2004). Furthermore, local moderate cooling to 28°C was shown to cause a rapid increase in mitochondrial reactive oxygen species activity in smooth muscle cells of mouse tail arteries, as shown by confocal microscopy using reactive oxygen species-sensitive probes (Bailey et al., 2005), as further discussed in the next chapter. This reactive oxygen species generation has been shown to stimulate the activation of RhoA and Rho kinase signalling and mobilisation of α_{2c}-adrenergic receptors to the cell surface, leading to constriction of the smooth muscle cell (Bailey et al., 2005). As shown in chapter 3, I have shown that cinnamaldehyde-induced vasodilatation following TRPA1 activation is dependent on superoxide, hydroxyl radicals and nitrotyrosine generation. In this chapter, I investigated the role of reactive oxygen species on cold-induced vascular responses using the same ROS inhibitors and scavengers as previously used in chapter 3.

In this study, I found that pre-treatment with reactive oxygen species scavenger N-acetylcysteine did not inhibit cold-induced vascular responses when compared to control. Interestingly, this similar dose of N-acetylcysteine was shown to significantly decrease cinnamaldehyde-induced vasodilatation in chapter 3. Nevertheless, Bailey *et al.* showed that N-acetylcysteine was able to reduce the α_2-receptor agonist UK14304-induced constriction when

cooled to 28°C (Bailey et al., 2005). Supplementation with antioxidant L-ascorbate was also shown to decrease local moderate cooling-induced vasoconstriction in human forearm skin when skin sites were cooled from 34°C to 24°C (Yamazaki, 2010). I further investigated the role of reactive oxygen species using a combination of treatment with SOD and catalase, which was previously shown to significantly reduce cinnamaldehyde-induced vasodilatation (chapter 3) and prevent cold-induced translocation of α_{2c}-adrenergic receptors(Bailey et al., 2005).

Interestingly, in the present study cold-induced vascular responses remained unchanged in the presence of SOD and catalase. SOD and catalase have been reported to reduce cold-induced injury (Bhaumik et al., 1995) and demonstrated to reduce hydroxyl radicals formation during the rewarming phase in studies where rabbit leg was exposed to cold (0°C) (Das et al., 1991). It may be possible that SOD and catalase are not transported to the site of action as they are not cell-permeable and hence, to further elucidate the role of superoxide and H_2O_2, studies will require cell-permeable SOD and catalase mimics. Furthermore, NOX4 and hydroxyl radicals were shown not to be involved in the cold-induced vascular response and this suggests that TRPA1-mediated vascular responses by cold are not dependent on reactive oxygen species derived from NOX4. I also found that there was no difference in the superoxide and H_2O_2 levels at 30 min following local cold treatment in hindpaw tissue when compared to untreated hindpaw tissue samples. This finding suggests or reinforces the evidence that the cold-induced vascular response is non-invasive, with normal restoration in baseline blood flow at 30 min. To further elucidate the role of reactive oxygen species in the cold-induced vascular responses, tissue samples will need to be collected at an earlier time point as shown in chapter 5.

There is evidence in the literature to suggest that superoxide plays an important role in cold-induced vasoconstriction (Bailey et al., 2005) and superoxide generated by local cooling can reduce NO bioavailability by reacting with NO to form peroxynitrite in the vasculature (Forstermann and Munzel, 2006). Preliminary studies using SOD showed that there was no change in cold-induced vascular response and this may be due to SOD being readily excreted and having a circulatory half-life of 8 min, as shown in rats (Turrens et al., 1984) or SOD not penetrating the cell membranes as it is a large molecule (Beckman et al., 1988). Pre-treatment with the cell permeable SOD mimic tempol was shown to significantly decrease cinnamaldehyde-induced vasodilatation *in vivo* and this finding led us to investigate the role of tempol in the cold-induced vascular responses. In agreement with our previous findings, I showed clearly that the cold-induced vascular responses were significantly reduced in the presence of tempol, when compared to control-treated groups. Tissue hypoxia during vasoconstriction has been shown to lead to increased mitochondrial superoxide release (Turrens,

2003). Interestingly, it is also known that endothelial cells are the initial site of tissue injury in local cold studies and provide a rich source of the superoxide-generating enzyme, xanthine oxidase in the rewarming phase of a cold-induce response (Jarasch et al., 1986).

Hence, it may be possible that in our study tempol is reducing the accumulation of superoxide in the vasculature by increasing its rate of breakdown into water and oxygen as well as free radical scavengers. This further decreases intracellular reactive oxygen species concentrations and reduces cold-induced vascular responses. Further experiments are required to elucidate in which phase superoxide participates in the cold-induced vascular response observed in this study, as well as how superoxide interacts with the sympathetic nervous system.

4.5 Conclusion

This chapter investigated the mechanisms underlying cold-induced vascular responses following local cold water (10°C) treatment for 5 min in the mouse hindpaw. Using genetically modified mice and pharmacological inhibitors, these results provide a new insight into the mechanisms of cold-induced responses, illustrating clearly that (1) cold (10°C) activates TRPA1 in the peripheral vasculature and causes a rapid transient decrease in blood flow, followed by prolonged vasodilatation to return blood flow to baseline. The role of TRPA1 as a cold sensor has been a controversial issue in the literature, and this current study presents novel findings showing that TRPA1 is a vascular cold sensor *in vivo* (Figure 4.8); and (2) the pharmacological blockade or gene deletion of the TRPM8 gene was shown to partially inhibit cold-induced vascular responses, suggesting that TRPM8 may be involved in mediating the vasodilatation phase but further studies are required to investigate these effects.

In this study, cold-induced vascular responses following activation of TRPA1 was demonstrated to be dependent on the release of the neuropeptide substance P and the potent microvascular vasodilator CGRP (Figure 4.9). This is in agreement with the traditional hypothesis that an axon reflex mediates neurogenic vasodilatation, which is essential in protecting against local cold-induced injury. Our study also introduces the novel concept that the β-CGRP isoforms (as shown in α-CGRP KO mice) and nNOS-derived nitric oxide have an important role in mediating the cold-induced vascular responses. Moreover, intracellular reactive oxygen species such as superoxide were shown to play a pivotal role in cold-induced vascular response. Overall, this study provides evidence that the cold-induced vascular response is clearly mediated by two phases: an initial vasoconstriction and vasodilatation to prevent against local cold-induced injury. It is evident from the present findings that the release of vasodilators such as CGRP, substance P, nitric oxide and superoxide, downstream of TRPA1 activation by local

cold exposure, play a pivotal role in returning blood flow back to baseline following the transient local cold-induced vasoconstriction. Indeed, this mechanism may be relevant in understanding the pathophysiology of the Raynaud's phenomenon where there is prolonged vasoconstriction following local cold exposure.

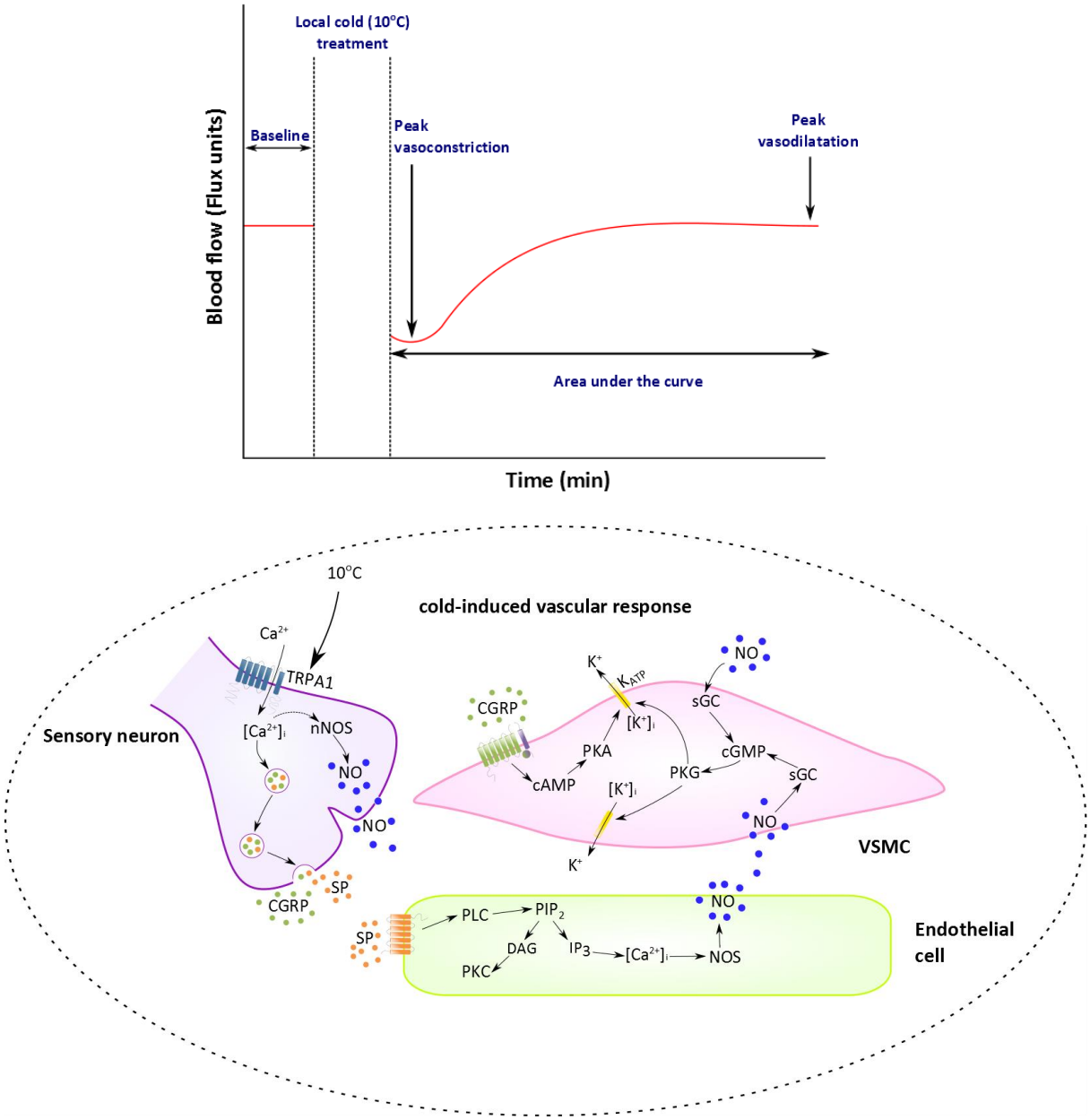

Figure 4.9 Signalling mechanisms underlying cold-induced vascular responses following action of TRPA1. The diagram summarises the signalling pathways involved in mediating cold (10°C)-induced vascular responses in the peripheral vasculature. Cold activates TRPA1 and causes stimulation of nerve endings from primary afferent neurons. This releases the neuropeptide calcitonin gene-realated peptide (CGRP), substance P and neuronal nitric oxide synthase (nNOS)-derived nitric oxide to mediate an increase blood flow in the vasculature. CGRP acts on CGRP receptor complex; CGRP receptor-like receptor (CRLR) and receptor activity-modifying protein-1 (RAMP1) to induce an increase in intracellular cyclic adenosine monophosphate (cAMP) via adenylyl cyclase and cAMP further phosphorylate protein kinase A (PKA) and open ATP-sensitive potassium (K_{ATP}) channels to mediate relaxation. Substance P promotes vasodilatation by acting on neurokinin-1 (NK_1) receptors on the endothelial cells via the release of nitric oxide. Nitric oxide acts on stimulating the soluble guanylate cylase (sGC) to subsequently form cyclic-guanosine monophosphate (cGMP), activating protein kinase G (PKG) which causes reuptake calcium and opens potassium channels, leading to hyperpolarization of the membrane and further relaxing the vascular smooth muscle cell (VSMC).

Chapter 5 – Investigating the constrictor and dilator components of cold-induced vascular responses

Chapter 5 – Investigating the constrictor and dilator components of cold-induced vascular responses

5.1 Introduction

Our findings from chapter 4 demonstrated clearly that TRPA1 acts as a vascular cold sensor *in vivo* and mediates cold-induced vascular responses, which are dependent on the release of the neuropeptides CGRP and substance P, iNOS and nNOS-derived nitric oxide as well as generation of superoxide. Similarly, the majority of these mediators also participate in TRPA1-mediated vasodilatation induced by the exogenous TRPA1 agonist cinnamaldehyde, as shown in chapter 3. It is assumed that cutaneous cold or pain sensors can stimulate nerves to release vasodilators as a result of an axon reflex, and I have provided clear evidence of a role of neuropeptides in mediating cold-induced vascular responses in our study. Moreover, it is well established that the sympathetic nervous system has an important role in initiating changes mediated by local reflexes or adrenergic receptor activation following local cold treatment in the vasculature. Traditionally, most studies investigating the effects of acute or long term exposure to cold at various temperatures have concentrated on the loss of sympathetic constrictor mechanisms as a primary driver of the decreased blood flow (Daanen and van der Struijs, 2005). It remains difficult to compare the findings from different studies due to the different variables in cooling procedures such as sites and temperature. This chapter will focus on understanding the mechanisms involved in sensing temperature in the skin to further comprehend the underlying protective mechanism.

From the results presented in chapter 4, it is evident that TRPA1 plays a prominent role in mediating the cold-induced vascular response. Whilst it is known that activation of TRPA1 can mediate vasorelaxation (Pozsgai et al., 2010), there is no evidence showing that TRPA1 mediates a vasoconstrictor response in the peripheral vasculature. It is interesting to note that as shown in chapter 4, the cold-induced vascular response consists of an initial rapid phase of vasoconstriction followed by vasodilatation. This vasodilator component is important in returning the blood flow back to basal levels.

The first aim of this chapter is to re-analyse the results for TRPA1 and CGRP from chapter 4 in order to examine their role in mediating either the constrictor or dilator component of the cold-induced vascular response. To accomplish this analysis, I investigate the effects of the pharmacological antagonists on the net vasoconstriction and vasodilatation phase, as previously described in section 2.8.2. Furthermore, I will elucidate the role of the sympathetic nerve in our cold (10°C)-induced vascular responses and investigate the potential link between TRPA1 activation and sympathetic nerves in this response.

5.1.1 Brief methods

Using the FLPI, cold-induced vascular responses were studied, as detailed in Chapter 2 (section 2.4). Briefly, skin blood flow was measured concomitantly in the whole area of both hindpaw of male mice anaesthetised with ketamine (75mg/kg) and medetomidine (1mg/kg). Following baseline measurement for 5-10 min, the mouse was subsequently removed from the heating mat and the ipsilateral paw was exposed up to the level of the joint between the tibia and the calcaneum to cold water (10°C) for 5 min. The contralateral hindpaw was left untreated at room temperature (~22°C). Hence, this protocol allowed the simultaneous assessment of blood flow responses in the cold-treated and control paws in the same mouse. Following treatment, the hindpaw was dried as detailed in section 2.4.4 and blood flow measurement was resumed for 30 min using the FLPI.

All the experiments studying cold-induced blood flow responses were conducted using FLPI in male mice. A range of pharmacological inhibitors was used to investigate the mediators involved in mediating cold-induced vascular responses (section 2.6).

The response to cooling consisted of an initial reduction in flux, in keeping with vasoconstriction, followed by a slow developing sustained increased flux, consistent with vasodilatation. This whole response observed following treatment is termed "*cold-induced vascular response*" in this chapter. Data was recorded as flux arbitrary units and in this chapter, data was analysed as AUC from time '0 min' following treatment (cold water immersion and drying of hindpaw) to 30 min recording, as detailed in section 2.8.2. Furthermore, a two-component analysis was introduced in this chapter to investigate the role of particular mediators in mediating the initial constrictor or dilator component of the cold-induced vascular response, as detailed in section 2.8.2.

Hindpaw tissue samples were collected at 2 min or 30 min following local cold treatment and *ex vivo* analysis was conducted to investigate noradrenaline generation using ELISA, superoxide release using the Lucigenin assay, and MLC protein expression using western blotting, as detailed in section 2.7.

5.2 Results

5.2.1 Role of TRPA1 in the constrictor and dilator components of cold-induced vascular responses

Since the discovery of TRPA1 by Story *et al.* (2003), studies have shown that TRPA1 has a polymodal activation profile including activation by low temperatures (Story et al., 2003) and has an important role in vasorelaxant effects, as discussed in chapter 1. It is widely established that TRPA1 is expressed on sensory neurons, but there is now increasing evidence of TRPA1 being expressed on non-neuronal cells. The acute cold model employed in this study was shown to have both constrictor and dilator components and it remains unknown whether TRPA1 is involved in mediating one or both phase of this response. From our previous results it is clear that TRPA1 is the cold sensor at 10°C but in contrast to the established role of TRPA1 in mediating neurogenic-dependent vasodilatation, its role in mediating constriction in the peripheral vasculature requires investigation.

In this study, the constrictor phase of the cold (10°C)-induced vascular responses occurred immediately between 0 to 2 min following the cold treatment of the hindpaw, where this phase is termed net vasoconstriction (see Figure 4.1 in chapter 4). It may be possible that the vasoconstriction is initiated during the active cooling period, but this could not be measured in the current study. The observed constrictor phase was followed by a vasodilator phase recorded over 30 min, where the blood flow returns to baseline level, and this response is termed as net vasodilatation. Our results provide clear evidence that local cold treatment causes a significant decrease in blood flow when compared to the untreated-hindpaw in the net vasoconstriction phase ($p<0.001$, $n=12$, Figure 5.1A). Furthermore, there was a significant increase in the maximum change of blood flow in the cold-treated hindpaw when compared to the respective untreated hindpaw in the vasodilator phase in TRPA1 WT mice ($p<0.001$, $n=12$, Figure 5.1A). It is important to note that the magnitude of the initial cold-induced constriction response can influence the dilator response, to return blood flow back to baseline. Interestingly, there was a significant decrease in both the constriction ($p<0.05$) and vasodilator ($p<0.001$) phase in the TRPA1 KO mice ($n=9$, Figure 5.1A).

To further confirm the role of TRPA1 in this response, I investigated the effects of the TRPA1 antagonists HC030031, at a previous dose shown to selectively block TRPA1-mediated responses (McNamara et al., 2007). Similarly to the results observed in TRPA1 KO mice, pre-treatment with HC030031 produced a significant decrease in both phases of the cold-induced vascular response ($n=8$-10, Figure 5.1B). Interestingly, there was a residual significant response in the cold-treated hindpaw in the HC030031-control treated when compared to the respective

untreated hindpaw ($p<0.01$, $n=8$, Figure 5.1B). This correlates to our previous reported findings with the effects of HC030031 on cold-induced vascular responses in chapter 4.

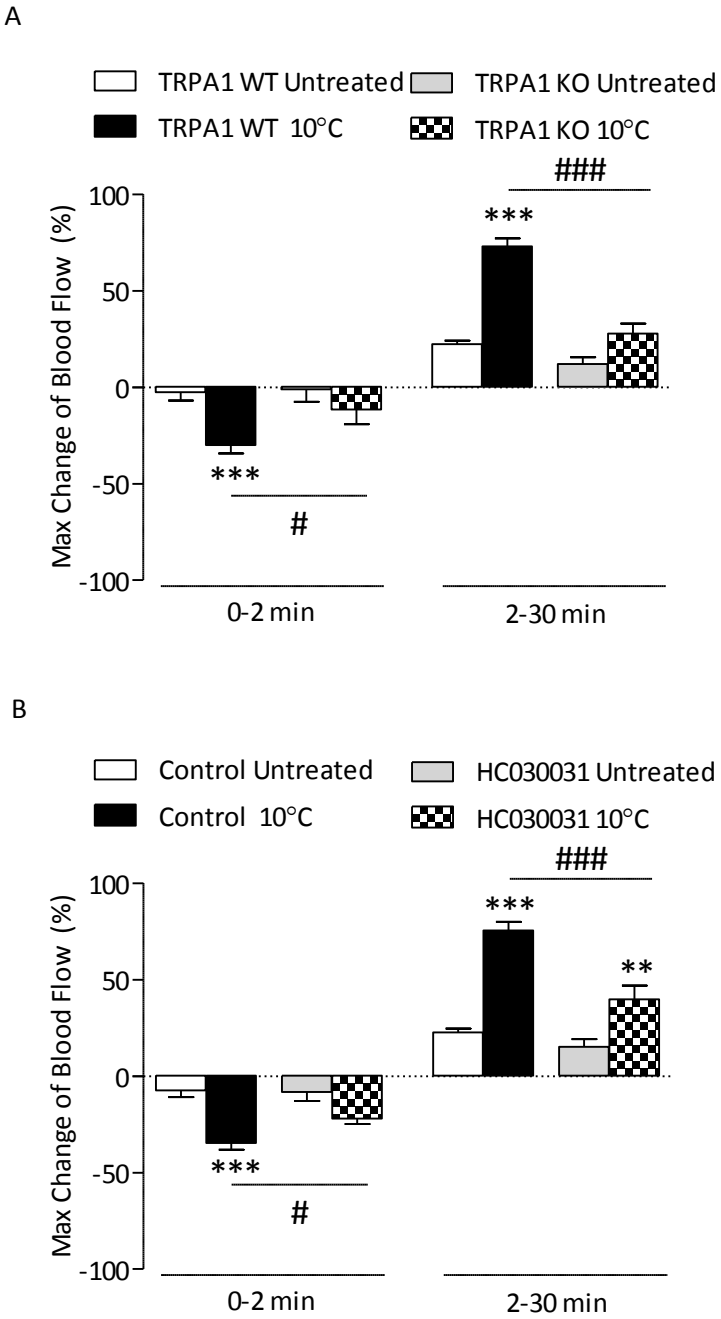

Figure 5.1 Evidence for the involvement of TRPA1 in the vasoconstrictor and vasodilator component of the cold-induced vascular response

Blood flow responses in mouse contralateral hindpaw following cold water (10°C) immersion and ipsilateral hindpaw remains untreated using FLPI. Blood flow ($\times 10^3$ flux units) recorded over 30 min following treatment and expressed as area under the curve (AUC). % maximum change in hindpaw blood flow from baseline to 0-2 min following cold treatment (net vasoconstriction) and from 2 min to 30 min following cold treatment (net vasodilatation) in **A**) TRPA1 WT and KO mice (n=9-12) and **B**) in CD1 WT mice pre-treated with the TRPA1 antagonist HC030031 (100mg/kg, *i.p.*, 30 min, n=10) or control (10% DMSO in saline, *i.p.*, 30 min, n=8). Results are shown as mean $\pm$ S.E.M. **p<0.01, ***p<0.001 compared to respective untreated, #p<0.05, ###p<0.001 compared to cold-treated hindpaw of mice using 2-way ANOVA followed by Bonferroni *post hoc* test.

5.2.2 *Role of CGRP in the constrictor and dilator components of cold-induced vascular responses*

It is well established that CGRP is a potent dilator in the microvasculature, and as illustrated in chapter 3 and 4, CGRP is involved in TRPA1-mediated vascular responses. CGRP-containing primary sensory neurons are known to play an important role in potent vasodilation. The control of the tone of the peripheral resistance vascular bed tone is mediated by both the sympathetic adrenergic nerves and CGRP-containing vasodilator nerves (Kawasaki et al., 1990, Takenaga and Kawasaki, 1999). In the cold (10°C)-induced response derived from the α-CGRP KO mice in this study, β-CGRP has been proposed to have an important role in influencing vascular tone. The role of α-CGRP in mediating vasodilatation has been widely studied since its discovery in 1985 and it has been reported that both α-CGRP and β-CGRP have equipotent properties. However, the role of β-CGRP in the peripheral vasculature is less known. As both isoforms of CGRP bind to the CGRP receptor to exert their effects, I investigated the role of CGRP in our cold model using the CGRP receptor antagonist BIBN4096BS. Importantly from our previous findings, I demonstrated that pre-treatment with BIBN4096BS did not alter baseline blood in the periphery.

Following pre-treatment with BIBN4096BS, as expected I observed that there was no significant change in the constrictor component of the cold-induced vascular response, when compared to control ($p>0.0$, n=9-10, Figure 5.25). However, there was a significant decrease in the vasodilator phase when compared to control treated group ($p<0.01$, n=9-10, Figure 5.2). As the vasodilator response was not completely abolished to the same extent seen in TRPA1 KO mice (Figure 5.1A), it is worth highlighting that other mediators are possibly involved.

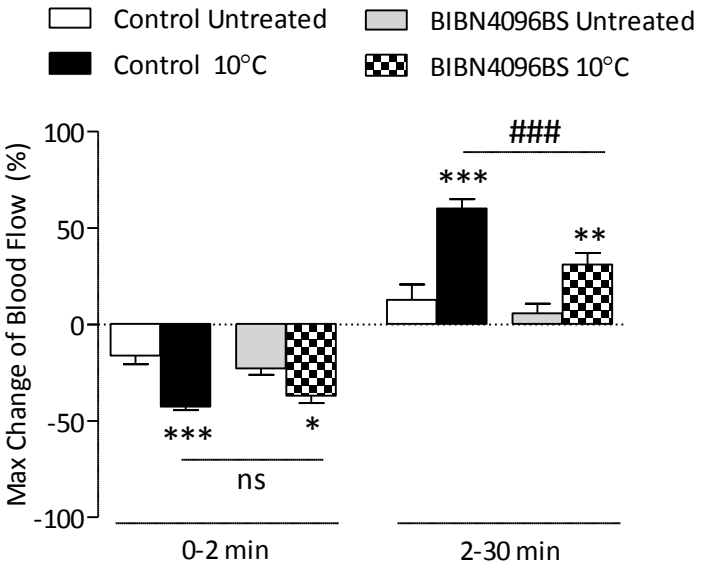

Figure 5.2 Evidence for the involvement of CGRP in the vasodilator component of the cold-induced vascular response

Blood flow responses in mouse contralateral hindpaw following cold water (10°C) immersion and ipsilateral hindpaw remains untreated using FLPI. Blood flow ($\times 10^3$ flux units) recorded over 30 min following treatment and expressed as % maximum change in hindpaw blood flow from baseline to 0-2 min following cold treatment (net vasoconstriction) and from 2 min to 30 min following cold treatment (net vasodilatation) in **A**) CD1 WT mice pre-treated with CGRP receptor antagonist BIBN40946S (0.3mg/kg, *i.v.*, 5 min, n=9) or respective control (saline, *i.v.*, 5 min, n=10). Results are shown as mean $\pm$ S.E.M. *p<0.05, **p<0.01, ***p<0.001 compared to respective untreated, ###p<0.001 compared to cold-treated hindpaw of mice using 2-way ANOVA followed by Bonferroni *post hoc* test.

5.2.3 Role of sympathetic nervous system in cold-induced vascular responses

It is well documented that the sympathetic nervous system plays an important role in the vasoconstrictor phase of the hunting response of cold reaction (Shepherd and Thompson, 1953) and there is an increased sensitivity of the vascular smooth muscle cells to adrenergic transmitter(s), in particular noradrenaline which participates in neurally-mediated vasoconstriction (Janssens and Vanhoutte, 1978, Rusch et al., 1981). There is clear evidence from our study, that the cold-induced vascular response initiates with an intense vasoconstriction, which is shown to be dependent on TRPA1 but not CGRP. It remains unknown whether this is dependent on the sympathetic nerve activity in the cutaneous vasculature.

I investigated the effects of local cold treatment on noradrenaline release in TRPA1 WT and KO mice. Interestingly, our results showed that 2 min after cold water immersion (peak vasoconstriction), there was a trend towards a decrease in noradrenaline levels when compared to untreated-hindpaw tissue in TRPA1 WT mice (n=7, Figure 5.3). However, there was no change observed in the TRPA1 KO mice (n=6), suggesting that noradrenaline release is dependent on TRPA1 activation in this model. Furthermore, at 30 min following cold treatment, which represents the vasodilator phase of the cold-induced vascular response, no change in the levels of noradrenaline in the cold-treated tissues were detected when compared to untreated tissues, in either TRPA1 WT or KO mice (n=3, Figure 5.3). It remains unknown whether there are any significant changes in noradrenaline levels at earlier time points of cold-water immersion, which represents the constrictor phase.

I further investigated the influence of the sympathetic nerve and adrenergic receptors in the cold-induced vascular response using pharmacological inhibitors for sympathetic nerve and adrenergic receptors. I did not find any significant change in cold-induced vascular responses in the WT mice pre-treated with the sympathetic nerve blocker guanethidine when compared to control ($p>0.05$, n=7-12, Figure 5.4B). Interestingly, pre-treatment with non-selective α-adrenergic receptors blocker phentolamine was shown to have no significant effect on the cold-induced vascular response when compared to control ($p>0.05$, n=8-9, Figure 5.4A). Interestingly, I found that pre-treatment with the α_2-adrenergic receptor blocker yohimbine was shown to cause a significant decrease in the overall cold-induced vascular responses when compared to control-treated group ($p<0.05$, n=5, Figure 5.4C). I further investigated the role of α_2-adrenergic receptors in each phase of the cold-induced vascular responses and I found that yohimbine caused a significant decrease in the maximum change in blood flow during the net vasoconstriction phase ($p<0.05$) and net vasodilator phase ($p<0.001$) (n=5, Figure 5.4D). It is also worth highlighting that there was no significant difference between the untreated- and cold-

treated hindpaw in the net vasoconstriction phase (0-2 min post treatment) in the yohimbine-treated mice (n=5, Figure 5.4D).

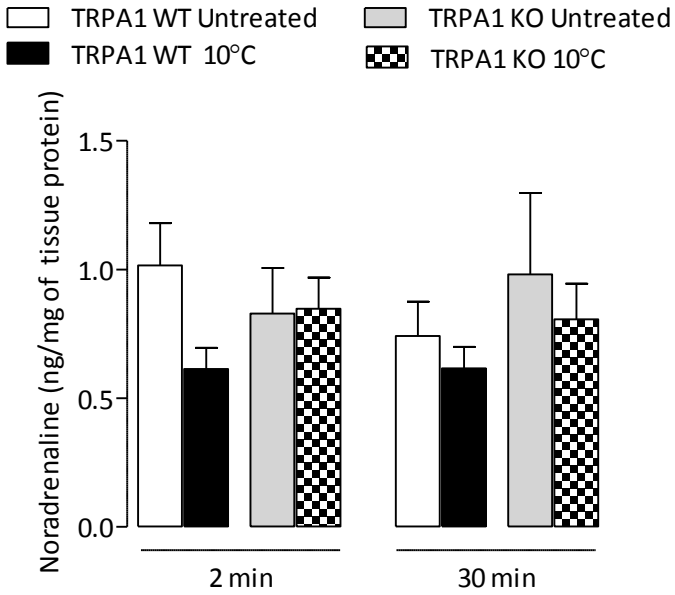

Figure 5.3 Effects of cold treatment on noradrenaline generation in TRPA1 WT and KO mice

The ipsilateral hindpaw was immersed in cold water (10°C) for 5 min, whilst the contralateral hindpaw was left untreated in anaesthetised mice. Hindpaw tissue homogenates were collected at 2 min or 30 min following cold water immersion from TRPA1 WT and KO mice. Noradrenaline concentrations as quantified by ELISA and values are expressed as noradrenaline concentration (ng) per mg of tissue protein (n=3-7). Data was analysed using 2-way ANOVA followed by Bonferroni *post hoc* test.

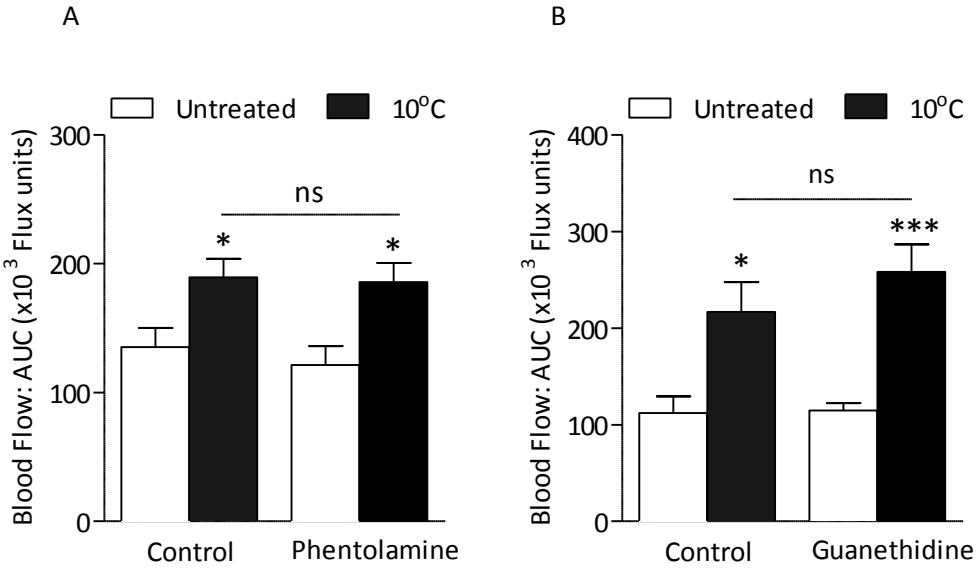
A
B
Untreated
10°C
Blood Flow: AUC (x10 3 Flux units)
300
200
100
0
ns
*
*
Control
Phentolamine
400
300
200
100
0
ns
*
***
Control
Guanethidine

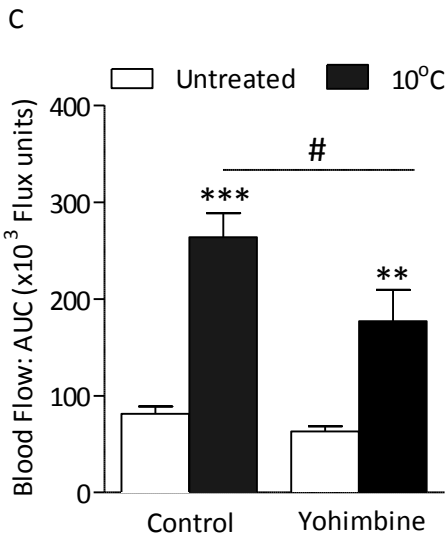
C
Untreated
10°C
Blood Flow: AUC (x10 3 Flux units)
400
300
200
100
0
#
***
**
Control
Yohimbine

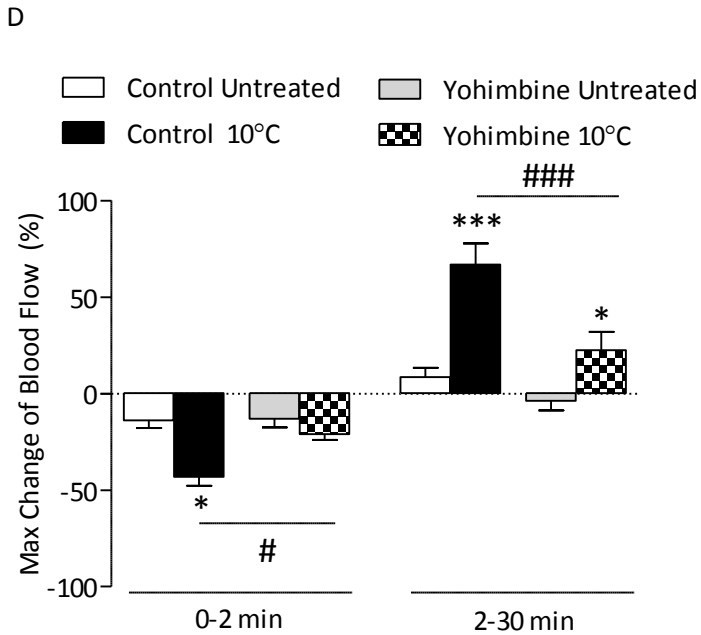
D
Control Untreated
Control 10°C
Yohimbine Untreated
Yohimbine 10°C
Max Change of Blood Flow (%)
100
50
0
-50
-100
###
***
*
*
#
0-2 min
2-30 min

Figure 5.4 The role of sympathetic nerves in the vasoconstrictor and vasodilator component of the cold-induced vascular response

Blood flow responses in mouse contralateral hindpaw following cold water (10°C) immersion and ipsilateral hindpaw remains untreated using FLPI. Blood flow ($\times 10^3$ flux units) recorded over 30 min following treatment and expressed as area under the curve (AUC). Cold-induced vascular responses in the hindpaw of CD1 mice pre-treated with **A**) non-selective α-adrenergic receptor antagonist phentolamine (5mg/kg, *i.p.*, 30min, n=8) or control (saline, *i.p.*, 30min, n=9), **B**) sympathetic nerve blocker guanethidine (30mg/kg, *s.c.*, 60 min, n=12) or control (saline, *s.c.*, 60 min, n=7) and **C**) α_2-adrenergic receptor antagonist yohimbine (10mg/kg, *s.c.*, 30 min, n=5) or control (saline, *s.c.*, 30 min, n=5). **D**) % Maximum change in hindpaw blood flow from baseline to 0-2 min following cold treatment (net vasoconstriction) and from 2 min to 30 min following cold treatment (net vasodilatation) in CD1 WT mice pre-treated with the α_2-adrenergic receptor antagonist yohimbine (10mg/kg, *s.c.*, 30 min, n=5) or control (saline, *s.c.*, 30 min, n=5). Results are shown as mean $\pm$ S.E.M. *p<0.05, **p<0.01, ***p<0.001 compared to respective untreated, #p<0.05, ###p<0.001 compared to cold-treated hindpaw of mice using 2-way ANOVA followed by Bonferroni *post hoc* test. 'ns' represents no significance.

5.2.4 Role of α_{2c}-adrenergic receptors in cold-induced vascular responses

The previous results illustrate clearly that α_2-adrenergic receptors play an important role in the cold-induced vascular response in both the constrictor and dilator phase. The α_2-adrenergic receptor is a presynaptic receptor which acts as a negative feedback mechanism for noradrenaline-induced responses and furthermore, it is also located on vascular smooth muscle cells. There are three different subtypes of α_2-adrenergic receptors; α_{2A}-, α_{2B}- and α_{2C}-adrenergic receptors. As previously mentioned in chapter 1, α_{2C}-adrenergic receptors are implicated in cold-induced vasoconstriction (Bailey et al., 2005) and hence, I investigated the potential role of this receptor in the cold-induced vascular response in our study. Pre-treatment with the selective α_{2C}-adrenergic receptor antagonist JP1302 caused a significant decrease in the overall cold-induced vascular response when compared to control ($p<0.05$, n=5, Figure 5.5A). Additionally, detailed analysis of the net vasoconstriction and net vasodilatation revealed that there was a significant decrease in the maximum change in blood flow at 0-2 min following treatment from baseline ($p<0.05$) and at 30 min following treatment from 2 min ($p<0.01$, n=6, Figure 5.5B). Whilst there was no significant difference between the untreated- and cold-treated hindpaws in the net vasoconstriction of the yohimbine-treated groups, I found a significant difference in the JP1302 -treated groups. The pharmacological blockade of α_{2c}-adrenergic receptors is able to suppress both the constrictor and dilator component of the cold-induced vascular response.

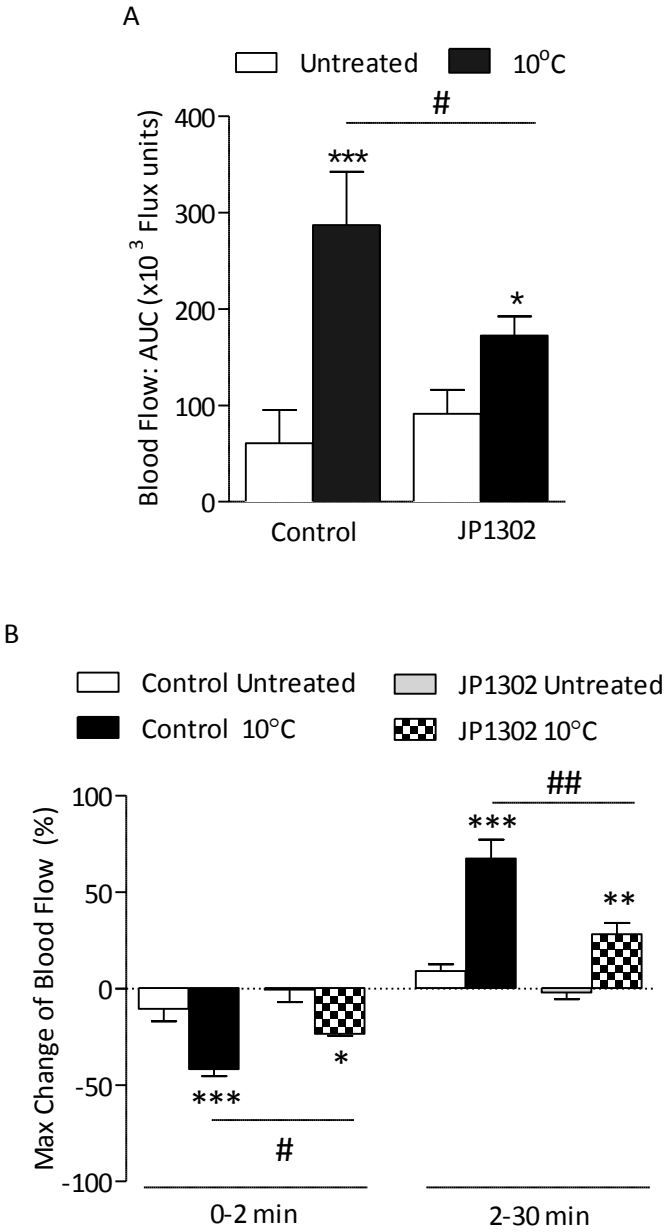

Figure 5.5 The role of α_{2c}-adrenceptor in the vasoconstrictor and vasodilator component component of the cold-induced vascular response

Blood flow responses in mouse contralateral hindpaw following cold water (10°C) immersion and ipsilateral hindpaw remains untreated using FLPI. Blood flow ($\times 10^3$ flux units) recorded over 30 min following treatment WT CD1 mice mice were pre-treated with selective α-adrenergic receptor antagonist JP1302 (3µg/kg, *s.c.*, 60 min, n=6) or control (saline, *s.c.*, 60 min, n=6). Blood flow data are expressed as **A**) area under the curve (AUC) and **B**) % maximum change in hindpaw blood flow from baseline to 0-2 min following cold treatment (net vasoconstriction) and from 2 min to 30 min following cold treatment (net vasodilatation). *p<0.05, **p<0.01, ***p<0.001 compared to respective untreated, #p<0.05, ##p<0.01 compared to cold-treated hindpaw of mice using 2-way ANOVA followed by Bonferroni *post hoc* test.

5.2.5 Role of superoxide in cold-induced vascular responses

This study thus far has provided clear evidence that TRPA1 and adrenergic receptors play an important role in mediating cold-induced vascular responses, where both are involved in the constrictor component. I further showed that α_{2c}-adrenergic receptors can mediate the constrictor component of the response. As previously discusssed in chapter 1, α_{2c}-adrenergic receptors are known to be silent at 37°C but in response to moderate cooling, the activity of α_{2c}-adrenergic receptors increases due to increased production of reactive oxygen species such as superoxide (Bailey et al., 2005). In chapter 4, I showed that pre-treatment with the highly potent, cell-permeable SOD mimic tempol reduced the local cold-induced vascular responses over the 30 min, as determined by AUC (Figure 4.8). In the current chapter, I will closely examine the role of superoxide in both the constrictor and dilator component of the cold-induced vascular response.

Interestingly, pre-treatment with tempol was able to significantly decrease the net vasoconstriction ($p<0.05$) and net vasodilatation ($p<0.001$) of the cold-induced vascular response when compared to control-treated groups (n=5-6, Figure 5.6). I further confirm this finding by investigating the generation of superoxide in TRPA1 WT and KO mice using lucigenin chemiluminescence assay at 2 min following cold treatment, which represents the peak vasoconstriction phase of the cold-induced vascular response. Interestingly, I found that there was a trend towards increased superoxide generation in the cold-treated hindpaw when compared to the respective untreated hindpaw tissue samples in the TRPA1 WT mice, but this difference did not reach significance (n=4-5, Figure 5.6B). Furthermore, there was no significant difference between the cold-treated and untreated hindpaw tissue samples in TRPA1 KO mice (n=4-5, Figure 5.6B). As shown in chapter 4, superoxide levels were not different at 30 min following cold treatment which confirms that our model may not be invasive and that the exposed hindpaw recovered fully at 30 min.

To further elucidate the role of TRPA1 in mediating the generation of superoxide at the net vasoconstriction phase following the local cold treatment, I used WT mice pre-treated with the selective TRPA1 antagonist HC030031. In this study, I observed that there was a significant increase in superoxide levels in the cold (10°C)-treated hindpaws from vehicle-treated mice compared to the respective untreated hindpaw at the net vasoconstriction phase or naive hindpaw tissue sample ($p<0.01$, n=3-5, Figure 5.6C). However, there was a significant decrease in superoxide levels in the cold (10°C)-treated hindpaws in the HC030031-treated group when compared to the control treated group ($p<0.05$, n=3-4, Figure 5.6C). INo significant change was observedbetween superoxide levels between the cold (10°C)-treated and untreated hindpaw

tissue samples in the HC030031-treated groups (Figure 5.6C) and the levels measured are similar to the naïve hindpaw tissue sample.

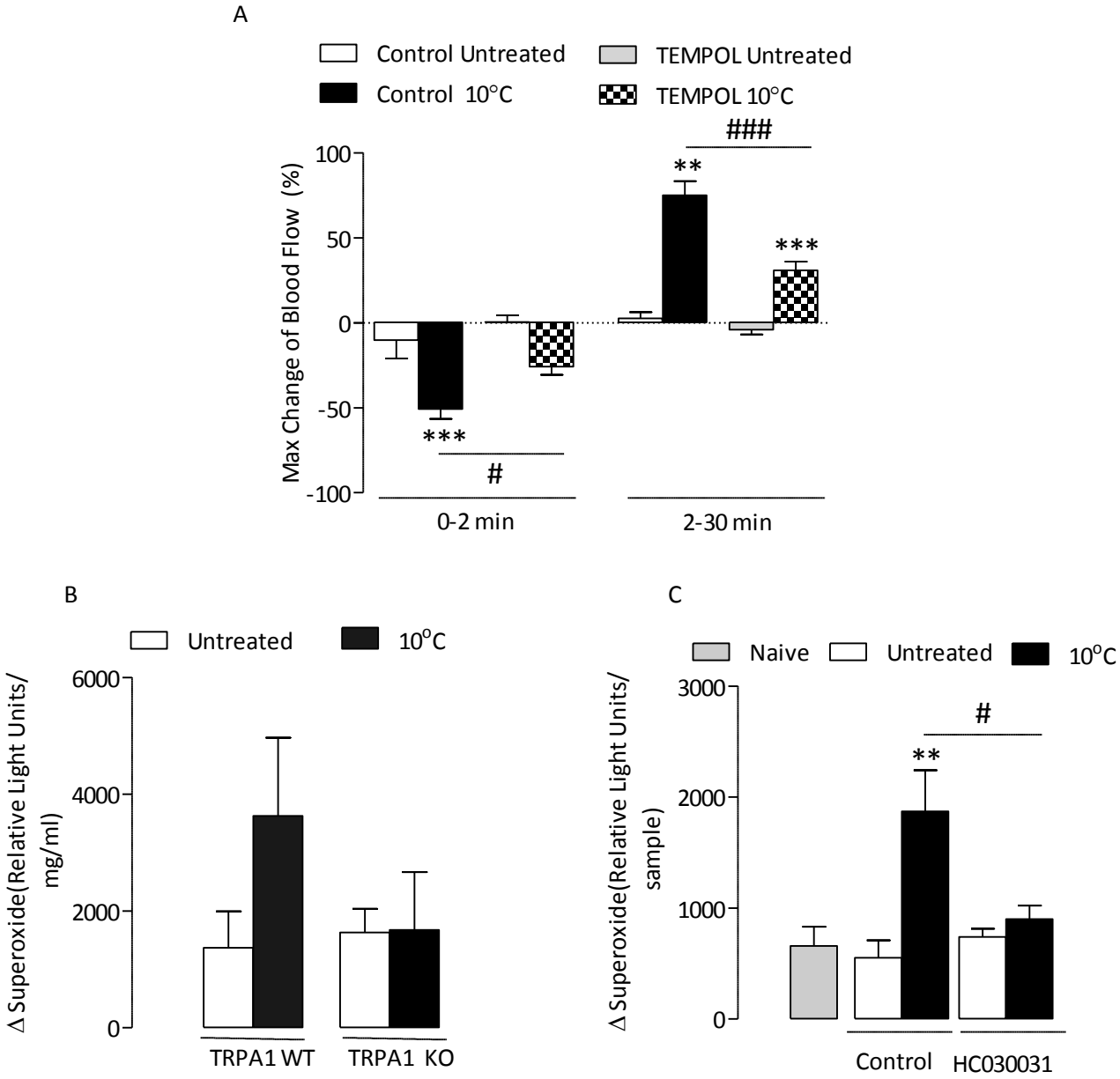

Figure 5.6 The role of superoxide in the vasoconstrictor and vasodilator component of the cold-induced vascular response

Cold-induced vascular responses in mouse contralateral hindpaw following cold water (10°C) immersion and ipsilateral hindpaw remain untreated. **A**) Blood flow ($\times 10^3$ flux units) recorded over 30 min following treatment using FLPI and expressed as % maximum change in hindpaw blood flow from baseline to 0-2 min following cold treatment (net vasoconstriction) and from 2 min to 30 min following cold treatment (net vasodilatation) in WT CD1 mice pre-treated with SOD mimic tempol (30mg/kg) or respective control (saline, *i.v.*, n=4). At 2 min following cold-treatment, hindpaw tissues were collected and superoxide levels were measured in the samples by lucigenin chemiluminescence assay and expressed as **B**) relative light units per mg of tissue homogenate in TRPA1 WT and KO mice (n=4-5) and **C**) relative light units per sample in naive WT mice (n=5) and WT mice pre-treated with TRPA1 antagonist HC030031 (100mg/kg, *i.p.*, 30 min) or control (10% DMSO in saline, *i.p.*, 30 min) (n=3-5). Results are shown as mean ± S.E.M. **p<0.01, ***p<0.001 compared to respective untreated, #p<0.05, ###p<0.001 compared to cold-treated hindpaw of mice using 2-way ANOVA followed by Bonferroni *post hoc* test.

5.2.6 Role of Rho-associated protein kinase in cold-induced vascular responses

This study has currently provided clear evidence that TRPA1 and sympathetic nerves play an important role in mediating the cold-induced vascular responses, with a greater involvement in the constrictor component. I further showed that α_{2c}-adrenergic receptors can mediate the constrictor component of the response and interestingly, smooth muscle cell contraction via adrenergic receptors has been reported to be highly dependent on Rho-associated kinase (Rho-kinase/ROCK) activity (Mori-Kawabe et al., 2009). The role of Rho-kinase was further investigated in the cold-induced vascular response by using the highly potent, cell-permeable and selective Rho-kinase inhibitor Y27632. Interestingly, I showed that pre-treatment with Y27632 was able to cause a significant decrease in the overall cold-induced vascular response when compared to control-treated groups ($p<0.01$, n=5-6, Figure 5.7A). It is worth noting that there was a small but significant increase in the cold-induced blood flow responses over the 30 min recording period in the cold-treated hindpaw compared to untreated hindpaw of the Y27632-treated group ($p<0.05$, n=6, Figure 5.7A). Furthermore, detailed analysis of the profile characteristics of Rho-kinase in our local cold-induced vascular responses illustrated that pre-treatment with Y27632 was able to completely abolish both the net vasoconstriction and net vasodilatation of the cold-induced vascular response when compared to control-treated group ($p<0.01$, n=5-6, Figure 5.7B).

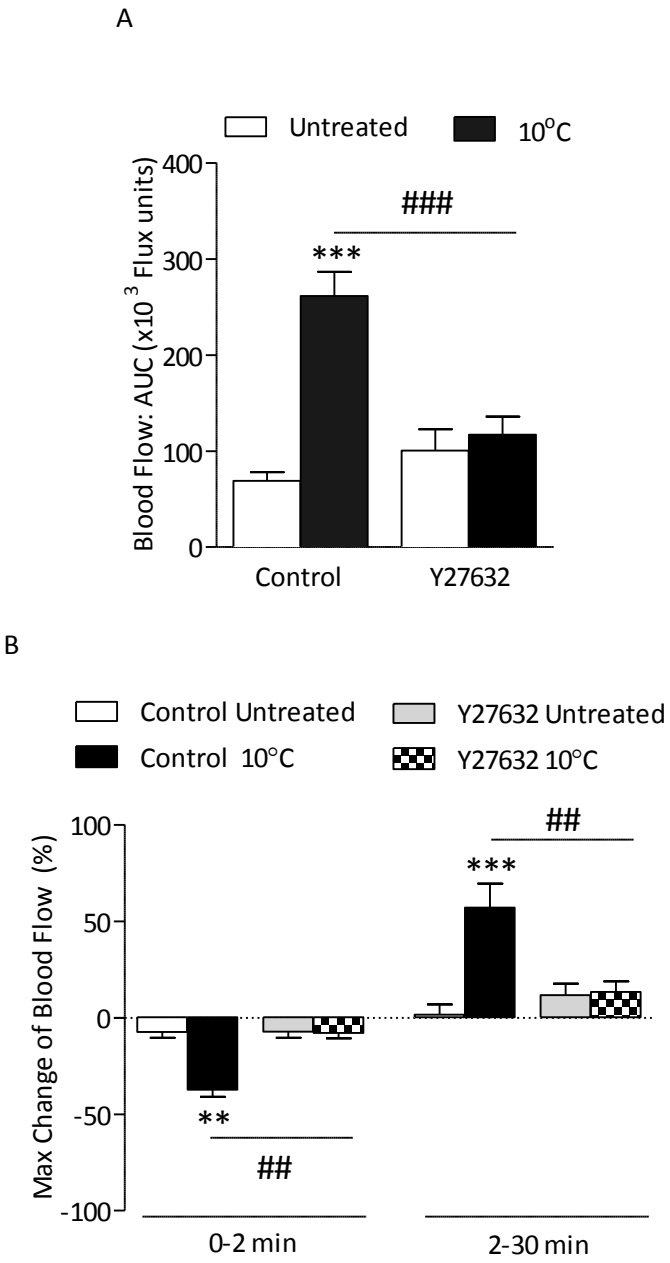

Figure 5.7 The role of Rho-associated protein kinase in the vasoconstrictor and vasodilator component of the cold-induced vascular response

Blood flow responses in mouse contralateral hindpaw following cold water (10°C) immersion and ipsilateral hindpaw remains untreated using FLPI. Blood flow ($\times 10^3$ flux units) recorded over 30 min following treatment WT CD1 mice were pre-treated with the selective Rho-associated protein kinase (ROCK) inhibitor Y27632 (5mg/kg, *i.p.*, 30 min, n=6) or vehicle (saline, *i.p.*, 30 min, n=5). Blood flow data are expressed as **A**) area under the curve (AUC) and **B**) % maximum change in hindpaw blood flow from baseline to 0-2 min following cold treatment (net vasoconstriction) and from 2 min to 30 min following cold treatment (net vasodilatation). *p<0.05, **p<0.01, ***p<0.001 compared to respective untreated; #p<0.05, ##p<0.01 compared to cold-treated hindpaw of mice using 2-way ANOVA followed by Bonferroni *post hoc* test.

5.2.7 Role of myosin light chain in cold-induced vascular responses

I have demonstrated clearly that α_{2C}-adrenergic receptors and Rho-kinase play an important role in mediating the constrictor component of the cold-induced vasoconstriction in the previous studies. The mechanism by which Rho-kinase results in vasoconstriction is due to the inhibition of myosin light chain phosphatase (MLCP), which causes an increase in the phosphorylation of MLC, leading to an increase in contraction of the vascular smooth muscle cell (Riento and Ridley, 2003, Somlyo and Somlyo, 2003). In smooth muscle, MLC is phosphorylated at threonine 18 (Thr18) and serine (Ser19) by MLC kinase in a calcium/calmodulin-dependent manner, increasing myosin ATPase activity and hence, contraction of smooth muscle (Ikebe and Hartshorne, 1985, Tan et al., 1992). Interestingly, Rho-kinase has been reported to phosphorylate Ser19 of MLC in smooth muscle *in vitro* (Totsukawa et al., 2000). I investigated whether the Rho-kinase mediated MLC activation signalling pathway was involved in our cold study by studying the phosphorylation of MLC protein at Ser19 in hindpaw tissue samples collected from untreated and cold-treated hindpaws at the net vasoconstriction phase which is 2 min following cold treatment.

Our results showed that there was an increase in phosphorylation of MLC in cold-treated when compared to untreated-hindpaw tissue samples (Figure 5.8A) and furthermore, a significant increase is noted in the ratio of phosphorylated MLC against total MLC ($p<0.001$, $n=3$, Figure 5.8B). This cold-induced increase in phosphorylated-MLC was only observed in WT mice but not TRPA1 KO mice and it is worth highlighting that this increase was inhibited in TRPA1 KO mice ($p<0.01$, $n=3$, Figure 5.8B). There was no significant difference observed in the ratio of phosphorylated MLC against total MLC protein expression between untreated- and cold-treated TRPA1 KO mice.

A

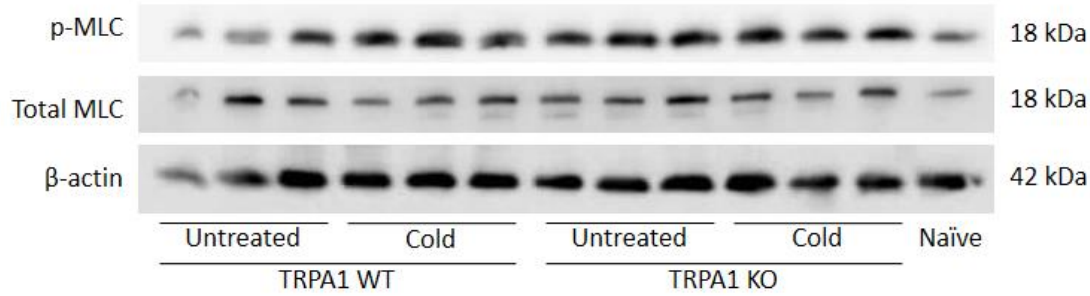

B

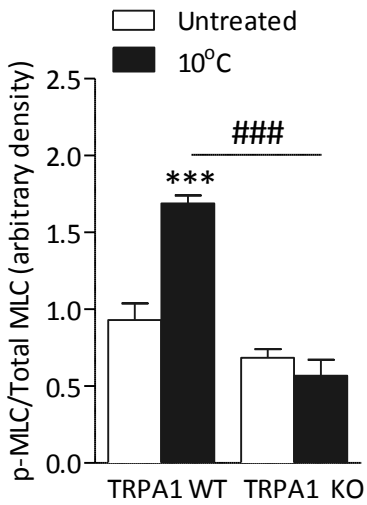

Figure 5.8 Effects of cold treatment on phosphorylated Ser19 of Myosin Light Chain 2 (p-MLC) in hindpaw tissues of TRPA1 WT and KO mice.

Cold-induced vascular responses in mouse contralateral hindpaw following cold water (10°C) immersion and ipsilateral hindpaw remain untreated. At 2 min following cold-treatment, hindpaw tissue samples were collected and, p-MLC at Ser19 of MLC and total MLC protein expression were **A)** determined by immunoblotting and **B)** analysed by densitometry relative to the loading control β-actin. Data denotes mean ± S.E.M, n=3. ***$p<0.001$ compared to respective untreated, ###$p<0.001$ compared to cold-treated hindpaw of mice using 2-way ANOVA followed by Bonferroni *post hoc* test.

5.3 Discussion

This chapter characterised the cold-induced vascular response by determining the profile of TRPA1 and the humoral mediators within the constrictor and dilator components of the response in mice. In order to quantify these responses separately, parameters were derived from the blood-flow response curve recording over the 30 min time period following local cold-treatment in the hindpaw. The peak decrease in blood flow responses occurs immediately, at the period corresponding to 0 to 2 min following cold-treatment and the maximum change in blood flow at this time point from baseline is referred to as the net vasoconstriction. Furthermore, over the 30 min period the blood flow returns to baseline, with a peak increase at 30 min and the maximum change in blood flow at this time point from 2 min following cold treatment represents the net vasodilatation. The major findings from the present section using these two parameters are that the initial vasoconstrictor component of the cold-induced vascular response is dependent on TRPA1 and α_{2C}-adrenergic receptor stimulation potentially via a Rho-kinase mediated MLC phosphorylation in the mouse hindpaw, whilst the dilator component is greatly dependent on the release of CGRP.

5.3.1 Role of TRPA1 in the constrictor and dilator components of cold-induced vascular responses

In the previous chapters, I demonstrated clearly that TRPA1 has a key role in mediating the cinnamaldehyde- and cold-induced vascular responses in the peripheral vasculature *in vivo*. These results highlight that TRPA1 is involved in mediating a vasodilator response, however the cold-induced vascular response is driven by an initial constrictor component. I have observed that the magnitude of the constrictor component influences the extent of the vasodilator response. Since the discovery of TRPA1 by Story *et al.* (2003), most studies have shown the important role of this channel in mediating vasorelaxant effects (Bodkin and Brain, 2011, Story et al., 2003). TRPA1 is widely expressed on sensory neurons and I showed that TRPA1-mediated vasodilatation is dependent on neuropeptide release. There is now increasing evidence showing expression of TRPA1 in non-neuronal cells (Fernandes et al., 2012) and it was recently demonstrated that TRPA1 is expressed in the rat proximal and distal colon smooth muscle layers using qRT-PCR (Dong et al., 2010). Interestingly, mustard oil was demonstrated to induce a dose-dependent increase in contractions in the isolated mouse intestine in a TRPA1-dependent manner (Penuelas et al., 2007) and in the guinea pig ileum via the release of serotonin downstream of TRPA1 activation (Nozawa et al., 2009). Dong *et al.* (2010) further showed that cold stimuli (from 37°C to 12°C) induced colonic smooth muscle contractions in a TRPA1-dependent manner and PLC/IP_3/Ca^{2+} pathway (Aarons et al., 2004, Dong et al., 2010).

In our study, the pharmacological blockade or genetic deletion of TRPA1 gene was shown to decrease the constrictor component of the cold-induced vascular response. Given that the magnitude of the initial vasoconstriction phase correlates with the vasodilator component of the blood flow responses following local cutaneous cold treatment, our results clearly showed that in WT mice pre-treated with the TRPA1 antagonist HC030031 or in TRPA1 KO mice, the net vasodilatation is significantly decreased when compared to control-treated groups or in TRPA1 WT mice. This observation suggests that there is a cross-talk between the two mechanisms mediating the two responses which control the cutaneous vasculature tone. Indeed, this finding is similar with previous studies investigating local heating by Hodges *et al.* (2008) where the inhibition of the vasoconstrictor response completely abolished the vasodilatation and they suggested that this is due to a noradrenaline-induced nitric oxide production by eNOS (Hodges et al., 2009, Cocks and Angus, 1983)

Our primary finding in this study implies that TRPA1 receptors are present in the peripheral vasculature, are selectively activated by cold (10°C), which further leads to a constrictor response possibly via an interaction and/or involvement of the sympathetic nerve or smooth muscle cell *in vivo*. At present, our knowledge in this study does not provide enough evidence to confirm whether functional TRPA1 is expressed on the sensory neuron, sympathetic nerve or in smooth muscle cells the vasculature of the hindpaw.

Cooling (20°C)-induced contractions of the smooth muscle cells of the rat fundus was previously shown to be mediated by TRPM8 and involved activation of the Rho-kinase signalling mechanisms (Mustafa and Oriowo, 2005). The evidences illustrating the mechanisms underlying cooling-induced contraction responses have been derived from studies conducted with non-vascular smooth muscle cells. The inhibition of the initial vasoconstriction response following low to moderate cooling is thought to potentially rely on (1) blockade of transmitter release from vasoconstrictor nerves, (2) antagonism of adrenergic receptors, (3) blockade of sensory nerves (Johnson et al., 2005, Pergola et al., 1993, Yamazaki et al., 2006) or antagonism of TRPA1. Hence, this highlights the importance for a better understanding of this pathway to understand how TRPA1 mediates its vascular effects in our model.

Furthermore, it is well established that there is a link between the Rho-kinase signalling system and the sympathetic nervous system, and therefore I investigated the role of the sympathetic nervous system in our local cold model to understand the role of TRPA1 in mediating a constriction response (section 5.3.3).

5.3.2 Role of CGRP in the dilator component of cold-induced vascular responses

As there was a significant decrease in the vasodilator component in the cold-induced vascular response in TRPA1 KO mice, and WT mice treated with TRPA1 antagonist HC030031 when compared to control, our finding suggests that TRPA1 activation is involved in mediating this response. It has been shown that stimulation of TRPA1 by methylglyoxal in the sciatic nerve, vagus nerve and paw skin can induce the release of CGRP via a TRPA1-dependent manner (Eberhardt et al., 2012). CGRP has been shown in chapter 3 and 4 to have a role in our cinnamaldehyde- and cold-induced vascular responses in the periphery *in vivo*. CGRP is known to be a potent dilator in the microvasculature and indeed, interestingly, our results in this chapter strongly support this finding. I show that pre-treatment with the CGRP receptor antagonist BIBN4096BS causes no significant difference in the net vasoconstriction response compared to control-treated groups while the vasodilatation component was significantly inhibited. The results suggest that CGRP is not involved in mediating the constrictor response.

However, there was a significant decrease in the dilator component of the cold-induced vascular response and this finding highlights the important role of CGRP in mediating the vasodilatation or the return of blood flow to baseline, which is important to protect against local cold-induced vasoconstriction. It is important to note that there was a residual effect in the vasodilator response following the pharmacological blockade of CGRP receptors. Hence, this result further implies that the other vasodilator mediators such as nitric oxide may have a role in mediating the vasodilator component, as shown in chapter 4.

Indeed, it was previously shown that endogenous CGRP when released from peptidergic nerves innervating the rat mesenteric vascular bed could suppress sympathetic adrenergic nerve function and hence regulate the tone of resistance blood vessels by overriding the sympathetic vasoconstriction (Takenaga and Kawasaki, 1999). Moreover, activation of β_2-adrenergic receptors in dental pulp has been shown to reduce exocytosis of neuropeptides from capsaicin-sensitive nociceptors (Bowles et al., 2003). This suggests that there is a possible interaction between the sympathetic nervous system and sensory nerves involving CGRP-induced vasodilatation, which controls vascular blood flow following local cold treatment. Indeed, sensory and sympathetic nerves are known to have a close overlapping distribution pattern around blood vessels in the periphery and a reciprocal trophic influence was observed following the denervation of either the sensory peptide- or catecholamine-containing sympathetic nerves (Terenghi et al., 1986).

5.3.3 *Effects of local cold treatment on sympathetic noradrenaline release in the vasoconstrictor and dilator component of cold-induced vascular responses*

The plantar, which is the glabrous surface of the hindpaw is known to be innervated by the sciatic nerve which consists of sensory, motor and autonomic nerve fibres (Greene, 2001). It has been previously reported that sympathetic denervation can reduce TRPV1-induced neurogenic responses in the vasculature (Xu et al., 2010). Local cooling has been reported to initiate a reflex increase in sympathetic output and vasoconstriction mediated by noradrenaline in the cutaneous vasculature (Vanhouette, 1980). The cutaneous sympathetic neurons are important for regulating skin blood flow to conserve heat in a cold environment (Hales et al., 1978). It has been previously hypothesised that the cold-induced vasoconstriction may be due to an increased sensitivity of the vascular smooth muscle cells to noradrenaline (Janssens and Vanhoutte, 1978, Rusch et al., 1981, Gardner and Webb, 1986). I investigated the role of the sympathetic nerve in the constrictor and dilator component of the cold-induced vascular response by measuring the concentrations of noradrenaline in the hindpaw skin tissue samples collected at 2 min or 30 min following cold-treatment in mice.

Moderate cooling of the skin (25°C) has been shown to release ATP, which stimulates purinoceptors on the sympathetic nerve terminals to facilitate the release of noradrenaline (Koganezawa et al., 2006). Our results showed that at the time representing the net vasoconstriction of the cold-induced vascular response, there was a trend towards a decrease in noradrenaline concentrations in the cold-treated hindpaw skin compared to untreated hindpaw skin tissue samples in the WT mice ($p<0.05$, $n=7$, Figure 5.3). Intriguingly, this finding was against our hypothesis where an increase in noradrenaline concentrations was expected in cold-treated hindpaws during the net vasoconstriction phase (2 min post cold water immersion). However, this result correlates with earlier findings from Vanhouette and Verbeurren (1976), who showed that cooling (from 37°C to 28°C) induced a decrease in tension with a decrease in ^{3}H-noradrenaline and metabolites in the cutaneous vein of dog (Vanhoutte and Verbeuren, 1976). There is also evidence from studies of Nakamoto (1990), where plasma noradrenaline concentrations decreased immediately following the immersion of the hand in 5°C water for 10 min (Nakamoto, 1990). Nevertheless, they demonstrated that during the treatment period, there was a peak increase in plasma noradrenaline concentrations compared to baseline levels in healthy subjects (Nakamoto, 1990).

In our current model, it may be possible that the noradrenaline concentrations peak during the cold water immersion and this further initiates the transient rapid decrease in blood flow responses immediately following treatment. Noradrenaline is known to have a very short half-life of 2 min and approximately 80-90% of the released noradrenaline undergoes re-uptake

through the neuronal noradrenaline transporter (Esler et al., 1990) where it is repackaged into vesicles via monoamine transporter-2 or degraded by monoaminooxidase into its various metabolites (Schroeder and Jordan, 2012). Once released from the presynaptic terminals, its roles include activating adrenergic receptors on effector cells and stimulating presynaptic α_{2A}-adrenergic receptor and α_{2C}-adrenergic receptor to further inhibit neurotransmitter release (Langer, 1974, Starke, 1987, Brede et al., 2003, Hein et al., 1999). As the blood flow returns to baseline from 2 min following treatment, it may be possible that at this phase there is a decrease in noradrenaline concentrations which correlate with our findings. A decrease in noradrenaline release from the nerves will lead to less noradrenaline available at the local site and this possibility awaits direct assessment of noradrenaline or its various metabolites concentrations at different time intervals. In our current model, the reduction in noradrenaline levels following local cold treatment may result as a compensatory mechanism to protects against prolonged vasoconstriction.

Nonetheless, I further investigated if the cold-induced decrease in noradrenaline release at 2 min following cold treatment is TRPA1 dependent. Interestingly, I showed that there was no significant change between untreated- and cold-treated hindpaw skin tissues in the TRPA1 KO mice, and this correlates well with our current *in vivo* results illustrating the lack of cold-induced vasoconstriction in the TRPA1 KO mice. Our results thus suggest that these changes in noradrenaline concentrations following cold treatment are dependent on TRPA1 and require more investigation.

I also provided evidence that there was no change in noradrenaline concentrations at 30 min following cold treatment in untreated- and cold- treated hindpaw tissues of TRPA1 WT and KO mice. Indeed, at 20 min or 40 min following immersion of the legs into 12°C water up the knee, there was no change in plasma levels of catecholamines (Jansky et al., 2006). Hence, I conclude that at 30 min following cold-treatment, as the blood flow returns to baseline and there is no change in noradrenaline concentrations. Hence, the normal vascular tone is restored.

It is important to note that our results do not provide any evidenceon the effects of local cold treatment on plasma noradrenaline and furthermore, sympathetic outflow is known to be regionalised and variable as circulating noradrenaline varies in specific vascular beds (Goldstein et al., 1983). It is worth studying the speed and pattern of cold-induced noradrenaline release in both plasma and hindpaw skin tissue sample at baseline and at different time intervals during and after the cold treatment to understand the role of noradrenaline in the cold-induced vascular response. These finding will hence provide key information when there is a peak in noradrenaline concentrations in local cold-treatment in the cutaneous vasculature and further delineate the role of noradrenaline and TRPA1 in local cold-induced vascular responses.

5.3.4 Role of sympathetic nerves in the vasoconstrictor and dilator component of cold-induced vascular responses

Following from our findings with noradrenaline levels in the local cold model, I further investigated whether the pharmacological inhibition of the sympathetic nervous system will have an effect on the constrictor and dilator component of the cold-induced vascular response. Guanethidine is known to exert its sympathetic blockade by directly acting on noradrenaline transporter protein (NET) on the sympathetic nerve terminals to occupy the intracellular vesicle and depletes noradrenaline (Dixit et al., 1961). Using guanethidine, I showed that there was no significant change in the overall cold-induced vascular responses in the cold-treated hindpaw in the control-treated and guanethidine-treated group. However, guanethidine given at 10mg/kg (*i.v.*) was shown to decrease plantar skin blood flow responses when the left foot was cooled from 25°C to 10°C (Koganezawa et al., 2006). It is also known that presynaptic blockade of sympathetic nerves with bretylium can reverse local cooling-induced vasoconstriction in the cutaneous vasculature (Pergola et al., 1993). Nevertheless, our finding is in agreement with previous reported evidence from Honda *et al.* (2007) who demonstrated that cooling the air temperature around the left paw from 25°C to 10°C induced a reduction of skin blood flow that was not inhibited following the administration of guanethidine or bretylium (Honda et al., 2007). Both drugs are known to inhibit the release of noradrenaline from the sympathetic nerve via depleting the nerves of noradrenaline.

Pharmacological sympathetic denervation with guanethidine (30mg/kg, *s.c.*) for 4 consecutive days has been shown to deplete the sympathetic nerve completely and diminish both the heat and cold sensitisation in rats with peripheral neuropathy (Neil et al., 1991). When sympathetic nerves are chemically sympathectomised with guanethidine, there is a significant increase in saphenous nerve-induced vasodilation (Kerezoudis et al., 1993a, Kerezoudis et al., 1993b). In our studies, it is possible that the lack of effect observed following guanethidine administration, using a dose characterised in rodents (Neil et al., 1991; Kerezoudis et al., 1993), was due to lack of sufficient depletion of noradrenaline in the sympathetic nerve. Furthermore, surgical denervation of sympathetic nerves has also been documented to require 7-10 days post-surgery (Zou et al., 2002; Lin et al., 2003) as confirmed anatomically with the fluorescent glyoxilic acid method (Furness & Costa, 1975). It would be interesting to investigate the effects of chronic guanethidine administration, and to anatomically confirm sufficient noradrenaline depletion in future studies.

If the sympathetic nerves have a role in the cold-induced vascular response, this will involve the stimulation of adrenergic receptors. The non-selective α_1- and α_2-adrenergic receptors antagonist phentolamine was used in this study and our results showed clearly that there was no

significant decrease in cold-induced blood flow responses between phentolamine-treated and control-treated hindpaws. Interestingly, previous studies have shown that cooling-induced constriction was completely blocked with phentolamine in rat cremaster skeletal muscle (Faber, 1988). There is also *in vivo* evidence showing that pre-treatment with phentolamine at the same dose (5mg/kg) can decrease plantar skin blood flow following local cooling treatment in rats (Koganezawa et al., 2006). It is worth highlighting that the pharmacological blockade of postsynaptic α_1-adrenergic receptors may still lead to spontaneous release of other vasoconstrictor transmitters such as ATP and neuropeptide Y (Lundberg, 1996) and hence, this may potentially explain the lack of inhibitory effects with phentolamine in our study.

Our results thus far are not clear on the precise role of noradrenaline or sympathetic nerve in the cold-induced vascular responses. Superficial cutaneous vessels exhibit increased responsiveness during cooling (Gardner and Webb, 1986, Janssens et al., 1981) and there is increasing evidence in the literature documenting the role of α-adrenergic receptors in cold-induced responses. Stimulation ofα-adrenergic receptors by noradrenaline predominantly results in vasoconstriction which is known to be mediated by α_1- and α_2-adrenergic receptors in the peripheral vessels (Timmermans and van Zwieten, 1982). Ekenvall *et al.* (1988) previously showed that cold (20°C)-induced vasoconstriction in human finger skin was abolished after the pre-treatment with α_2-adrenergic receptor antagonist rauwolscine (Ekenvall et al., 1988). An increase in post-junctional α_2-adrenergic receptor mediated vasoconstriction has been reported following local tissue cooling (Aarons et al., 2004, Faber, 1988, Flavahan et al., 1985) as it is known to have an increased affinity for noradrenaline. To further investigate the role of α_2-adrenergic receptors in the cold-induced vascular responses in this study, I investigated the effects of the α_2-adrenergic receptors antagonist yohimbine at a dose previously shown to be selective for α_2-adrenergic receptors (van Oene et al., 1984). In agreement with previous published findings, our results also showed that the administration of yohimbine caused a significant decrease in the total cold (10°C)-induced vascular response when compared to control-treated groups. I also demonstrated that the constrictor component of the cold-induced vascular response was abolished following pre-treatment with yohimbine, with a significant decrease in the vasodilator component. Indeed, the inhibition of noradrenergic constriction with yohimbine induced a transient dilation in terminal arterioles of rat cremaster skeletal muscle in cooling (26°C) studies (Faber, 1988) and abolished local-cooling induced vasoconstriction in finger blood flow in normal subjects (Cooke and Marshall, 2005). Altogether, our results are consistent with previous findings and highlight an important role of α_2-adrenergic receptors in regulating adrenergic regulation of the cold-induced vascular responses.

Our results thus far provide clear evidence that cold treatment causes constriction in the cutaneous blood vessels of the hindpaws by increasing reactivity of α_2-adrenergic receptors on

vascular smooth muscle. It is important to note that α_2-adrenergic receptors are not widely distributed in the entire vascular system but are localised in small veins and arteries (Faber, 1988). It is well established that there are different subtypes of α_2-adrenergic receptors and there are previous *in vitro* findings which demonstrated that cold-treatment can amplify α_{2C}-adrenergic receptors in isolated mouse tail arteries (Chotani et al., 2000). I investigated the role of α_{2C}-adrenergic receptors in our local cold model using JP1302, which has previously been shown to be a selective α_{2C}-adrenergic receptors antagonist *in vivo* and *in vitro* (Sallinen et al., 2007). Our results showed that the pharmacological antagonism of α_{2C}-adrenergic receptors with JP1302 caused a significant decrease in total cold-induced vascular responses. Interestingly, detailed analysis of this response also provides clear evidence that there was a significant decrease in both the constrictor and dilator component of the cold-induced blood flow responses. In agreement with previous published findings, I provide evidence of the possible activation of α_{2C}-adrenergic receptors in the vasculature in the hindpaw following cold (10°C) treatment *in vivo*.

In HEK293 cells expressing α_{2C}-adrenergic receptors, it was shown that α_{2C}-adrenergic receptors are normally silent, localised predominantly in the Golgi compartment and non-functional at ambient temperature (37°C). After cooling at 28°C, α_{2C}-adrenergic receptors were distributed to the plasma membrane and allows the normal function of α_{2C}-adrenergic receptors which has been speculated to be involved in thermoregulating the cutaneous circulation (Jeyaraj et al., 2001). The mechanisms underlying this translocation of α_{2C}-adrenergic receptors remain unknown, however it has been suggested that reactive oxygen species and Rho kinase may both play an important role (Bailey et al., 2004).

Moreover, tissue hypoxia during vasoconstriction may lead to an increase in mitochondrial reactive oxygen species (Turrens, 2003) which acts as a positive feedback to further potentiate the sympathetic α_2-adrenergic receptors signalling mechanism. Based on our previous evidence in chapter 4 that superoxide was shown to play a role in the cold-induced responses, I used the SOD mimic tempol to investigate the involvement of superoxide on the constrictor and dilator component of the cold-induced vascular responses. Our results showed that there was a significant decrease in both components following administration of tempol when compared to control groups. Our results indicate clearly that as tempol reduces the accumulation of reactive oxygen species by increasing the conversion of superoxide to water and oxygen in addition to radical scavengers in the vasculature, this reduced sympathetic-induced vasoconstriction in local cooling. Our current finding also suggests that cold-induced vasoconstriction may involve the generation of superoxide.

To confirm this finding, I measured the levels of superoxide in cold-treated and untreated-hindpaw tissue samples at 2 min following cold treatment, which represents the net vasoconstriction phase of the cold-induced vascular response. Our results showed that cold (10°C) treatment induces an increase in superoxide generation in comparison to untreated hindpaws in a TRPA1 dependent manner as shown in WT mice pre-treated with the TRPA1 antagonist HC030031 did not demonstrate an increase in superoxide levels. A similar trend was observed in TRPA1 KO mice, although this difference did not reach significance, which may be due to the small sample size. Our results here are consistent with those of Bailey *et al.* (2005), where the cell-permeable mimic of SOD myosin phosphatase targeting subunit 1 (MnTMPyP) was demonstrated to abolish the cold-induced increase in constrictor activity in isolated tail artery (Bailey et al., 2005). This response has been proposed to be mediated by α_{2C}-adrenergic receptors stimulation.

In summary, these results suggest that the constrictor component of the cold-induced vascular response contributes to superoxide generation, possibly in smooth muscle cells. It was previously suggested that an increase in reactive oxygen species activity can result in an increase in RhoA activity, further leading to translocation and stimulation of α_{2C}-adrenergic receptors which results in cold-induced vasoconstriction (Bailey et al., 2005). I provide novel evidence that these changes in superoxide generation are dependent on TRPA1 and the key questions which remained to be answered are (1) whether the superoxide is being produced downstream of TRPA1 activation by the cold stimulus and (2) if RhoA plays a role in our model.

5.3.5 Role of Rho associated protein kinase in the vasoconstrictor and dilator component of cold-induced vascular responses

Superoxide has been suggested to induce vasoconstriction through Rho-kinase/ROCK mediated pathways (Jin et al., 2004). The mediator Rho-kinase is known to regulate vascular smooth muscle calcium sensitivity and tone. It can also be stimulated by noradrenaline or mitochondrial superoxide generated in response to localised cooling; this further results in the translocation of α_{2C}-adrenergic receptors (Bailey et al., 2005, Somlyo and Somlyo, 2000).

I provide novel evidence for a potential role of TRPA1-dependent increase in superoxide generation following cold treatment during the net vasoconstriction phase as discussed previously. To investigate whether Rho-kinase mediated pathways play a role in the cold-induced vascular responses, I pre-treated mice with the selective cell permeable Rho-kinase inhibitor Y27632. Y27632 has been previously shown to have no effects on the modulation of α_2-adrenergic receptors *in vitro* in control experiments (37°C) (Bailey et al., 2004) and

interestingly, as expected I did not observe any change in the untreated-hindpaw blood flow responses in our study. Pre-treatment with Y27632 was demonstrated to cause a significant decrease in overall cold-induced vascular responses when compared to control pre-treated groups.

Further detailed analysis of the cold-induced vascular responses showed that pre-treatment with Y27632 completely abolished both the net constrictor and net vasodilator response following cold treatment. Indeed, a similar effect was observed with administration of Y27632 in studies looking at local cooling (28°C)-induced constriction in addition to α_2-adrenergic receptors stimulation in mouse tail arteries using pressure myography (Bailey et al., 2004). Bailey and colleagues showed that moderate cooling causes a time-dependent activation of RhoA in cultured cutaneous human vascular smooth muscle cells (Bailey et al., 2004). Interestingly, there is also *in vivo* evidence, which show that cooling (24°C)-induced cutaneous vasoconstriction is significantly reduced in human forearms following administration with another Rho-kinase inhibitor Fasudil (Thompson-Torgerson et al., 2007). Hence, our results support all these findings and provide new evidence demonstrating that cold-induced vasoconstriction at a lower temperature (10°C) is dependent on the generation of superoxide following activation of TRPA1, which further leads to activation of Rho-kinase and translocation of α_{2C}-adrenergic receptors to the cell surface membrane for activation in the mouse hindpaws.

5.3.6 Role of MLC in the vasoconstrictor component of cold-induced vascular responses

Rho-kinase is known to be widely expressed in the body and it has been shown to modulate smooth muscle contraction in both a calcium-dependent manner where ion channels are possibly involved and a calcium-independent manner which involves depletion of intracellular calcium stores or an increase in MLC activity (Somlyo and Somlyo, 2003). Rho-kinase has been reported to directly phosphorylate MYPT1, which also inhibits the activity of the phosphatases. This in turn, increases phosphorylation of MLC and maintains vascular contraction (Somlyo and Somlyo, 2003). Intriguingly, Aburto *et al.* (1993) used spiral strips of the rabbit saphenous vein to shown that stimulation of high density of postsynaptic α_2-adrenergic receptors using a selective α_2-agonist, UK14304 leads to an increase in vascular tone which was dependent on an increase in intracellular calcium and phosphorylation of MLC (Aburto et al., 1993). Since there is a profound initial decrease in blood flow responses following the cold-treatment, as indicated by an increase in net vasoconstriction in our local cold model in the cutaneous vasculature, I hypothesised that there would be an increase in MLC phosphorylation at this time point.

Our results clearly show that there was an increase in phosphorylated MLC protein during the net vasoconstriction period in the cold-treated hindpaws in the net vasoconstriction when compared to untreated hindpaws in WT mice. This result reveals that the localised cooling (10°C)-induced vasoconstriction is therefore mediated by the phosphorylation of MLC in the mouse hindpaw. I further showed that the increase in MLC phosphorylation following the cold-treatment relies on the presence of functional TRPA1 channels, as no change was observed in the TRPA1 KO mice. Cumulatively, these data provide novel mechanism of how Rho-kinase mediated phosphorylation of MLC results in vasoconstriction in the hindpaw following cold treatment, which is dependent on the activation of TRPA1 channels in the mouse hindpaw.

5.4 Conclusion

The results from the present chapter provide a new insight into the mechanisms underlying cold-induced vascular responses, which was first discovered by Sir Thomas Lewis (1930). I thought that it was important to determine the distinct role of TRPA1 and the humoral mediators in mediating vasoactive response at different phases of the cold-induced blood flow responses in the mouse hindpaw. Using genetically modified mice and pharmacological inhibitors, I provide novel evidence demonstrating clearly that activation of TRPA1 on the sensory neurons drives the cold-induced vascular responses at 10°C. I confirmed the traditional proposed hypotheses that sympathetic nerves, post-junctional α_2-adrenergic receptors and reactive oxygen species are major contributors to cold-induced vasoconstriction. I further provide novel evidence demonstrating clearly that local cold exposure in the mouse hindpaw causes an increase in intracellular superoxide production, in a TRPA1-dependent manner, which activate the Rho-kinase/ROCK-mediated pathways and possibly mediates translocation of α_{2C}-adrenergic receptors from the Golgi to the surface membrane to increase cold-induced α_{2C}-adrenergic activity. Our results introduce the concept that cold-induced vasoconstriction increases the phosphorylation of MLC in a TRPA1-dependent manner in the mouse hindpaw. This current mechanism underlying the constrictor component of cold-induced vasoconstriction may be important in understanding the pathophysiology underlying Raynaud's phenomenon where there is a prolonged increase in vasoconstriction following local cold exposure in digit areas of the fingers and toes of patients. Following the initial phase of vasoconstriction, our results demonstrated CGRP-induced vasodilatation downstream of TRPA1 activation is essential to protect against local cold-induced injury. The proposed mechanisms identified in this chapter are illustrated in Figure 5.9. To the best of our knowledge, I are the first to demonstrate the role of TRPA1 as a vascular cold sensor and provided evidence that both phases of the local cold-induced vascular responses are dependent on TRPA1.

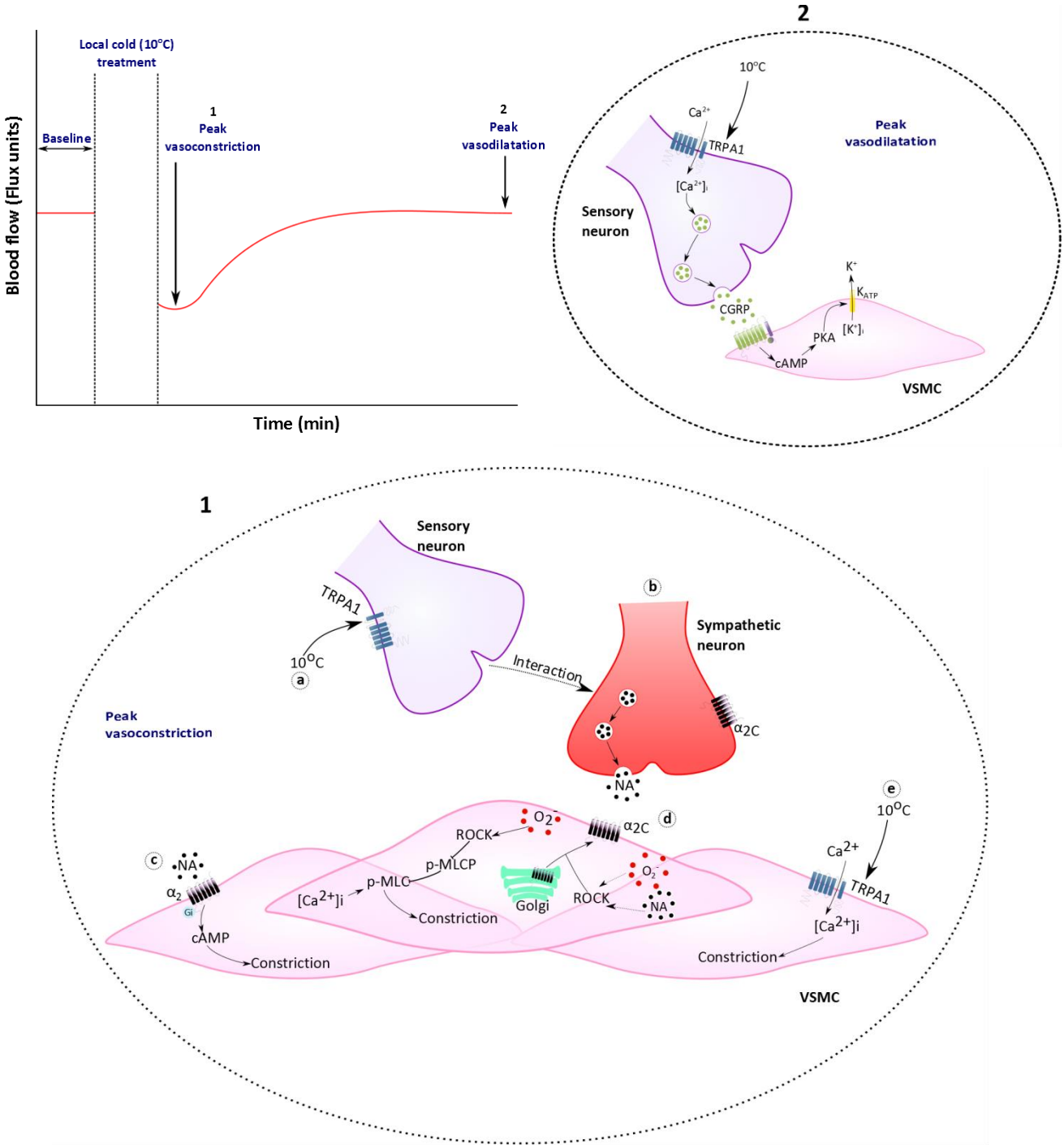

Figure 5.9 Schematic diagram of the proposed TRPA1-dependent activation mechanism following local cold exposure Local cold (10°C) exposure causes a transient and rapid decrease in blood flow (1), followed by a vasodilatation phase to bring blood flow back to baseline (2). The initial phase of cold-induced vasoconstriction consists of (a) activation of TRPA1 expressed on sensory neurons, which may further lead to the (b) activation of sympathetic neurons and mediate the release of (c) noradrenaline. Local cooling can also produce a hypoxic condition with (d) increased reactive oxygen species such as superoxide generation, which in turns induce the translocation of α_{2C}-adrenergic receptors from the Golgi to the surface membrane and increase adrenergic activity in the VSMC. Superoxide can also activate the ROCK-mediated pathways and increase constriction via phosphotylated MLC-induced increase in $[Ca^{2+}]_i$. (e) Local cooling may also directly activate TRPA1 on VSMC to mediate vasoconstriction. The prolonged vasodilator component of the cold-induced vascular response is mediated by the release of CGRP downstream of TRPA1 activation of sensory neuron, which returns blood flow to baseline. Abbreviations: cAMP, cyclic adenosine monophosphate; p-MLC; phosphorylated myosin light chain; MLC-P, myosin light chain phosphatase; NA, noradrenaline; ROCK, Rho-kinase; TRPA1, transient receptor potential ankyrin-1; superoxide, $O_{2;}$ VSMC, vascular smooth muscle cell.

Chapter 6 – General Discussion

Chapter 6 – General Discussion

6.1 Summary of results

This study investigated the mechanisms underlying TRPA1-mediated vascular responses *in vivo* using the exogenous agonist cinnamaldehyde in the mouse ear model and a cold (10°C) stimuli in the mouse hindpaw. Our results provided novel evidence showing that topical administration of cinnamaldehyde activates TRPA1 and causes vasodilatation which is mediated by the release of the microvascular vasodilator CGRP, but not the tachykinin neuropeptide substance P. nNOS derived-nitric oxide was also shown to be involved in this response. Additionally, I demonstrated clearly that cinnamaldehyde-induced vasodilatation involves the participation of reactive oxygen species.

This TRPA1-mediated pathway was further investigated in a cold model as TRPA1 has been reported to act as a cold sensor at low temperature (<17°C). An acute cold model was developed and characterised in the peripheral vasculature using the mouse hindpaw. Initial studies showed that following cold (10°C) water immersion for a 5 min period, there was an initial rapid and transient decrease in blood flow, followed by a vasodilatation phase where blood flow returns to baseline level to protect against the detrimental cold-induced vasocontriction. This cold-induced vascular response was shown to be primarily mediated by TRPA1 and this is the first study to illustrate that TRPA1 acts as a vascular cold sensor. The cold-sensitive TRPM8 channel was shown to be partially involved in the cold-induced vascular response. Furthermore, I provided clear evidence that CGRP is not involved in the initial local-cold induced vasoconstriction but has an essential role in mediating the vasodilator response, which is important in protecting against local cold-induced injury by returning the blood flow to basal levels.

Cold-induced vasoconstriction in our model was shown to be dependent on the (1) activation of Rho-kinase which increases phosphorylated MLC activity and (2) translocation of α_{2C}-adrenergic receptors, possibly mediated by increase in superoxide generation in this phase. Local cold-induced increase in superoxide generation and phosphorylated MLC in the vasoconstriction phase was shown to be dependent on TRPA1 activation.

Thus, this study demonstrates an essential role for TRPA1 in mediating cold-induced vasoconstriction as well as subsequent dilatation and rewarming in the mouse peripheral vasculature. Hence, the delineation of these underlying mechanisms provides a new perspective into the understanding of a well-established protective mechanism for localcold-induced injury.

6.2 Mechanisms involved in TRPA1-mediated vasodilatation using cinnamaldehyde

Perivascular sensory neurons are known to play a key role in vascular homeostasis, and hence it was necessary to understand the signalling pathways involved in sensory nerve activation. TRPA1 is known to be expressed on a large proportion of TRPV1-expressing sensory nerves, where its activation causes peripheral vasodilatation (Graepel et al., 2011, Fernandes et al., 2011). The primary focus of this study is characterising the downstream mechanisms underlying TRPA1-mediated vascular responses.

6.2.1 Cinnamaldehyde activates TRPA1 and mediates neurogenic-dependent vasodilatation

It was previously demonstrated in our group that cinnamaldehyde-mediated responses in the mouse hindpaw *in vivo* and in isolated mouse mesenteric arteries *in vitro* were dependent on TRPA1 (Pozsgai et al., 2010). This thesis has further contributed to our understanding on the mechanisms involved in TRPA1-mediated vasodilatation using the mouse ear model. Our results clearly demonstrated that cinnamaldehyde-induced vasodilatation was dependent on the activation of TRPA1, but not TRPV1 or TRPM8 channels. Collectively, these results demonstrate that cinnamaldehyde can influence blood flow in the peripheral vasculature mediated via TRPA1. Hence, this finding reflects the ability of cinnamaldehyde to influence blood flow in the peripheral vasculature solely via TRPA1.

The microcirculation of the mouse ear is innervated by trigeminal sensory neurons, expressing TRPA1 (Huang et al., 2012). This thesis provided clear evidence that cinnamaldehyde involves a neurogenic-dependent vasodilatation, as (1) α-CGRP and β-CGRP mRNA expression increased following cinnamaldehyde treatment, (2) cinnamaldehyde-induced vasodilatation was significantly reduced in α-CGRP KO mice, and in WT mice pre-treated with CGRP receptor antagonist and (3) cinnamaldehyde-induced vasodilatation was significantly reduced following the pharmacological blockade of K_{ATP} channels through glibenclamide, a known downstream target of CGRP. It is evident from our study that the sensory neurons play a major role downstream of TRPA1 activation to elicit neurogenic-dependent vasodilatation and future studies examining the effects of sensory nerve denervation can confirm this finding.

Nevertheless, I cannot exclude the potential role of cinnamaldehyde to directly influence the vasculature independent of sensory nerve mechanisms, for example by activating non-neuronal TRPA1 on keratinocytes (Atoyan et al., 2009) which also expresses β-CGRP (Hou et al., 2011). This concept warrants further investigation as the characteristic profiles of both non-neuronal TRPA1 and CGRP are at an early stage of research. Indeed, the application of cinnamaldehyde on keratinocytes have been shown to increase intracellular calcium level (Tsutsumi et al., 2010). Furthermore, keratinocytes can directly communicate with sensory neurons by possibly

activating TRPA1 via neuromodulators or keratinocyte-derived mediators, as shown in itch conditions (Wilson et al., 2013). I proposed that understanding the interaction between the keratinocytes and sensory neuron following TRPA1 activation using co-culturing techniques, would assist in understanding the pathophysiology of inflammatory skin conditions such as psoriasis and itch.

6.2.2 Cinnamaldehyde-induced vasodilatation is dependent on nitric oxide

Interestingly, this project also showed that cinnamaldehyde-induced vasodilatation is dependent on nNOS-derived nitric oxide, without any major role for eNOS or iNOS as shown in studies using selective NOS inhibitors. Our emerging data here further confirms previous findings that nNOS plays an important role in local regulation of vasculature tone and provides clear and novel *in vivo* evidence that nNOS-derived nitric oxide participates in TRPA1-induced vasodilatation. However, the question that arises is whether nNOS-derived nitric oxide is released together with CGRP from the sensory neuron following activation of TRPA1 or by other non-neuronal cell types such as smooth muscle and endothelial cells where physiologically active nNOS was shown to be expressed.

I conclude that CGRP and nNOS-derived nitric oxide participate in cinnamaldehyde-induced vasodilatation, downstream of TRPA1 activation in our model and thus, I propose that this mechanism may be potentially involved in the pathophysiology of headaches which are associated with endogenous NO metabolism. In migraine sufferers, increased CGRP release (Kunkler et al., 2011) and positive nNOS expression (Ramachandran et al., 2010) is located in tissue surrounding the trigeminal nerve associated with this pathology, where both contribute to the enhanced vasodilatation. Indeed, environmental irritants have been shown to activate TRPA1 and trigger neuronal excitation and subsequent neurogenic inflammation, contributing to migraine attacks (Kunkler et al., 2011, Edelmayer et al., 2012). I show a novel mechanism here linking TRPA1 activation with both the release of CGRP and nNOS-derived nitric oxide in the vasculature and this evidence adds to accumulating scientific evidence showing the role of TRPA1 in mediating neurogenic-dependent vascular responses. Ultimately, TRPA1 may be a potential new target in migraine pathophysiology.

6.2.3 Cinnamaldehyde-induced vasodilatation is dependent on reactive oxygen species

The previous discovery that neuropeptide-induced vasodilatation is dependent on reactive oxygen species generation (Starr et al., 2008) led us to investigate its role in cinnamaldehyde-induced vasodilatation. Our studies illustrated clearly that cinnamaldehyde-induced vasodilatation is dependent on the generation of superoxide and hydroxyl radicals, as shown in studies using the membrane-permeable SOD mimic tempol and the iron chelator deferoxamine,

respectively. However, the source of superoxide generation remains currently unknown in our model, although I propose that NOX2-containing NADPH oxidase and not NOX4 may be involved. The mitochondria may also be involved in generating superoxide following cinnamaldehyde application and further investigations are required to validate these hypotheses.

There was no involvement of H_2O_2, but an increase in the peroxynitrite marker nitrotyrosine in cinnamaldehyde-induced vasodilatation was observed possibly due to an interaction between superoxide and nNOS-derived nitric oxide. Interestingly, I have recently shown that TRPA1 activation by leukotriene-B_4 (LTB_4) can contribute to superoxide production in an itch model (Fernandes et al., 2013) and hence, providing further providing further evidence that reactive oxygen species are generated downstream of TRPA1 activation.

This emerging novel data suggests that the activation of TRPA1 by cinnamaldehyde results in an increase of intracellular calcium concentrations at nerve terminals which stimulates the release of CGRP into the periphery and mediates neurogenic-dependent vasodilatation. Additionally, TRPA1 is known as a major oxidant sensor (Andersson et al., 2008, Bessac et al., 2008) and our study further delineates that reactive oxygen species are involved downstream of TRPA1 activation in this proposed sensory stimulation by cinnamaldehyde. Thus, I propose that reactive oxygen species may be generated (1) downstream of CGRP signalling contributing to the vascular changes or (2) in the sensory nerve terminals or keratinocytes (Turner et al., 1998) via an increase in intracellular calcium downstream of TRPA1 activation. Another possible mechanisms may be that (3) cinnamaldehyde can initially induce reactive oxygen species signalling by interacting with the mitochondria (Wu et al., 2004), which in turn activates TRPA1 on the sensory nerve and mediates neurogenic-dependent vasodilatation. Our proposed mechanism of reactive oxygen species-modulated TRPA1 signalling may be relevant in understanding the pathophysiology underlying ischemia/reperfusion-induced injury, vascular permeability and itch sensation which are associated with an increase in oxidative stress. Furthermore, non-neuronal TRPA1 has been recently shown to be present within the rat cerebral vascular endothelium, localised to myoendothelial junctions and its activation using 4-HNE and NADPH produces TRPA1-mediated vasodilatation. This has led to the generation of endothelial cell-specific TRPA1 KO mice to directly test the effects of TRPA1 loss in cerebrovascular diseases associated with endothelial dysfunction such as stroke (Earley, 2013). It would be interesting to investigate the role of TRPA1 expressed on endothelial cells in mediating cinnamaldehyde-induced vasodilatation.

6.3 Mechanisms involved in cold-induced vascular responses

6.3.1 Characterising a cold model in the vasculature

Physiological human studies have described cold pain perception at low temperatures (<15°C) (Morin and Bushnell, 1998). A novel model of acute local cold-induced vascular responses was developed in our group by Dr Graepel (Graepel, 2009)and was used in this study to be able to investigate the potential role of TRPA1 (1) as a vascular cold (10°C) sensor *in vivo* and (2) to mediate vascular responses similar to cinnamaldehyde following activation with a cold stimulus. The newly developed cold model in this thesis allows quantifiable measurement of cold-induced vascular responses in anaesthetised mouse following local cold exposure.

Local cold (10°C) exposure for 5 min was shown to initially result in vasoconstriction followed by a vasodilatation phase where the blood flow returns to baseline. Collectively, this response consists of both the vasoconstriction and vasodilatation component and is termed 'cold-induced vascular response' in this study. Whilst the vasoconstriction phase is generally agreed in the literature, there is still some confliction with using the term 'vasodilatation' as it can be argued that the second phase of the cold-induced vascular response is a reversal of the initial vasoconstriction. The magnitude of the vasoconstriction directs the intensity of the vasodilatation, where in conditions where the vessels constrict at a high level, a greater magnitude of vasodilatation is required to bring the blood flow back to baseline without causing a hyperaemic response. If a pharmacological antagonist inhibits the vasoconstriction component, less change in blood flow is observed at the maximum vasodilatation phase from the maximum constriction phase. Other terms used for the vasodilatation phase used in the literature are 'rewarming' or 'rebound state'. The term vasodilatation was used in our study as I focussed on investigating the maximum increase in blood flow from the vasoconstrictor phase, to return blood flow to baseline.

It is also important to note that the response observed in this study is different to the Hunting response in CIVD which consists of a cyclic oscillations in blood flow induced by subsequent vasoconstrictions and vasodilatations in the extremities during cold exposure (Lewis, 1930, Gardner and Webb, 1986, Daanen, 2003, Duraku et al., 2012). Cold applications can cause blood flow to increase either during or following exposure. In our study, I did not investigate the changes in blood flow responses during the active cooling phase but following the local cold water immersion. Our current blood flow monitoring tools do not allow simultaneous blood flow measurements whilst the hindpaw is undergoing cold immersion and hence, it remains unknown whether CIVD is present during the treatment period. However, I were able to show a decrease in subcutaneous skin temperature during the treatment phase. Using the previous

knowledge and the proposed published mechanisms of CIVD, I investigated whether the axon reflex, sympathetic nerve or adrenergic receptors are involved in the cold-induced vascular response to understand the protective mechanisms underlying local cold-induced injury.

6.3.2 Cold-induced vascular response is dependent on TRPA1

The results initially presented in this study were assessed as area under the response curve and represented the changes in vascular blood flow for 30 min following local cold treatment. These results demonstrated conclusively that cold-induced vascular responses were dependent on TRPA1. This striking result supports the concept that TRPA1 is activated by cold and further provides novel evidence of the essential and primary role of TRPA1 as a vascular cold sensor in the periphery *in vivo* in the mouse. Surprisingly, further analysis of the cold-induced vascular responses, demonstrated clearly that TRPA1 is involved in the vasoconstriction phase. Our emerging data indicates that TRPA1 senses the temperature change from the thermoneutral zone, and is activated by low temperature at 10°C, mediating the cold-induced vascular response. When the TRPA1 gene is deleted or pharmacologically blocked, the vasoconstriction response was inhibited, and hence, blood flow stayed or fluctuated near basal levels and illustrated no significant change in the vasodilator component in our study.

The heat sensitive TRPV1 and warm sensitive TRPV4 channels were shown to have no involvement in affecting cold-induced vascular responses, as expected in our model. To address the controversy surrounding TRPA1 as a cold sensor, I demonstrated clearly for the first time that TRPM8 plays a secondary role to TRPA1 in the cold-induced vascular responses. I conclude that cold (10°C) directly activate TRPA1 and propose that TRPM8 may potentially be involved in the vasodilatation responses as it was previously characterised with a temperature threshold of activation is >10°C.

The question that arises from this novel finding is how TRPA1 mediates the cold-response and induces vasoconstriction. I can speculate that this may result following (1) the activation of non-neuronal TRPA1 on vascular smooth muscle cells. There is evidence showing that cold (17°C)-mediated constriction is inhibited by pre-treatment with non-selective cation channel blocker ruthenium red in the colon (Dong et al., 2010). However, non-neuronal TRPA1 is not as well characterised as neuronal TRPA1 and it remains unknown if smooth muscle cells in the mouse hindpaw express functional TRPA1; this requires further investigation which was beyond the scope of the current study, (2) Activation of TRPA1 on sympathetic nerves may mediate noradrenaline release and this will be dependent on evidence showing functional TRPA1 expression on sympathetic nerve, and increased noradrenaline levels in the hindpaw tissue in the vasoconstriction phase (discussed in the next section); (3) cross talk mechanisms between

sympathetic nerves and sensory neurons as it is well established that TRPA1 is widely expressed on sensory neurons; (4) increased superoxide generation in a TRPA1-dependent manner (see section 6.3.3) or (5) activation of TRPA1 on keratinocytes and this will rely on investigating the role of keratinocytes as independent cold sensors. Keratinocytes are known to express TRPA1 and activation of TRPA1 using exogenous agonists and cold can cause an increase in intracellular calcium (Tsutsumi et al., 2010). Simultaneously, TRPA1 activation on keratinocytes may mediate reactive oxygen species generation which may lead to downstream calcium-induced vasoconstriction in the effector cells. Furthermore, it is tempting to speculate that keratinocytes can release different mediators to activate primary afferent neurons and TRPA1 may also act as an essential regulator of CGRP release from keratinocytes. Understanding the signalling mechanisms between keratinocytes, smooth muscle cells and sensory neurons is necessary to determine the role of TRPA1 in mediating the cold-induced vascular responses.

6.3.3 Superoxide and adrenergic receptors drives the cold-induced vasoconstriction in a TRPA1-dependent manner

Following on from our evidence that TRPA1 is involved as a primary driver of the cold-induced vascular response, I showed that cold-induced vasoconstriction is dependent on adrenergic receptor activity, potentially caused by activation of α_{2C}-adrenergic receptors on vascular smooth muscle cells present in the mouse hindpaw. α_{2C}-adrenergic receptors are known to be silent at basal conditions near the thermoneutral zone (37°C), and are activated in the presence of increased superoxide generation, which is also known to increase in hypoxic conditions (Bailey et al., 2005). I further showed that (1) the catalysis of superoxide using tempol was able to suppress cold-induced vasoconstriction and illustrated clearly for the first time that (2) cold-induced increase in superoxide levels during the vasoconstriction phase is dependent on TRPA1. In this study, I were able to show an association between TRPA1 activation and superoxide generation using two TRPA1 agonists; cinnamaldehyde and cold. Thus, I conclude that superoxide may be produced downstream of TRPA1 activation by cold stimulus in the peripheral vasculature.

To strengthen our findings with superoxide, I also investigated the mechanism underlying superoxide-induced vasoconstriction of the smooth muscle cells by targeting the Rho-kinase mediated pathway. I demonstrated that (1) the pharmacological blockade of Rho-kinase was able to inhibit cold-induced vasoconstriction and (2) the cold-induced increase in phosphorylation of MLC, which is mediated by Rho-kinase, was dependent on TRPA1. Cumulatively, our novel findings here propose that local cold exposure activates TRPA1, which causes an increase in superoxide generation and activates Rho-kinase to phosphorylate MLC

and/or translocate α_{2C}-adrenergic receptors, ultimately leading to vasoconstriction in the mouse hindpaw (Figure 5.9). It is also important to note that both superoxide and noradrenaline are known to stimulate the Rho-kinase pathway. Since a direct link between noradrenaline and cold-induced vasoconstriction was not observed in the current study, it can be speculated that superoxide is activating this pathway, but the role of noradrenaline cannot be excluded.

It has previously been shown that the catalysis of superoxide reduces cold-induced injury in the hind leg of rabbits (Das et al., 1991) and vasogenic brain oedema (Ikeda et al., 1990, Ando et al., 1989). Our pathway illustrating the link between cold-induced TRPA1 activation and superoxide generation may be relevant in understanding the pathophysiology of prolonged environmental cold-induced injury which is characterised by oxygen-derived free radicals.

6.3.4 Role of vasodilators in the cold-induced vascular response

The vasodilatation phase of the cold-induced vascular response is important as it returns blood flow back to baseline to prevent cold-induced injury. Since I presented evidence supporting the role of TRPA1 as a vascular sensor, I further investigated the effects of pharmacological blockade of the mediators involved downstream of TRPA1 activation.

The role of the sensory axon reflex in mediating cold-induced responses has been previously proposed and remains debatable with conflicting evidence in the literature. I addressed this issue by demonstrating that the pharmacological blockade of (1) sodium channels using local anaesthetics, (2) substance P NK_1 receptors using SR140333 and (3) CGRP receptor antagonists using $CGRP_{8-37}$ or BIBN4096BS significantly reduced the cold-induced vascular response. This is the first study to clearly illustrate the involvement of a sensory neuron-dependent vasodilatation in cold-induced vascular responsein the mouse vasculature.

Although α-CGRP is known to have potent microvascular vasodilator properties, I provide novel results showing that cold-induced vascular responses were independent of α-CGRP but dependent on β-CGRP, using BIBN4096BS in α-CGRP WT and KO mice. Although the role of β-CGRP in vasoactive responses is not as well characterised as α-CGRP, I present clearly that there was an upregulation of β-CGRP mRNA in α-CGRP KO mice. In fact, our study confirms the vasodilator nature of CGRP as I demonstrated clearly that BIBN4096BS had no effect in inhibiting the cold-induced vasoconstriction, but inhibited the vasodilatation phase. CGRP is thus being demonstrated here to have a protective role in preventing cold-induced injury. The questions that arise are (1) whether CGRP is released downstream of sensory neuron stimulation by TRPA1 activation (2) if CGRP is released from a non-neuronal source such as keratinocytes (Hou et al., 2011) or (3) whether the sympathetic-sensory coupling pathway is involved in mediating the vasodilator component in the cold-induced vascular response. Previous studies

have shown that CGRP can dose-dependently increase cAMP accumulation and inhibit noradrenaline-induced IP_3 production and calcium mobilisation. This further leads to a decrease in phosphorylation of MLC protein and subsequently inhibits muscle contraction in a dose-dependent manner (Yousufzai and Abdel-Latif, 1998). Furthermore, both noradrenaline and the neuropeptide substance P are released simultaneously from the sympathetic and sensory nerves, respectively following cold stimulation, and as the noradrenaline sympathetic response occurs faster this results in vasoconstriction (Ochoa et al., 1993). However, the noradrenaline response is shortly diminished by its re-uptake into the nerve terminals and decreased neurotransmitter release by negative feedback through the pre-synaptic α_2-adrenergic receptors, while the vasodilator response through sensory-mediated release of neuropeptides such as substance P and CGRP, is maintained for longer, hence dominating the vascular response, resulting in the re-warming/vasodilatation phase. This suggests a cross-talk between sympathetic and sensory nervous system whereby CGRP-containing sensory nerve fibres could play an important role in regulating vascular smooth muscle function.

In support of the earlier proposed CIVD theory by Aschoff (1944) that an unknown vasodilator such as nitric oxide is involved, in this study I demonstrated that nitric oxide has a prominent role in cold-induced vascular responses. Whilst a selective eNOS inhibitor is unavailable, I showed that the thermosensitive iNOS might have a partial role in cold-induced vascular responses. Furthermore, pre-treatment with the neuropeptide receptor antagonists and the nNOS inhibitor completely abolished the cold-induced vascular response. I conclude that neuropeptide and nNOS-derived nitric oxide mediate their vasodilator effects downstream of TRPA1 activation and this mechanism is important in mediating the recovery of normal blood flow following the initial constrictor response to local cooling to protect against local cold-induced injury. This response may be relevant to painful conditions in peripheral vascular diseases such as Raynaud's disease.

6.3.5 Clinical relevance to diseases: local cooling and Raynaud's disease

Raynaud's disease is known to be more prevalent in women than men, where there are 10 million patients with Raynaud's in UK, and 2% of the adult population worldwide (NHS, 2013, Goundry et al., 2012). Raynaud's disease is multifactorial and complex with both vascular and neural abnormalities (Roustit et al., 2011), characterised by a loss of cold-induced reflex vasodilatation (Brain et al., 1990) and CGRP-containing nerve fibres (Bunker et al., 1990). A severe restriction of blood supply in the vasculature can lead to higher risk of causing complications such as frostbite in extreme cold conditions. Although various pharmacologic (calcium channel blockers and phosphodiesterase V inhibitors) and invasive therapies have been studied to treat the symptoms of Raynaud's disease, no specific treatments are currently

approved by the U.S. Food and Drug Administration (Landry, 2013, Herrick, 2013). There is a current need to understand the underlying mechanism of the symptoms of Raynaud's disease, with a focus on factors such as reduced in local blood supply in the peripheral vasculature.

Recent studies in our group have demonstrated that TRPA1 can play a critical role in mediating chronic pain associated with CFA-induced monarthritis in the mouse knee joint (Fernandes et al., 2011). All the pathways investigated in our current project have been linked with Raynaud's phenomenon. Local cold exposure leads to exaggerated vasoconstriction and ischemia reperfusion injury in the cutaneous vasculature and the main causes of this response has been attributed to activation of sympathetic nervous system, modulation of the expression of post-junctional α_2-adrenergic receptors, diminished release of CGRP and endothelial dysfunction with depressed or limited dilating action of nitric oxide (Cooke and Marshall, 2005). Interestingly, the administration of CGRP was shown to increase blood flow in Raynaud disease patients (Bunker et al., 1993), however it is important to note that the side effects experienced by these patients included flushing, diarrhoea, headache and mild hypotension.

Considering the conclusive finding in our current study that TRPA1 plays a primary role in cold-induced vascular response, it is tempting to suggest that the pharmacological blockade of TRPA1 may reduce cold-induced vasoconstriction in Raynaud's phenomenon. However, it may also be worth investigating whether the topical application of a TRPA1 agonist at a sub-maximal dose can reverse cold-induced vasoconstriction in digit areas of the fingers and toes. This will rely on investigating the role of TRPA1 in terms of expression and function in the pathophysiology of Raynaud's disease.

Furthermore, the airway is also known to be susceptible to temperature changes, as fluctuations in ambient temperature and cold weather has been reported to be a major environmental factor that worsens existing asthma conditions (Butcher, 2006). Cold air exposure can result in respiratory responses such as cough, bronchoconstriction and mucosal secretion (Koskela, 2007) and skin cooling can produce mild airway obstruction in asthmatic patients (Skowronski et al., 1998). TRPA1 is expressed on the vagal sensory nerves innervating the mouse airways and cinnamaldehyde inhalation was shown to elicit strong central-reflex changes in breathing pattern *in vivo*(Nassenstein et al., 2008). Indeed, 15.3% of the bronchopulmonary receptors can be activated by cold (8°C) in an *ex vivo* rat lung preparation (Zhou et al., 2011). In our study, I showed that activation of TRPA1 with cinnamaldehyde and cold can mediate neurogenic-dependent vascular processes with an interaction of nerves and vessels, which may be relevant in understanding the pathophysiology of airway inflammatory diseases.

6.3.6 Study limitations, practical considerations and future directions

This project used both a two-channel laser Doppler flowmeter and FLPI to study blood flow non-invasively in the mouse ear and hindpaw, respectively. Whilst the laser Doppler flowmeter is ideal for investigating blood flow changes in the skin microvasculature, it has limitations with its single point measurement. Special care was taken with the use of the optic fibre probe to position it on the same vessel of the ear each time, with avoidance of movements between the probe tip and the underlying tissue as structures other than blood cells can generate Doppler shifts. This is important and minimises variability in blood flow responses, as shown in experiments with cinnamaldehyde-induced vasodilatation in Chapter 3. The use of AUC as data analysis provides a measure for the magnitude of the response, allowing clear distinction between vehicle- and drug-treated ears with reproducible results as shown in this project. Increasing sample size (n=8) could further reduce variations between measurements. Nevertheless, this could not be employed for all experiments due to unavailability of transgenic mice or time limitations. The limitation in this study using laser Doppler flowmetry with cinnamaldehyde on the mouse ear (chapter 3) is the fact that the responses obtained is generated from a single point of the blood vessel of the ear and hence, does not provide a complete representative changes in the whole ear vasculature. A single reading may misrepresent the spatial heterogeneity of blood flow in the surrounding area of the ear. In future studies, it would be interesting to confirm the overall change in the whole ear area with the FLPI.

The FLPI offers a global evaluation of the blood flow responses over a larger area and avoids contact with the skin surface. Studies investigating cold-induced vascular responses were focussed on measuring blood flow in the whole area of each hindpaw (Chapter 4 and 5) with the FLPI. The primary limitation here consisted of proper positioning of the mice, as in the cold model following baseline measurement, the mice were removed for local cold treatment. Blood flow was not measured during the active cooling period. Following treatment, special care had to be taken to re-position the mice in the previous position in a small time window which requires training. However, the optimised methods using the FLPI allowed reproducible data to be obtained, as shown in this project (chapter 4 and 5). Whilst the use of AUC allowed clear distinction of the differences between the cold-treated and untreated hindpaw, subsequent analysis using the two-component analysis provided a better understanding of the different phases of the physiological response to local cold exposure. The use of both the laser Doppler and the FLPI in both models in this study allowed each mouse to serve as its own control. In the mouse ear model, the response in the cinnamaldehyde-treated ipsilateral ear was compared to the vehicle-treated contralateral ear. In the cold model, the same principle was applied in the mouse hindpaw. The bilateral measurement reduced sample size in this study and is therefore within the principle of the 3R's.

Although it is conclusive that cold (10°C) activates TRPA1 expressed on the peripheral vasculature, it remains unknown whether CIVD occurs during the active local cooling period in our model. Future studies examining the role of TRPA1 in mediating CIVD in the active cooling period will be necessary to resolve confusion of this phenomenon and further contribute to Lewis' findings.

The periphery responds to less extreme cold exposure including temperature encountered in daily normal lifestyles (<30°C) and the functioning of the digits is determined by several physiological parameters such as skin temperature, which is in turn known to be influenced by physiological parameters (Van der Struijs et al., 2008). Our model focussed on a short local cooling period using a water medium and hence, an improved model investigating the effects of cold (10°C) air exposure over a prolonged period will be essential to understand the role of TRPA1 in the mechanisms underlying cutaneous temperature regulation.

The data from the present study do not provide strong evidence to distinguish between the neuronal and non-neuronal function or location of TRPA1 in the vasculature, but it is evident from earlier studies that initial local cooling-induced vasoconstriction requires both intact function of the sympathetic and sensory nerve. Further studies examining sensory nerve denervation are required to confirm the role of neuronal CGRP in mediating the vasodilator component of the cold-induced vascular response to return blood flow to baseline. However, sensory denervation after capsaicin treatment has been shown to cause a sharp decrease in CGRP-containing nerves, as expected but with an increase in sympathetic nerves and this evidence highlights the close overlapping distribution patterns of both nerves around blood vessels and indicates a close interaction between both nerve populations in the periphery (Terenghi et al., 1986).

The role of TRPA1 as a cold sensor remains controversial in the literature and our current study addresses this controversy showing that cold (10°C) can activate TRPA1 in the peripheral vasculature. Interestingly, a recent study by Chen *et al.* demonstrated that lowering the temperature in steps (from 24 to 8°C) evoked progressively larger calcium influx in HEK293-F cells expressing mTRPA1 and rTRPA1 but not hTRPA1 and rhTRPA1 (Chen et al., 2013). These data suggest that cold activates rodent but not primate TRPA1 and hence, raises concerns on extrapolating our findings in rodents to humans, because of the lack of cold sensitivity of hTRPA1. Indeed, rodents have been used as the default species in TRPA1 research and drug discovery, with the availability of selective TRPA1 antagonists and TRPA1 KO mice (Bautista et al., 2006, Kwan et al., 2006, McNamara et al., 2007). Species-specific differences have been a major difficulty in TRPA1 research and drug discovery (Chen and Kym, 2009). Since rhesus monkey and human TRPA1 channels share a similar pharmacology profile (Bianchi et al., 2012,

Chen et al., 2013), it would be interesting to use non-human primates to further investigate the effects of (1) cold on primary cultured DRG neurons *in vitro* and (2) local cooling on peripheral blood flow to validate the role of TRPA1 as a cold sensor and subsequently, confirm findings on the role of rhTRPA1 as a cold sensor.

Nevertheless, on a positive note there is increasing clinical evidence suggesting that TRPA1 is important for cold pain sensation in humans. Kremeyer *et al.* (2010) showed a gain-of-function mutation in TRPA1 causes familial episodic pain syndrome which is characterised by episodes of debilitating upper body pain. The mutant TRPA1 channels have a normal pharmacological profile with altered biophysical properties at normal resting potentials (Kremeyer et al., 2010). Moreover, the non-synonymous genetic variant E179K of hTRPA1 gene was shown to induce paradoxical heat sensation in neuropathic pain patients which carry the Lys-179 variant (Binder et al., 2011). HEK cells expressing the variant Lys-179 TRPA1 are not activated by cold (4°C). These findings suggest that variations in the TRPA1 gene can alter pain perception in humans and hence, TRPA1 antagonists may be a useful therapy for pathological pain conditions.

6.3.7 Conclusion

It is well established through the studies of Lewis, Daanen, Johnson, Kellogg, Flavahan and Bailey that the reflex control of cutaneous blood in response to local cooling is accomplished through both efferent vasoconstrictor and vasodilator pathways. This thesis highlights the complex combination of the autonomic and sensory neuron-induced responses underlying the microvasculature in response to local cold exposure. An important aspect of this PhD project has been to address the controversial issue underlying the role of TRPA1 as a cold sensor and to introduce the concept that cold (10°C) can activate TRPA1 in the vasculature which drives the cold-induced vascular response. This initially consists of neurotransmitter release such as noradrenaline and/or generation of superoxide, adrenergic receptor translocation, and vascular smooth muscle cell contraction in the cutaneous vasculature. On the other hand, stimulation of TRPA1 presumably on the sensory neurons mediates the release of the potent microvascular vasodilator CGRP which is involved in reducing the α_{2C}-adrenergic receptor-mediated vasoconstriction, by relaxing blood vessels and returning blood flow to baseline. This TRPA1-mediated vasodilator response is important to protect against local cold-induced injury. Hence, this thesis has provided a new perspective into the understanding of the mechanisms underlying the well-established protective response for local-cold injury that has been studied for the last 80 years.

Chapter 7 – References

Chapter 7 – References

AARONS, E., GRANT, P., SOLDAN, K., LUTON, P., TANG, J. & TEDDER, R. 2004. Failure to diagnose recent hepatitis C virus infections in London injecting drug users. *Journal of Medical Virology,* 73**,** 548-553.

ABURTO, T. K., LAJOIE, C. & MORGAN, K. G. 1993. Mechanisms of signal transduction during alpha 2-adrenergic receptor-mediated contraction of vascular smooth muscle. *Circ Res,* 72**,** 778-85.

ADAIR, R. K. 1999. A model of the detection of warmth and cold by cutaneous sensors through effects on voltage-gated membrane channels. *Proc Natl Acad Sci U S A,* 96**,** 11825-9.

AHLQUIST, R. P. 1948. A study of the adrenotropic receptors. *Am J Physiol,* 153**,** 586-600.

AKERMAN, S., WILLIAMSON, D. J., KAUBE, H. & GOADSBY, P. J. 2002. Nitric oxide synthase inhibitors can antagonize neurogenic and calcitonin gene-related peptide induced dilation of dural meningeal vessels. *Br J Pharmacol,* 137**,** 62-8.

AKOPIAN, A. N. 2011. Regulation of nociceptive transmission at the periphery via TRPA1-TRPV1 interactions. *Curr Pharm Biotechnol,* 12**,** 89-94.

AKOPIAN, A. N., RUPAREL, N. B., JESKE, N. A. & HARGREAVES, K. M. 2007. Transient receptor potential TRPA1 channel desensitization in sensory neurons is agonist dependent and regulated by TRPV1-directed internalization. *J Physiol,* 583**,** 175-93.

AL-HADITHI, B. A., STAUBER, V. & MITCHELL, J. 1988. The co-localisation of substance P and VIP in cholinergic-type terminals of the rat parotid gland. *J Anat,* 159**,** 83-92.

ALAWI, K. & KEEBLE, J. 2010. The paradoxical role of the transient receptor potential vanilloid 1 receptor in inflammation. *Pharmacol Ther,* 125**,** 181-95.

ALMEIDA, M. C., HEW-BUTLER, T., SORIANO, R. N., RAO, S., WANG, W., WANG, J., TAMAYO, N., OLIVEIRA, D. L., NUCCI, T. B., ARYAL, P., GARAMI, A., BAUTISTA, D., GAVVA, N. R. & ROMANOVSKY, A. A. 2012. Pharmacological blockade of the cold receptor TRPM8 attenuates autonomic and behavioral cold defenses and decreases deep body temperature. *J Neurosci,* 32**,** 2086-99.

AMARA, S. G., EVANS, R. M. & ROSENFELD, M. G. 1984. Calcitonin/calcitonin gene-related peptide transcription unit: tissue-specific expression involves selective use of alternative polyadenylation sites. *Mol Cell Biol,* 4**,** 2151-60.

AMARA, S. G., JONAS, V., O'NEIL, J. A., VALE, W., RIVIER, J., ROOS, B. A., EVANS, R. M. & ROSENFELD, M. G. 1982. Calcitonin COOH-terminal cleavage peptide as a model for identification of novel neuropeptides predicted by recombinant DNA analysis. *J Biol Chem,* 257**,** 2129-32.

ANAND, U., OTTO, W. R., FACER, P., ZEBDA, N., SELMER, I., GUNTHORPE, M. J., CHESSELL, I. P., SINISI, M., BIRCH, R. & ANAND, P. 2008. TRPA1 receptor localisation in the human peripheral nervous system and functional studies in cultured human and rat sensory neurons. *Neurosci Lett,* 438**,** 221-7.

ANDERSSON, D. A., GENTRY, C. & BEVAN, S. 2012. TRPA1 has a key role in the somatic pro-nociceptive actions of hydrogen sulfide. *PLoS One,* 7**,** e46917.

ANDERSSON, D. A., GENTRY, C., MOSS, S. & BEVAN, S. 2008. Transient receptor potential A1 is a sensory receptor for multiple products of oxidative stress. *J Neurosci,* 28**,** 2485-94.

ANDO, K., PEGRAM, B. L. & FROHLICH, E. D. 1990. Hemodynamic effects of calcitonin gene-related peptide in spontaneously hypertensive rats. *Am J Physiol,* 258**,** R425-9.

ANDO, Y., INOUE, M., HIROTA, M., MORINO, Y. & ARAKI, S. 1989. Effect of a superoxide dismutase derivative on cold-induced brain edema. *Brain Res,* 477**,** 286-91.

ANDRADE, E. L., LUIZ, A. P., FERREIRA, J. & CALIXTO, J. B. 2008. Pronociceptive response elicited by TRPA1 receptor activation in mice. *Neuroscience,* 152**,** 511-20.

ANDRE, E., CAMPI, B., MATERAZZI, S., TREVISANI, M., AMADESI, S., MASSI, D., CREMINON, C., VAKSMAN, N., NASSINI, R., CIVELLI, M., BARALDI, P. G., POOLE, D. P., BUNNETT, N. W., GEPPETTI, P. & PATACCHINI, R. 2008. Cigarette smoke-induced neurogenic inflammation is mediated by alpha,beta-unsaturated aldehydes and the TRPA1 receptor in rodents. *J Clin Invest,* 118**,** 2574-82.

ANTONY, I., APTECAR, E., LEREBOURS, G. & NITENBERG, A. 1994. Coronary artery constriction caused by the cold pressor test in human hypertension. *Hypertension,* 24**,** 212-9.

ARMSTEAD, W. M. 1996. Role of ATP-sensitive K+ channels in cGMP-mediated pial artery vasodilation. *Am J Physiol,* 270**,** H423-6.

ARUNODAYA, G. R. & TALY, A. B. 1995. Sympathetic skin response: a decade later. *J Neurol Sci,* 129**,** 81-9.

ARUOMA, O. I., HALLIWELL, B., HOEY, B. M. & BUTLER, J. 1989. The antioxidant action of N-acetylcysteine: its reaction with hydrogen peroxide, hydroxyl radical, superoxide, and hypochlorous acid. *Free Radic Biol Med,* 6**,** 593-7.

ASCHOFF, J. 1944. Uber der Kiiltedilation der Extremitiit des Menschen in Eiswasser,. *Pflugers Arch,* 248**,** 183-196.

ATOYAN, R., SHANDER, D. & BOTCHKAREVA, N. V. 2009. Non-neuronal expression of transient receptor potential type A1 (TRPA1) in human skin. *J Invest Dermatol,* 129**,** 2312-5.

AUBDOOL, A., GRAPEL, R., BRAIN, S. 2010. Interactions between TRPA1 and TRPV1 in the peripheral vasculature. *pA2 online,* Proceedings of the British Pharmacological Society.

AUBDOOL, A. A. & BRAIN, S. D. 2011. Neurovascular aspects of skin neurogenic inflammation. *J Investig Dermatol Symp Proc,* 15**,** 33-9.

BABES, A., ZORZON, D. & REID, G. 2004. Two populations of cold-sensitive neurons in rat dorsal root ganglia and their modulation by nerve growth factor. *Eur J Neurosci,* 20**,** 2276-82.

BACHETTI, T., COMINI, L., CURELLO, S., BASTIANON, D., PALMIERI, M., BRESCIANI, G., CALLEA, F. & FERRARI, R. 2004. Co-expression and modulation of neuronal and endothelial nitric oxide synthase in human endothelial cells. *J Mol Cell Cardiol,* 37**,** 939-45.

BAILEY, S. R., EID, A. H., MITRA, S., FLAVAHAN, S. & FLAVAHAN, N. A. 2004. Rho kinase mediates cold-induced constriction of cutaneous arteries: role of alpha2C-adrenoceptor translocation. *Circ Res,* 94**,** 1367-74.

BAILEY, S. R., MITRA, S., FLAVAHAN, S. & FLAVAHAN, N. A. 2005. Reactive oxygen species from smooth muscle mitochondria initiate cold-induced constriction of cutaneous arteries. *Am J Physiol Heart Circ Physiol,* 289**,** H243-50.

BANDELL, M., STORY, G. M., HWANG, S. W., VISWANATH, V., EID, S. R., PETRUS, M. J., EARLEY, T. J. & PATAPOUTIAN, A. 2004. Noxious cold ion channel TRPA1 is activated by pungent compounds and bradykinin. *Neuron,* 41**,** 849-57.

BANG, S. & HWANG, S. W. 2009. Polymodal ligand sensitivity of TRPA1 and its modes of interactions. *J Gen Physiol,* 133**,** 257-62.

BANVOLGYI, A., POZSGAI, G., BRAIN, S. D., HELYES, Z. S., SZOLCSANYI, J., GHOSH, M., MELEGH, B. & PINTER, E. 2004. Mustard oil induces a transient receptor potential vanilloid 1 receptor-independent neurogenic inflammation and a non-neurogenic cellular inflammatory component in mice. *Neuroscience,* 125**,** 449-59.

BARALDI, P. G., PRETI, D., MATERAZZI, S. & GEPPETTI, P. 2010. Transient receptor potential ankyrin 1 (TRPA1) channel as emerging target for novel analgesics and anti-inflammatory agents. *J Med Chem,* 53**,** 5085-107.

BAUTISTA, D. M., JORDT, S. E., NIKAI, T., TSURUDA, P. R., READ, A. J., POBLETE, J., YAMOAH, E. N., BASBAUM, A. I. & JULIUS, D. 2006. TRPA1 mediates the inflammatory actions of environmental irritants and proalgesic agents. *Cell,* 124**,** 1269-82.

BAUTISTA, D. M., MOVAHED, P., HINMAN, A., AXELSSON, H. E., STERNER, O., HOGESTATT, E. D., JULIUS, D., JORDT, S. E. & ZYGMUNT, P. M. 2005. Pungent products from garlic activate the sensory ion channel TRPA1. *Proc Natl Acad Sci U S A,* 102**,** 12248-52.

BAUTISTA, D. M., PELLEGRINO, M. & TSUNOZAKI, M. 2013. TRPA1: A gatekeeper for inflammation. *Annu Rev Physiol,* 75**,** 181-200.

BAUTISTA, D. M., SIEMENS, J., GLAZER, J. M., TSURUDA, P. R., BASBAUM, A. I., STUCKY, C. L., JORDT, S. E. & JULIUS, D. 2007. The menthol receptor TRPM8 is the principal detector of environmental cold. *Nature,* 448**,** 204-8.

BAYLISS, W. M. 1901. On the origin from the spinal cord of the vaso-dilator fibres of the hind-limb, and on the nature of these fibres. *J Physiol,* 26**,** 173-209.

BECKMAN, J. S. & KOPPENOL, W. H. 1996. Nitric oxide, superoxide, and peroxynitrite: the good, the bad, and ugly. *Am J Physiol,* 271**,** C1424-37.

BECKMAN, J. S., MINOR, R. L., JR., WHITE, C. W., REPINE, J. E., ROSEN, G. M. & FREEMAN, B. A. 1988. Superoxide dismutase and catalase conjugated to polyethylene glycol increases endothelial enzyme activity and oxidant resistance. *J Biol Chem,* 263**,** 6884-92.

BENNETT, D. L., DMIETRIEVA, N., PRIESTLEY, J. V., CLARY, D. & MCMAHON, S. B. 1996. trkA, CGRP and IB4 expression in retrogradely labelled cutaneous and visceral primary sensory neurones in the rat. *Neurosci Lett,* 206**,** 33-6.

BERGERSEN, T. K., ERIKSEN, M. & WALLOE, L. 1997. Local constriction of arteriovenous anastomoses in the cooled finger. *Am J Physiol,* 273**,** R880-6.

BERGERSEN, T. K., HISDAL, J. & WALLOE, L. 1999. Perfusion of the human finger during cold-induced vasodilatation. *Am J Physiol,* 276**,** R731-7.

BERRIDGE, M. J. & IRVINE, R. F. 1984. Inositol trisphosphate, a novel second messenger in cellular signal transduction. *Nature,* 312**,** 315-21.

BESSAC, B. F., SIVULA, M., VON HEHN, C. A., ESCALERA, J., COHN, L. & JORDT, S. E. 2008. TRPA1 is a major oxidant sensor in murine airway sensory neurons. *J Clin Invest,* 118**,** 1899-910.

BHAUMIK, G., SRIVASTAVA, K. K., SELVAMURTHY, W. & PURKAYASTHA, S. S. 1995. The role of free radicals in cold injuries. *Int J Biometeorol,* 38**,** 171-5.

BIANCHI, B. R., ZHANG, X. F., REILLY, R. M., KYM, P. R., YAO, B. B. & CHEN, J. 2012. Species comparison and pharmacological characterization of human, monkey, rat, and mouse TRPA1 channels. *J Pharmacol Exp Ther,* 341**,** 360-8.

BICKERS, D., CALOW, P., GREIM, H., HANIFIN, J. M., ROGERS, A. E., SAURAT, J. H., SIPES, I. G., SMITH, R. L., TAGAMI, H. & PANEL, R. E. 2005. A toxicologic and dermatologic assessment of cinnamyl alcohol, cinnamaldehyde and cinnamic acid when used as fragrance ingredients. *Food Chem Toxicol,* 43**,** 799-836.

BINDER, A., MAY, D., BARON, R., MAIER, C., TOLLE, T. R., TREEDE, R. D., BERTHELE, A., FALTRACO, F., FLOR, H., GIERTHMUHLEN, J., HAENISCH, S., HUGE, V., MAGERL, W., MAIHOFNER, C., RICHTER, H., ROLKE, R., SCHERENS, A., UCEYLER, N., UFER, M., WASNER, G., ZHU, J. & CASCORBI, I. 2011. Transient receptor potential channel polymorphisms are associated with the somatosensory function in neuropathic pain patients. *PLoS One,* 6**,** e17387.

BINTI MD ISA, K., KAWASAKI, N., UEYAMA, K., SUMII, T. & KUDO, S. 2011. Effects of cold exposure and shear stress on endothelial nitric oxide synthase activation. *Biochem Biophys Res Commun,* 412**,** 318-22.

BIRO, T. & KOVACS, L. 2009. An "ice-cold" TR(i)P to skin biology: the role of TRPA1 in human epidermal keratinocytes. *J Invest Dermatol,* 129**,** 2096-9.

BLESSING, W. W. & NALIVAIKO, E. 2000. Regional blood flow and nociceptive stimuli in rabbits: patterning by medullary raphe, not ventrolateral medulla. *Journal of Physiology-London,* 524**,** 279-292.

BLOCK, J. A. & SEQUEIRA, W. 2001. Raynaud's phenomenon. *Lancet,* 357**,** 2042-8.

BODKIN, J. V. & BRAIN, S. D. 2011. Transient receptor potential ankyrin 1: emerging pharmacology and indications for cardiovascular biology. *Acta Physiol (Oxf),* 203**,** 87-98.

BOSSALLER, C., REITHER, K., HEHLERT-FRIEDRICH, C., AUCH-SCHWELK, W., GRAF, K., GRAFE, M. & FLECK, E. 1992. In vivo measurement of endothelium-dependent vasodilation with substance P in man. *Herz,* 17**,** 284-90.

BOULANGER, C. M., HEYMES, C., BENESSIANO, J., GESKE, R. S., LEVY, B. I. & VANHOUTTE, P. M. 1998. Neuronal nitric oxide synthase is expressed in rat vascular smooth muscle cells: activation by angiotensin II in hypertension. *Circ Res,* 83**,** 1271-8.

BOURNE, M. H., PIEPKORN, M. W., CLAYTON, F. & LEONARD, L. G. 1986. Analysis of microvascular changes in frostbite injury. *J Surg Res,* 40**,** 26-35.

BOWLES, W. R., FLORES, C. M., JACKSON, D. L. & HARGREAVES, K. M. 2003. beta 2-Adrenoceptor regulation of CGRP release from capsaicin-sensitive neurons. *J Dent Res,* 82**,** 308-11.

BRAIN, S. D. 1996. *The innevation of skin vasculature: The emerging importance of neuropeptides* UK, Harwood academic publishers.

BRAIN, S. D. 1997. Sensory neuropeptides: their role in inflammation and wound healing. *Immunopharmacology,* 37**,** 133-52.

BRAIN, S. D. & COX, H. M. 2006. Neuropeptides and their receptors: innovative science providing novel therapeutic targets. *Br J Pharmacol,* 147 Suppl 1**,** S202-11.

BRAIN, S. D. & GRANT, A. D. 2004. Vascular actions of calcitonin gene-related peptide and adrenomedullin. *Physiological Reviews,* 84**,** 903-934.

BRAIN, S. D., HUGHES, S. R., CAMBRIDGE, H. & O'DRISCOLL, G. 1993. The contribution of calcitonin gene-related peptide (CGRP) to neurogenic vasodilator responses. *Agents Actions,* 38 Spec No**,** C19-21.

BRAIN, S. D., PETTY, R. G., LEWIS, J. D. & WILLIAMS, T. J. 1990. Cutaneous blood flow responses in the forearms of Raynaud's patients induced by local cooling and intradermal injections of CGRP and histamine. *Br J Clin Pharmacol,* 30**,** 853-9.

BRAIN, S. D., TIPPINS, J. R., MORRIS, H. R., MACINTYRE, I. & WILLIAMS, T. J. 1986. Potent vasodilator activity of calcitonin gene-related peptide in human skin. *J Invest Dermatol,* 87**,** 533-6.

BRAIN, S. D., WILLIAMS, T. J., TIPPINS, J. R., MORRIS, H. R. & MACINTYRE, I. 1985. Calcitonin Gene-Related Peptide Is a Potent Vasodilator. *Nature,* 313**,** 54-56.

BRAVERMAN, I. M. 1997. The cutaneous microcirculation: ultrastructure and microanatomical organization. *Microcirculation,* 4**,** 329-40.

BRAVERMAN, I. M. 2000. The cutaneous microcirculation. *J Investig Dermatol Symp Proc,* 5**,** 3-9.

BREDE, M., NAGY, G., PHILIPP, M., SORENSEN, J. B., LOHSE, M. J. & HEIN, L. 2003. Differential control of adrenal and sympathetic catecholamine release by alpha 2-adrenoceptor subtypes. *Mol Endocrinol,* 17**,** 1640-6.

BRIERLEY, S. M., CASTRO, J., HARRINGTON, A. M., HUGHES, P. A., PAGE, A. J., RYCHKOV, G. Y. & BLACKSHAW, L. A. 2011. TRPA1 contributes to specific mechanically activated currents and sensory neuron mechanical hypersensitivity. *J Physiol,* 589**,** 3575-93.

BUCKINGHAM, R. E., HAMILTON, T. C., HOWLETT, D. R., MOOTOO, S. & WILSON, C. 1989. Inhibition by glibenclamide of the vasorelaxant action of cromakalim in the rat. *Br J Pharmacol,* 97**,** 57-64.

BUNKER, C. B., REAVLEY, C., O'SHAUGHNESSY, D. J. & DOWD, P. M. 1993. Calcitonin gene-related peptide in treatment of severe peripheral vascular insufficiency in Raynaud's phenomenon. *Lancet,* 342**,** 80-3.

BUNKER, C. B., TERENGHI, G., SPRINGALL, D. R., POLAK, J. M. & DOWD, P. M. 1990. Deficiency of calcitonin gene-related peptide in Raynaud's phenomenon. *Lancet,* 336**,** 1530-3.

BURGESS, G. M., GODFREY, P. P., MCKINNEY, J. S., BERRIDGE, M. J., IRVINE, R. F. & PUTNEY, J. W., JR. 1984. The second messenger linking receptor activation to internal Ca release in liver. *Nature,* 309**,** 63-6.

BURTON, A. C., EDHOLM, O.G. 1955. Man in a cold environment. London EdwardArnold Ltd.

BUSTIN, S. A., BENES, V., GARSON, J. A., HELLEMANS, J., HUGGETT, J., KUBISTA, M., MUELLER, R., NOLAN, T., PFAFFL, M. W., SHIPLEY, G. L., VANDESOMPELE, J. & WITTWER, C. T. 2009. The MIQE guidelines: minimum information for publication of quantitative real-time PCR experiments. *Clin Chem,* 55**,** 611-22.

BUTCHER, J. D. 2006. Exercise-induced asthma in the competitive cold weather athlete. *Curr Sports Med Rep,* 5**,** 284-8.

BUYUKAFSAR, K., YALCIN, I., KURT, A. H., TIFTIK, R. N., SAHAN-FIRAT, S. & AKSU, F. 2006. Rho-kinase inhibitor, Y-27632, has an antinociceptive effect in mice. *Eur J Pharmacol,* 541**,** 49-52.

CAIN, D. M., KHASABOV, S. G. & SIMONE, D. A. 2001. Response properties of mechanoreceptors and nociceptors in mouse glabrous skin: an in vivo study. *J Neurophysiol,* 85**,** 1561-74.

CALS-GRIERSON, M. M. & ORMEROD, A. D. 2004. Nitric oxide function in the skin. *Nitric Oxide,* 10**,** 179-93.

CAMARA, A. K., RIESS, M. L., KEVIN, L. G., NOVALIJA, E. & STOWE, D. F. 2004. Hypothermia augments reactive oxygen species detected in the guinea pig isolated perfused heart. *Am J Physiol Heart Circ Physiol,* 286**,** H1289-99.

CAO, T., GERARD, N. P. & BRAIN, S. D. 1999. Use of NK(1) knockout mice to analyze substance P-induced edema formation. *Am J Physiol,* 277**,** R476-81.

CAO, Y. Q., MANTYH, P. W., CARLSON, E. J., GILLESPIE, A. M., EPSTEIN, C. J. & BASBAUM, A. I. 1998. Primary afferent tachykinins are required to experience moderate to intense pain. *Nature,* 392**,** 390-4.

CASPANI, O. & HEPPENSTALL, P. A. 2009. TRPA1 and cold transduction: an unresolved issue? *J Gen Physiol,* 133**,** 245-9.

CATERINA, M. J. & JULIUS, D. 2001. The vanilloid receptor: a molecular gateway to the pain pathway. *Annu Rev Neurosci,* 24**,** 487-517.

CATERINA, M. J., LEFFLER, A., MALMBERG, A. B., MARTIN, W. J., TRAFTON, J., PETERSEN-ZEITZ, K. R., KOLTZENBURG, M., BASBAUM, A. I. & JULIUS, D. 2000. Impaired nociception and pain sensation in mice lacking the capsaicin receptor. *Science,* 288**,** 306-13.

CATERINA, M. J., ROSEN, T. A., TOMINAGA, M., BRAKE, A. J. & JULIUS, D. 1999. A capsaicin-receptor homologue with a high threshold for noxious heat. *Nature,* 398**,** 436-41.

CATERINA, M. J., SCHUMACHER, M. A., TOMINAGA, M., ROSEN, T. A., LEVINE, J. D. & JULIUS, D. 1997. The capsaicin receptor: a heat-activated ion channel in the pain pathway. *Nature,* 389**,** 816-24.

CAVANAUGH, E. J., SIMKIN, D. & KIM, D. 2008. Activation of transient receptor potential A1 channels by mustard oil, tetrahydrocannabinol and Ca2+ reveals different functional channel states. *Neuroscience,* 154**,** 1467-76.

CERNUDA-MOROLLON, E., PINEDA-MOLINA, E., CANADA, F. J. & PEREZ-SALA, D. 2001. 15-Deoxy-Delta 12,14-prostaglandin J2 inhibition of NF-kappaB-DNA binding through covalent modification of the p50 subunit. *J Biol Chem,* 276**,** 35530-6.

CHANG, M. M., LEEMAN, S. E. & NIALL, H. D. 1971. Amino-acid sequence of substance P. *Nat New Biol,* 232**,** 86-7.

CHAO, L. K., HUA, K. F., HSU, H. Y., CHENG, S. S., LIN, I. F., CHEN, C. J., CHEN, S. T. & CHANG, S. T. 2008. Cinnamaldehyde inhibits pro-inflammatory cytokines secretion from monocytes/macrophages through suppression of intracellular signaling. *Food Chem Toxicol,* 46**,** 220-31.

CHARKOUDIAN, N. 2003. Skin blood flow in adult human thermoregulation: how it works, when it does not, and why. *Mayo Clin Proc,* 78**,** 603-12.

CHARKOUDIAN, N. 2010. Mechanisms and modifiers of reflex induced cutaneous vasodilation and vasoconstriction in humans. *J Appl Physiol (1985),* 109**,** 1221-8.

CHEN, J., JOSHI, S. K., DIDOMENICO, S., PERNER, R. J., MIKUSA, J. P., GAUVIN, D. M., SEGRETI, J. A., HAN, P., ZHANG, X. F., NIFORATOS, W., BIANCHI, B. R., BAKER, S. J., ZHONG, C., SIMLER, G. H., MCDONALD, H. A., SCHMIDT, R. G., MCGARAUGHTY, S. P., CHU, K. L., FALTYNEK, C. R., KORT, M. E., REILLY, R. M. & KYM, P. R. 2011. Selective blockade of TRPA1 channel attenuates pathological pain without altering noxious cold sensation or body temperature regulation. *Pain,* 152**,** 1165-72.

CHEN, J., KANG, D., XU, J., LAKE, M., HOGAN, J. O., SUN, C., WALTER, K., YAO, B. & KIM, D. 2013. Species differences and molecular determinant of TRPA1 cold sensitivity. *Nat Commun,* 4**,** 2501.

CHEN, J. & KYM, P. R. 2009. TRPA1: the species difference. *J Gen Physiol,* 133**,** 623-5.

CHEN, R. Y. & GUTH, P. H. 1995. Interaction of endogenous nitric oxide and CGRP in sensory neuron-induced gastric vasodilation. *Am J Physiol,* 268**,** G791-6.

CHENG, X. & PANG, C. C. 2004. Increased vasoconstriction to noradrenaline by 1400W, inhibitor of iNOS, in rats with streptozotocin-induced diabetes. *Eur J Pharmacol,* 484**,** 263-8.

CHEUNG, S. S. & DAANEN, H. A. 2012. Dynamic adaptation of the peripheral circulation to cold exposure. *Microcirculation,* 19**,** 65-77.

CHIBA, T., YAMAGUCHI, A., YAMATANI, T., NAKAMURA, A., MORISHITA, T., INUI, T., FUKASE, M., NODA, T. & FUJITA, T. 1989. Calcitonin gene-related peptide receptor antagonist human CGRP-(8-37). *Am J Physiol,* 256**,** E331-5.

CHOI, C. M. & BENNETT, R. G. 2003. Laser Dopplers to determine cutaneous blood flow. *Dermatol Surg,* 29**,** 272-80.

CHOMCZYNSKI, P. & SACCHI, N. 1987. Single-step method of RNA isolation by acid guanidinium thiocyanate-phenol-chloroform extraction. *Anal Biochem,* 162**,** 156-9.

CHOTANI, M. A., FLAVAHAN, S., MITRA, S., DAUNT, D. & FLAVAHAN, N. A. 2000. Silent alpha(2C)-adrenergic receptors enable cold-induced vasoconstriction in cutaneous arteries. *Am J Physiol Heart Circ Physiol,* 278**,** H1075-83.

CHUNG, M. K. & CATERINA, M. J. 2007. TRP channel knockout mice lose their cool. *Neuron,* 54**,** 345-7.

CIARA, M. 1939. Die arterio-venosen Anastomosen. Barth, Leipzig.

CLARA, M. 1959. Le Anastomosi Arteriovenosi. Casa Editrice Dr.Francesco Vallardi: Milano.

CLOUGH, G. F. 1999. Role of nitric oxide in the regulation of microvascular perfusion in human skin in vivo. *J Physiol,* 516 (Pt 2)**,** 549-57.

CLOUGH, G. F. & CHURCH, M. K. 2002. Vascular responses in the skin: an accessible model of inflammation. *News Physiol Sci,* 17**,** 170-4.

COCKS, T. M. & ANGUS, J. A. 1983. Endothelium-dependent relaxation of coronary arteries by noradrenaline and serotonin. *Nature,* 305**,** 627-30.

COFFMAN, J. D. & COHEN, R. A. 1988. Role of alpha-adrenoceptor subtypes mediating sympathetic vasoconstriction in human digits. *Eur J Clin Invest,* 18**,** 309-13.

COLBURN, R. W., LUBIN, M. L., STONE, D. J., JR., WANG, Y., LAWRENCE, D., D'ANDREA, M. R., BRANDT, M. R., LIU, Y., FLORES, C. M. & QIN, N. 2007. Attenuated cold sensitivity in TRPM8 null mice. *Neuron,* 54**,** 379-86.

COLEMAN, J. W., HUANG, Q. & STANWORTH, D. R. 1986. The mast cell response to substance P: effects of neuraminidase, limulin, and some novel synthetic peptide antagonists. *Peptides,* 7**,** 171-5.

CONTI, B., SANCHEZ-ALAVEZ, M., WINSKY-SOMMERER, R., MORALE, M. C., LUCERO, J., BROWNELL, S., FABRE, V., HUITRON-RESENDIZ, S., HENRIKSEN, S., ZORRILLA, E. P., DE LECEA, L. & BARTFAI, T. 2006. Transgenic mice with a reduced core body temperature have an increased life span. *Science,* 314**,** 825-8.

COOKE, J. P. & MARSHALL, J. M. 2005. Mechanisms of Raynaud's disease. *Vasc Med,* 10**,** 293-307.

CORDERO-MORALES, J. F., GRACHEVA, E. O. & JULIUS, D. 2011. Cytoplasmic ankyrin repeats of transient receptor potential A1 (TRPA1) dictate sensitivity to thermal and chemical stimuli. *Proc Natl Acad Sci U S A,* 108**,** E1184-91.

CORDOVA, M. M., WERNER, M. F., SILVA, M. D., RUANI, A. P., PIZZOLATTI, M. G. & SANTOS, A. R. 2011. Further antinociceptive effects of myricitrin in chemical models of overt nociception in mice. *Neurosci Lett,* 495**,** 173-7.

COREY, D. P., GARCIA-ANOVEROS, J., HOLT, J. R., KWAN, K. Y., LIN, S. Y., VOLLRATH, M. A., AMALFITANO, A., CHEUNG, E. L., DERFLER, B. H., DUGGAN, A., GELEOC, G. S., GRAY, P. A., HOFFMAN, M. P., REHM, H. L., TAMASAUSKAS, D. & ZHANG, D. S. 2004. TRPA1 is a candidate for the mechanosensitive transduction channel of vertebrate hair cells. *Nature,* 432**,** 723-30.

COSENS, D. J. & MANNING, A. 1969. Abnormal electroretinogram from a Drosophila mutant. *Nature,* 224**,** 285-7.

COUTURE, R., LANEUVILLE, O., GUIMOND, C., DRAPEAU, G. & REGOLI, D. 1989. Characterization of the peripheral action of neurokinins and neurokinin receptor selective agonists on the rat cardiovascular system. *Naunyn Schmiedebergs Arch Pharmacol,* 340**,** 547-57.

CRAIG, A. D., REIMAN, E. M., EVANS, A. & BUSHNELL, M. C. 1996. Functional imaging of an illusion of pain. *Nature,* 384**,** 258-260.

CVETKOV, T. L., HUYNH, K. W., COHEN, M. R. & MOISEENKOVA-BELL, V. Y. 2011. Molecular architecture and subunit organization of TRPA1 ion channel revealed by electron microscopy. *J Biol Chem,* 286**,** 38168-76.

DAANEN, H. A. 2001. Cold injury risk of marines *TNO Human factors.* Soesterberg.

DAANEN, H. A. 2003. Finger cold-induced vasodilation: a review. *Eur J Appl Physiol,* 89**,** 411-26.

DAANEN, H. A. & DUCHARME, M. B. 2000. Axon reflexes in human cold exposed fingers. *Eur J Appl Physiol,* 81**,** 240-4.

DAANEN, H. A. & VAN DE LINDE, F. J. 1992. Comparison of four noninvasive rewarming methods for mild hypothermia. *Aviat Space Environ Med,* 63**,** 1070-6.

DAANEN, H. A., VAN DE LINDE, F. J., ROMET, T. T. & DUCHARME, M. B. 1997. The effect of body temperature on the hunting response of the middle finger skin temperature. *Eur J Appl Physiol Occup Physiol,* 76**,** 538-43.

DAANEN, H. A. & VAN DER STRUIJS, N. R. 2005. Resistance Index of Frostbite as a predictor of cold injury in arctic operations. *Aviat Space Environ Med,* 76**,** 1119-22.

DAANEN, H. A. M. 1991. Arterio-venous anastomoses and thermoregulation. The Netherlands: TNO Institute for Perception Group: Thermophysiology.

DALE, H. H. & FELDBERG, W. 1934. The chemical transmission of secretory impulses to the sweat glands of the cat. *J Physiol,* 82**,** 121-8.

DAS, D. K., RUSSELL, J. C. & JONES, R. M. 1991. Reduction of cold injury by superoxide dismutase and catalase. *Free Radic Res Commun,* 12-13 Pt 2**,** 653-62.

DE HOON, J. N., PICKKERS, P., SMITS, P., STRUIJKER-BOUDIER, H. A. & VAN BORTEL, L. M. 2003. Calcitonin gene-related peptide: exploring its vasodilating mechanism of action in humans. *Clin Pharmacol Ther,* 73**,** 312-21.

DEFALCO, J., STEIGER, D., GUSTAFSON, A., EMERLING, D. E., KELLY, M. G. & DUNCTON, M. A. 2010. Oxime derivatives related to AP18: Agonists and antagonists of the TRPA1 receptor. *Bioorg Med Chem Lett,* 20**,** 276-9.

DEL CAMINO, D., MURPHY, S., HEIRY, M., BARRETT, L. B., EARLEY, T. J., COOK, C. A., PETRUS, M. J., ZHAO, M., D'AMOURS, M., DEERING, N., BRENNER, G. J., COSTIGAN, M., HAYWARD, N. J., CHONG, J. A., FANGER, C. M., WOOLF, C. J., PATAPOUTIAN, A. & MORAN, M. M. 2010. TRPA1 contributes to cold hypersensitivity. *J Neurosci,* 30**,** 15165-74.

DENDA, M., TSUTSUMI, M. & DENDA, S. 2010a. Topical application of TRPM8 agonists accelerates skin permeability barrier recovery and reduces epidermal proliferation induced by barrier insult: role of cold-sensitive TRP receptors in epidermal permeability barrier homoeostasis. *Exp Dermatol,* 19**,** 791-5.

DENDA, M., TSUTSUMI, M., GOTO, M., IKEYAMA, K. & DENDA, S. 2010b. Topical application of TRPA1 agonists and brief cold exposure accelerate skin permeability barrier recovery. *J Invest Dermatol,* 130**,** 1942-5.

DENNIS, T., FOURNIER, A., ST PIERRE, S. & QUIRION, R. 1989. Structure-activity profile of calcitonin gene-related peptide in peripheral and brain tissues. Evidence for receptor multiplicity. *J Pharmacol Exp Ther,* 251**,** 718-25.

DHAKA, A., MURRAY, A. N., MATHUR, J., EARLEY, T. J., PETRUS, M. J. & PATAPOUTIAN, A. 2007. TRPM8 is required for cold sensation in mice. *Neuron,* 54**,** 371-8.

DIXIT, B. N., GULATI, O. D. & GOKHALE, S. D. 1961. Action of bretylium and guanethidine at the neuromuscular junction. *Br J Pharmacol Chemother,* 17**,** 372-9.

DONG, Y., SHI, H. L., SHI, J. R. & WU, D. Z. 2010. Transient receptor potential A1 is involved in cold-induced contraction in the isolated rat colon smooth muscle. *Sheng Li Xue Bao,* 62**,** 349-56.

DOODS, H., HALLERMAYER, G., WU, D., ENTZEROTH, M., RUDOLF, K., ENGEL, W. & EBERLEIN, W. 2000. Pharmacological profile of BIBN4096BS, the first selective small molecule CGRP antagonist. *Br J Pharmacol,* 129**,** 420-3.

DUBOIS-RANDE, J. L., DUPOUY, P., APTECAR, E., BHATIA, A., TEIGER, E., HITTINGER, L., BERDEAUX, A., CASTAIGNE, A. & GESCHWIND, H. 1995. Comparison of the effects of exercise and cold pressor test on the vasomotor response of normal and atherosclerotic coronary arteries and their relation to the flow-mediated mechanism. *Am J Cardiol,* 76**,** 467-73.

DUNHAM, J. P., LEITH, J. L., LUMB, B. M. & DONALDSON, L. F. 2010. Transient receptor potential channel A1 and noxious cold responses in rat cutaneous nociceptors. *Neuroscience,* 165**,** 1412-9.

DUNN, A. K., BOLAY, H., MOSKOWITZ, M. A. & BOAS, D. A. 2001. Dynamic imaging of cerebral blood flow using laser speckle. *J Cereb Blood Flow Metab,* 21**,** 195-201.

DUNN, W. R., WALLIS, S. J. & GARDINER, S. M. 1998. Remodelling and enhanced myogenic tone in cerebral resistance arteries isolated from genetically hypertensive Brattleboro rats. *J Vasc Res,* 35**,** 18-26.

DURAKU, L. S., SMITS, E. S., NIEHOF, S. P., HOVIUS, S. E., WALBEEHM, E. T. & SELLES, R. W. 2012. Thermoregulation in peripheral nerve injury-induced cold-intolerant rats. *J Plast Reconstr Aesthet Surg,* 65**,** 771-9.

EARLEY, S. 2012. TRPA1 channels in the vasculature. *Br J Pharmacol,* 167**,** 13-22.

EARLEY, S. TRP channels in cerebral arteries. 37th Congress of IUPS, 2013 (Birmingham, UK. Proceedings of The Physiological Society, SA227.

EARLEY, S., GONZALES, A. L. & CRNICH, R. 2009. Endothelium-dependent cerebral artery dilation mediated by TRPA1 and Ca2+-Activated K+ channels. *Circ Res,* 104**,** 987-94.

EBERHARDT, M. J., FILIPOVIC, M. R., LEFFLER, A., DE LA ROCHE, J., KISTNER, K., FISCHER, M. J., FLEMING, T., ZIMMERMANN, K., IVANOVIC-BURMAZOVIC, I., NAWROTH, P. P., BIERHAUS, A., REEH, P. W. & SAUER, S. K. 2012. Methylglyoxal activates nociceptors through transient receptor potential channel A1 (TRPA1): a possible mechanism of metabolic neuropathies. *J Biol Chem,* 287**,** 28291-306.

EBNER, K. & SINGEWALD, N. 2006. The role of substance P in stress and anxiety responses. *Amino Acids,* 31**,** 251-72.

EDBROOKE, M. R., PARKER, D., MCVEY, J. H., RILEY, J. H., SORENSON, G. D., PETTENGILL, O. S. & CRAIG, R. K. 1985. Expression of the human calcitonin/CGRP gene in lung and thyroid carcinoma. *EMBO J,* 4**,** 715-24.

EDELMAYER, R. M., LE, L. N., YAN, J., WEI, X., NASSINI, R., MATERAZZI, S., PRETI, D., APPENDINO, G., GEPPETTI, P., DODICK, D. W., VANDERAH, T. W., PORRECA, F. & DUSSOR, G. 2012. Activation of TRPA1 on dural afferents: a potential mechanism of headache pain. *Pain,* 153**,** 1949-58.

EDVINSSON, L., FREDHOLM, B. B., HAMEL, E., JANSEN, I. & VERRECCHIA, C. 1985. Perivascular peptides relax cerebral arteries concomitant with stimulation of cyclic adenosine monophosphate accumulation or release of an endothelium-derived relaxing factor in the cat. *Neurosci Lett,* 58**,** 213-7.

EDWARDS, M. A. 1967. The role of arteriovenous anastomoses in cold-induced vasodilation, rewarming, and reactive hyperemia as determined by 24Na clearance. *Can J Physiol Pharmacol,* 45**,** 39-48.

EGHIANRUWA, K. I. & EYRE, P. 1991. The isolated, perfused bovine ear. A model for pharmacological study of cutaneous vasculature and anaphylaxis. *Vet Res Commun,* 15**,** 117-25.

EID, A. H., MAITI, K., MITRA, S., CHOTANI, M. A., FLAVAHAN, S., BAILEY, S. R., THOMPSON-TORGERSON, C. S. & FLAVAHAN, N. A. 2007. Estrogen increases smooth muscle expression of alpha2C-adrenoceptors and cold-induced constriction of cutaneous arteries. *Am J Physiol Heart Circ Physiol,* 293**,** H1955-61.

EID, S. R., CROWN, E. D., MOORE, E. L., LIANG, H. A., CHOONG, K. C., DIMA, S., HENZE, D. A., KANE, S. A. & URBAN, M. O. 2008. HC-030031, a TRPA1 selective antagonist, attenuates inflammatory- and neuropathy-induced mechanical hypersensitivity. *Mol Pain,* 4**,** 48.

EIDE, R. 1976. Physiological and behavioral reactions to repeated tail cooling in the white rat. *J Appl Physiol,* 41**,** 292-4.

EISENHOFER, G., KOPIN, I. J. & GOLDSTEIN, D. S. 2004. Catecholamine metabolism: a contemporary view with implications for physiology and medicine. *Pharmacol Rev,* 56**,** 331-49.

EKENVALL, L., LINDBLAD, L. E., NORBECK, O. & ETZELL, B. M. 1988. alpha-Adrenoceptors and cold-induced vasoconstriction in human finger skin. *Am J Physiol,* 255**,** H1000-3.

EL KARIM, I. A., LINDEN, G. J., CURTIS, T. M., ABOUT, I., MCGAHON, M. K., IRWIN, C. R., KILLOUGH, S. A. & LUNDY, F. T. 2011. Human dental pulp fibroblasts express the "cold-sensing" transient receptor potential channels TRPA1 and TRPM8. *J Endod,* 37**,** 473-8.

ELKINGTON, E. J. 1968. Finger blood flow in Antarctica. *J Physiol,* 199**,** 1-10.

EMERY, R. W., ESTRIN, J. A., WAHLER, G. M. & FOX, I. J. 1983. The left ventricular mechanoreceptor reflex: characterisation of the afferent pathway. *Cardiovasc Res,* 17**,** 214-22.

EMONDS-ALT, X., DOUTREMEPUICH, J. D., HEAULME, M., NELIAT, G., SANTUCCI, V., STEINBERG, R., VILAIN, P., BICHON, D., DUCOUX, J. P., PROIETTO, V. & ET AL. 1993. In vitro and in vivo biological activities of SR140333, a novel potent non-peptide tachykinin NK1 receptor antagonist. *Eur J Pharmacol,* 250**,** 403-13.

ENGEL, M. A., LEFFLER, A., NIEDERMIRTL, F., BABES, A., ZIMMERMANN, K., FILIPOVIC, M. R., IZYDORCZYK, I., EBERHARDT, M., KICHKO, T. I., MUELLER-TRIBBENSEE, S. M., KHALIL, M., SIKLOSI, N., NAU, C., IVANOVIC-

BURMAZOVIC, I., NEUHUBER, W. L., BECKER, C., NEURATH, M. F. & REEH, P. W. 2011. TRPA1 and substance P mediate colitis in mice. *Gastroenterology,* 141**,** 1346-58.

ESLER, M., JENNINGS, G., LAMBERT, G., MEREDITH, I., HORNE, M. & EISENHOFER, G. 1990. Overflow of catecholamine neurotransmitters to the circulation: source, fate, and functions. *Physiol Rev,* 70**,** 963-85.

EULER, H. V. & NILSSON, R. 1931. Note on the activation of oxido-reductions by co-zymase. *Biochem J,* 25**,** 2168-71.

EVANS, B. N., ROSENBLATT, M. I., MNAYER, L. O., OLIVER, K. R. & DICKERSON, I. M. 2000. CGRP-RCP, a novel protein required for signal transduction at calcitonin gene-related peptide and adrenomedullin receptors. *J Biol Chem,* 275**,** 31438-43.

EVERAERTS, W., VRIENS, J., OWSIANIK, G., APPENDINO, G., VOETS, T., DE RIDDER, D. & NILIUS, B. 2010. Functional characterization of transient receptor potential channels in mouse urothelial cells. *Am J Physiol Renal Physiol,* 298**,** F692-701.

FABER, J. E. 1988. Effect of local tissue cooling on microvascular smooth muscle and postjunctional alpha 2-adrenoceptors. *Am J Physiol,* 255**,** H121-30.

FANG, L., CHEN, M. F., XIAO, Z. L., LIU, Y., YU, G. L., CHEN, X. B. & XIE, X. M. 2011. Calcitonin gene-related peptide released from endothelial progenitor cells inhibits the proliferation of rat vascular smooth muscle cells induced by angiotensin II. *Mol Cell Biochem,* 355**,** 99-108.

FERNANDES, E. S., FERNANDES, M. A. & KEEBLE, J. E. 2012. The functions of TRPA1 and TRPV1: moving away from sensory nerves. *Br J Pharmacol,* 166**,** 510-21.

FERNANDES, E. S., RUSSELL, F. A., SPINA, D., MCDOUGALL, J. J., GRAEPEL, R., GENTRY, C., STANILAND, A. A., MOUNTFORD, D. M., KEEBLE, J. E., MALCANGIO, M., BEVAN, S. & BRAIN, S. D. 2011. A distinct role for transient receptor potential ankyrin 1, in addition to transient receptor potential vanilloid 1, in tumor necrosis factor alpha-induced inflammatory hyperalgesia and Freund's complete adjuvant-induced monarthritis. *Arthritis Rheum,* 63**,** 819-29.

FERNANDES, E. S., VONG, C. T., QUEK, S., CHEONG, J., AWAL, S., GENTRY, C., AUBDOOL, A. A., LIANG, L., BODKIN, J. V., BEVAN, S., HEADS, R. & BRAIN, S. D. 2013. Superoxide generation and leukocyte accumulation: key elements in the mediation of leukotriene B(4)-induced itch by transient receptor potential ankyrin 1 and transient receptor potential vanilloid 1. *FASEB J,* 27**,** 1664-73.

FERNANDES, M., KEEBLE, J. 2011a. The Differing Effects Of Various TRPV1 And TRPA1 Antagonists On Capsaicin- And Mustard Oil- Induced Changes In Blood Flow In Mice. *Proceedings of the British Pharmacological Society.***,** pA2 online.

FERNANDES, M. A., KEEBLE, J. 2011b. The Effects Of The TRPA1 Antagonists TCS5861528 And HC030031 On Core Body Temperature And Activity Of Conscious Mice. *BPS Winter Meeting 2011*. London: PA2 online

FERNANDEZ, N., MONGE, L., GARCIA-VILLALON, A. L., GARCIA, J. L., GOMEZ, B. & DIEGUEZ, G. 1994. Cooling effects on nitric oxide production by rabbit ear and femoral arteries during cholinergic stimulation. *Br J Pharmacol,* 113**,** 550-4.

FIEBICH, B. L., SCHLEICHER, S., BUTCHER, R. D., CRAIG, A. & LIEB, K. 2000. The neuropeptide substance P activates p38 mitogen-activated protein kinase resulting in IL-6 expression independently from NF-kappa B. *J Immunol,* 165**,** 5606-11.

FLAVAHAN, N. A., LINDBLAD, L. E., VERBEUREN, T. J., SHEPHERD, J. T. & VANHOUTTE, P. M. 1985. Cooling and alpha 1- and alpha 2-adrenergic responses in cutaneous veins: role of receptor reserve. *Am J Physiol,* 249**,** H950-5.

FLOURIS, A. D. & CHEUNG, S. S. 2009. Influence of thermal balance on cold-induced vasodilation. *J Appl Physiol (1985),* 106**,** 1264-71.

FLOURIS, A. D., WESTWOOD, D. A., MEKJAVIC, I. B. & CHEUNG, S. S. 2008. Effect of body temperature on cold induced vasodilation. *Eur J Appl Physiol,* 104**,** 491-9.

FOLKOW, B., FOX, R. H., KROG, J., ODELRAM, H. & THOREN, O. 1963. Studies on the Reactions of the Cutaneous Vessels to Cold Exposure. *Acta Physiol Scand,* 58**,** 342-54.

FOREMAN, J. & JORDAN, C. 1983. Histamine release and vascular changes induced by neuropeptides. *Agents Actions,* 13**,** 105-16.

FORSTERMANN, U. & KLEINERT, H. 1995. Nitric oxide synthase: expression and expressional control of the three isoforms. *Naunyn Schmiedebergs Arch Pharmacol,* 352**,** 351-64.

FORSTERMANN, U. & MUNZEL, T. 2006. Endothelial nitric oxide synthase in vascular disease: from marvel to menace. *Circulation,* 113**,** 1708-14.

FOX, R. H. & WYATT, H. T. 1962. Cold-induced vasodilatation in various areas of the body surface of man. *J Physiol,* 162**,** 289-97.

FRANZ, D. R. 1985. The effects of indomethacin on cold-induced vasodilation in the cat. *J Therm Biol,* 10**,** 245-248.

FREEDMAN, R. R., SABHARWAL, S. C., MOTEN, M. & MIGALY, P. 1992. Local temperature modulates alpha 1- and alpha 2-adrenergic vasoconstriction in men. *Am J Physiol,* 263**,** H1197-200.

GANTEN, D., PAUL, M. & LANG, R. E. 1991. The role of neuropeptides in cardiovascular regulation. *Cardiovasc Drugs Ther,* 5**,** 119-30.

GARCIA-ANOVEROS, J. & NAGATA, K. 2007. Trpa1. *Handb Exp Pharmacol***,** 347-62.

GARCIA-VILLALON, A. L., FERNANDEZ, N., MONGE, L., GARCIA, J. L., GOMEZ, B. & DIEGUEZ, G. 1995. Role of nitric oxide and potassium channels in the cholinergic relaxation of rabbit ear and femoral arteries: effects of cooling. *J Vasc Res,* 32**,** 387-97.

GARCIA-VILLALON, A. L., MONGE, L., MONTOYA, J. J., GARCIA, J. L., FERNANDEZ, N., GOMEZ, B. & DIEGUEZ, G. 1992. Cooling and response to adrenoceptor agonists of rabbit ear and femoral artery: role of the endothelium. *Br J Pharmacol,* 106**,** 727-32.

GARDINER, S. M., COMPTON, A. M., KEMP, P. A., BENNETT, T., BOSE, C., FOULKES, R. & HUGHES, B. 1991. Antagonistic effect of human alpha-calcitonin gene-related peptide (8-37) on regional hemodynamic actions of rat islet amyloid polypeptide in conscious Long-Evans rats. *Diabetes,* 40**,** 948-51.

GARDNER, C. A. & WEBB, R. C. 1986. Cold-induced vasodilatation in isolated, perfused rat tail artery. *Am J Physiol,* 251**,** H176-81.

GARVEY, E. P., OPLINGER, J. A., FURFINE, E. S., KIFF, R. J., LASZLO, F., WHITTLE, B. J. & KNOWLES, R. G. 1997. 1400W is a slow, tight binding, and highly selective inhibitor of inducible nitric-oxide synthase in vitro and in vivo. *J Biol Chem,* 272**,** 4959-63.

GAVVA, N. R., TAMIR, R., QU, Y., KLIONSKY, L., ZHANG, T. J., IMMKE, D., WANG, J., ZHU, D., VANDERAH, T. W., PORRECA, F., DOHERTY, E. M., NORMAN, M. H., WILD, K. D., BANNON, A. W., LOUIS, J. C. & TREANOR, J. J. 2005. AMG 9810 [(E)-3-(4-t-butylphenyl)-N-(2,3-dihydrobenzo[b][1,4] dioxin-6-yl)acrylamide], a novel vanilloid receptor 1 (TRPV1) antagonist with antihyperalgesic properties. *J Pharmacol Exp Ther,* 313**,** 474-84.

GENNARI, C. & FISCHER, J. A. 1985. Cardiovascular action of calcitonin gene-related peptide in humans. *Calcif Tissue Int,* 37**,** 581-4.

GENTRY, C., STOAKLEY, N., ANDERSSON, D. A. & BEVAN, S. 2010. The roles of iPLA2, TRPM8 and TRPA1 in chemically induced cold hypersensitivity. *Mol Pain,* 6**,** 4.

GIBBINS, I. L., FURNESS, J. B., COSTA, M., MACINTYRE, I., HILLYARD, C. J. & GIRGIS, S. 1985. Co-localization of calcitonin gene-related peptide-like immunoreactivity with substance P in cutaneous, vascular and visceral sensory neurons of guinea pigs. *Neurosci Lett,* 57**,** 125-30.

GOLDSTEIN, D. S., MCCARTY, R., POLINSKY, R. J. & KOPIN, I. J. 1983. Relationship between plasma norepinephrine and sympathetic neural activity. *Hypertension,* 5**,** 552-9.

GOUNDRY, B., BELL, L., LANGTREE, M. & MOORTHY, A. 2012. Diagnosis and management of Raynaud's phenomenon. *BMJ,* 344**,** e289.

GOZAL, D., TORRES, J. E., GOZAL, Y. M. & LITTWIN, S. M. 1996. Effect of nitric oxide synthase inhibition on cardiorespiratory responses in the conscious rat. *J Appl Physiol (1985),* 81**,** 2068-77.

GRAEPEL, R. 2009. *An investigation of the TRPA1 and TRPV1 receptors in peripheral nociception and vascular responses.* Doctor of Philosophy, King's College London

GRAEPEL, R., FERNANDES, E. S., AUBDOOL, A. A., ANDERSSON, D. A., BEVAN, S. & BRAIN, S. D. 2011. 4-oxo-2-nonenal (4-ONE): evidence of transient receptor potential ankyrin 1-dependent and -independent nociceptive and vasoactive responses in vivo. *J Pharmacol Exp Ther,* 337**,** 117-24.

GRANT, A. D., GERARD, N. P. & BRAIN, S. D. 2002. Evidence of a role for NK1 and CGRP receptors in mediating neurogenic vasodilatation in the mouse ear. *Br J Pharmacol,* 135**,** 356-62.

GRANT, A. D., PINTER, E., SALMON, A. M. & BRAIN, S. D. 2005. An examination of neurogenic mechanisms involved in mustard oil-induced inflammation in the mouse. *Eur J Pharmacol,* 507**,** 273-80.

GRANT, A. D., TAM, C. W., LAZAR, Z., SHIH, M. K. & BRAIN, S. D. 2004. The calcitonin gene-related peptide (CGRP) receptor antagonist BIBN4096BS blocks CGRP and adrenomedullin vasoactive responses in the microvasculature. *Br J Pharmacol,* 142**,** 1091-8.

GRANT, R. T. 1930. Observations and direct communication between arteries and veins in the rabbit ear *Heart* 5**,** 281-303.

GRANT, R. T., BLAND, E.F. 1931. Observations on arteriovenous anastomoses in human skin and the bird's foot with special reference to the reaction to cold *Heart* 15**,** 385-407.

GRAVES, J. E., LEWIS, S. J. & KOOY, N. W. 1998. Peroxynitrite-mediated vasorelaxation: evidence against the formation of circulating S-nitrosothiols. *Am J Physiol,* 274**,** H1001-8.

GRAY, D. W. & MARSHALL, I. 1992a. Human alpha-calcitonin gene-related peptide stimulates adenylate cyclase and guanylate cyclase and relaxes rat thoracic aorta by releasing nitric oxide. *Br J Pharmacol,* 107**,** 691-6.

GRAY, D. W. & MARSHALL, I. 1992b. Nitric oxide synthesis inhibitors attenuate calcitonin gene-related peptide endothelium-dependent vasorelaxation in rat aorta. *Eur J Pharmacol,* 212**,** 37-42.

GRAY, D. W. & MARSHALL, I. 1992c. A pharmacological profile of the endothelium-derived relaxant factor released by calcitonin gene-related peptide in rat aorta. *Ann N Y Acad Sci,* 657**,** 517-8.

GREENE, E. G. 2001. *Anatomy of the rat* New York, Hafner Press.

GREENFIELD, A. D., SHEPHERD, J. T. & WHELAN, R. F. 1951a. The part played by the nervous system in the response to cold of the circulation through the finger tip. *Clin Sci (Lond),* 10**,** 347-60.

GREENFIELD, A. D., SHEPHERD, J. T. & WHELAN, R. F. 1951b. The part played by the nervous system in the response to cold of the circulation through the finger tip. *J Physiol,* 115**,** 10p-1p.

GREISHMAN, S. E. 1954. The reaction of the capillary bed of the nailfold to the continous intravenous infusion of levo-norepihephrine in patients with normal blood pressure and with essential hypertension. *Journal of Clinical Investigation* 33**,** 975-983.

GRIFFITH, O. W. & STUEHR, D. J. 1995. Nitric oxide synthases: properties and catalytic mechanism. *Annu Rev Physiol,* 57**,** 707-36.

GULER, A. D., LEE, H., IIDA, T., SHIMIZU, I., TOMINAGA, M. & CATERINA, M. 2002. Heat-evoked activation of the ion channel, TRPV4. *J Neurosci,* 22**,** 6408-14.

GUZIK, T. J. & CHANNON, K. M. 2005. Measurement of vascular reactive oxygen species production by chemiluminescence. *Methods Mol Med,* 108**,** 73-89.

HALE, A. R. & BURCH, G. E. 1960. The arteriovenous anastomoses and blood vessels of the human finger. Morphological and functional aspects. *Medicine (Baltimore),* 39**,** 191-240.

HALES, J. R., FAWCETT, A. A., BENNETT, J. W. & NEEDHAM, A. D. 1978. Thermal control of blood flow through capillaries and arteriovenous anastomoses in skin of sheep. *Pflugers Arch,* 378**,** 55-63.

HALLIWELL, B. 1997. What nitrates tyrosine? Is nitrotyrosine specific as a biomarker of peroxynitrite formation in vivo? *FEBS Lett,* 411**,** 157-60.

HAMBERG, M., SVENSSON, J. & SAMUELSSON, B. 1975. Thromboxanes: a new group of biologically active compounds derived from prostaglandin endoperoxides. *Proc Natl Acad Sci U S A,* 72**,** 2994-8.

HARADA, M., HIRAYAMA, Y. & YAMAZAKI, R. 1982. Pharmacological studies on Chinese cinnamon. V. Catecholamine releasing effect of cinnamaldehyde in dogs. *J Pharmacobiodyn,* 5**,** 539-46.

HARADA, M. & YANO, S. 1975. Pharmacological studies on Chinese cinammon. II. Effects of cinnamaldehyde on the cardiovascular and digestive systems. *Chem Pharm Bull (Tokyo),* 23**,** 941-7.

HARDIE, R. C. & MINKE, B. 1992. The trp gene is essential for a light-activated Ca2+ channel in Drosophila photoreceptors. *Neuron,* 8**,** 643-51.

HARGREAVES, R., FERREIRA, J. C., HUGHES, D., BRANDS, J., HALE, J., MATTSON, B. & MILLS, S. 2011. Development of aprepitant, the first neurokinin-1 receptor antagonist for the prevention of chemotherapy-induced nausea and vomiting. *Ann N Y Acad Sci,* 1222**,** 40-8.

HARLAN, J. M. & HARKER, L. A. 1981. Hemostasis, thrombosis, and thromboembolic disorders. The role of arachidonic acid metabolites in platelet-vessel wall interactions. *Med Clin North Am,* 65**,** 855-80.

HARMAR, A., SCHOFIELD, J. G. & KEEN, P. 1981. Substance P biosynthesis in dorsal root ganglia: an immunochemical study of [35S]methionine and [3H]proline incorporation in vitro. *Neuroscience,* 6**,** 1917-22.

HATANO, N., ITOH, Y., SUZUKI, H., MURAKI, Y., HAYASHI, H., ONOZAKI, K., WOOD, I. C., BEECH, D. J. & MURAKI, K. 2012. Hypoxia-inducible factor-1alpha (HIF1alpha) switches on transient receptor potential ankyrin repeat 1 (TRPA1) gene expression via a hypoxia response element-like motif to modulate cytokine release. *J Biol Chem,* 287**,** 31962-72.

HEIN, L., ALTMAN, J. D. & KOBILKA, B. K. 1999. Two functionally distinct alpha2-adrenergic receptors regulate sympathetic neurotransmission. *Nature,* 402**,** 181-4.

HEISS, E., HERHAUS, C., KLIMO, K., BARTSCH, H. & GERHAUSER, C. 2001. Nuclear factor kappa B is a molecular target for sulforaphane-mediated anti-inflammatory mechanisms. *J Biol Chem,* 276**,** 32008-15.

HERRICK, A. L. 2013. Management of Raynaud's phenomenon and digital ischemia. *Curr Rheumatol Rep,* 15**,** 303.

HEYER, G., HORNSTEIN, O. P. & HANDWERKER, H. O. 1991. Reactions to intradermally injected substance P and topically applied mustard oil in atopic dermatitis patients. *Acta Derm Venereol,* 71**,** 291-5.

HINMAN, A., CHUANG, H. H., BAUTISTA, D. M. & JULIUS, D. 2006. TRP channel activation by reversible covalent modification. *Proc Natl Acad Sci U S A,* 103**,** 19564-8.

HIRAI, K., HORVATH, S. M. & WEINSTEIN, V. 1970. Differences in the vascular hunting reaction between Caucasians and Japanese. *Angiology,* 21**,** 502-10.

HODGES, G. J., KOSIBA, W. A., ZHAO, K. & JOHNSON, J. M. 2009. The involvement of heating rate and vasoconstrictor nerves in the cutaneous vasodilator response to skin warming. *Am J Physiol Heart Circ Physiol,* 296**,** H51-6.

HODGES, G. J., TRAEGER, J. A., 3RD, TANG, T., KOSIBA, W. A., ZHAO, K. & JOHNSON, J. M. 2007. Role of sensory nerves in the cutaneous vasoconstrictor response to local cooling in humans. *Am J Physiol Heart Circ Physiol,* 293**,** H784-9.

HODGES, G. J., ZHAO, K., KOSIBA, W. A. & JOHNSON, J. M. 2006. The involvement of nitric oxide in the cutaneous vasoconstrictor response to local cooling in humans. *J Physiol,* 574**,** 849-57.

HOLOM, V. H., MESSLINGER, K. & FISCHER, M. J. 2008. Temperature-dependent neuronal regulation of arterial blood flow in rat cranial dura mater. *J Neurosci Res,* 86**,** 158-64.

HOLSTEGE, G., KUYPERS, H. G. & DEKKER, J. J. 1977. The organization of the bulbar fibre connections to the trigeminal, facial and hypoglossal motor nuclei. II. An autoradiographic tracing study in cat. *Brain,* 100**,** 264-86.

HOLZER, P. 1991. Capsaicin: cellular targets, mechanisms of action, and selectivity for thin sensory neurons. *Pharmacol Rev,* 43**,** 143-201.

HOLZER, P. 1992. Peptidergic sensory neurons in the control of vascular functions: mechanisms and significance in the cutaneous and splanchnic vascular beds. *Rev Physiol Biochem Pharmacol,* 121**,** 49-146.

HONDA, M., SUZUKI, M., NAKAYAMA, K. & ISHIKAWA, T. 2007. Role of alpha2C-adrenoceptors in the reduction of skin blood flow induced by local cooling in mice. *Br J Pharmacol,* 152**,** 91-100.

HORNYAK, M. E., NAVER, H. K., RYDENHAG, B. & WALLIN, B. G. 1990. Sympathetic activity influences the vascular axon reflex in the skin. *Acta Physiol Scand,* 139**,** 77-84.

HOU, Q., BARR, T., GEE, L., VICKERS, J., WYMER, J., BORSANI, E., RODELLA, L., GETSIOS, S., BURDO, T., EISENBERG, E., GUHA, U., LAVKER, R., KESSLER, J., CHITTUR, S., FIORINO, D., RICE, F. & ALBRECHT, P. 2011. Keratinocyte expression of calcitonin gene-related peptide beta: implications for neuropathic and inflammatory pain mechanisms. *Pain,* 152**,** 2036-51.

HU, W., YANG, M., CHANG, J., SHEN, Z., GU, T., DENG, A. & GU, X. 2012. Laser doppler perfusion imaging of skin territory to reflect autonomic functional recovery following sciatic nerve autografting repair in rats. *Microsurgery,* 32**,** 136-43.

HUANG, D., LI, S., DHAKA, A., STORY, G. M. & CAO, Y. Q. 2012. Expression of the transient receptor potential channels TRPV1, TRPA1 and TRPM8 in mouse trigeminal primary afferent neurons innervating the dura. *Mol Pain,* 8**,** 66.

HUMEAU, A., CHAPEAU-BLONDEAU, F., ROUSSEAU, D. & ABRAHAM, P. 2007a. Numerical simulation of laser Doppler flowmetry signals based on a model of nonlinear coupled oscillators. Comparison with real data in the frequency domain. *Conf Proc IEEE Eng Med Biol Soc,* 2007**,** 4068-71.

HUMEAU, A., STEENBERGEN, W., NILSSON, H. & STROMBERG, T. 2007b. Laser Doppler perfusion monitoring and imaging: novel approaches. *Med Biol Eng Comput,* 45**,** 421-35.

HURLEY, H. J., JR. & MESCON, H. 1956. Cholinergic innervation of the digital arteriovenous anastomoses of human skin; a histochemical localization of cholinesterase. *J Appl Physiol,* 9**,** 82-4.

HWANG, S. J., OH, J. M. & VALTSCHANOFF, J. G. 2005. The majority of bladder sensory afferents to the rat lumbosacral spinal cord are both IB4- and CGRP-positive. *Brain Res,* 1062**,** 86-91.

IKEBE, M. & HARTSHORNE, D. J. 1985. Phosphorylation of smooth muscle myosin at two distinct sites by myosin light chain kinase. *J Biol Chem,* 260**,** 10027-31.

IKEDA, Y., BRELSFORD, K. L., IKEDA, K., BULKLEY, G. B. & LONG, D. M. 1990. Effect of superoxide dismutase in cats with cold-induced edema. *Adv Neurol,* 52**,** 203-10.

INOKUCHI, K., HIROOKA, Y., SHIMOKAWA, H., SAKAI, K., KISHI, T., ITO, K., KIMURA, Y. & TAKESHITA, A. 2003. Role of endothelium-derived hyperpolarizing factor in human forearm circulation. *Hypertension,* 42**,** 919-24.

INOUE, H., ASAKA, T., NAGATA, N. & KOSHIHARA, Y. 1997. Mechanism of mustard oil-induced skin inflammation in mice. *Eur J Pharmacol,* 333**,** 231-40.

ITABASHI, A., KASHIWABARA, H., SHIBUYA, M., TANAKA, K., MASAOKA, H., KATAYAMA, S. & ISHII, J. 1988. The interaction of calcitonin gene-related peptide with angiotensin II on blood pressure and renin release. *J Hypertens Suppl,* 6**,** S418-20.

ITO, N., RUEGG, U. T., KUDO, A., MIYAGOE-SUZUKI, Y. & TAKEDA, S. 2013. Activation of calcium signaling through Trpv1 by nNOS and peroxynitrite as a key trigger of skeletal muscle hypertrophy. *Nat Med,* 19**,** 101-6.

IWASE, S., CUI, J., WALLIN, B. G., KAMIYA, A. & MANO, T. 2002. Effects of increased ambient temperature on skin sympathetic nerve activity and core temperature in humans. *Neurosci Lett,* 327**,** 37-40.

IZZARD, A. S., BUND, S. J. & HEAGERTY, A. M. 1996. Myogenic tone in mesenteric arteries from spontaneously hypertensive rats. *Am J Physiol,* 270**,** H1-6.

JACQUOT, L., MONNIN, J., LUCARZ, A. & BRAND, G. 2005. Trigeminal sensitization and desensitization in the nasal cavity: a study of cross interactions. *Rhinology,* 43**,** 93-8.

JAIN, A., BRONNEKE, S., KOLBE, L., STAB, F., WENCK, H. & NEUFANG, G. 2011. TRP-channel-specific cutaneous eicosanoid release patterns. *Pain,* 152**,** 2765-72.

JANCSO, N., JANCSO-GABOR, A. & SZOLCSANYI, J. 1967. Direct evidence for neurogenic inflammation and its prevention by denervation and by pretreatment with capsaicin. *Br J Pharmacol Chemother,* 31**,** 138-51.

JANSKY, L., MATOUSKOVA, E., VAVRA, V., VYBIRAL, S., JANSKY, P., JANDOVA, D., KNIZKOVA, I. & KUNC, P. 2006. Thermal, cardiac and adrenergic responses to repeated local cooling. *Physiol Res,* 55**,** 543-9.

JANSSENS, W. J. & VANHOUTTE, P. M. 1978. Instantaneous changes of alpha-adrenoceptor affinity caused by moderate cooling in canine cutaneous veins. *Am J Physiol,* 234**,** H330-7.

JANSSENS, W. J., VERBEUREN, T. J. & VANHOUTTE, P. M. 1981. Effect of moderate cooling on adrenergic neuroeffector interaction in canine cutaneous veins. *Blood Vessels,* 18**,** 281-95.

JAQUEMAR, D., SCHENKER, T. & TRUEB, B. 1999. An ankyrin-like protein with transmembrane domains is specifically lost after oncogenic transformation of human fibroblasts. *J Biol Chem,* 274**,** 7325-33.

JARASCH, E. D., BRUDER, G. & HEID, H. W. 1986. Significance of xanthine oxidase in capillary endothelial cells. *Acta Physiol Scand Suppl,* 548**,** 39-46.

JEYARAJ, S. C., CHOTANI, M. A., MITRA, S., GREGG, H. E., FLAVAHAN, N. A. & MORRISON, K. J. 2001. Cooling evokes redistribution of alpha2C-adrenoceptors from Golgi to plasma membrane in transfected human embryonic kidney 293 cells. *Mol Pharmacol,* 60**,** 1195-200.

JI, G., ZHOU, S., KOCHUKOV, M. Y., WESTLUND, K. N. & CARLTON, S. M. 2007. Plasticity in intact A delta- and C-fibers contributes to cold hypersensitivity in neuropathic rats. *Neuroscience,* 150**,** 182-93.

JIN, L., YING, Z. & WEBB, R. C. 2004. Activation of Rho/Rho kinase signaling pathway by reactive oxygen species in rat aorta. *Am J Physiol Heart Circ Physiol,* 287**,** H1495-500.

JOHNSON, J. M., TAYLOR, W. F., SHEPHERD, A. P. & PARK, M. K. 1984. Laser-Doppler measurement of skin blood flow: comparison with plethysmography. *J Appl Physiol Respir Environ Exerc Physiol,* 56**,** 798-803.

JOHNSON, J. M., YEN, T. C., ZHAO, K. & KOSIBA, W. A. 2005. Sympathetic, sensory, and nonneuronal contributions to the cutaneous vasoconstrictor response to local cooling. *Am J Physiol Heart Circ Physiol,* 288**,** H1573-9.

JOLLY, S. R., KANE, W. J., BAILIE, M. B., ABRAMS, G. D. & LUCCHESI, B. R. 1984. Canine myocardial reperfusion injury. Its reduction by the combined administration of superoxide dismutase and catalase. *Circ Res,* 54**,** 277-85.

JORDT, S. E., BAUTISTA, D. M., CHUANG, H. H., MCKEMY, D. D., ZYGMUNT, P. M., HOGESTATT, E. D., MENG, I. D. & JULIUS, D. 2004. Mustard oils and cannabinoids excite sensory nerve fibres through the TRP channel ANKTM1. *Nature,* 427**,** 260-5.

JUNG, J., SHIN, J. S., LEE, S. Y., HWANG, S. W., KOO, J., CHO, H. & OH, U. 2004. Phosphorylation of vanilloid receptor 1 by Ca2+/calmodulin-dependent kinase II regulates its vanilloid binding. *J Biol Chem,* 279**,** 7048-54.

KA, H., PARK, H. J., JUNG, H. J., CHOI, J. W., CHO, K. S., HA, J. & LEE, K. T. 2003. Cinnamaldehyde induces apoptosis by ROS-mediated mitochondrial permeability transition in human promyelocytic leukemia HL-60 cells. *Cancer Lett,* 196**,** 143-52.

KAJEKAR, R., GUPTA, P., SHEPPERSON, N. B. & BRAIN, S. D. 1995. Effect of a 5-HT1 receptor agonist, CP-122,288, on oedema formation induced by stimulation of the rat saphenous nerve. *Br J Pharmacol,* 115**,** 1-2.

KALSNER, S. 1972. Differential activation of the inner and outer muscle cell layers of the rabbit ear artery. *Eur J Pharmacol,* 20**,** 122-4.

KANG, K., PULVER, S. R., PANZANO, V. C., CHANG, E. C., GRIFFITH, L. C., THEOBALD, D. L. & GARRITY, P. A. 2010. Analysis of Drosophila TRPA1 reveals an ancient origin for human chemical nociception. *Nature,* 464**,** 597-600.

KARASHIMA, Y., PRENEN, J., MESEGUER, V., OWSIANIK, G., VOETS, T. & NILIUS, B. 2008. Modulation of the transient receptor potential channel TRPA1 by phosphatidylinositol 4,5-biphosphate manipulators. *Pflugers Arch,* 457**,** 77-89.

KARASHIMA, Y., PRENEN, J., TALAVERA, K., JANSSENS, A., VOETS, T. & NILIUS, B. 2010. Agonist-induced changes in Ca(2+) permeation through the nociceptor cation channel TRPA1. *Biophys J,* 98**,** 773-83.

KARASHIMA, Y., TALAVERA, K., EVERAERTS, W., JANSSENS, A., KWAN, K. Y., VENNEKENS, R., NILIUS, B. & VOETS, T. 2009. TRPA1 acts as a cold sensor in vitro and in vivo. *Proc Natl Acad Sci U S A,* 106**,** 1273-8.

KASTING, G. B., FRANCIS, W. R., BOWMAN, L. A. & KINNETT, G. O. 1997. Percutaneous absorption of vanilloids: in vivo and in vitro studies. *J Pharm Sci,* 86**,** 142-6.

KATSURA, H., OBATA, K., MIZUSHIMA, T., YAMANAKA, H., KOBAYASHI, K., DAI, Y., FUKUOKA, T., TOKUNAGA, A., SAKAGAMI, M. & NOGUCHI, K. 2006. Antisense knock down of TRPA1, but not TRPM8, alleviates cold hyperalgesia after spinal nerve ligation in rats. *Exp Neurol,* 200**,** 112-23.

KAWASAKI, H., NUKI, C., SAITO, A. & TAKASAKI, K. 1990. Role of calcitonin gene-related peptide-containing nerves in the vascular adrenergic neurotransmission. *J Pharmacol Exp Ther,* 252**,** 403-9.

KAWASAKI, H., TAKASAKI, K., SAITO, A. & GOTO, K. 1988. Calcitonin gene-related peptide acts as a novel vasodilator neurotransmitter in mesenteric resistance vessels of the rat. *Nature,* 335**,** 164-7.

KEATINGE, W. R. 1957. The effect of general chilling on the vasodilator response to cold. *J Physiol,* 139**,** 497-507.

KEATINGE, W. R. 1961. The return of blood flow to fingers in ice-water after suppression by adrenaline or noradrenaline. *J Physiol,* 159**,** 101-10.

KEATINGE, W. R. 1970. *Direct effect of temperature on blood vessels: their role in cold vasodilation* Charles C Thomas, Springfield.

KEATINGE, W. R., HARMAN,M.C. 1980. *Local mechanisms controlling blood vessels,* London, Academic Press.

KEATINGE, W. R. & NADEL, J. A. 1965. Immediate Respiratory Response to Sudden Cooling of the Skin. *J Appl Physiol,* 20**,** 65-9.

KEEBLE, J. E., BODKIN, J. V., LIANG, L., WODARSKI, R., DAVIES, M., FERNANDES, E. S., COELHO CDE, F., RUSSELL, F., GRAEPEL, R., MUSCARA, M. N., MALCANGIO, M. & BRAIN, S. D. 2009. Hydrogen peroxide is a novel mediator of inflammatory hyperalgesia, acting via transient receptor potential vanilloid 1-dependent and independent mechanisms. *Pain,* 141**,** 135-42.

KELLOGG, D. L., JR., LIU, Y., KOSIBA, I. F. & O'DONNELL, D. 1999. Role of nitric oxide in the vascular effects of local warming of the skin in humans. *J Appl Physiol (1985),* 86**,** 1185-90.

KEREZOUDIS, N. P., FUNATO, A., EDWALL, L. & OLGART, L. 1993a. Activation of sympathetic nerves exerts an inhibitory influence on afferent nerve-induced vasodilation unrelated to vasoconstriction in rat dental pulp. *Acta Physiol Scand,* 147**,** 27-35.

KEREZOUDIS, N. P., OLGART, L., FUNATO, A. & EDWALL, L. 1993b. Inhibitory influence of sympathetic nerves on afferent nerve-induced extravasation in the rat incisor pulp upon direct electrical stimulation of the tooth. *Arch Oral Biol,* 38**,** 483-90.

KESSLER, J. A., BELL, W. O. & BLACK, I. B. 1983. Interactions between the sympathetic and sensory innervation of the iris. *J Neurosci,* 3**,** 1301-7.

KEVIN, L. G., CAMARA, A. K., RIESS, M. L., NOVALIJA, E. & STOWE, D. F. 2003. Ischemic preconditioning alters real-time measure of O2 radicals in intact hearts with ischemia and reperfusion. *Am J Physiol Heart Circ Physiol,* 284**,** H566-74.

KHATTAB, M. M. 2006. TEMPOL, a membrane-permeable radical scavenger, attenuates peroxynitrite- and superoxide anion-enhanced carrageenan-induced paw edema and hyperalgesia: a key role for superoxide anion. *Eur J Pharmacol,* 548**,** 167-73.

KIM, H., MITTAL, D. P., IADAROLA, M. J. & DIONNE, R. A. 2006. Genetic predictors for acute experimental cold and heat pain sensitivity in humans. *J Med Genet,* 43**,** e40.

KIM, H. Y., CHUNG, J. M. & CHUNG, K. 2008. Increased production of mitochondrial superoxide in the spinal cord induces pain behaviors in mice: the effect of mitochondrial electron transport complex inhibitors. *Neurosci Lett,* 447**,** 87-91.

KIRCHMAIR, R., MARKSTEINER, J., TROGER, J., MAHATA, S. K., MAHATA, M., DONNERER, J., AMANN, R., FISCHER-COLBRIE, R., WINKLER, H. & SARIA, A. 1994. Human and rat primary C-fibre afferents store and release secretoneurin, a novel neuropeptide. *Eur J Neurosci,* 6**,** 861-8.

KLEDE, M., CLOUGH, G., LISCHETZKI, G. & SCHMELZ, M. 2003. The effect of the nitric oxide synthase inhibitor N-nitro-L-arginine-methyl ester on neuropeptide-induced vasodilation and protein extravasation in human skin. *J Vasc Res,* 40**,** 105-14.

KLIONSKY, L., TAMIR, R., GAO, B., WANG, W., IMMKE, D. C., NISHIMURA, N. & GAVVA, N. R. 2007. Species-specific pharmacology of Trichloro(sulfanyl)ethyl benzamides as transient receptor potential ankyrin 1 (TRPA1) antagonists. *Mol Pain,* 3**,** 39.

KNOWLTON, W. M., BIFOLCK-FISHER, A., BAUTISTA, D. M. & MCKEMY, D. D. 2010. TRPM8, but not TRPA1, is required for neural and behavioral responses to acute noxious cold temperatures and cold-mimetics in vivo. *Pain,* 150**,** 340-50.

KNOWLTON, W. M., DANIELS, R. L., PALKAR, R., MCCOY, D. D. & MCKEMY, D. D. 2011. Pharmacological blockade of TRPM8 ion channels alters cold and cold pain responses in mice. *PLoS One,* 6**,** e25894.

KNOWLTON, W. M., PALKAR, R., LIPPOLDT, E. K., MCCOY, D. D., BALUCH, F., CHEN, J. & MCKEMY, D. D. 2013. A sensory-labeled line for cold: TRPM8-expressing sensory neurons define the cellular basis for cold, cold pain, and cooling-mediated analgesia. *J Neurosci,* 33**,** 2837-48.

KOBAYASHI, K., FUKUOKA, T., OBATA, K., YAMANAKA, H., DAI, Y., TOKUNAGA, A. & NOGUCHI, K. 2005. Distinct expression of TRPM8, TRPA1, and TRPV1 mRNAs in rat primary afferent neurons with adelta/c-fibers and colocalization with trk receptors. *J Comp Neurol,* 493**,** 596-606.

KOGANEZAWA, T., ISHIKAWA, T., FUJITA, Y., YAMASHITA, T., TAJIMA, T., HONDA, M. & NAKAYAMA, K. 2006. Local regulation of skin blood flow during cooling involving presynaptic P2 purinoceptors in rats. *Br J Pharmacol,* 148**,** 579-86.

KOON, H. W., ZHAO, D., ZHAN, Y., RHEE, S. H., MOYER, M. P. & POTHOULAKIS, C. 2006. Substance P stimulates cyclooxygenase-2 and prostaglandin E2 expression through JAK-STAT activation in human colonic epithelial cells. *J Immunol,* 176**,** 5050-9.

KOSKELA, H. O. 2007. Cold air-provoked respiratory symptoms: the mechanisms and management. *Int J Circumpolar Health,* 66**,** 91-100.

KRAMER, K. & SCHULZE, W. 1948. [Not Available]. *Pflugers Arch Gesamte Physiol Menschen Tiere,* 250**,** 141-70.

KREMEYER, B., LOPERA, F., COX, J. J., MOMIN, A., RUGIERO, F., MARSH, S., WOODS, C. G., JONES, N. G., PATERSON, K. J., FRICKER, F. R., VILLEGAS, A., ACOSTA, N., PINEDA-TRUJILLO, N. G., RAMIREZ, J. D., ZEA, J., BURLEY, M. W., BEDOYA, G., BENNETT, D. L., WOOD, J. N. & RUIZ-LINARES, A. 2010. A

gain-of-function mutation in TRPA1 causes familial episodic pain syndrome. *Neuron,* 66**,** 671-80.

KU, D. D., ABDEL-RAZEK, T. T., DAI, J., KIM-PARK, S., FALLON, M. B. & ABRAMS, G. A. 2002. Garlic and its active metabolite allicin produce endothelium- and nitric oxide-dependent relaxation in rat pulmonary arteries. *Clin Exp Pharmacol Physiol,* 29**,** 84-91.

KUNKLER, P. E., BALLARD, C. J., OXFORD, G. S. & HURLEY, J. H. 2011. TRPA1 receptors mediate environmental irritant-induced meningeal vasodilatation. *Pain,* 152**,** 38-44.

KUNTZ, A. & HAMILTON, J. W. 1938. Afferent innervation of the skin. *Anatomical Record,* 71**,** 387-400.

KUSTERS, F. J., WALBEEHM, E. T. & NIEHOF, S. P. 2010. Neural influence on cold induced vasodilatation using a new set-up for bilateral measurement in the rat hind limb. *J Neurosci Methods,* 193**,** 100-5.

KWAN, K. Y., ALLCHORNE, A. J., VOLLRATH, M. A., CHRISTENSEN, A. P., ZHANG, D. S., WOOLF, C. J. & COREY, D. P. 2006. TRPA1 contributes to cold, mechanical, and chemical nociception but is not essential for hair-cell transduction. *Neuron,* 50**,** 277-89.

KWAN, K. Y., GLAZER, J. M., COREY, D. P., RICE, F. L. & STUCKY, C. L. 2009. TRPA1 modulates mechanotransduction in cutaneous sensory neurons. *J Neurosci,* 29**,** 4808-19.

LANDRY, G. J. 2013. Current medical and surgical management of Raynaud's syndrome. *J Vasc Surg,* 57**,** 1710-6.

LANGER, S. Z. 1974. Presynaptic regulation of catecholamine release. *Biochem Pharmacol,* 23**,** 1793-800.

LANGLEY, J. N. 1923. Antidromic action: Part II. Stimulation of the peripheral nerves of the cat's hind foot. *J Physiol,* 58**,** 49-69.

LASHINGER, E. S., STEIGINGA, M. S., HIEBLE, J. P., LEON, L. A., GARDNER, S. D., NAGILLA, R., DAVENPORT, E. A., HOFFMAN, B. E., LAPING, N. J. & SU, X. 2008. AMTB, a TRPM8 channel blocker: evidence in rats for activity in overactive bladder and painful bladder syndrome. *Am J Physiol Renal Physiol,* 295**,** F803-10.

LAWSON, S. N., PERRY, M. J., PRABHAKAR, E. & MCCARTHY, P. W. 1993. Primary sensory neurones: neurofilament, neuropeptides, and conduction velocity. *Brain Res Bull,* 30**,** 239-43.

LEBLANC, J., DULAC, S., COTE, J. & GIRARD, B. 1975. Autonomic Nervous-System and Adaptation to Cold in Man. *Journal of Applied Physiology,* 39**,** 181-186.

LEE, J. Y., BAKRI, I., MATSUO, A. & TOCHIHARA, Y. 2013. Cold-induced vasodilation and vasoconstriction in the finger of tropical and temperate indigenes. *Journal of Thermal Biology,* 38**,** 70-78.

LEE, S. M., CHO, Y. S., KIM, T. H., JIN, M. U., AHN, D. K., NOGUCHI, K. & BAE, Y. C. 2012. An ultrastructural evidence for the expression of transient receptor potential ankyrin 1 (TRPA1) in astrocytes in the rat trigeminal caudal nucleus. *J Chem Neuroanat,* 45**,** 45-9.

LEMBECK, F. 1953. [Central transmission of afferent impulses. III. Incidence and significance of the substance P in the dorsal roots of the spinal cord]. *Naunyn Schmiedebergs Arch Exp Pathol Pharmakol,* 219**,** 197-213.

LEMBECK, F., DONNERER, J., TSUCHIYA, M. & NAGAHISA, A. 1992. The non-peptide tachykinin antagonist, CP-96,345, is a potent inhibitor of neurogenic inflammation. *Br J Pharmacol,* 105**,** 527-30.

LEMBECK, F. & HOLZER, P. 1979. Substance P as neurogenic mediator of antidromic vasodilation and neurogenic plasma extravasation. *Naunyn Schmiedebergs Arch Pharmacol,* 310**,** 175-83.

LEVINE, J. D., CLARK, R., DEVOR, M., HELMS, C., MOSKOWITZ, M. A. & BASBAUM, A. I. 1984. Intraneuronal substance P contributes to the severity of experimental arthritis. *Science,* 226**,** 547-9.

LEWIS, T. 1927. *The blood vessels of the human skin and their response,* London, Shaw and Sons.

LEWIS, T. 1930. Observations upon the reactions of the vessels of the human skin to cold. *Heart-a Journal for the Study of the Circulation,* 15**,** 177-208.

LI, J. M. & SHAH, A. M. 2004. Endothelial cell superoxide generation: regulation and relevance for cardiovascular pathophysiology. *Am J Physiol Regul Integr Comp Physiol,* 287**,** R1014-30.

LIEDTKE, W. & FRIEDMAN, J. M. 2003. Abnormal osmotic regulation in trpv4-/- mice. *Proc Natl Acad Sci U S A,* 100**,** 13698-703.

LINDEROTH, B., FEDORCSAK, I. & MEYERSON, B. A. 1991. Peripheral vasodilatation after spinal cord stimulation: animal studies of putative effector mechanisms. *Neurosurgery,* 28**,** 187-95.

LINDEROTH, B., GAZELIUS, B., FRANCK, J. & BRODIN, E. 1992. Dorsal column stimulation induces release of serotonin and substance P in the cat dorsal horn. *Neurosurgery,* 31**,** 289-96; discussion 296-7.

LINDEROTH, B., GHERARDINI, G., REN, B. & LUNDEBERG, T. 1995. Preemptive spinal cord stimulation reduces ischemia in an animal model of vasospasm. *Neurosurgery,* 37**,** 266-71; discussion 271-2.

LINDEROTH, B., HERREGODTS, P. & MEYERSON, B. A. 1994. Sympathetic mediation of peripheral vasodilation induced by spinal cord stimulation: animal studies of the role of cholinergic and adrenergic receptor subtypes. *Neurosurgery,* 35**,** 711-9.

LOESCH, A. & BURNSTOCK, G. 1988. Ultrastructural localisation of serotonin and substance P in vascular endothelial cells of rat femoral and mesenteric arteries. *Anat Embryol (Berl),* 178**,** 137-42.

LOUIS, S. M., JOHNSTONE, D., RUSSELL, N. J., JAMIESON, A. & DOCKRAY, G. J. 1989. Antibodies to calcitonin-gene related peptide reduce inflammation induced by topical mustard oil but not that due to carrageenin in the rat. *Neurosci Lett,* 102**,** 257-60.

LOWENSTEIN, C. J., DINERMAN, J. L. & SNYDER, S. H. 1994. Nitric oxide: a physiologic messenger. *Ann Intern Med,* 120**,** 227-37.

LOWRY, O. H., ROSEBROUGH, N. J., FARR, A. L. & RANDALL, R. J. 1951. Protein measurement with the Folin phenol reagent. *J Biol Chem,* 193**,** 265-75.

LU, J. T., SON, Y. J., LEE, J., JETTON, T. L., SHIOTA, M., MOSCOSO, L., NISWENDER, K. D., LOEWY, A. D., MAGNUSON, M. A., SANES, J. R. & EMESON, R. B. 1999. Mice lacking alpha-calcitonin gene-related peptide exhibit normal cardiovascular regulation and neuromuscular development. *Mol Cell Neurosci,* 14**,** 99-120.

LUEBKE, A. E., DAHL, G. P., ROOS, B. A. & DICKERSON, I. M. 1996. Identification of a protein that confers calcitonin gene-related peptide responsiveness to oocytes by using a cystic fibrosis transmembrane conductance regulator assay. *Proc Natl Acad Sci U S A,* 93**,** 3455-60.

LUMPKIN, E. A. & CATERINA, M. J. 2007. Mechanisms of sensory transduction in the skin. *Nature,* 445**,** 858-65.

LUNDBERG, J. M. 1996. Pharmacology of cotransmission in the autonomic nervous system: integrative aspects on amines, neuropeptides, adenosine triphosphate, amino acids and nitric oxide. *Pharmacol Rev,* 48**,** 113-78.

LUNDBERG, J. M., FRANCO-CERECEDA, A., HUA, X., HOKFELT, T. & FISCHER, J. A. 1985. Co-existence of substance P and calcitonin gene-related peptide-like immunoreactivities in sensory nerves in relation to cardiovascular and bronchoconstrictor effects of capsaicin. *Eur J Pharmacol,* 108**,** 315-9.

MACPHERSON, L. J., DUBIN, A. E., EVANS, M. J., MARR, F., SCHULTZ, P. G., CRAVATT, B. F. & PATAPOUTIAN, A. 2007. Noxious compounds activate TRPA1 ion channels through covalent modification of cysteines. *Nature,* 445**,** 541-5.

MACPHERSON, L. J., GEIERSTANGER, B. H., VISWANATH, V., BANDELL, M., EID, S. R., HWANG, S. & PATAPOUTIAN, A. 2005. The pungency of garlic: activation of TRPA1 and TRPV1 in response to allicin. *Curr Biol,* 15**,** 929-34.

MACPHERSON, L. J., HWANG, S. W., MIYAMOTO, T., DUBIN, A. E., PATAPOUTIAN, A. & STORY, G. M. 2006. More than cool: promiscuous relationships of menthol and other sensory compounds. *Mol Cell Neurosci,* 32**,** 335-43.

MAGGI, C. A., GIULIANI, S., SANTICIOLI, P., REGOLI, D. & MELI, A. 1987. Peripheral effects of neurokinins: functional evidence for the existence of multiple receptors. *J Auton Pharmacol,* 7**,** 11-32.

MAGGI, C. A. & MELI, A. 1988. The sensory-efferent function of capsaicin-sensitive sensory neurons. *Gen Pharmacol,* 19**,** 1-43.

MARTIN, W., VILLANI, G. M., JOTHIANANDAN, D. & FURCHGOTT, R. F. 1985. Selective blockade of endothelium-dependent and glyceryl trinitrate-induced relaxation by hemoglobin and by methylene blue in the rabbit aorta. *J Pharmacol Exp Ther,* 232**,** 708-16.

MATERAZZI, S., NASSINI, R., ANDRE, E., CAMPI, B., AMADESI, S., TREVISANI, M., BUNNETT, N. W., PATACCHINI, R. & GEPPETTI, P. 2008. Cox-dependent fatty acid metabolites cause pain through activation of the irritant receptor TRPA1. *Proc Natl Acad Sci U S A,* 105**,** 12045-50.

MAYEUX, P. R., AGRAWAL, K. C., TOU, J. S., KING, B. T., LIPPTON, H. L., HYMAN, A. L., KADOWITZ, P. J. & MCNAMARA, D. B. 1988. The pharmacological effects of allicin, a constituent of garlic oil. *Agents Actions,* 25**,** 182-90.

MCCOY, E. S., TAYLOR-BLAKE, B., STREET, S. E., PRIBISKO, A. L., ZHENG, J. & ZYLKA, M. J. 2013. Peptidergic CGRPalpha primary sensory neurons encode heat and itch and tonically suppress sensitivity to cold. *Neuron,* 78**,** 138-51.

MCGARAUGHTY, S., CHU, K. L., PERNER, R. J., DIDOMENICO, S., KORT, M. E. & KYM, P. R. 2010. TRPA1 modulation of spontaneous and mechanically evoked firing of spinal neurons in uninjured, osteoarthritic, and inflamed rats. *Mol Pain,* 6**,** 14.

MCKEMY, D. D., NEUHAUSSER, W. M. & JULIUS, D. 2002. Identification of a cold receptor reveals a general role for TRP channels in thermosensation. *Nature,* 416**,** 52-8.

MCLATCHIE, L. M., FRASER, N. J., MAIN, M. J., WISE, A., BROWN, J., THOMPSON, N., SOLARI, R., LEE, M. G. & FOORD, S. M. 1998. RAMPs regulate the transport and ligand specificity of the calcitonin-receptor-like receptor. *Nature,* 393**,** 333-9.

MCNAMARA, C. R., MANDEL-BREHM, J., BAUTISTA, D. M., SIEMENS, J., DERANIAN, K. L., ZHAO, M., HAYWARD, N. J., CHONG, J. A., JULIUS, D., MORAN, M. M. & FANGER, C. M. 2007. TRPA1 mediates formalin-induced pain. *Proc Natl Acad Sci U S A,* 104**,** 13525-30.

MELIKIAN, N., SEDDON, M. D., CASADEI, B., CHOWIENCZYK, P. J. & SHAH, A. M. 2009. Neuronal nitric oxide synthase and human vascular regulation. *Trends Cardiovasc Med,* 19**,** 256-62.

MILLAN, M. J. 1999. The induction of pain: an integrative review. *Prog Neurobiol,* 57**,** 1-164.

MILNER, P., BODIN, P., GUIDUCCI, S., DEL ROSSO, A., KAHALEH, M. B., MATUCCI-CERINIC, M. & BURNSTOCK, G. 2004. Regulation of substance P mRNA expression in human dermal microvascular endothelial cells. *Clin Exp Rheumatol,* 22**,** S24-7.

MILNER, P., BODIN, P., LOESCH, A. & BURNSTOCK, G. 1995. Interactions between sensory perivascular nerves and the endothelium in brain microvessels. *Int J Microcirc Clin Exp,* 15**,** 1-9.

MILNER, P., RALEVIC, V., HOPWOOD, A. M., FEHER, E., LINCOLN, J., KIRKPATRICK, K. A. & BURNSTOCK, G. 1989. Ultrastructural localisation of substance P and choline acetyltransferase in endothelial cells of rat coronary artery and release of substance P and acetylcholine during hypoxia. *Experientia,* 45**,** 121-5.

MINKE, B. 2006. TRP channels and Ca2+ signaling. *Cell Calcium,* 40**,** 261-75.

MIYAMOTO, T., DUBIN, A. E., PETRUS, M. J. & PATAPOUTIAN, A. 2009. TRPV1 and TRPA1 mediate peripheral nitric oxide-induced nociception in mice. *PLoS One,* 4**,** e7596.

MOINI ZANJANI, T. & SABETKASAEI, M. 2010. Study of the intraplantar injection of lidocaine and morphine on pain perception and the influence of morphine dependence and withdrawal on lidocaine-induced analgesia in rats. *Iran Biomed J,* 14**,** 164-70.

MONAHAN, K. D., WILSON, T. E. & RAY, C. A. 2004. Omega-3 fatty acid supplementation augments sympathetic nerve activity responses to physiological stressors in humans. *Hypertension,* 44**,** 732-8.

MONCADA, S., HIGGS, A. & FURCHGOTT, R. 1997. International Union of Pharmacology Nomenclature in Nitric Oxide Research. *Pharmacol Rev,* 49**,** 137-42.

MONTELL, C. & RUBIN, G. M. 1989. Molecular characterization of the Drosophila trp locus: a putative integral membrane protein required for phototransduction. *Neuron,* 2**,** 1313-23.

MORI-KAWABE, M., TSUSHIMA, H., FUJIMOTO, S., TADA, T. & ITO, J. 2009. Role of Rho/Rho-kinase and NO/cGMP signaling pathways in vascular function prior to atherosclerosis. *J Atheroscler Thromb,* 16**,** 722-32.

MORI, Y., KAJIMOTO, T., NAKAO, A., TAKAHASHI, N. & KIYONAKA, S. 2011. Receptor signaling integration by TRP channelsomes. *Adv Exp Med Biol,* 704**,** 373-89.

MORIN, C. & BUSHNELL, M. C. 1998. Temporal and qualitative properties of cold pain and heat pain: a psychophysical study. *Pain,* 74**,** 67-73.

MORRIS, H. R., PANICO, M., ETIENNE, T., TIPPINS, J., GIRGIS, S. I. & MACINTYRE, I. 1984. Isolation and characterization of human calcitonin gene-related peptide. *Nature,* 308**,** 746-8.

MOSAVI, L. K., CAMMETT, T. J., DESROSIERS, D. C. & PENG, Z. Y. 2004. The ankyrin repeat as molecular architecture for protein recognition. *Protein Sci,* 13**,** 1435-48.

MULDERRY, P. K., GHATEI, M. A., SPOKES, R. A., JONES, P. M., PIERSON, A. M., HAMID, Q. A., KANSE, S., AMARA, S. G., BURRIN, J. M., LEGON, S. & ET AL. 1988. Differential expression of alpha-CGRP and beta-CGRP by primary sensory neurons and enteric autonomic neurons of the rat. *Neuroscience,* 25**,** 195-205.

MUSTAFA, S. & ORIOWO, M. 2005. Cooling-induced contraction of the rat gastric fundus: mediation via transient receptor potential (TRP) cation channel TRPM8 receptor and Rho-kinase activation. *Clin Exp Pharmacol Physiol,* 32**,** 832-8.

MUSTAFA, S. M. D. & THULESIUS, O. 2001. Cooling is a potent vasodilator of deep vessels in the rat. *Canadian Journal of Physiology and Pharmacology,* 79**,** 899-904.

NAGAI, K., SAITOH, Y., SAITO, S. & TSUTSUMI, K. 2012. Structure and hibernation-associated expression of the transient receptor potential vanilloid 4 channel (TRPV4) mRNA in the Japanese grass lizard (Takydromus tachydromoides). *Zoolog Sci,* 29**,** 185-90.

NAGATA, K., DUGGAN, A., KUMAR, G. & GARCIA-ANOVEROS, J. 2005. Nociceptor and hair cell transducer properties of TRPA1, a channel for pain and hearing. *J Neurosci,* 25**,** 4052-61.

NAKAJIMA, Y., TSUCHIDA, K., NEGISHI, M., ITO, S. & NAKANISHI, S. 1992. Direct linkage of three tachykinin receptors to stimulation of both phosphatidylinositol hydrolysis and cyclic AMP cascades in transfected Chinese hamster ovary cells. *J Biol Chem,* 267**,** 2437-42.

NAKAMOTO, M. 1990. Responses of sympathetic nervous system to cold exposure in vibration syndrome subjects and age-matched healthy controls. *Int Arch Occup Environ Health,* 62**,** 177-81.

NAKAMURA, Y., UNE, Y., MIYANO, K., ABE, H., HISAOKA, K., MORIOKA, N. & NAKATA, Y. 2012. Activation of transient receptor potential ankyrin 1 evokes nociception through substance P release from primary sensory neurons. *J Neurochem,* 120**,** 1036-47.

NAKATSUKA, K., GUPTA, R., SAITO, S., BANZAWA, N., TAKAHASHI, K., TOMINAGA, M. & OHTA, T. 2013. Identification of Molecular Determinants for a Potent Mammalian TRPA1 Antagonist by Utilizing Species Differences. *J Mol Neurosci*.

NAMER, B., KLEGGETVEIT, I. P., HANDWERKER, H., SCHMELZ, M. & JORUM, E. 2008. Role of TRPM8 and TRPA1 for cold allodynia in patients with cold injury. *Pain,* 139**,** 63-72.

NAMER, B., SEIFERT, F., HANDWERKER, H. O. & MAIHOFNER, C. 2005. TRPA1 and TRPM8 activation in humans: effects of cinnamaldehyde and menthol. *Neuroreport,* 16**,** 955-9.

NASH, G. B., ABBITT, K. B., TATE, K., JETHA, K. A. & EGGINTON, S. 2001. Changes in the mechanical and adhesive behaviour of human neutrophils on cooling in vitro. *Pflugers Arch,* 442**,** 762-70.

NASSENSTEIN, C., KWONG, K., TAYLOR-CLARK, T., KOLLARIK, M., MACGLASHAN, D. M., BRAUN, A. & UNDEM, B. J. 2008. Expression and function of the ion channel TRPA1 in vagal afferent nerves innervating mouse lungs. *J Physiol,* 586**,** 1595-604.

NATIVI, C., GUALDANI, R., DRAGONI, E., DI CESARE MANNELLI, L., SOSTEGNI, S., NORCINI, M., GABRIELLI, G., LA MARCA, G., RICHICHI, B., FRANCESCONI, O., MONCELLI, M. R., GHELARDINI, C. & ROELENS, S. 2013. A TRPA1 antagonist reverts oxaliplatin-induced neuropathic pain. *Sci Rep,* 3**,** 2005.

NEIL, A., ATTAL, N. & GUILBAUD, G. 1991. Effects of guanethidine on sensitization to natural stimuli and self-mutilating behaviour in rats with a peripheral neuropathy. *Brain Res,* 565**,** 237-46.

NELMS, J. D. 1963. Functional anatomy of skin related to temperature regulation. *Fed Proc,* 22**,** 933-6.

NELSON, M. T., HUANG, Y., BRAYDEN, J. E., HESCHELER, J. & STANDEN, N. B. 1990. Arterial dilations in response to calcitonin gene-related peptide involve activation of K+ channels. *Nature,* 344**,** 770-3.

NHS. 2013. *Raynaud's phenomenon* [Online]. UK.

NIEHOF, S. P., HUYGEN, F. J., VAN DER WEERD, R. W., WESTRA, M. & ZIJLSTRA, F. J. 2006. Thermography imaging during static and controlled thermoregulation in complex regional pain syndrome type 1: diagnostic value and involvement of the central sympathetic system. *Biomed Eng Online,* 5**,** 30.

NILIUS, B. 2007. Transient receptor potential (TRP) cation channels: rewarding unique proteins. *Bull Mem Acad R Med Belg,* 162**,** 244-53.

NILIUS, B., APPENDINO, G. & OWSIANIK, G. 2012. The transient receptor potential channel TRPA1: from gene to pathophysiology. *Pflugers Arch,* 464**,** 425-58.

NILIUS, B., PRENEN, J. & OWSIANIK, G. 2011. Irritating channels: the case of TRPA1. *J Physiol,* 589**,** 1543-9.

NILSSON, G. E., TENLAND, T. & OBERT, P. A. 1980. A new instrument for continuous measurement of tissue blood flow by light beating spectroscopy. *IEEE Trans Biomed Eng,* 27**,** 12-9.

NISOLI, E., TONELLO, C., BRISCINI, L. & CARRUBA, M. O. 1997. Inducible nitric oxide synthase in rat brown adipocytes: implications for blood flow to brown adipose tissue. *Endocrinology,* 138**,** 676-82.

NOGUCHI, K., SENBA, E., MORITA, Y., SATO, M. & TOHYAMA, M. 1990. Alpha-CGRP and beta-CGRP mRNAs are differentially regulated in the rat spinal cord and dorsal root ganglion. *Brain Res Mol Brain Res,* 7**,** 299-304.

NORBERG, K. A., HAMBERGER, B. 1964. The sympathetic adrenergic neuron: some characteristics revealed by histochemical studies on the intraneuronal distribution of the transmitter. *Acta Physiol Scand Suppl,* 238**,** 1-42.

NORISUE, M., TODOKI, K. & OKABE, E. 1997. Inhibition by hydroxyl radicals of calcitonin gene-related peptide-mediated neurogenic vasorelaxation in isolated canine lingual artery. *J Pharmacol Exp Ther,* 280**,** 492-500.

NOZAWA, K., KAWABATA-SHODA, E., DOIHARA, H., KOJIMA, R., OKADA, H., MOCHIZUKI, S., SANO, Y., INAMURA, K., MATSUSHIME, H., KOIZUMI, T., YOKOYAMA, T. & ITO, H. 2009. TRPA1 regulates gastrointestinal motility through serotonin release from enterochromaffin cells. *Proc Natl Acad Sci U S A,* 106**,** 3408-13.

OBATA, K., KATSURA, H., MIZUSHIMA, T., YAMANAKA, H., KOBAYASHI, K., DAI, Y., FUKUOKA, T., TOKUNAGA, A., TOMINAGA, M. & NOGUCHI, K. 2005. TRPA1 induced in sensory neurons contributes to cold hyperalgesia after inflammation and nerve injury. *J Clin Invest,* 115**,** 2393-401.

OCHOA, J. L., YARNITSKY, D., MARCHETTINI, P., DOTSON, R. & CLINE, M. 1993. Interactions between sympathetic vasoconstrictor outflow and C nociceptor-induced antidromic vasodilatation. *Pain,* 54**,** 191-6.

OGAWA, H., TAKAHASHI, K., MIURA, S., IMAGAWA, T., SAITO, S., TOMINAGA, M. & OHTA, T. 2012. H(2)S functions as a nociceptive messenger through transient receptor potential ankyrin 1 (TRPA1) activation. *Neuroscience,* 218**,** 335-43.

OHTA, T., IMAGAWA, T. & ITO, S. 2007. Novel agonistic action of mustard oil on recombinant and endogenous porcine transient receptor potential V1 (pTRPV1) channels. *Biochem Pharmacol,* 73**,** 1646-56.

OKUBO, K., MATSUMURA, M., KAWAISHI, Y., AOKI, Y., MATSUNAMI, M., OKAWA, Y., SEKIGUCHI, F. & KAWABATA, A. 2012. Hydrogen sulfide-induced mechanical hyperalgesia and allodynia require activation of both Cav3.2 and TRPA1 channels in mice. *Br J Pharmacol,* 166**,** 1738-43.

ORMEROD, A. D., KOBZA BLACK, A., DAWES, J., MURDOCH, R. D., KORO, O., BARR, R. M. & GREAVES, M. W. 1988. Prostaglandin D2 and histamine release in cold urticaria unaccompanied by evidence of platelet activation. *J Allergy Clin Immunol,* 82**,** 586-9.

PARNAVELAS, J. G., KELLY, W. & BURNSTOCK, G. 1985. Ultrastructural localization of choline acetyltransferase in vascular endothelial cells in rat brain. *Nature,* 316**,** 724-5.

PATACCHINI, R., MAGGI, C. A. & MELI, A. 1990. Capsaicin-like activity of some natural pungent substances on peripheral endings of visceral primary afferents. *Naunyn Schmiedebergs Arch Pharmacol,* 342**,** 72-7.

PATAPOUTIAN, A., PEIER, A. M., STORY, G. M. & VISWANATH, V. 2003. ThermoTRP channels and beyond: mechanisms of temperature sensation. *Nat Rev Neurosci,* 4**,** 529-39.

PATEL, P., QI, W. N., ALLEN, D. M., CHEN, L. E., SEABER, A. V., STAMLER, J. S. & URBANIAK, J. R. 2004. Inhibition of iNOS with 1400W improves contractile function

and alters nos gene and protein expression in reperfused skeletal muscle. *Microsurgery,* 24**,** 324-31.

PEIER, A. M., MOQRICH, A., HERGARDEN, A. C., REEVE, A. J., ANDERSSON, D. A., STORY, G. M., EARLEY, T. J., DRAGONI, I., MCINTYRE, P., BEVAN, S. & PATAPOUTIAN, A. 2002. A TRP channel that senses cold stimuli and menthol. *Cell,* 108**,** 705-15.

PENUELAS, A., TASHIMA, K., TSUCHIYA, S., MATSUMOTO, K., NAKAMURA, T., HORIE, S. & YANO, S. 2007. Contractile effect of TRPA1 receptor agonists in the isolated mouse intestine. *Eur J Pharmacol,* 576**,** 143-50.

PERGOLA, P. E., JOHNSON, J. M., KELLOGG, D. L., JR. & KOSIBA, W. A. 1996. Control of skin blood flow by whole body and local skin cooling in exercising humans. *Am J Physiol,* 270**,** H208-15.

PERGOLA, P. E., KELLOGG, D. L., JR., JOHNSON, J. M., KOSIBA, W. A. & SOLOMON, D. E. 1993. Role of sympathetic nerves in the vascular effects of local temperature in human forearm skin. *Am J Physiol,* 265**,** H785-92.

PERRY, M. J. & LAWSON, S. N. 1998. Differences in expression of oligosaccharides, neuropeptides, carbonic anhydrase and neurofilament in rat primary afferent neurons retrogradely labelled via skin, muscle or visceral nerves. *Neuroscience,* 85**,** 293-310.

PETRUS, M., PEIER, A. M., BANDELL, M., HWANG, S. W., HUYNH, T., OLNEY, N., JEGLA, T. & PATAPOUTIAN, A. 2007. A role of TRPA1 in mechanical hyperalgesia is revealed by pharmacological inhibition. *Mol Pain,* 3**,** 40.

PETTITT, D., GOLDSTEIN, J. L., MCGUIRE, A., SCHWARTZ, J. S., BURKE, T. & MANIADAKIS, N. 2000. Overview of the arthritis Cost Consequence Evaluation System (ACCES): a pharmacoeconomic model for celecoxib. *Rheumatology (Oxford),* 39 Suppl 2**,** 33-42; discussion 57-9.

POKORSKI, M., TAKEDA, K., SATO, Y. & OKADA, Y. 2013. The hypoxic ventilatory response and trpa1 antagonism in conscious mice. *Acta Physiol (Oxf).*

POLLOCK, D. C., LI, Z., ROSENCRANCE, E., KROME, J., KOMAN, L. A. & SMITH, T. L. 1997. Acute effects of periarterial sympathectomy on the cutaneous microcirculation. *J Orthop Res,* 15**,** 408-13.

POOLE, D. P., PELAYO, J. C., CATTARUZZA, F., KUO, Y. M., GAI, G., CHIU, J. V., BRON, R., FURNESS, J. B., GRADY, E. F. & BUNNETT, N. W. 2011. Transient receptor potential ankyrin 1 is expressed by inhibitory motoneurons of the mouse intestine. *Gastroenterology,* 141**,** 565-75, 575 e1-4.

POWERS, E. W., 3RD & FRAYER, W. W. 1978. Laser Doppler measurement of blood flow in the microcirculation. *Plast Reconstr Surg,* 61**,** 250-5.

POZSGAI, G., BODKIN, J. V., GRAEPEL, R., BEVAN, S., ANDERSSON, D. A. & BRAIN, S. D. 2010. Evidence for the pathophysiological relevance of TRPA1 receptors in the cardiovascular system in vivo. *Cardiovasc Res,* 87**,** 760-8.

POZSGAI, G., HAJNA, Z., BAGOLY, T., BOROS, M., KEMENY, A., MATERAZZI, S., NASSINI, R., HELYES, Z., SZOLCSANYI, J. & PINTER, E. 2012. The role of transient receptor potential ankyrin 1 (TRPA1) receptor activation in hydrogen-sulphide-induced CGRP-release and vasodilation. *Eur J Pharmacol,* 689**,** 56-64.

PRADO, M. A., EVANS-BAIN, B., OLIVER, K. R. & DICKERSON, I. M. 2001. The role of the CGRP-receptor component protein (RCP) in adrenomedullin receptor signal transduction. *Peptides,* 22**,** 1773-81.

PREIBISZ, J. J. 1993. Calcitonin gene-related peptide and regulation of human cardiovascular homeostasis. *Am J Hypertens,* 6**,** 434-50.

PURKAYASTHA, S. S., SELVAMURTHY, W. & ILAVAZHAGAN, G. 1992. Peripheral vascular response to local cold stress of tropical men during sojourn in the Arctic cold region. *Jpn J Physiol,* 42**,** 877-89.

QIN, N., NEEPER, M. P., LIU, Y., HUTCHINSON, T. L., LUBIN, M. L. & FLORES, C. M. 2008. TRPV2 is activated by cannabidiol and mediates CGRP release in cultured rat dorsal root ganglion neurons. *J Neurosci,* 28**,** 6231-8.

QUAYLE, J. M., BONEV, A. D., BRAYDEN, J. E. & NELSON, M. T. 1994. Calcitonin gene-related peptide activated ATP-sensitive K+ currents in rabbit arterial smooth muscle via protein kinase A. *J Physiol,* 475**,** 9-13.

RAIMURA, M., TASHIMA, K., MATSUMOTO, K., TOBE, S., CHINO, A., NAMIKI, T., TERASAWA, K. & HORIE, S. 2013. Neuronal Nitric Oxide Synthase-Derived Nitric Oxide Is Involved in Gastric Mucosal Hyperemic Response to Capsaicin in Rats. *Pharmacology,* 92**,** 60-70.

RAMACHANDRAN, R., PLOUG, K. B., HAY-SCHMIDT, A., OLESEN, J., JANSEN-OLESEN, I. & GUPTA, S. 2010. Nitric oxide synthase (NOS) in the trigeminal vascular system and other brain structures related to pain in rats. *Neurosci Lett,* 484**,** 192-6.

RAMSEY, I. S., DELLING, M. & CLAPHAM, D. E. 2006. An introduction to TRP channels. *Annu Rev Physiol,* 68**,** 619-47.

RAUEN, U. & DE GROOT, H. 1998. Cold-induced release of reactive oxygen species as a decisive mediator of hypothermia injury to cultured liver cells. *Free Radic Biol Med,* 24**,** 1316-23.

REILLY, D. M., FERDINANDO, D., JOHNSTON, C., SHAW, C., BUCHANAN, K. D. & GREEN, M. R. 1997. The epidermal nerve fibre network: characterization of nerve fibres in human skin by confocal microscopy and assessment of racial variations. *Br J Dermatol,* 137**,** 163-70.

RIBEIRO-DA-SILVA, A. & HOKFELT, T. 2000. Neuroanatomical localisation of Substance P in the CNS and sensory neurons. *Neuropeptides,* 34**,** 256-71.

RIENTO, K. & RIDLEY, A. J. 2003. Rocks: multifunctional kinases in cell behaviour. *Nat Rev Mol Cell Biol,* 4**,** 446-56.

ROACH, A., ADLER, J. E. & BLACK, I. B. 1987. Depolarizing influences regulate preprotachykinin mRNA in sympathetic neurons. *Proc Natl Acad Sci U S A,* 84**,** 5078-81.

ROBERTS, K., SHENOY, R. & ANAND, P. 2011. A novel human volunteer pain model using contact heat evoked potentials (CHEP) following topical skin application of transient receptor potential agonists capsaicin, menthol and cinnamaldehyde. *J Clin Neurosci,* 18**,** 926-32.

ROBERTSON, D., JOHNSON, G. A., ROBERTSON, R. M., NIES, A. S., SHAND, D. G. & OATES, J. A. 1979. Comparative assessment of stimuli that release neuronal and adrenomedullary catecholamines in man. *Circulation,* 59**,** 637-43.

ROSSI, A., KAPAHI, P., NATOLI, G., TAKAHASHI, T., CHEN, Y., KARIN, M. & SANTORO, M. G. 2000. Anti-inflammatory cyclopentenone prostaglandins are direct inhibitors of IkappaB kinase. *Nature,* 403**,** 103-8.

ROUSTIT, M., BLAISE, S., MILLET, C. & CRACOWSKI, J. L. 2011. Impaired transient vasodilation and increased vasoconstriction to digital local cooling in primary Raynaud's phenomenon. *Am J Physiol Heart Circ Physiol,* 301**,** H324-30.

RUCH, D. S., VALLEE, J., LI, Z., SMITH, B. P., HOLDEN, M. & KOMAN, L. A. 2003. The acute effect of peripheral nerve transection on digital thermoregulatory function. *J Hand Surg Am,* 28**,** 481-8.

RUIJS, A. C., NIEHOF, S. P., SELLES, R. W., JAQUET, J. B., DAANEN, H. A. & HOVIUS, S. E. 2009. Digital rewarming patterns after median and ulnar nerve injury. *J Hand Surg Am,* 34**,** 54-64.

RUPAREL, N. B., PATWARDHAN, A. M., AKOPIAN, A. N. & HARGREAVES, K. M. 2008. Homologous and heterologous desensitization of capsaicin and mustard oil responses utilize different cellular pathways in nociceptors. *Pain,* 135**,** 271-9.

RUSCH, N. J., SHEPHERD, J. T. & VANHOUTTE, P. M. 1981. The effect of profound cooling on adrenergic neurotransmission in canine cutaneous veins. *J Physiol,* 311**,** 57-65.

RYCKMANS, T., AUBDOOL, A. A., BODKIN, J. V., COX, P., BRAIN, S. D., DUPONT, T., FAIRMAN, E., HASHIZUME, Y., ISHII, N., KATO, T., KITCHING, L., NEWMAN, J., OMOTO, K., RAWSON, D. & STROVER, J. 2011. Design and pharmacological evaluation of PF-4840154, a non-electrophilic reference agonist of the TrpA1 channel. *Bioorg Med Chem Lett,* 21**,** 4857-9.

SADOFSKY, L. R., BOA, A. N., MAHER, S. A., BIRRELL, M. A., BELVISI, M. G. & MORICE, A. H. 2011. TRPA1 is activated by direct addition of cysteine residues to the N-hydroxysuccinyl esters of acrylic and cinnamic acids. *Pharmacol Res,* 63**,** 30-6.

SAGAN, S., CHASSAING, G., PRADIER, L. & LAVIELLE, S. 1996. Tachykinin peptides affect differently the second messenger pathways after binding to CHO-expressed human NK-1 receptors. *J Pharmacol Exp Ther,* 276**,** 1039-48.

SALAS, M. M., HARGREAVES, K. M. & AKOPIAN, A. N. 2009. TRPA1-mediated responses in trigeminal sensory neurons: interaction between TRPA1 and TRPV1. *Eur J Neurosci,* 29**,** 1568-78.

SALLINEN, J., HOGLUND, I., ENGSTROM, M., LEHTIMAKI, J., VIRTANEN, R., SIRVIO, J., WURSTER, S., SAVOLA, J. M. & HAAPALINNA, A. 2007. Pharmacological characterization and CNS effects of a novel highly selective alpha2C-adrenoceptor antagonist JP-1302. *Br J Pharmacol,* 150**,** 391-402.

SALMON, A. M., DAMAJ, I., SEKINE, S., PICCIOTTO, M. R., MARUBIO, L. & CHANGEUX, J. P. 1999. Modulation of morphine analgesia in alphaCGRP mutant mice. *Neuroreport,* 10**,** 849-54.

SALVATORE, C. A. & KANE, S. A. 2011. CGRP receptor antagonists: toward a novel migraine therapy. *Curr Pharm Biotechnol,* 12**,** 1671-80.

SAMS, A., YENIDUNYA, A., ENGBERG, J. & JANSEN-OLESEN, I. 1999. Equipotent in vitro actions of alpha- and beta-CGRP on guinea pig basilar artery are likely to be mediated via CRLR derived CGRP receptors. *Regul Pept,* 85**,** 67-75.

SANDOR, K., HELYES, Z., ELEKES, K. & SZOLCSANYI, J. 2009. Involvement of capsaicin-sensitive afferents and the Transient Receptor Potential Vanilloid 1 Receptor in xylene-induced nocifensive behaviour and inflammation in the mouse. *Neurosci Lett,* 451**,** 204-7.

SAPAN, C. V., LUNDBLAD, R. L. & PRICE, N. C. 1999. Colorimetric protein assay techniques. *Biotechnol Appl Biochem,* 29 (Pt 2)**,** 99-108.

SAWADA, S. & YAMAMOTO, S. 1983. Stability of individual difference of cold-induced vasodilatation response at different room and water temperatures and immersion time. *Sangyo Igaku,* 25**,** 116-7.

SAWADA, Y., HOSOKAWA, H., HORI, A., MATSUMURA, K. & KOBAYASHI, S. 2007. Cold sensitivity of recombinant TRPA1 channels. *Brain Res,* 1160**,** 39-46.

SCHMIDT, M., DUBIN, A. E., PETRUS, M. J., EARLEY, T. J. & PATAPOUTIAN, A. 2009. Nociceptive signals induce trafficking of TRPA1 to the plasma membrane. *Neuron,* 64**,** 498-509.

SCHMIDT, R., SCHMELZ, M., FORSTER, C., RINGKAMP, M., TOREBJORK, E. & HANDWERKER, H. 1995. Novel classes of responsive and unresponsive C nociceptors in human skin. *J Neurosci,* 15**,** 333-41.

SCHOFIELD, I., MALIK, R., IZZARD, A., AUSTIN, C. & HEAGERTY, A. 2002. Vascular structural and functional changes in type 2 diabetes mellitus: evidence for the roles of abnormal myogenic responsiveness and dyslipidemia. *Circulation,* 106**,** 3037-43.

SCHROEDER, C. & JORDAN, J. 2012. Norepinephrine transporter function and human cardiovascular disease. *Am J Physiol Heart Circ Physiol,* 303**,** H1273-82.

SCHUTZ, B., MAUER, D., SALMON, A. M., CHANGEUX, J. P. & ZIMMER, A. 2004. Analysis of the cellular expression pattern of beta-CGRP in alpha-CGRP-deficient mice. *J Comp Neurol,* 476**,** 32-43.

SCOTLAND, R. S., CHAUHAN, S., DAVIS, C., DE FELIPE, C., HUNT, S., KABIR, J., KOTSONIS, P., OH, U. & AHLUWALIA, A. 2004. Vanilloid receptor TRPV1, sensory C-fibers, and vascular autoregulation: a novel mechanism involved in myogenic constriction. *Circ Res,* 95**,** 1027-34.

SENDOWSKI, I., SAVOUREY, G., BESNARD, Y. & BITTEL, J. 1997. Cold induced vasodilatation and cardiovascular responses in humans during cold water immersion of various upper limb areas. *Eur J Appl Physiol Occup Physiol,* 75**,** 471-7.

SENDOWSKI, I., SAVOUREY, G., LAUNAY, J. C., BESNARD, Y., COTTET-EMARD, J. M., PEQUIGNOT, J. M. & BITTEL, J. 2000. Sympathetic stimulation induced by hand cooling alters cold-induced vasodilatation in humans. *Eur J Appl Physiol,* 81**,** 303-9.

SHEPHERD, J. T., RUSCH, N. J. & VANHOUTTE, P. M. 1983. Effect of cold on the blood vessel wall. *Gen Pharmacol,* 14**,** 61-4.

SHEPHERD, J. T. & THOMPSON, I. D. 1953. The response to cold of the blood vessels of denervated fingers during the regeneration of the nerves. *Ir J Med Sci***,** 208-11.

SHIGETOMI, E., JACKSON-WEAVER, O., HUCKSTEPP, R. T., O'DELL, T. J. & KHAKH, B. S. 2013. TRPA1 channels are regulators of astrocyte basal calcium levels and long-term potentiation via constitutive D-serine release. *J Neurosci,* 33**,** 10143-53.

SILVA, C. R., OLIVEIRA, S. M., ROSSATO, M. F., DALMOLIN, G. D., GUERRA, G. P., DA SILVEIRA PRUDENTE, A., CABRINI, D. A., OTUKI, M. F., ANDRE, E. & FERREIRA, J. 2011. The involvement of TRPA1 channel activation in the inflammatory response evoked by topical application of cinnamaldehyde to mice. *Life Sci,* 88**,** 1077-87.

SIMON, S. A. & LIEDTKE, W. 2008. How irritating: the role of TRPA1 in sensing cigarette smoke and aerogenic oxidants in the airways. *J Clin Invest,* 118**,** 2383-6.

SIMONE, D. A. & KAJANDER, K. C. 1996. Excitation of rat cutaneous nociceptors by noxious cold. *Neurosci Lett,* 213**,** 53-6.

SIMONE, D. A. & KAJANDER, K. C. 1997. Responses of cutaneous A-fiber nociceptors to noxious cold. *J Neurophysiol,* 77**,** 2049-60.

SIMONS, C. T., SUDO, S., SUDO, M. & CARSTENS, E. 2004. Mustard oil has differential effects on the response of trigeminal caudalis neurons to heat and acidity. *Pain,* 110**,** 64-71.

SKOWRONSKI, M. E., CIUFO, R., NELSON, J. A. & MCFADDEN, E. R., JR. 1998. Effects of skin cooling on airway reactivity in asthma. *Clin Sci (Lond),* 94**,** 525-9.

SMILLIE, S. J. 2012. *Pathological effects of calcitonin gene-related peptide in a model of cardiovascular dysfunction and remodelling.* Doctor of Philosophy, King's College London.

SMILLIE, S. J. & BRAIN, S. D. 2011. Calcitonin gene-related peptide (CGRP) and its role in hypertension. *Neuropeptides,* 45**,** 93-104.

SMITH, M. P., BEACHAM, D., ENSOR, E. & KOLTZENBURG, M. 2004. Cold-sensitive, menthol-insensitive neurons in the murine sympathetic nervous system. *Neuroreport,* 15**,** 1399-403.

SMITH, T. L., GORDON, S., HOLDEN, M. B., SMITH, B. P., RUSSELL, G. B. & KOMAN, L. A. 1994. A rabbit ear model for cold stress testing. *Microsurgery,* 15**,** 563-7.

SMITS, E. S., DURAKU, L. S., NIEHOF, S. P., DAANEN, H. A., HOVIUS, S. E., SELLES, R. W. & WALBEEHM, E. T. 2013a. Cold-induced vasodilatation in cold-intolerant rats after nerve injury. *J Plast Reconstr Aesthet Surg,* 66**,** 1279-86.

SMITS, E. S., DURAKU, L. S., NIEHOF, S. P., KUSTERS, F. J., HOVIUS, S. E., DAANEN, H. A., SELLES, R. W. & WALBEEHM, E. T. 2013b. Comments to the term "cold-induced vasodilatation" in "laser doppler perfusion imaging of skin territory to reflect autonomic functional recovery following sciatic nerve autografting repair in rats". *Microsurgery,* 33**,** 83-4.

SNIDER, R. M., CONSTANTINE, J. W., LOWE, J. A., 3RD, LONGO, K. P., LEBEL, W. S., WOODY, H. A., DROZDA, S. E., DESAI, M. C., VINICK, F. J., SPENCER, R. W. & ET AL. 1991. A potent nonpeptide antagonist of the substance P (NK1) receptor. *Science,* 251**,** 435-7.

SOMLYO, A. P. & SOMLYO, A. V. 2000. Signal transduction by G-proteins, rho-kinase and protein phosphatase to smooth muscle and non-muscle myosin II. *J Physiol,* 522 Pt 2**,** 177-85.

SOMLYO, A. P. & SOMLYO, A. V. 2003. Ca2+ sensitivity of smooth muscle and nonmuscle myosin II: modulated by G proteins, kinases, and myosin phosphatase. *Physiol Rev,* 83**,** 1325-58.

STARKE, K. 1987. Presynaptic alpha-autoreceptors. *Rev Physiol Biochem Pharmacol,* 107**,** 73-146.

STARR, A., GRAEPEL, R., KEEBLE, J., SCHMIDHUBER, S., CLARK, N., GRANT, A., SHAH, A. M. & BRAIN, S. D. 2008. A reactive oxygen species-mediated component in neurogenic vasodilatation. *Cardiovasc Res,* 78**,** 139-47.

STARUSCHENKO, A., JESKE, N. A. & AKOPIAN, A. N. 2010. Contribution of TRPV1-TRPA1 interaction to the single channel properties of the TRPA1 channel. *J Biol Chem,* 285**,** 15167-77.

STOKES, A., WAKANO, C., KOBLAN-HUBERSON, M., ADRA, C. N., FLEIG, A. & TURNER, H. 2006. TRPA1 is a substrate for de-ubiquitination by the tumor suppressor CYLD. *Cell Signal,* 18**,** 1584-94.

STORY, G. M. & GEREAU, R. W. T. 2006. Numbing the senses: role of TRPA1 in mechanical and cold sensation. *Neuron,* 50**,** 177-80.

STORY, G. M., PEIER, A. M., REEVE, A. J., EID, S. R., MOSBACHER, J., HRICIK, T. R., EARLEY, T. J., HERGARDEN, A. C., ANDERSSON, D. A., HWANG, S. W., MCINTYRE, P., JEGLA, T., BEVAN, S. & PATAPOUTIAN, A. 2003. ANKTM1, a TRP-like channel expressed in nociceptive neurons, is activated by cold temperatures. *Cell,* 112**,** 819-29.

TAGAWA, T., MOHRI, M., TAGAWA, H., EGASHIRA, K., SHIMOKAWA, H., KUGA, T., HIROOKA, Y. & TAKESHITA, A. 1997. Role of nitric oxide in substance P-induced vasodilation differs between the coronary and forearm circulation in humans. *J Cardiovasc Pharmacol,* 29**,** 546-53.

TAKAHASHI, N., KUWAKI, T., KIYONAKA, S., NUMATA, T., KOZAI, D., MIZUNO, Y., YAMAMOTO, S., NAITO, S., KNEVELS, E., CARMELIET, P., OGA, T., KANEKO, S., SUGA, S., NOKAMI, T., YOSHIDA, J. & MORI, Y. 2011. TRPA1 underlies a sensing mechanism for O2. *Nat Chem Biol,* 7**,** 701-11.

TAKENAGA, M. & KAWASAKI, H. 1999. Endogenous calcitonin gene-related peptide suppresses vasoconstriction mediated by adrenergic nerves in rat mesenteric resistance blood vessels. *Eur J Pharmacol,* 367**,** 239-45.

TAN, J. L., RAVID, S. & SPUDICH, J. A. 1992. Control of nonmuscle myosins by phosphorylation. *Annu Rev Biochem,* 61**,** 721-59.

TANAKA, S., BARRON, K. W., CHANDLER, M. J., LINDEROTH, B. & FOREMAN, R. D. 2003. Local cooling alters neural mechanisms producing changes in peripheral blood flow by spinal cord stimulation. *Auton Neurosci,* 104**,** 117-27.

TANG, H. B., LI, Y. S., ARIHIRO, K. & NAKATA, Y. 2007. Activation of the neurokinin-1 receptor by substance P triggers the release of substance P from cultured adult rat dorsal root ganglion neurons. *Mol Pain,* 3**,** 42.

TANG, J. A., XU, D., YUAN, Q. X., MENG, Z. H., CHENG, F. R., CHEN, M. Z., LIU, G. Z., LIU, L. S. & ZHANG, Z. K. 1989. Calcitonin gene-related peptide in the pathogenesis and treatment of hypertension. *Chin Med J (Engl),* 102**,** 897-901.

TAYLOR-CLARK, T. E., UNDEM, B. J., MACGLASHAN, D. W., JR., GHATTA, S., CARR, M. J. & MCALEXANDER, M. A. 2008. Prostaglandin-induced activation of nociceptive neurons via direct interaction with transient receptor potential A1 (TRPA1). *Mol Pharmacol,* 73**,** 274-81.

TAYLOR, A. C., MCCARTHY, J. J. & STOCKER, S. D. 2008. Mice lacking the transient receptor vanilloid potential 1 channel display normal thirst responses and central Fos activation to hypernatremia. *Am J Physiol Regul Integr Comp Physiol,* 294**,** R1285-93.

TERENGHI, G., ZHANG, S. Q., UNGER, W. G. & POLAK, J. M. 1986. Morphological changes of sensory CGRP-immunoreactive and sympathetic nerves in peripheral tissues following chronic denervation. *Histochemistry,* 86**,** 89-95.

TEW, G. A., KLONIZAKIS, M., MOSS, J., RUDDOCK, A. D., SAXTON, J. M. & HODGES, G. J. 2011. Role of sensory nerves in the rapid cutaneous vasodilator response to local heating in young and older endurance-trained and untrained men. *Exp Physiol,* 96**,** 163-70.

THAKOR, A. S. & GIUSSANI, D. A. 2005. Role of nitric oxide in mediating in vivo vascular responses to calcitonin gene-related peptide in essential and peripheral circulations in the fetus. *Circulation,* 112**,** 2510-6.

THOMAS, J. R., SHURTLEFF, D., SCHROT, J. & AHLERS, S. T. 1994. Cold-induced perturbation of cutaneous blood flow in the rat tail: a model of nonfreezing cold injury. *Microvasc Res,* 47**,** 166-76.

THOMPSON-TORGERSON, C. S., HOLOWATZ, L. A., FLAVAHAN, N. A. & KENNEY, W. L. 2007. Cold-induced cutaneous vasoconstriction is mediated by Rho kinase in vivo in human skin. *Am J Physiol Heart Circ Physiol,* 292**,** H1700-5.

TIMMERMANS, P. B. & VAN ZWIETEN, P. A. 1982. alpha 2 adrenoceptors: classification, localization, mechanisms, and targets for drugs. *J Med Chem,* 25**,** 1389-401.

TOTSUKAWA, G., YAMAKITA, Y., YAMASHIRO, S., HARTSHORNE, D. J., SASAKI, Y. & MATSUMURA, F. 2000. Distinct roles of ROCK (Rho-kinase) and MLCK in spatial regulation of MLC phosphorylation for assembly of stress fibers and focal adhesions in 3T3 fibroblasts. *J Cell Biol,* 150**,** 797-806.

TREEDE, R. D. & MAGERL, W. 1995. Modern Concepts of Pain and Hyperalgesia - Beyond the Polymodal C-Nociceptor. *News in Physiological Sciences,* 10**,** 216-228.

TREEDE, R. D., MEYER, R. A. & CAMPBELL, J. N. 1990. Comparison of Heat and Mechanical Receptive-Fields of Cutaneous C-Fiber Nociceptors in Monkey. *Journal of Neurophysiology,* 64**,** 1502-1513.

TREEDE, R. D., MEYER, R. A., RAJA, S. N. & CAMPBELL, J. N. 1992. Peripheral and Central Mechanisms of Cutaneous Hyperalgesia. *Progress in Neurobiology,* 38**,** 397-421.

TREEDE, R. D., RAJA, S. N., DAVIS, K. D., MEYER, R. A. & CAMPBELL, J. N. 1991. Evidence That Peripheral Alpha-Adrenergic Receptors Mediate Sympathetically Maintained Pain. *Proceedings of the Vith World Congress on Pain,* 4**,** 377-382.

TREVISAN, G., ROSSATO, M. F., HOFFMEISTER, C., OLIVEIRA, S. M., SILVA, C. R., MATHEUS, F. C., MELLO, G. C., ANTUNES, E., PREDIGER, R. D. & FERREIRA, J. 2013. Mechanisms involved in abdominal nociception induced by either TRPV1 or TRPA1 stimulation of rat peritoneum. *Eur J Pharmacol,* 714**,** 332-44.

TREVISANI, M., SIEMENS, J., MATERAZZI, S., BAUTISTA, D. M., NASSINI, R., CAMPI, B., IMAMACHI, N., ANDRE, E., PATACCHINI, R., COTTRELL, G. S., GATTI, R., BASBAUM, A. I., BUNNETT, N. W., JULIUS, D. & GEPPETTI, P. 2007. 4-Hydroxynonenal, an endogenous aldehyde, causes pain and neurogenic inflammation through activation of the irritant receptor TRPA1. *Proc Natl Acad Sci U S A,* 104**,** 13519-24.

TSUTSUMI, M., DENDA, S., IKEYAMA, K., GOTO, M. & DENDA, M. 2010. Exposure to low temperature induces elevation of intracellular calcium in cultured human keratinocytes. *J Invest Dermatol,* 130**,** 1945-8.

TURNER, C. P., TOYE, A. M. & JONES, O. T. 1998. Keratinocyte superoxide generation. *Free Radic Biol Med,* 24**,** 401-7.

TURRENS, J. F. 2003. Mitochondrial formation of reactive oxygen species. *J Physiol,* 552**,** 335-44.

TURRENS, J. F., CRAPO, J. D. & FREEMAN, B. A. 1984. Protection against oxygen toxicity by intravenous injection of liposome-entrapped catalase and superoxide dismutase. *J Clin Invest,* 73**,** 87-95.

UDDMAN, R., EDVINSSON, L., EKBLAD, E., HAKANSON, R. & SUNDLER, F. 1986. Calcitonin gene-related peptide (CGRP): perivascular distribution and vasodilatory effects. *Regul Pept,* 15**,** 1-23.

US, V. E. & GADDUM, J. H. 1931. An unidentified depressor substance in certain tissue extracts. *J Physiol,* 72**,** 74-87.

VAN DER STRUIJS, N. R., VAN ES, E. M., RAYMANN, R. J. & DAANEN, H. A. 2008. Finger and toe temperatures on exposure to cold water and cold air. *Aviat Space Environ Med,* 79**,** 941-6.

VAN OENE, J. C., DE VRIES, J. B. & HORN, A. S. 1984. The effectiveness of yohimbine in blocking rat central dopamine autoreceptors in vivo. *Naunyn Schmiedebergs Arch Pharmacol,* 327**,** 304-11.

VANDESOMPELE, J., DE PRETER, K., PATTYN, F., POPPE, B., VAN ROY, N., DE PAEPE, A. & SPELEMAN, F. 2002. Accurate normalization of real-time quantitative RT-PCR data by geometric averaging of multiple internal control genes. *Genome Biol,* 3**,** RESEARCH0034.

VANGGAARD, L. 1975. Physiological reactions to wet-cold. *Aviat Space Environ Med,* 46**,** 33-6.

VANHOUETTE, P. M. 1980. *Physical factors and regulation.,* Bethesda, M.D., American Physiological Society.

VANHOUTTE, P. M. & VERBEUREN, T. J. 1976. Depression by local cooling of 3H-norepinephrine release evoked by nerve stimulation in cutaneous veins. *Blood Vessels,* 13**,** 92-9.

VANMOLKOT, F. H., VAN DER SCHUEREN, B. J. & DE HOON, J. N. 2006. Calcitonin gene-related peptide-induced vasodilation in the human forearm is antagonized by CGRP8-37: evaluation of a human in vivo pharmacodynamic model. *Clin Pharmacol Ther,* 79**,** 263-73.

VAUSE, C. V. & DURHAM, P. L. 2009. CGRP stimulation of iNOS and NO release from trigeminal ganglion glial cells involves mitogen-activated protein kinase pathways. *J Neurochem,* 110**,** 811-21.

VENTURINI, G., COLASANTI, M., FIORAVANTI, E., BIANCHINI, A. & ASCENZI, P. 1999. Direct effect of temperature on the catalytic activity of nitric oxide synthases types I, II, and III. *Nitric Oxide,* 3**,** 375-82.

VICTOR, R. G., LEIMBACH, W. N., JR., SEALS, D. R., WALLIN, B. G. & MARK, A. L. 1987. Effects of the cold pressor test on muscle sympathetic nerve activity in humans. *Hypertension,* 9**,** 429-36.

VONGSAVAN, N. & MATTHEWS, B. 1993. Measuring Rates of Fluid-Flow through Dentin Invivo. *International Endodontic Journal,* 26**,** 10-11.

VRIENS, J., APPENDINO, G. & NILIUS, B. 2009. Pharmacology of vanilloid transient receptor potential cation channels. *Mol Pharmacol,* 75**,** 1262-79.

WANG, D., RUAN, L., HONG, Y., CHABOT, J. G. & QUIRION, R. 2013. Involvement of PKA-dependent upregulation of nNOS-CGRP in adrenomedullin-initiated mechanistic pathway underlying CFA-induced response in rats. *Exp Neurol,* 239**,** 111-9.

WANG, L., CVETKOV, T. L., CHANCE, M. R. & MOISEENKOVA-BELL, V. Y. 2012. Identification of in vivo disulfide conformation of TRPA1 ion channel. *J Biol Chem,* 287**,** 6169-76.

WANG, S., DAI, Y., FUKUOKA, T., YAMANAKA, H., KOBAYASHI, K., OBATA, K., CUI, X., TOMINAGA, M. & NOGUCHI, K. 2008a. Phospholipase C and protein kinase A mediate bradykinin sensitization of TRPA1: a molecular mechanism of inflammatory pain. *Brain,* 131**,** 1241-51.

WANG, Y. Y., CHANG, R. B., WATERS, H. N., MCKEMY, D. D. & LIMAN, E. R. 2008b. The nociceptor ion channel TRPA1 is potentiated and inactivated by permeating calcium ions. *J Biol Chem,* 283**,** 32691-703.

WATANABE, H., VRIENS, J., SUH, S. H., BENHAM, C. D., DROOGMANS, G. & NILIUS, B. 2002. Heat-evoked activation of TRPV4 channels in a HEK293 cell expression system and in native mouse aorta endothelial cells. *J Biol Chem,* 277**,** 47044-51.

WEHRFRITZ, A., NAMER, B., IHMSEN, H., MUELLER, C., FILITZ, J., KOPPERT, W. & LEFFLER, A. 2011. Differential effects on sensory functions and measures of epidermal nerve fiber density after application of a lidocaine patch (5%) on healthy human skin. *Eur J Pain,* 15**,** 907-12.

WEI, E. P., MOSKOWITZ, M. A., BOCCALINI, P. & KONTOS, H. A. 1992. Calcitonin gene-related peptide mediates nitroglycerin and sodium nitroprusside-induced vasodilation in feline cerebral arterioles. *Circ Res,* 70**,** 1313-9.

WEI, H., CHAPMAN, H., SAARNILEHTO, M., KUOKKANEN, K., KOIVISTO, A. & PERTOVAARA, A. 2010a. Roles of cutaneous versus spinal TRPA1 channels in mechanical hypersensitivity in the diabetic or mustard oil-treated non-diabetic rat. *Neuropharmacology,* 58**,** 578-84.

WEI, H., HAMALAINEN, M. M., SAARNILEHTO, M., KOIVISTO, A. & PERTOVAARA, A. 2009. Attenuation of mechanical hypersensitivity by an antagonist of the TRPA1 ion channel in diabetic animals. *Anesthesiology,* 111**,** 147-54.

WEI, H., KARIMAA, M., KORJAMO, T., KOIVISTO, A. & PERTOVAARA, A. 2012. Transient receptor potential ankyrin 1 ion channel contributes to guarding pain and mechanical hypersensitivity in a rat model of postoperative pain. *Anesthesiology,* 117**,** 137-48.

WEI, H., KOIVISTO, A. & PERTOVAARA, A. 2010b. Spinal TRPA1 ion channels contribute to cutaneous neurogenic inflammation in the rat. *Neurosci Lett,* 479**,** 253-6.

WEI, H., SAARNILEHTO, M., FALCK, L., VIISANEN, H., LASIERRA, M., KOIVISTO, A. & PERTOVAARA, A. 2013a. Spinal transient receptor potential ankyrin 1 channel induces mechanical hypersensitivity, increases cutaneous blood flow, and mediates the pronociceptive action of dynorphin A. *J Physiol Pharmacol,* 64**,** 331-40.

WEI, H., VIISANEN, H., AMORIM, D., KOIVISTO, A. & PERTOVAARA, A. 2013b. Dissociated modulation of conditioned place-preference and mechanical hypersensitivity by a TRPA1 channel antagonist in peripheral neuropathy. *Pharmacol Biochem Behav,* 104**,** 90-6.

WEIDNER, C., KLEDE, M., RUKWIED, R., LISCHETZKI, G., NEISIUS, U., SKOV, P. S., PETERSEN, L. J. & SCHMELZ, M. 2000. Acute effects of substance P and calcitonin gene-related peptide in human skin--a microdialysis study. *J Invest Dermatol,* 115**,** 1015-20.

WEIHE, E. & HARTSCHUH, W. 1988. Multiple peptides in cutaneous nerves: regulators under physiological conditions and a pathogenetic role in skin disease? *Semin Dermatol,* 7**,** 284-300.

WHITE, B. J., SMITH, P. A. & DUNN, W. R. 2013. Hydrogen sulphide-mediated vasodilatation involves the release of neurotransmitters from sensory nerves in pressurized mesenteric small arteries isolated from rats. *Br J Pharmacol,* 168**,** 785-93.

WIDMER, R. J., LAURINEC, J. E., YOUNG, M. F., LAINE, G. A. & QUICK, C. M. 2006. Local heat produces a shear-mediated biphasic response in the thermoregulatory microcirculation of the Pallid bat wing. *Am J Physiol Regul Integr Comp Physiol,* 291**,** R625-32.

WILSON, S. R., NELSON, A. M., BATIA, L., MORITA, T., ESTANDIAN, D., OWENS, D. M., LUMPKIN, E. A. & BAUTISTA, D. M. 2013. The ion channel TRPA1 is required for chronic itch. *J Neurosci,* 33**,** 9283-94.

WIMALAWANSA, S. J., MORRIS, H. R., ETIENNE, A., BLENCH, I., PANICO, M. & MACINTYRE, I. 1990. Isolation, purification and characterization of beta-hCGRP from human spinal cord. *Biochem Biophys Res Commun,* 167**,** 993-1000.

WONG, B. J., TUBLITZ, N. J. & MINSON, C. T. 2005. Neurokinin-1 receptor desensitization to consecutive microdialysis infusions of substance P in human skin. *J Physiol,* 568**,** 1047-56.

WU, S. J., NG, L. T. & LIN, C. C. 2004. Effects of vitamin E on the cinnamaldehyde-induced apoptotic mechanism in human PLC/PRF/5 cells. *Clin Exp Pharmacol Physiol,* 31**,** 770-6.

XIAO, R., ZHANG, B., DONG, Y., GONG, J., XU, T., LIU, J. & XU, X. Z. 2013. A genetic program promotes C. elegans longevity at cold temperatures via a thermosensitive TRP channel. *Cell,* 152**,** 806-17.

XU, X., WANG, P., ZOU, X., LI, D., FANG, L., GONG, K. & LIN, Q. 2010. The effects of sympathetic outflow on upregulation of vanilloid receptors TRPV(1) in primary afferent neurons evoked by intradermal capsaicin. *Exp Neurol,* 222**,** 93-107.

XUE, Y. L., SHI, H. X., MURAD, F. & BIAN, K. 2011. Vasodilatory effects of cinnamaldehyde and its mechanism of action in the rat aorta. *Vasc Health Risk Manag,* 7**,** 273-80.

YAMAZAKI, F. 2010. Local ascorbate administration inhibits the adrenergic vasoconstrictor response to local cooling in the human skin. *J Appl Physiol,* 108**,** 328-33.

YAMAZAKI, F., SONE, R., ZHAO, K., ALVAREZ, G. E., KOSIBA, W. A. & JOHNSON, J. M. 2006. Rate dependency and role of nitric oxide in the vascular response to direct cooling in human skin. *J Appl Physiol,* 100**,** 42-50.

YANAGA, A., GOTO, H., NAKAGAWA, T., HIKIAMI, H., SHIBAHARA, N. & SHIMADA, Y. 2006. Cinnamaldehyde induces endothelium-dependent and -independent vasorelaxant action on isolated rat aorta. *Biol Pharm Bull,* 29**,** 2415-8.

YOKOYAMA, T., OHBUCHI, T., SAITO, T., SUDO, Y., FUJIHARA, H., MINAMI, K., NAGATOMO, T., UEZONO, Y. & UETA, Y. 2011. Allyl isothiocyanates and cinnamaldehyde potentiate miniature excitatory postsynaptic inputs in the supraoptic nucleus in rats. *Eur J Pharmacol,* 655**,** 31-7.

YOUSUFZAI, S. Y. & ABDEL-LATIF, A. A. 1998. Calcitonin gene-related peptide relaxes rabbit iris dilator smooth muscle via cyclic AMP-dependent mechanisms: cross-talk between the sensory and sympathetic nervous systems. *Curr Eye Res,* 17**,** 197-204.

ZERPA, H., BERHANE, Y., ELLIOTT, J. & BAILEY, S. R. 2007. Cooling augments vasoconstriction mediated by 5-HT1 and alpha2-adrenoceptors in the isolated equine digital vein: involvement of Rho kinase. *Eur J Pharmacol,* 569**,** 212-21.

ZERPA, H., BERHANE, Y., ELLIOTT, J. & BAILEY, S. R. 2010a. Functional role of alpha2-adrenoceptor subtypes in the cooling-enhanced vasoconstriction of isolated cutaneous digital veins of the horse. *Eur J Pharmacol,* 627**,** 194-202.

ZERPA, H., BERHANE, Y., WOODCOCK, H., ELLIOTT, J. & BAILEY, S. R. 2010b. Rho kinase activation and ROS production contributes to the cooling enhanced contraction in cutaneous equine digital veins. *J Appl Physiol (1985),* 109**,** 11-8.

ZHANG, M., BREWER, A. C., SCHRODER, K., SANTOS, C. X., GRIEVE, D. J., WANG, M., ANILKUMAR, N., YU, B., DONG, X., WALKER, S. J., BRANDES, R. P. & SHAH, A. M. 2010. NADPH oxidase-4 mediates protection against chronic load-induced stress in mouse hearts by enhancing angiogenesis. *Proc Natl Acad Sci U S A,* 107**,** 18121-6.

ZHOLOS, A. 2010. Pharmacology of transient receptor potential melastatin channels in the vasculature. *Br J Pharmacol,* 159**,** 1559-71.

ZHOU, Y., SUN, B., LI, Q., LUO, P., DONG, L. & RONG, W. 2011. Sensitivity of bronchopulmonary receptors to cold and heat mediated by transient receptor potential cation channel subtypes in an ex vivo rat lung preparation. *Respir Physiol Neurobiol,* 177**,** 327-32.

ZURBORG, S., YURGIONAS, B., JIRA, J. A., CASPANI, O. & HEPPENSTALL, P. A. 2007. Direct activation of the ion channel TRPA1 by Ca2+. *Nat Neurosci,* 10**,** 277-9.

ZWINGMANN, C. & BILODEAU, M. 2006. Metabolic insights into the hepatoprotective role of N-acetylcysteine in mouse liver. *Hepatology,* 43**,** 454-63.